ANNALES
UNIVERSITATIS SCIENTIARUM BUDAPESTINENSIS DE ROLANDO EÖTVÖS NOMINATAE

SECTIO GEOLOGICA

TOMUS XVI
1973

REDIGUNT
B. GÉCZY
J. KISS
L. STEGENA

BUDAPEST
1973

ANNALES
UNIVERSITATIS SCIENTIARUM BUDAPESTINENSIS DE ROLANDO EÖTVÖS NOMINATAE

SECTIO BIOLOGICA
incepit anno MCMLVII

SECTIO CHIMICA
incepit anno MCMLIX

SECTIO GEOLOGICA
incepit anno MCMLVII

SECTIO GEOGRAPHICA
incepit anno MCMLXV

SECTIO HISTORICA
incepit anno MCMLVII

SECTIO IURIDICA
incepit anno MCMLIX

SECTIO LINGUISTICA
incepit anno MCMLXIX

SECTIO MATHEMATICA
incepit anno MCMLVIII

SECTIO PAEDAGOGICA ET PSYCHOLOGICA
incepit anno MCMLXIX

SECTIO PHILOLOGICA
incepit anno MCMLVII

SECTIO PHILOSOPHICA ET SOCIOLOGICA
incepit anno MCMLXII

GEOCHEMICAL INVESTIGATIONS OF SEDIMENTARY ROCKS IN THE NORTHERN CSERHÁT HILLS

by
J. ANDÓ

(Department of Petrography and Geochemistry, L. Eötvös University, Budapest)
(Received: 31st March, 1972)

РЕЗЮМЕ

Верхнеолигоценовые, а также нижне- и среднемиоценовые песчанистые, алевритовые и глинистые породы северной части гор Черхат являются относительно бедными редкими и рассеянными элементами, о чем свидетельствуют результаты анализов 400 образцов. Среднее содержание серебра (Ag 0,1 ppm), хрома (Cr 87 ppm), титана (Ti 3830 ppm) и лития (Li 70 ppm) в олигоценовых отложениях, содержание цинка (Zn 84 ppm), кобальта (Co 18 ppm), серебра (Ag 0,1 ppm), марганца (Mn 627 ppm), лития (Li 57 ppm) и стронция (410 ppm) в миоценовых осадочных отложениях, а также содержание серебра (Ag 0,1 ppm) и свинца (Pb 17 ppm) в плейстоцено-голоценовых отложениях соответствуют примерно средним значениям, установленным Виноградовым для осадочных пород. Несколько повышенные концентрации берилия (Be 8,5 ppm) наблюдаются в миоценовых отложениях. Несмотря на небольшие средние значения, региональное изучение распределения рассеянных элементов на земной поверхности позволяет выделить встречающиеся спорадически или небольшими пятнами локальные аномалии. Судя по минералого-петрографическим исследованиям и стратиграфическо-тектоническим наблюдениям, аномалии чаще всего обусловлены адсорбционной связью элементов, эвентуально – миграцией вдоль тектонических плоскостей или вулканизмом.

Under the National Rare Element Prospecting Project the staff of the Department of Petrography and Geochemistry of L. Eötvös University carried out petrographical-geochemical investigations in the Cserhát Hills relying on the surveying-sampling work directed by Dr. I. Kubovics, the head of the Department. The investigations were conducted by subareas readily dinstinguishable on the basis of the geological and geomorphological characteristics.

The Cserhát's western, northern and central subareas of relatively high structural position and intensively eroded, are characterized by the predominance of Upper Oligocene-Lower Eocene sediments and subvolcanic andesite dikes. The type of the east-southeastern subarea of geologically lower position is defined by the presence of young Middle to Upper Miocene and Pliocene sedimentary rocks and a stratovolcanic andesite complex.

During the investigations in the western subarea the investigators could rely merely on surface sampling, except for the territory of the horsts occuring on the left bank of the Danube. In the eastern subarea the materials recovered from drilling by the mapping team of the Hungarian Geological Institute were also made use of.

Subject to petrographical and geochemical investigations were detrital sedimentary rocks of varying grain size containing more or less pelite and $CaCO_3$. The basis for work was provided by sampling of all rock types along profiles and by tracing laterally the particular horizons. All in all, a total of 400 samples (80 from the Upper Oligocene, 302 from the Lower and Middle Oligocene and 18 from the Pleistocene-Holocene) as well as 13 000 geochemical data were at the author's disposal.

During this interpretation the writer aimed mainly at determining the trace element averages of the area and at finding out local anomalies and thus examining the regional distribution pattern.

The determination of trace elements, which served as a basis for geochemical interpretations, was performed spectrographically with a quartz spectrograph Q – 24. The results were evaluated semi-quantitatively by *J. Balogh – Nagy* using the combination of concentration and "Y" scales. The limits of detectability with an Al-electrode have been shown in Table 1.

Table 1

Detectability limits and sensitivity factors (S%) as found for particular elements by the spectographic method during the geochemical investigations of the Cserhát Hills

Element	Detectability limit ppm	S %	Element	Detectability limit ppm	S %
Ag	1	10	Be	60	5
Ga	1	3000	Sb	60	3
Tl	1	100	Te	60	0.02
Cr	2.5	400	Ti	60	7500
In	4	1	Ba	100	800
Ni	6	1580	Sc	100	10
Pb	6	334	Sr	100	450
V	6	2166	W	100	2
B	10	1000	Zn	100	80
Ge	10	20	As	160	4
Mo	10	20	Hg	250	0.2
Cu	10	570	Nb	250	8
Sn	10	100	Y	300	10
Co	16	125	Li	400	15
Mn	16	4180	Ta	1000	0.3
Bi	40	0.025	Zr	1000	20
Cd	40	0.75			

In evaluating the results, the ratio of the detectability limits of the particular elements to their global frequencies characteristic of the examined rock type have to be taken into consideration. This ratio may be called the *sensitivity factor*, $S\%$, of the method under consideration, a factor varying by elements and rock types:

$$S\% = \frac{\text{global average}}{\text{detectability limit}} \times 100$$

Table 1 also shows the S % obtained for the elements examined by this method in sedimentary rocks. As evident from the tabulation, the method has proved to be of high sensitivity ($S\% > 1000$: Mn and Ti) or of fair sensitivity ($S\%$ 100 to 1000: Ba and Sr) in the case of elements that cannot be ranked among the trace elements in the strict sense. Of the elements characterized by frequencies lower than 200 ppm, Ga, Ni, V, and B can be detected with high sensitivity ($S\% > 1000$), Cr, Pb, Cu, Ti, Sn, and Co with a fair sensitivity ($S\%$ 100 to 999), Ag, In, Ge, Mo, Be, Sb, Sc, W, Zn, As, Nb, Y, Li and Zr with a low sensitivity ($S\%$ 1 to 99), and Bi, Cd, Te, Hg and Ta with a very poor one ($S\% < 1$). It can be concluded that the above method yields satisfactory results suitable for the determination of the average distributions of elements necessary for locating geochemical anomalies, enrichments of economic significance for most of the examined trace elements.

In processing the data the analyses were grouped according to different principles and the quantities below the detectability limit were taken to be *minimum average* and those higher than this limit to be *maximum average*. The *geometrical mean* of these two figures is the value that is closest to the virtual average. This is why this mean was used in the subsequent calculations. Its values were calculated for sedimentary rocks of different ages, viz. Upper Oligocene, Lower Miocene, Pleistocene-Holocene (Table 2). The various rock types of different trace element content are represented on earth's surface in proportions differring from the virtual abundances, which is due to the different petrophysical characteristics of the surficial rocks. Since no statistical data of rocks are available, because of the lack of deep drilling information, the trace element mean values based upon surficial sampling do not apply to the entire vertical section. According to the data of the tabulation, the surficial, exclusively detrital, sedimentary rocks of the northern Cserhát Hills are rather poor in trace elements: a fact well reflected by the enrichment factors (ef) of the individual elements

$$ef = \frac{\text{observed mean}}{\text{Vinogradov's sedimentary average}}.$$

Belonging to the group of *siderophile* elements, Co and Ni show essentially the same behaviour in rocks of different age, their quantity does not attain the mean values characteristic of sedimentary rocks (ef = $= 0.3-0.9$ and $0.3-0.4$, respectively). Of the *sulphocalcophile* elements, positively valuable data have been obtained only for Cu and Ag whereas in the case of Cd, Hg, As, Sb, Bi and Te only quantities below the detectability limit could be found. Because of the very low sensitivity of the method in respect of the afore-mentioned elements (see Table 1), no precise conclusion as to their distribution patterns can be drawn unless the method is improved. The mean of Cu in the rocks of different age shows very little fluctuation, if any. The highest concentration (32 ppm) occurs in the Miocene, the lowest (27 ppm) in the Oligocene rocks, though

Table 2

Mean values and enrichment factors of trace elements in the surficial sedimentary rocks of the northern Cserhát Hills

	ELEMENTE	OLIGOCENE		MIOCENE		PLEISTOCENE – HOLOCENE		Vinogradov's average for sedimentary rocks
		mean (ppm)	enrichment factors	mean (ppm)	enrichment factors	mean (ppm)	enrichment factors	
siderophile	Co	16.0	0,8	17.6	0,90	6.6	0.3	20.0
	Ni	38.0	0.4	34.0	0.4	27.0	0.3	95.0
sulphocalcophile	Cu	27.0	0.5	32.0	0.6	30.0	0.5	57.0
	Ag	0.1	1.0	0.1	1.0	0.09	0.9	0.1
	Cd	0	0	0	0	0	0	0.3
	Hg	0	0	0	0	0	0	0.4
	As	0	0	0	0	0	0	6.6
	Sb	0	0	0	0	0	0	2.0
	Bi	0	0	0	0	0	0	0.01
	Te	0	0	0	0	0	0	0.01
oxicalcophile	Zn	65.0	0.8	84.0	1.1	53.0	0.7	80.0
	Ga	7.3	0.2	11.0	0.4	3.0	0.1	30.0
	Ge	0	0	0.1	0.05	0	0	2.0
	In	0	0	0	0	0	0	0.05
	Sn	4.0	0.4	4.0	0.4	0	0	10.0
	Tl	0	0	5.0	5.0	0	0	1.0
	Pb	13.0	0.6	16.0	0.8	17.0	0.9	20.0
light pegmatophile	Sc	0	0	0	0	0	0	10.0
	V	58,0	0.4	47.0	0.4	15.0	0.1	130.0
	Cr	87.0	0.9	64.0	0.6	45.0	0.4	100.0
	Mn	396,0	0.6	627.0	0.9	366.0	0.5	670.0
	Ti	3830.0	0.9	2065.0	0.5	1643.0	0.4	4500.0
pegmatophile	Y	0	0	0	0	0	0	30.0
	Zr	0	0	8.8	0.04	0	0	200.0
	Nb	0	0	0	0	0	0	20.0
	Mo	1.2	0.6	4.7	2.4	0	0	2.0
	Ta	0	0	0	0	0	0	3.5
	W	0	0	0	0	0	0	2.0
litophile	Li	70.0	1.2	57.0	1.0	0	0	60.0
	Be	0	0	8.5	2.8	0	0	3.0
	Ba	487.0	0.6	345.0	0.4	315.0	0.4	800.0
	Sr	291.0	0.6	410.0	0.9	77.0	0.2	450.0
sedimentophile	B	27.0	0.3	45.0	0.5	40.0	0.4	100.0

O means quantities lower than the detectability limit.

even these values fall short of the standard sedimentary average *(ef = = 0.5–0.6)*. Silver in the younger rocks is contained in gradually decreasing concentrations, though even the Oligocene rocks, showing the highest mean value of Ag, can be characterized by an average enrichment

factor as low as ef = 2. Of the *oxicalcophile* elements, Ge and In are present in quantities lower than the detectability limit a fact due to the low sensitivity of the method for these elements under consideration – (S% = 20 and 1, resp.). Pb and Ga show concentrations lower than the global sedimentary average and the divergencies in mean concentrations observable in rocks of different age are negligible (Pb: ef = 0.6 – 0.8; Ga: ef = 0.1 – 0.4).

The slight increase (peak) of the mean Ga content observed in Miocene rocks is due to the presence of lignite seams of low rank within this sequence. Zn in the Oligocene and Pleistocene-Holocene rocks is a little lower than the average, whereas in the Miocene strata its value is somewhat higher than the average as a result of the Zn-concentrating effect of the silt and pelite fractions present in considerable amount. Calculated from heavily scattered data, the mean value of Sn does not attain the Vinogradov's average in any of the rock types studied (ef = 0.04). Other authors (*Turekian – Wedepohl*, 1961), however, believe that this value would imply for detrital sedimentary rocks an enrichment by one order of magnitude.

In the group of *pegmatophile* elements, an account of the low sensitivity (*S*% = 0.30 – 20), no evaluable result was obtained for Sc, Y, Zr, Nb, Ta and W. Because of the inaccuracies observable in the higher concentration ranges, the mean values of Mn and Ti, elements not belonging to the trace elements in the narrower sense, seem to be somewhat lower than the virtual average. Thus in the northern Cserhát Hills, Mn is supposed to occur in quantities around, or somewhat lower than, the global average, whereas in case of Ti, values characterizable by enrichment factors 0.5 – 1.0 can be reckoned with. With exception of Mo, showing occasionally considerable concentration peaks in the Miocene, all the pegmatophile elements characterized by positive analyses (V, Cr, Mn, Ti) – though otherwise present in concentrations lower than the sedimentary average – show mean values tending to decrease with geological age.

Of the *litophile* elements, Li is present in all but the youngest formations in quantities around the sedimentary average; Sr in the Miocene rocks of higher average $CaCO_3$ content is somewhat richer, Ba poorer than in the Oligocene. Be in the Oligocene and Pleistocene – Holocene formations falls short of the sedimentary average, showing distinct concentration peaks in the Miocene sedimentary rocks (ef = 2,8). All of the lithophile elements are poorest in the Pleistocene – Holocene formations.

Sedimentophile B in the different surficial sedimentary formations is present in quantities lower than the sedimentary average. As evident from Table 2, the B : Ga ratio, considered as a rule to be an indicator of facies, does not reflect the sharp lithological boundary existing between the predominantly marine Oligocene – Miocene and the terrestrial Pleistocene – Holocene.

It can be stated on the basis of the above, that the mean trace element content of the exposed Oligocene, Miocene and Pleistocene – Holocene sediments of the northern Cserhát Hills usually falls short of Vino-

gradov's sedimentary average. The mean Cr, Ti and Li contents of the Oligocene, the Co, Ag, Mn, Li and Sr contents of the Miocene and the Ag and Pb contents of the Pleistocene – Holocene are around this figure. A low degree of enrichment is observable only in the case of the Ag content of the Oligocene and the Be (Tl) content of the Miocene sediments.

Although, as shown above, there are only minor divergencies in the mean trace element contents of the formations of different age and facies (sandy, silty-clayey), some isolated peaks of relative concentrations, with occasionally striking figures, can be observed nevertheless. In Table 3 the maximal values of the analyses of rocks of different age and the enrichment factors calculable therefrom have been shown. According to the data of the tabulation, the relevant figures for Ag ($ef_{max} = 60$), Be ($ef_{max} = 200$) and Li ($ef_{max} = 42$) of the Miocene sediments are noteworthy. In the case of these elements, on the basis of their figures substantially higher than the sedimentary average, maps of statistical surficial *distribution* have been compiled for locating potential anomalies.

Table 3

Trace element concentration peaks observed in the surficial sedimentary deposits of the northern Cserhát Hills

Elements	Oligocene maximum		Miocene maximum		Pleistocene-Holocene maximum	
	ppm	ef	ppm	ef	ppm	ef
Co	40	2	60	3	40	2
Ni	160	1,7	160	1.7	160	1.7
Cu	250	4.4	250	4.4	160	2.8
Ag	1	10	6	60	1.6	16
Zn	400	5.5	400	5.0	250	3.1
Ga	25	0.8	25	0.8	25	0.8
Sn	40	4	25	2.5	0	–
Tl	0	–	200	200	0	–
Pb	100	5	250	12.5	100	5.0
V	250	1.9	600	4.6	60	0.5
Cr	400	4	250	2.5	160	1.6
Mn	6 000	9	>10 000	>15.0	2 500	3.7
Ti	>10 000	>2.2	>10 000	> 2.2	10 000	2.2
Mo	16	8	16	8	0	–
Li	600	10.0	2 500	42	400	6.0
Be	0	0	600	200	0	–
Ba	> 1 000	>1.2	1 000	1.2	1 000	1.2
Sr	> 1 000	>2.2	1 000	2.2	400	0.9
B	250	2.5	400	4	250	2.5

Remark: Cd, Hg, As, Sb, Bi, Te, Ge, In, Sc, Y, Zr, Nb, Ta and W have in none of the samples yielded figures higher than the Vinogradov's average for sediments.

In compiling isoconcentration maps, the author calculated averages by ages for units (subareas) of a grid of 1 km spacing of the areas examinable in exposures. The 1-square kilometre subareas yielded on the average

4 samples of Oligocene and 5 samples of Miocene age: a satisfactory density of data in an area covered for about 80% by younger formations. In the case of the Pleistocene – Holocene formations, on account of the relatively low number of samples, an evaluation of this kind was impossible. For a few elements characterized by locally striking concentration peaks and an indetectability in the majority of the cases, just a map of dispersed anomaly dots could be plotted (Fig. 1.). On the basis of the data of Table 3 and the applicability as indicators of facies, the elements Ag, Zn, Sn, Mn, Mo, Be, Sr and B were examined for spatial distribution.

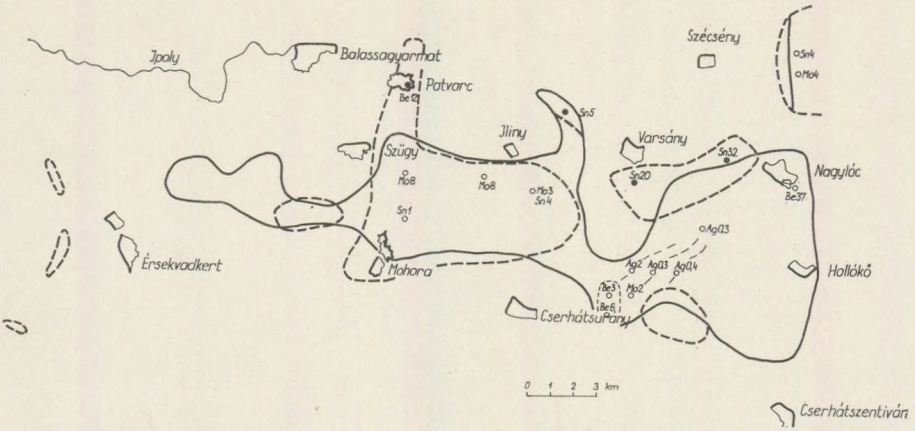

Fig. 1. Surficial anomalies of Ag, Sn, Mo and Be in the northern Cserhát Hills, Hungary

The occurrence of Ag in the sediments of the northern Cserhát Hills, as a rule, are confined to spaces of limited extension, thus showing distinct anomalies (Fig. 1). An Ag concentration peak independent of sandy or silty facies can be located in the country rock accompanying an Ottnangian lignite seam (abandoned mine at Nógrádsipek) and the contact wall rock of an andesite dike (dike range N and S of Nógrádsipek). As shown by micromineralogical analyses, the rocks of both environments of enrichment derived overwhelmingly from metamorphic sources (Table 4.). No mineral assemblages suggestive convincingly of magmatic rocks and their eventual hydrothermal associates can be identified. The analysis of calcareous siltstones for heavy minerals has not furnished any virtually interpretable data, as it is commonly the case with silty-clayey rocks. Sandy rocks are characterized by a relatively high tourmaline content. Because of the absence of aby direct relationship between the Ag content and the detrital components of the rocks, the most plausible assumption is an enrichment due to adsorption (clay minerals, iron oxihydroxides) of silver locally accumulated in the course of volcanism and coal deposition.

Sn attains, primarily in Oligocene rocks, subareal averages as high as twice or thrice the figure obtained for the total area (Fig. 1.). Rocks in

Table 4

Heavy mineral composition of the Ag-bearing sedimentary rocks of the northern Cserhát Hills

	heavy minerals (% by specimens) / rock type	garnet	staurolite	zoisite	andalusite	serpentine	glauconite	tourmaline	chlorite (chloritoid)	rutile	titanite	opaque	biotite	rhombic pyroxene	apatite	zircon	limonite
country rock of lignite	cross-bedded, friable sandstone	40	4	2	1	1	–	8	–	–	–	12	1	–	5	–	26
	thinly laminated (foliated), finegrained, friable sandstone	38	2	–	–	–	1	12	10	2	1	15	1	1	–	2	15
wall rock of dike	calcareous siltstone	5	–	–	–	–	–	–	31	–	–	–	53	–	–	–	7
	medium-grained friable sandstone	57	2	–	–	–	–	8	-	–	–	2	–	1	–	–	30

which it is concentrated are the Egerian clayey siltstones forming the wall of the andesite dike as well as friable, limonitic-clayey sandstones, clayey conglomerates and clays occuring at the top of the Oligocene. Worth of attention is the ENE – WSW trend of the Sn-shows (indications) parallel to the andesite dike swarms of the northern Cserhát Hills as well as the distinct eastward increase of concentration values. No mineral of tin can be identified among the detrital components of the rocks, though the common occurrence of *tourmaline* may suggest a granitic source area. The enrichment of tin in siallitic rocks may be due to adsorption.

The minor Mo anomalies of the northern Cserhát Hills (Fig. 1.) occur in the small-grained gravels and sands of the Egerian – Eggenburgian. Since, as shown in the literature, the enrichment of Mo in sedimentary rocks is enhanced by the clayey-sapropelitic facies, the altogether different lithofacies of the area seems to owe its concentrating influence to inclusions of detrital components (mainly quartz).

As for the distribution of Be, here again areally restricted anomalies can be recognized (Fig. 1.). The anomaly observable in the grey clays near Patvarc (ef = 4) and the Be-shows occurring in Miocene sandstones near Herencsény indicate just minor accumulations restricted to particular subareas. In certain horizons of the Lower Miocene at Nagylóc, however, considerable anomalies can be observed per subarea (ef = 12 – 67). The Lower Miocene formations of Nagylóc are very diversified in lithology: coarse- and fine-grained sands alternate with clayey rocks and

terrestrial variegated clays. Of these, rather significant enrichment of Be could be shown to occur in the 10- to 100-cm-thick layers of grey clay and of hard, purple sandstone. As shown by micromineralogical analyses, the quantity of heavy minerals belonging to the group of overwhelmingly magmatogenic rock constituents is significant in two rock types (Table 5.). On the basis of derivatographic results, the <0.02 mm grain fractions of the two rock types are constituted by pure halloysite (kaolinite?) (Fig. 2.).

Table 5

Micromineralogical composition of Be-bearing Lower Miocene rocks

components (% by specimens) / rock	Heavy minerals													Light minerals		
	rutile	zircon	titanite	augite	pyroxene	hornblende	garnet	tourmaline	biotite	chlorite	glaucophane	epidote	weight %	weight %	quartz	altered volcanic glass
grey clay	2	5	1	18	11	11	11	3	23	6	1	8	1.8	98.2	81	19
* red sandstone	3	2	2	22	5	11	9	2	27	5	2	10	2.0	98.0	88	12

* Because of the heavy desaggregation of red sandstone by HCl, limonite could not be interpreted.

Micromineralogical analyses testify to an andesitic-dacitic volcanism to have taken place during the accumulation of grey clays and red sandstones at the base of the schlier sequence. On the basis of the mineralogical composition these qualify as tuffaceous-tuffitic sediments. A distinct

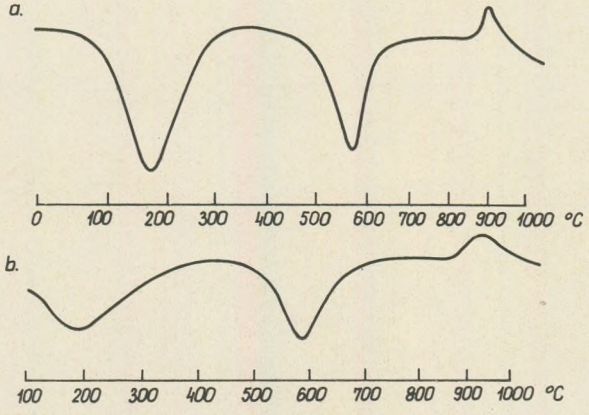

Fig. 2. DTA graphs of the < 0.02 mm fractions of Lower Miocene grey clays *(a)* and red sandstones *(b)*, Nagyl6c, Cserhát Hills, Hungary

enrichment of Ni, Zn, Sn, Pb and Sr can be shown to occur in these strata, too: a fact undoubtedly due to the connection of these formations with the volcanism of the so-called Lower Rhyolitic Tuff. The considerable amount of micromineralogically identified pyroxene as well as the poverty in trace elements of the Lower Rhyolitic Tuff typical of the Cserhát suggests local volcanological and geochemical agents to have manifested themselves in this area. The comparatively high concentrations of Ni, Zn, Sn, Pb and Sr may also be connected with the clay minerals of tuffitic rocks, but the striking values of Be are difficult to explain by a concentration due to adsorption, particulary so in the case of the red sandstone consisting overwhelmingly of detrital components. As known from the relevant literature, there exist rhyolitic tuffs altered by postvolcanic processes, containing commercial accumulations of Be. The Be-carrying mineral of these is finely crystalline bertrandite ($Be_4(SiO_4-SiO_3)(OH)_2$). Detrital components of very fine grained-size, thus indetectable micromineralogically, may also have been involved in the above enrichments.

Despite their regional investigations, the grey clays and red sandstones proved to be local formations. Therefore the remarkable enrichment of Be can be regarded just a local anomaly.

In addition, the surficial distribution of a few elements was also examined, elements which cannot be of economic value despite their local anomalies but which seem to be of interest from the geochemical point of view. It is merely in minor isolated patches that the quantity of Zn in the Oligocene rocks attains values round Vinogradov's sedimentary average. The mean Zn content tends to increase eastwards to some extent.

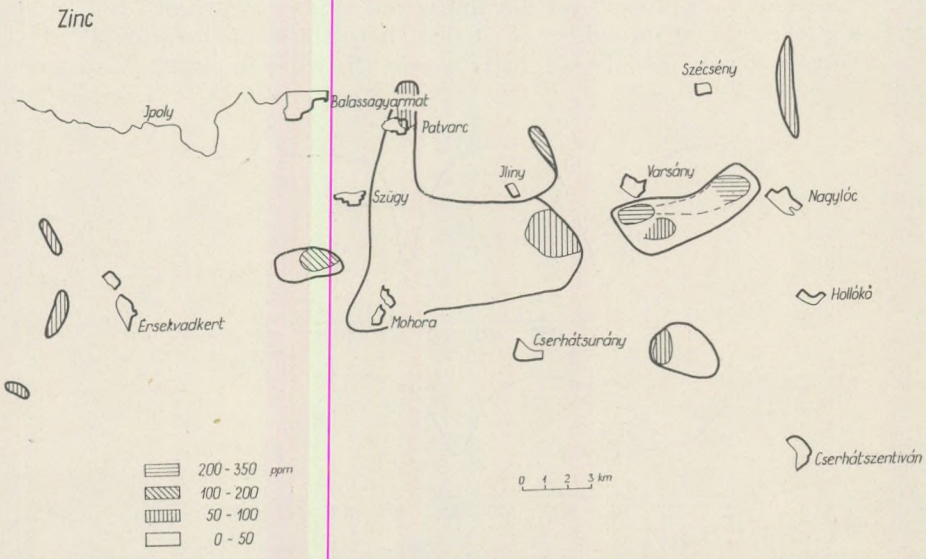

Fig. 3. Spatial distribution of Zn in the surficial Oligocene formations of the northern Cserhát Hills, Hungary

Anomalies showing three to four times the average can be observed to occur in the Egerian clayey-gravelly sediments, concentrators of Sn too, west of Nagylóc (Fig. 1.) and in the siltstones along the andesite dike (Fig. 3.).

The Miocene formations are characterized by a Zn content somewhat higher than the Oligocene average. Nevertheless, the quantity of Zn does not attain even the half of Vinogradov's sedimentary average over much of the Miocene-covered territory Whereas Zn values around the average in the western part of the area are restricted to isolated patches, in the east they can be traced over relatively large, continuous subareas. In the vicinity of Nagylóc and south of Hollókő, in fact, vast concentration fields characterized by ef = 1.5 to 2.5 can be located (Fig. 4.).

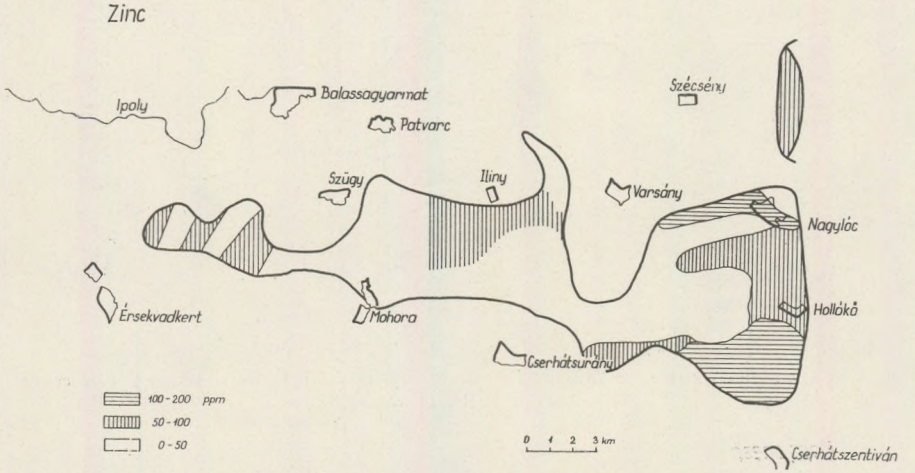

Fig. 4. Spatial distribution of Zn in the surficial Miocene formations of the northern Cserhát Hills, Hungary

The above peculiarity of the surficial distribution of Zn can be explained partly by the concentrating role of the schlier formation of the Carpathian Stage gradually gaining predominance to the east, partly by a migration along the fault zone of NE—SW trend extending a little west Hollókő and serving as a natural boundary between the western and eastern Cserhát Hills.

The mean Mn content obtained for the Oligocene and Miocene rocks of the northern Cserhát Hills is somewhat lower than or corresponds to the standard sedimentary average. The areal distribution found for the exposed Oligocene formations is very uneven: the subareal mean values over a considerable part of the examined surface area are much lower than the Vinogradov value, anomalous concentration peaks being confined to small areas (Fig. 5.).

In the Mn-concentrating psammitic rocks there are thin manganese mineral coats and layers occasionally visible to the naked eye (subareal

maximum, ef = 6, west of Mohora). Similar to the above is the Mn distribution pattern in the surficial Lower Miocene sediments as well, though the areas characterized by ef = 1 – 2 are somewhat larger. Rocks with an enrichment factor higher than this, ef = 2 – 3, however, are very small in number, being confined to a very small subarea (Fig. 6.).

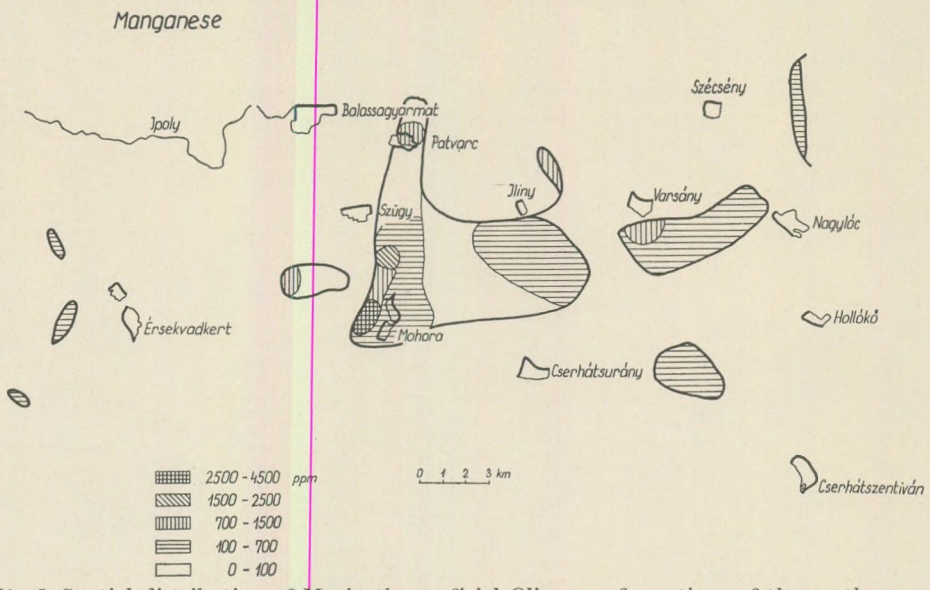

Fig. 5. Spatial distribution of Mn in the surficial Oligocene formations of the northern Cserhát Hills, Hungary

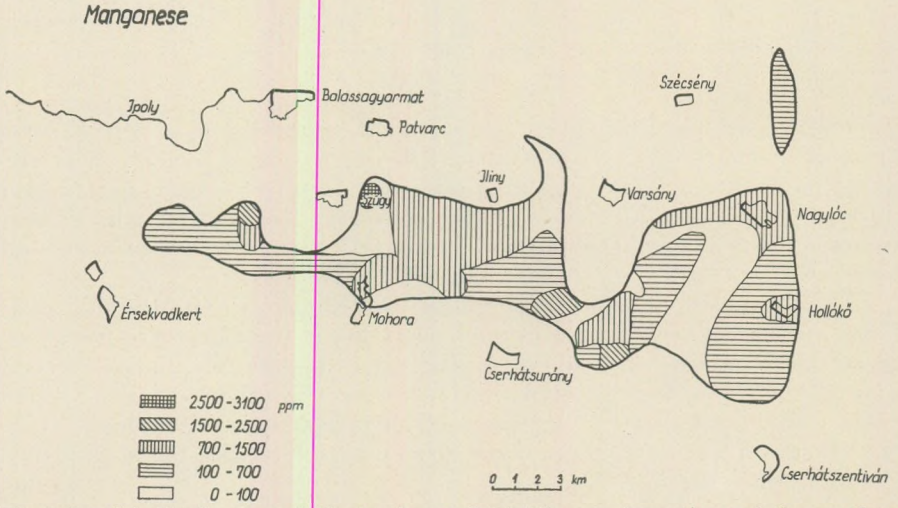

Fig. 6. Spatial distribution of Mn in the surficial Miocene formations of the northern Cserhát Hills, Hungary

The subareal enrichments, like it has been the case with the Oligocene rocks, occur predominantly in medium-to coarse-grained sandstones and conglomerates: a phenomenon suggesting direct precipitation from rather agitated sea waters of high oxygen content.

The average Sr content of the carbonate-poor Oligocene rocks is very low, its areal distribution being rather uniform, too. In addition to being regionally lower than the sedimentary standard, Sr shows some enrich-

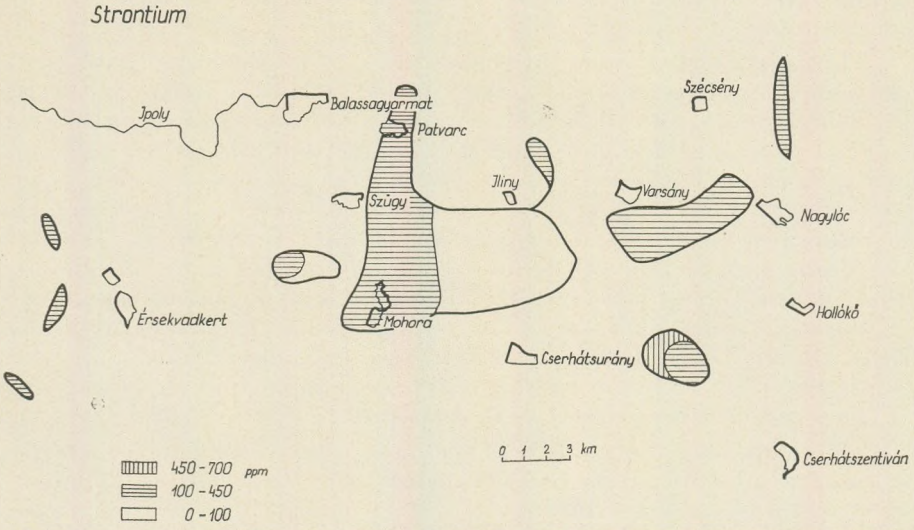

Fig. 7. Spatial distribution of Sr in the Oligocene formations of the northern Cserhát Hills, Hungary

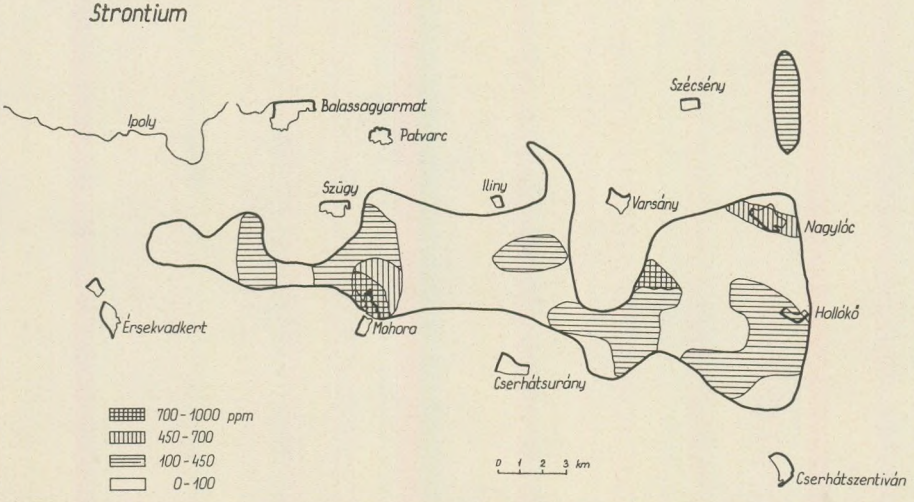

Fig. 8. Spatial distribution of Sr in the surficial Miocene formations of the northern Cserhát Hills, Hungary

ment of limited extent merely in the medium-grained sandstones of the vicinity of Herencsény (Fig. 7.).

As for the spatial distribution of Sr in the Miocene rocks, it is mainly the sandstones and siltstones of higher carbonate content as well as some of the wall rocks of andesite dikes (Mohora, Herencsény) that something like an anomaly can be observed. That the Sr content of the poorly calcareous country rocks "burnt" by the magma of dikes is different from the sedimentary average is an evidence of the Sr-accumulating role of the contact effect of the magma (Fig. 8.).

The spatial distribution of B showing very low average in the surficial sedimentary rocks of the northern Cserhát Hills is controlled by the surficial extension of the clayey-silty rocks. Subareal mean values corresponding to about, or slightly higher than, the sedimentary average indicate in both the Oligocene and the Miocene the presence of a clayey-silty (schlier) lithofacies (Fig. 9—10.). Figuring as an indicator of marine facies in references on geochemistry and sedimentary petrography, B in the Oligocene and Miocene of the area shows in both the more offshore and the lagoonal-terrestrial clays, an enrichment with regard to the average of boron (B) characteristic of the sediments of the northern Cserhát Hills. On the basis of the above, the regular connection of boron with pelitic rocks can be taken for sure, whereas its application as an indicator of facies can be accepted only with some reserve.

All in all, let us conclude that the mean quantities of trace elements in the surficial sedimentary rocks of the northern Cserhát Hills fall mostly short of the standard sedimentary average. Local concentration peaks,

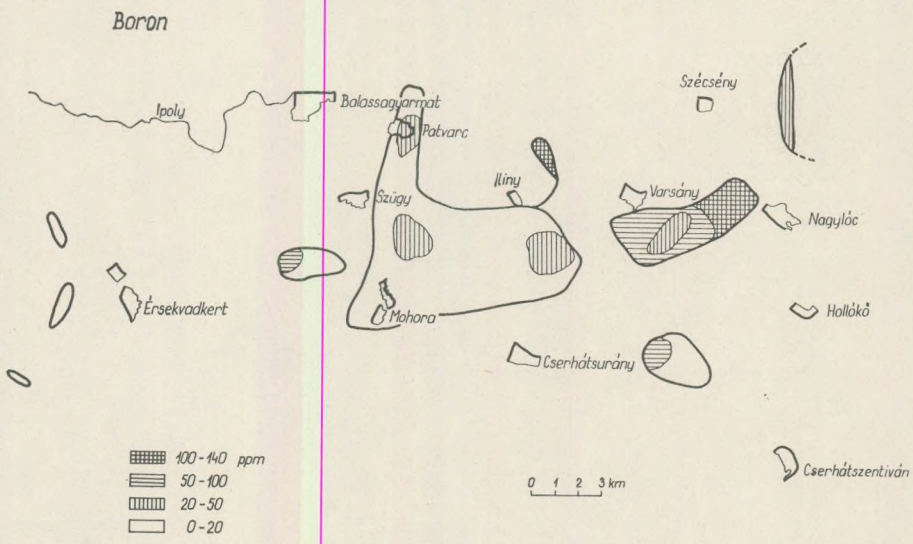

Fig. 9. Spatial distribution of boron (B) in the surficial Oligocene formations of the northern Cserhát Hills, Hungary

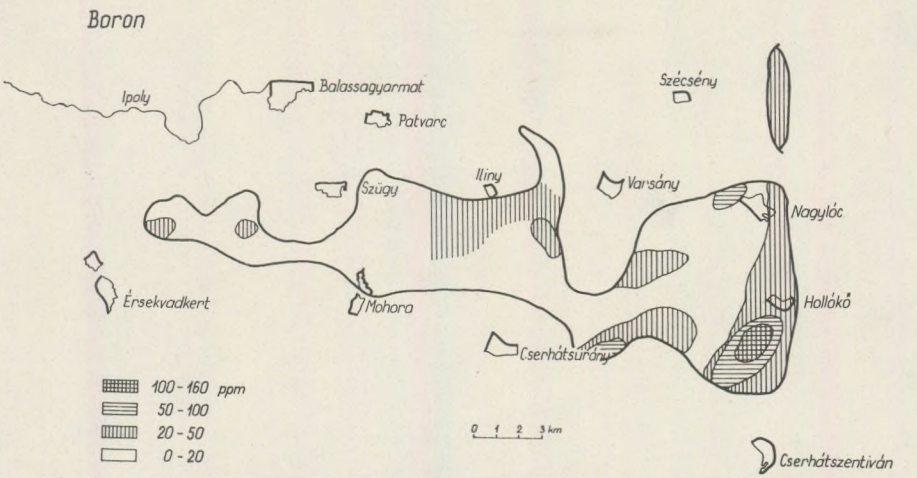

Fig. 10. Spatial distribution of boron (B) in the surficial Miocene formations of the northern Cserhát Hills, Hungary

anomalies, are usually due to fixation of elements by adsorption and to eventual migration or volcanic supply along deep-reaching tectonic planes. No placer-like accumulation of mineral raw materials connected with detrital components can be shown to occur.

REFERENCES

Bartkó, L. (1939): Nummulinás kvarckavicsok. (Quartz gravels with Nummulina.) Földtani Közlöny 69. p. 58–61.

Báldi, T. (1966): A magyarországi felsőoligocén molluszkafauna. (Mollusc fauna of Hungary's Upper Oligocene.) Dissertation (Manuscript).

Csiky, G. (1968): A szénhidrogénkutatások újabb eredményei és kilátásai az északi paleogén medencében. (Recent results and prospects of hydrocarbon exploration of the northern Paleogene basin.) Földtani Közlöny, 98. p. 29–40.

Ferenczi, I. (1933/35): Adatok az Ipoly-medence Sóshartyán–Karancsság, illetve Balassagyarmat körüli részének földtani ismeretéhez. (Contribution to the geology of the Ipoly Basin near Sóshartyán–Karancs and Balassagyarmat.) Magyar Állami Földtani Intézet Évi Jelentése. 2. p. 789–836.

Ferenczi, I. (1936–38): Újabb adatok az Ipoly-medence földtani viszonyainak ismeretéhez. (New data on the geology of the Ipoly Basin.) Magyar Állami Földtani Intézet Évi Jelentése. 2. p. 1035–1075.

Kubovics, I. – Pécsiné – Donáth, É. – Rózsavölgyi, J. – Andó, J. – Nagyné – Balogh, J. (1971): A Cserhát hegységi üledékes és vulkáni képződmények komplex kőzettani-geokémiai-vulkanológiai vizsgálata. (Complex petrographical-geochemical-volcanological investigations of the sedimentary and volcanic rocks of the Cserhát Hills) (Manuscript). MÁFI Adattár.

Szádeczky-Kardoss, E. (1953): Geokémia. (Geochemistry). Akadémiai Kiadó, Budapest.

Turekian, K. K. – Wedepohl, K. H. (1961): Distribution of the elements in some major units of the Earth's crust. Bull. Geol. Soc. Amer. 72. No. 2. p. 175–191.

Vadász, E. (1960): Magyarország földtana. (Geology of Hungary.) Budapest.

Vinogradov, A. P. (1962): Srednye soderzhaniya khimicheskikh elementov glavnykh tipah izvershennykh gornykh porod zemnoy kory. Geokhimiya 7. p. 555–572.

GEOCHEMICAL STUDY ON THE EARLY TORTONIAN ANDESITIC VOLCANISM OF THE CENTRAL AND SOUTH-WESTERN CSERHÁT HILLS

by
P. ÁRKAI

(Geochemical Research Laboratory of the Hungarian Academy of Sciences, Budapest)
(Received: 10th March, 1972)

SUMMARY

The aim of the present paper is a study of the temporal and spatial variations in the chemical and trace element composition of the volcanic complex of the Cserhát Hills, previously subdivided by mineralo-petrographical and paleomagnetic methods. The author – after a comparision with the literature – applied the regulations yielded through statistical evaluation of the data, to outline the presumed differentiation of the volcanism. From the linear and cyclic changes of the main and trace element amount, the different mechanism of the secondary magma chambers can be concluded.

After the previous publications (Árkai, 1967, 1968, 1970) on the mineralo-petrographical subdividing, relationship of the rock texture, mineralogical composition and rate of cooling, as well as the correlation between of rock-structure and textural orientation of the Central and SW Cserhát volcanic formations, consisting a part of the inner-Carpathian, mainly Neogene subsequent andesitic-rhyolitic volcanism, the purpose of the present work is to charakterize geochemically the volcanic activity.

For a better understanding of the geochemical data, the summarizing table of the temporal and spatial distribution of the volcanic rocks and facies on the studied area is quoted below (Table 1.).

The behaviour of the main elements

According to Vendl A. (1932) the andesites of the Cserhát Hills are dominantly of normal-dioritic, in some occurances are of normal-dioritic – gabbrodioritic, and the dacite of Buják is of quarzdioritic – normal-granitic character. The differentiation of the Pacific-type volcanics is normal, in several occurances Si-excess is demonstrable (si > 160), but the quarz starts to crystallize at only a *si* = 255 value. Vendl, after Lacroix, named the rocks of Si excess, but lacking in quarz to dacitoids (= phenoandesite). The volcanics are characterized by great titanium content and they are of nearly the same character as the andesites of the Mátra Hills.

According to Póka T. (1968), the andesites of the Cserhát Hills are less differentiated. The *si* value in the dyke developments is 154, at the eruption centres 164, and in the lava flows 175.

The subdividing of the volcanic rocks and the parallelization of the dyke and lava flow facies in the Central and SW Cserhát Hills permitted a statistical evaluation of the properly arranged chemical analyses.

On the basis of the differentiation characteristics figured in AFM graphs (Fig. 1.) the first lava eruption formed by bronzitic augite andesite is the least differentiated, most basic member, with its greatest magnesium, smallest alkaline and medium iron content. The hypersthenic augite andesite and dacite of the second eruption, with its smallest mag-

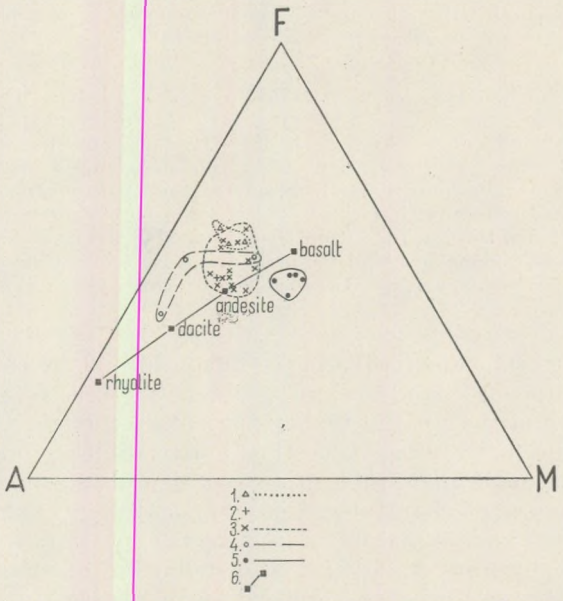

Fig. 1. The differentiational developments of the Central and SW Cserhát volcanics.

1. microandesite; 2. vesicular andesite; 3. amafic andesite; 4. hypersthenic augite andesite, dacite; 5. bronzitic augite andesite; 6. Daly-averages

nesium and great alkaline content is the most acidic phase of the cycle. The amafic, vacuolar and microandesites are of medium differentiation grade.

Fig. 2. shows the differentiation characteristics of the congenetic andesites of the Cserhát and Mátra Hills, applying the data of Kubovics I. (1966), Póka T. (1968), Varga Gy. (1964) and Csillagné T. E. (1963). In the Mátra Hills the average magnesium content increases and the average iron content decreases through the succeeding cycles. On the other hand by the comparison of the Middle Andesitic Group of the Mátra and Cserhát Hills a regional change is observable. The andesitic group of the Central and SW Cserhát Hills comprises the most basic and

SW Cserhát Hills		Acsa – Galgaguta area	Central Cserhát Hills		W Mátra Hills (According to Kubovics I.)	NE Mátra Hills (According to Kubovics I.)	The subdividing of the volcanic complex (According to Kubovics I.)		Magnetic polarity (According to Márton P.–Szalay E.)
dykes	volcanics	volcanics	dykes	volcanics					
–	–	–	–	–	–	overlying andesite	UPPER ANDESITE GROUP		positive
–	–	–	–	–	andesitogenic potash trachyte (sanidinite, adularite)	–	MIDDLE ANDESITE GROUP	MIDDLE VOLCANIC COMPLEX	
–	patchstone-like microandesite typical microandesite	–	microandesite of intermediate character	microandesite microandesite of intermediate character	patchstone-like microandesite typical microandesite vacuolar microandesite microandesite of intermediate character (with small porfiric plagioclase content)	–			
–	vacuolar microandesite vacuolar amafic andesite	vacuolar microandesite	–	vacuolar microandesite vacuolar amafic andesite	pseudo-tuff, pseudo-agglomerate vacuolar glauconitic andesite vacuolar microandesite vacuolar amafic andesite	–			negative
amafic andesite of Szanda-type		–	amafic andesite of Szanda-type amafic andesite of Bercel-type		amafic andesite	–			
–	–	–	–	–	andesite with augitic matrix	andesite with augitic matrix			
	lapilli-bearing, pumiceous andesite tuff, agglomerate	lapilli-bearing, pumiceous andesite tuff, agglomerate	–	lapilli-bearing, pumiceous andesite tuff, agglomerate	fine-grained andesite tuff	–			
bronzitic augite andesite		hypersthenic augite andesite andesitodacite	–	hypersthenic augite andesite andesitodacite bronzitic augite andesite	andesitodacite bronzitic augite andesite augite-bronzite andesite augite-bronzite-hypersthene andesite	bonzitic pyroxene andesite			
–	andesite tuff?	andesite tuff?	–	–	lapilli-bearing, pumiceous andesite tuff hypersthene andesite andesite-dacite tuff –	lapilli-bearing andesite tuff dacite tuff dacite laccoliths?			positive
–	plagioclase-bearing middle rhyolitic tuff	plagioclase-bearing middle rhyolitic tuff	–	plagioclase-bearing middle rhyolitic tuff	plagioclase-bearing middle rhyolitic tuff	plagioclase-bearing middle rhyolitic tuff			
–	–	–	–	–	hypersthene andesite tuff	andesite tuff	LOWER ANDESITE GROUP	LOWER VOLCANIC COMPLEX	negative

most acidic developments, their magnesium content generally is greater and their iron content is smaller than those of the counterparts in the N Cserhát and W Mátra Hills.

The differentiation characteristics are more precisely shown by the felsic and mafic indices suggested by S i m p s o n, E. S. W. (1954) (Fig. 3., 4.).

In accordance with the normal differentiation of the cak-alkaline rocks, the felsic index rises with the mafic index increase. The bronzitic

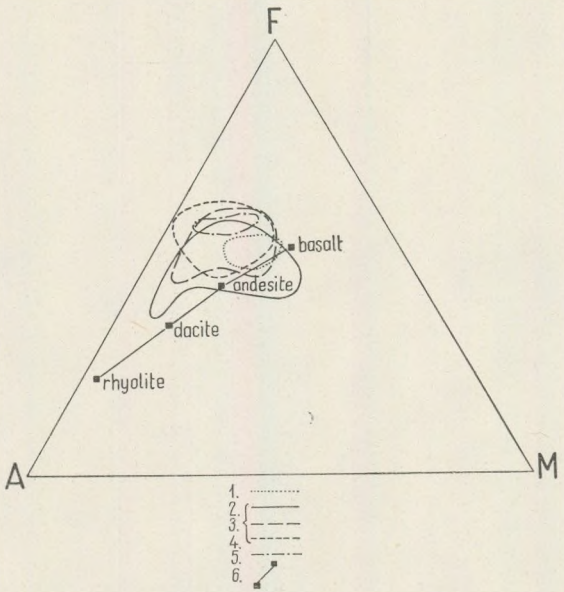

Fig. 2. The comparison of the differentiational developments of the Cserhát volcanics and the Lower, Middle and Upper Andesite Group of the Mátra Hills

1. Upper Andesite Group, Central Mátra Hills; 2. – 4. Middle Andesite Group; 2. Central and SW Cserhát Hills; 3. N Cserhát and northern part of the Central Cserhát Hills; 4. W Mátra Hills; 5. Lower Andesite Group, W Mátra Hills; 6. Daly-averages

augite andesite and the amafic andesite firstly differs by the Mg/Fe ration, but the calcium excess is characteristic to both of them. The felsic index of the hypersthenic augite andesite – dacite is transitory between the amafic and microandesite, and judging by its mafic index it is the most differentiated type. The vacuolar andesites agree with the amafic andesites, and to the microandesites the alkaline excess and the high, but as compared to the dacites somewhat lower mafic differentiation is characteristic.

The andesitic groups of the Mátra Hills differ solely in the mafic indices, i.e. the mafic index decreases in time.

In the Middle Andesitic Group of the SW, Central Cserhát and N Cserhát and W Mátra Hills the values of the mafic index increase in the above order.

The mol-percent Mg/Fe ratio of the pyroxene andesites' sum-chemism is closely followed by the average chemical composition of the ortho-

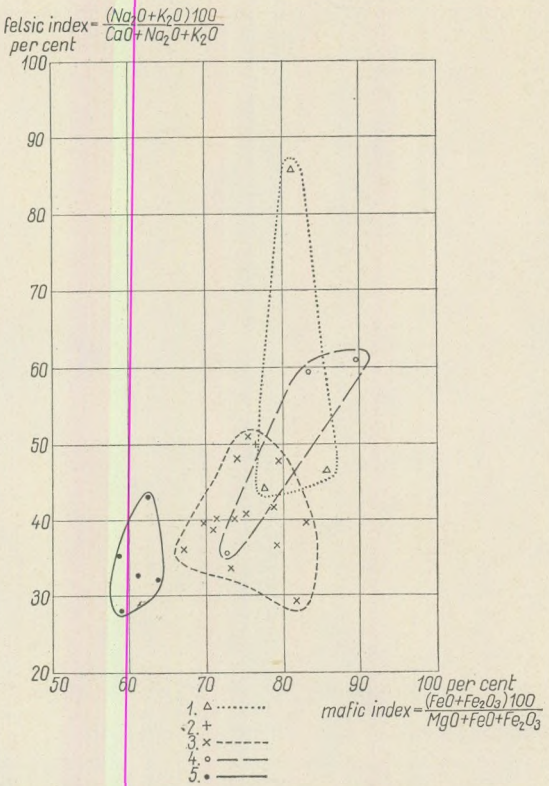

Fig. 3. The differentiational developments of the Central and SW Cserhát volcanics on the basis of felsic and mafic indices.

1. microandesite; 2. vesicular andesite; 3. amafic andesite; 4. hypersthene augite andesite, dacite; 5. Bronzitic augite andesite.

and clino-pyroxene phenocrysts, determined by microscopic method (H e s s, H. H. (1949), R u e g g, N. B. (1964). (Fig. 5.).

The temporal differentional processes of the volcanism are illustrated in the Table II. and Fig. 6., including the average Niggli-values. The *alk*, *k* and *o* curves run parallelly to the si values, but the *fm*, *c* and *mg* average curves run inconsistantly. The al curve rises graditionally from the

Table II

The average Niggli-values of the Cserhát volcanics

		si	al	fm	c	alk	k	mg	o
microandesite	SW Cserhát lava flows ...	155	26,4	34,6	20,8	18,2	0,40	0,29	0,15
	Central Cserhát lava flows.	212	32,5	37,0	13,6	16,9	0,33	0,35	0,43
	average	193	30,5	36,2	16,0	17,3	0,36	0,33	0,34
vacuolar andesite	SW Cserhát lava flow	159	37,1	27,8	18,2	15,9	0,30	0,37	0,32
amafic andesite of Szanda-type	SW Cserhát	172	31,7	32,9	20,2	15,2	0,34	0,35	0,18
	Central Cserhát	163	31,5	28,6	26,7	13,2	0,31	0,38	0,19
	dykes	164	29,3	31,8	24,8	14,1	0,30	0,34	0,21
	volcanic shield	163	31,5	28,6	26,6	13,3	0,34	0,41	0,14
	volcanic lava flow	168	37,7	24,5	24,9	12,9	0,29	0,34	0,30
	average	164	31,5	29,2	25,7	13,6	0,31	0,37	0,19
amafic andesite of Bercel-type	Central Cserhát volcanic shield	148	32,3	28,8	28,0	10,9	0,32	0,40	0,18
hyperstenic augite andesite, dacite	Central Cserhát, Acsa-Galgaguta lava flows	244	30,0	28,3	22,5	19,2	0,39	0,29	0,30
bronzitic augite andesite	SW Cserhát	153	23,5	41,8	23,2	11,5	0,29	0,55	0,17
	Central Cserhát	144	21,7	37,7	26,7	9,6	0,32	0,54	0,19
	dykes	151	23,7	38,9	27,6	9,8	[illegible]	[illegible]	0,13
	volcanics	145	21,7	36,1	24,7	10,[illegible]	[illegible]	[illegible]	0,23
	average	148	22,5	39,3	25,8	10,4	0,31	0,54	0,19
average of the SW and Central Cserhát volcanics		173	29,8	31,8	24,2	14,2	0,33	0,39	0,29
average of the N Cserhát volcanics		159	33,8	29,2	24,3	10,7	0,31	0,35	0,26
average of the Cserhát volcanics		167	31,5	30,6	24,2	12,7	0,32	0,37	0,24

bronzitic augite andesite up to the vacuolar andesite, and falls again at the microandesite.

The average chemical composition of the dyke, volcanic shield and lava-flow formations of the certain rock-types differ unsignificantly: the volcanic lava-flows are the most differentiated types generally.

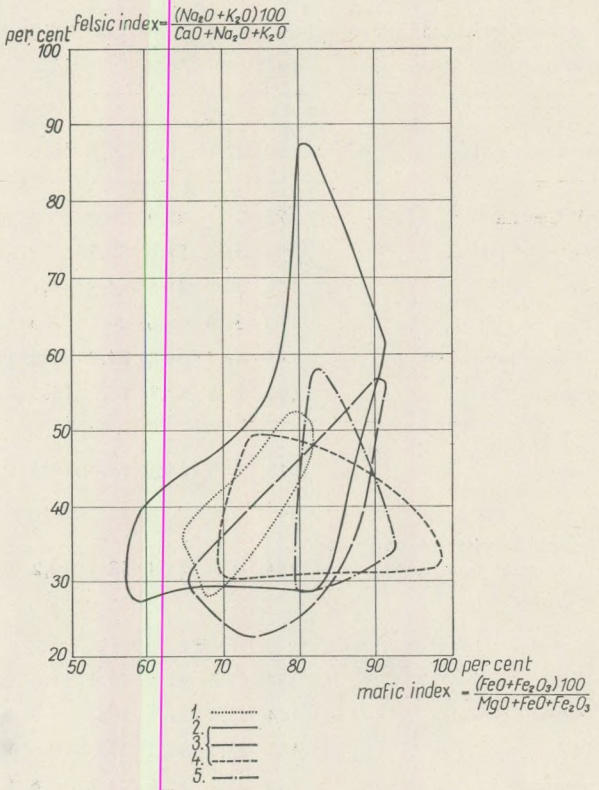

Fig. 4. The differentiational developments of the Cserhát volcanics and the Lower, Middle and Upper Andesite Group of the Mátra Hills, on the basis of the felsic and mafic indices

1. Upper Andesite Group, Central Mátra Hills; 2. — 4. Middle Andesite Group; 2. Central and SW Cserhát Hills; 3. N Cserhát and northern part of the Central Cserhát Hills; 4. W Mátra Hills; 5. Lower Andesite Group, W Mátra Hills.

The differentiation of the Cserhát Hills' volcanics is of normal Pacific character. Parallelly with the *si* value increase, the *alk* and *o* considerably, the *al* and *k* slightly grows, on the other hand the *mg* and *c* markedly, the *fm* gently decreases.

Table III.

rock-type	development	Ag	As	B	Ba	Be	Bi	Cd	Co	Cr	Cu	Ga	Ge	Hg	In	Li	Mn	Mo	Nb	Ni	Pb	Sb	Sn	Sr	Te	Ti	Tl	V	W	Zn
microandesite	SW Cserhát, lava flows	0	0	<10	2 275	0	0	0	21	1,5	37,5	3,6	0	0	0	<400	2 000	0	0	tr	tr	0	0	1 300	0	16 000	0	440	0	<100
	Central Cserhát, lava flows	0	<100	52	2 250	0	0	0	42	15	27	7,0	0	0	0	520	2 670	0	0	23,5	~9	0	0	1 570	0	20 200	0	190	0	<100
	average	0	<100	30	2 260	0	0	0	33	9	31,5	5,5	0	0	0	~400	2 380	0	0	16	~5,5	0	0	1 450	0	18 400	0	300	0	<100
intermediate microandesite	Central Cserhát, lava flows	0	0	<10	1 930	0	0	0	51	17	38	5,2	0	0	0	<400	750	0	0	44	<10	0	0	2 300	0	19 500	0	253	0	<100
amafic andesite of Szanda-type	SW Cserhát, dykes	0	0	<10	2 300	0	0	0	50	39	90	2,7	0	0	0	560	3 180	0	0	20	~11	0	0	1 430	0	9 600	0	430	0	<100
	SW Cserhát, lava flows	0	0	10	3 000	0	0	0	40	3	48	2,2	0	0	0	400	2 200	0	0	0	~9	0	0	1 270	0	9 600	0	533	0	<100
	SW Cserhát, average	0	0	<10	2 440	0	0	0	48	31	82	2,6	0	0	0	525	2 980	0	0	16	~10	0	0	1 430	0	9 600	0	450	0	<100
	Central Cserhát, Szanda dyke	0	0	10	1 300	0	0	0	29	15	43	4,1	0	0	0	<400	380	0	0	9	tr	0	0	1 010	0	23 000	0	149	0	<100
	Central Cserhát, Szanda volcanic shield	0	0	10	1 200	0	0	0	35	8,5	26	4,1	0	0	0	~400	745	0	0	20	0	0	0	1 380	0	19 000	0	180	0	<100
	Central Cserhát, lava flows	0	0	10	1 750	0	0	0	30	9	23	3,6	0	0	0	~400	690	0	0	9	<10	0	0	2 220	0	17 400	0	145	0	<100
	Central Cserhát, average	0	0	10	1 420	0	0	0	31	10	30	3,9	0	0	0	~400	635	0	0	13	<10	0	0	1 670	0	19 200	0	157	0	<100
	average of the dykes	0	0	<10	1 740	0	0	0	38	25	63	3,5	0	0	0	~400	1 580	0	0	14	~5	0	0	1 200	0	17 400	0	270	0	<100
	average of the volcanics	0	0	<10	1 590	0	0	0	32	8,5	25	3,7	0	0	0	~400	790	0	0	13	<10	0	0	1 820	0	17 600	0	179	0	<100
	average	0	0	<10	1 610	0	0	0	34	14	39	3,6	0	0	0	~400	1 060	0	0	14	<10	0	0	1 620	0	17 500	0	210	0	<100
amafic andesite of Bercel-type	average of dykes and volcanic shield	0	0	<10	2 500	0	0	0	37	21	58	5,3	0	0	0	<400	1 700	0	0	22	<10	0	0	1 170	0	25 000	0	295	0	<100
Hyperstenic augite andesite, dacite	Acsa, Galgaguta, Central Cserhát, lava flows	0,3	0	<10	1 920	0	0	0	29	12	<10	3,4	0	0	0	<1600	390	0	0	12	<10	0	0	2 080	0	9 500	0	63	0	<100
bronzitic augite andesite	SW Cserhát, dykes	0	0	<10	1 400	0	0	0	47	220	37	1,4	0	0	0	<400	1 200	0	0	33	0	0	0	1 070	0	6 700	0	220	0	<100
	SW Cserhát, volcanic shield	0	<160	<10	2 380	0	0	0	70	435	45	4,0	0	0	0	<400	2 130	0,7	0	134	~6	0	0	1 880	0	13 000	0	135	0	<100
	SW Cserhát, average	0	<160	<10	2 250	0	0	0	68	408	44	3,6	0	0	0	<400	2 020	0,5	0	122	~5	0	0	1 780	0	11 600	0	145	0	<100
	Central Cserhát, dykes	0	0	<10	1 660	0	0	0	59	372	65	5,3	0	0	0	<400	975	0	0	54	tr.	0	0	1 490	0	23 000	0	284	0	<100
	Central Cserhát, volcanic-schield	0,5	0	<10	2 210	0	0	0	47	540	41	6,4	0	0	0	<400	3 750	0	0	105	<10	0	0	1 510	0	18 700	0	220	0	<100
	Central Cserhát, average	0,2	0	<10	1 760	0	0	0	55	437	55	5,7	0	0	0	<400	2 030	0	0	73	<10	0	0	1 500	0	21 300	0	260	0	<100
	average of dykes	0	0	<10	1 600	0	0	0	56	345	60	4,5	0	0	0	<400	1 020	0	0	50	<10	0	0	1 410	0	19 900	0	272	0	<100
	average of the volcanics	0,1	<160	<10	2 260	0	0	0	64	460	44	4,6	0	0	0	<400	2 570	0,5	0	126	<10	0	0	1 780	0	14 500	0	168	0	<100
	average	0,1	<160	<10	1 990	0	0	0	60	410	49	4,5	0	0	0	<400	1 980	0,3	0	98	<10	0	0	1 620	0	16 000	0	194	0	<100
andesite tuff, agglomerate	SW Cserhát	0	0	<10	1 650	0	0	0	20	33	31	4,5	0	0	0	0	680	0	0	7	tr	0	0	600	0	9 200	0	141	0	<100
	Acsa – Galgaguta	0	0	<10	2 270	0	0	0	35	47	29	2,2	0	0	0	<600	267	0	0	16	<10	0	0	2 950	0	9 200	0	162	0	<100
	Central Cserhát	0	0	<10	1 130	0	0	0	25	13	10	3,0	0	0	0	<400	296	0	0	15	<10	0	0	1 560	0	14 500	0	170	0	<100
Middle plagioclase-rhyolitic tuff	Acsa – Galgaguta	2	0	<10	350	0	0	0	16	88	10	<1	0	0	0	0	40	0	0	3,3	30	0	0	250	0	860	0	15	0	<100
average of lava rocks of andesitic composition		0,04	<160	<10	1 910	0	0	0	41	103	42	4,3	0	0	0	<400	1 390	0	0	35	<10	0	0	1 600	0	18 200	0	215	0	<100
average of volcanics of andesitic composition		0	<160	<10	1 900	0	0	0	39	97	40	4,2	0	0	0	<400	1 290	0	0	33	<10	0	0	1 600	0	17 400	0	210	0	<100

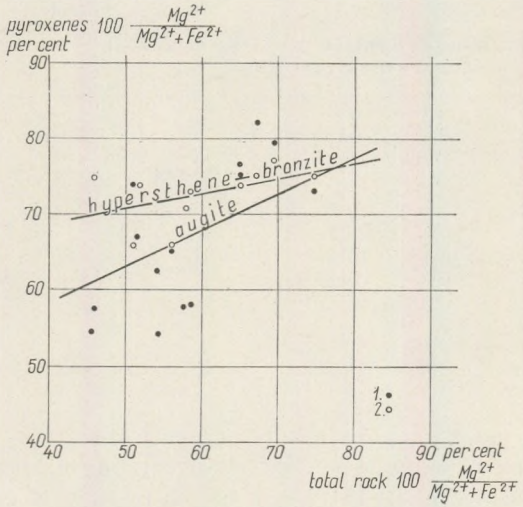

Fig. 5. Relationship between the $Mg^{2+}/Mg^{2+} + Fe^{2+}$ ratios of ortho- and clino-pyroxene phenocrysts and of counted from the rock-chemism mol-percentages.

1. augite; 2. hypersthene — bronzite.

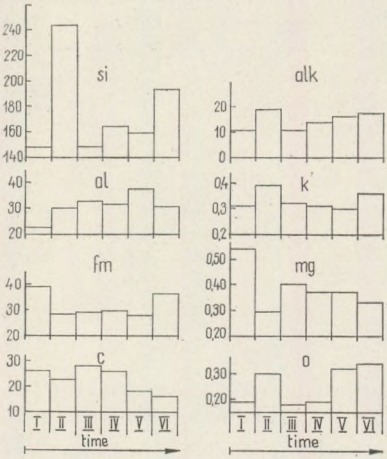

Fig. 6. The temporal differentiational processes of the Cenrtal and SW Cserhát volcanics, on the basis of the average Niggli-values.

I. bronzitic augite andesite — II. hypersthenic augite andesite, dacite — III. amafic andesite (Bercel-type) — IV. amafic andesite (Szanda-type) — V. vesicular andesite — VI. micro-andesite.

The change of trace element content in the volcanic complex

The following genetical evaluation is based on the data of half-quantitative trace element analyses of a total of 280 samples. The spectrographic determinations were carried out by Mrs N a g y B. In the course of the statistical evaluation of the data, the average trace element content of the certain rock-types, facies and regions were also determined (Table III.).

The frequency distribution of the nickel, chrome and manganese content is, corresponding with the conclusion of A h r e n s, L. H. (1954, 1963) typically lognormal, the distribution of the cobalt, vanadium, copper, barium and strontium content is transitory between the normal and log-normal types, and of the gallium is nearly normal (Figs. 7.).

The closeness of the relation between the certain trace element contents was determined by counting the correlation coefficients (Table IV.).

The close correlations (Co-Ni, Ni-Cr, Ba-Sr) can be interpreted with the similar electronic structure, or the element replacement, geochemical affinity, primer-magmatic differentiation, but the moderate correlations can be explained only by changes of trace element content, in accordance with magma-chemical province, have been taken place during the hypo-magmatic and secondary (endo- and exometamagmatic) processes. Under

Table IV

The correlation coefficients of the trace elements in the pyroxene andesite complex of the Central and SW Cserhát Hills

	Ba	Co	Cr	Cu	Ga	Mn	Ni	Sr
V	0.18	0.11	−0.01	0.28	0.20	0.37	−0.06	−0.12
Sr	0.45	0.35	0.12	0.03	0.21	0.13	0.24	
Ni	0.24	0.49	0.69	0.07	0.14	0.10		
Mn	0.30	0.10	0.26	0.11	0.09			
Ga	0.34	0.28	0.14	0.21				
Cu	0.01	0.25	−0.03					
Cr	0.03	0.25						
Co	0.38							

the influence of these latter processes in the amounts of electronic-structurally and geochemically different elements similar changes can be observed.

On the basis of temporal change study of the trace element content (Fig. 8.) the trace elements of the SW Cserhát Hills' volcanics can be ranged into three groups.

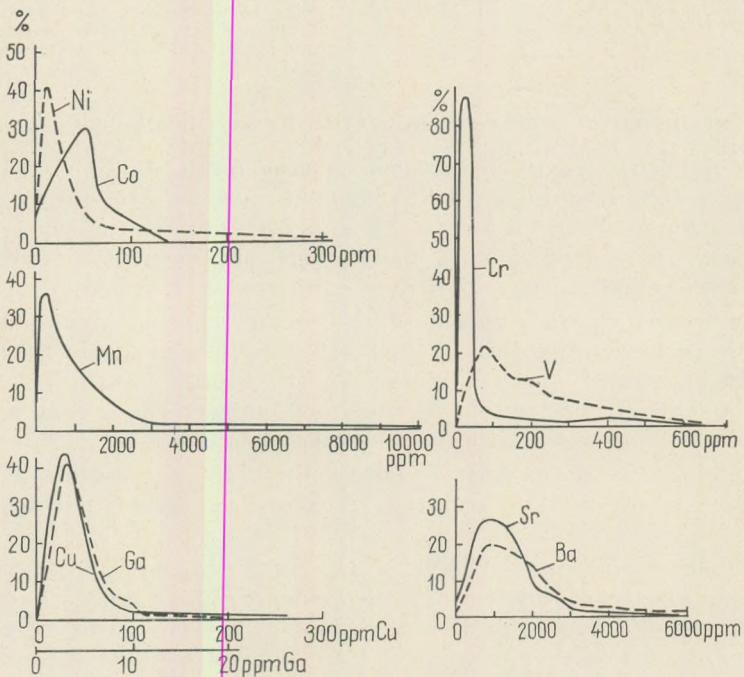

Fig. 7. The frequency-distribution of the trace element content of the Cserhát volcanics

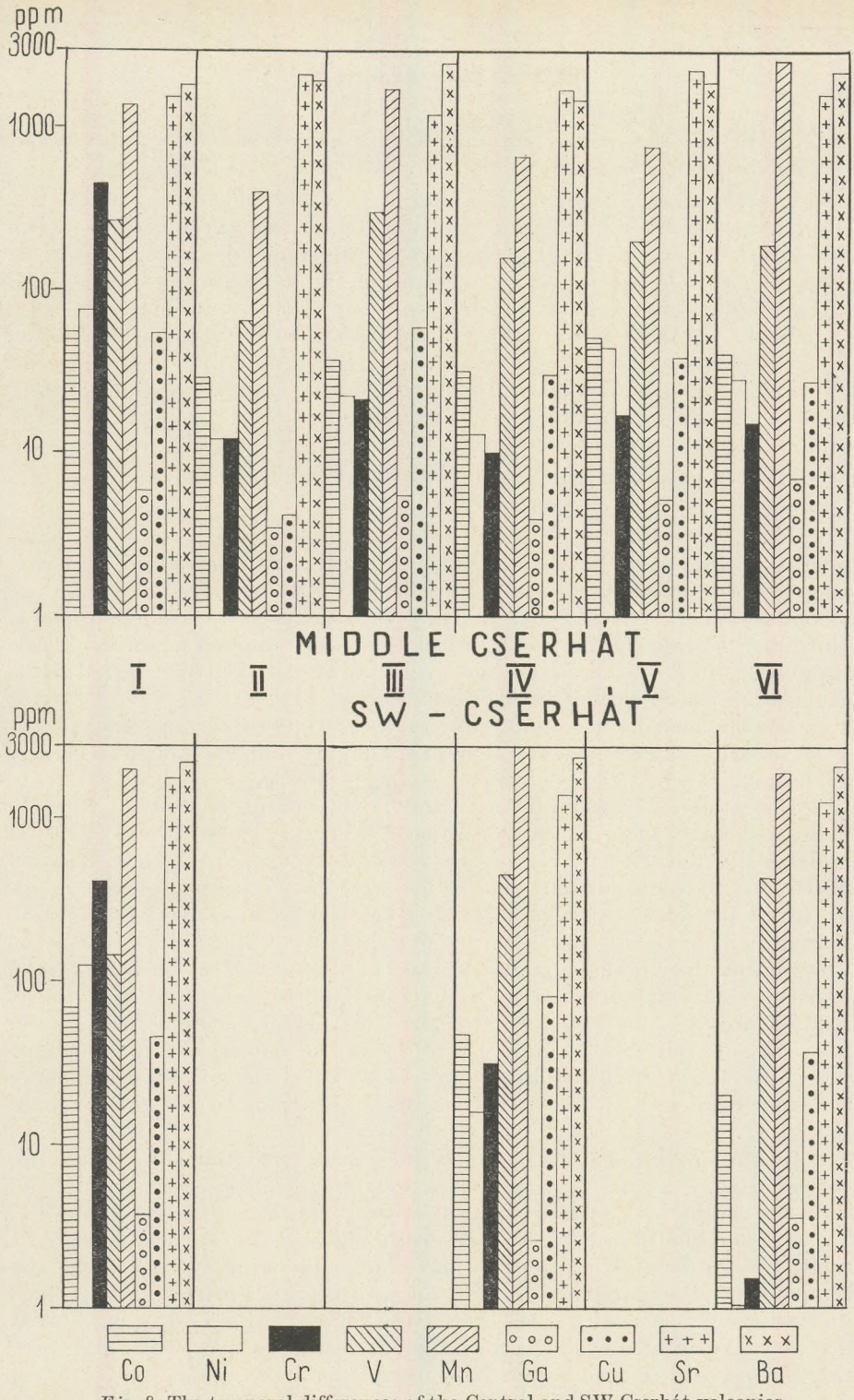

Fig. 8. The temporal differences of the Central and SW Cserhát volcanics

I. bronzitic augite andesite, dacite — II. hypersthenic augite andesite, dacite — III. amafic andesite (Bercel-type) — IV amafic andesite (Szanda – type) — V vesicular andesite — VI. microandesite

1. The cobalt, nickel, chrome and strontium amount gradually decreases in the course of the volcanism.

2. The vanadium, manganese, barium, copper and lithium amount is the greatest in the amafic andesites: the copper amount is greater in the bronzitic augite andesite, the amount of the other elements is lower as compared to the corresponding averages of the microandesite.

3. The gallium amount in the amafic andesites is minimal.

In the Central Cserhát Hills two trace element groups can be separated:

1. The cobalt, nickel, chrome, vanadium, manganese and gallium amount changes cyclically, the cobalt, nickel and chrome content in the bronzitic augite andesite is maximal.

2. In the case of the lithium, strontium and barium amounts the cyclicity is reverse, i.e. their summit falls into the microandesites.

The different changes of the two areas, firstly the change of the siderofile elements and the chrome content can be interpreted by plutonic, magma differentiation processes and by the different characters of the secondary magma chambers. In the SW Cserhát Hills merely a single "infilling" and gradual draining of the secondary magma chamber can be supposed, on the other hand the cyclicity in the Central Cserhát Hills suggests repeated infilling and draining.

The trace element content differences of the subvolcanic and volcanic facies are smaller than the temporal changes and can be statistically evaluated.

The copper, vanadium, lead and zinc amount in the subvolcanic dykes is greater than in the volcanic rock-types. The strontium, arsenic and barium enriches rather in the volcanic facies. The former may be partly due to the usually positive transvaporization in the volcanic facies or can be presumably explained with volatile escape occuring at volcanic horizons. The arsenic and barium enrichment in the volcanics can be presumably due to slight postmagmatic exhalations. On the basis of the mineralo-petrographic analyses the transvaporization processes in the studied area can be explained by the volatile intake have been taken place at low temperature and pressure (at the surface, or near-surface position). On the other hand these pricesses had, if any, slight influence on the trace element content of the volcanics (according to the greater ionic potential).

By endometamagmatic processes the cobalt, nickel, chrome, vanadium, copper, zinc, gallium and lead content of the volcanics decreases slightly, but the manganese, strontium and barium content increases markedly. In the hydrothermal dykes of Bercel the chrome and vanadium amount relatively the greatest in the montmorillonite- nontronite phase of highest temperature, the manganese, strontium and barium enriches in the dusting calcitic phase, and the trace element content of the opal-chrystobalite phase is usually minimal. Consequently the low temperature hydrothermal activity of the Cserhát Hills (developed merely to embrionic form

generally) was not connected with heavy or precious metallic enrichment.

By exometamagmatic influence (weathering, leaching) the trace element content of the volcanics decreases usually.

Differentiation developments

The activity of the Mátra–Cserhát volcano, as a member of the inner-Carpathian Neogene andesitic-rhyolitic volcanism can be interpreted on the basis of the sythesis on the regional and deepstructural situation of the Carpathian internid mass (Szádeczky – Kardoss, E. (1968). The presumably basaltic primary magma of the volcanism originates along deep-faults formed by tensional stresses in the Styrian phase of the Alpine orogeny from the peridotitic upper mantle, through selective migration and practically by tap of the deep currents. According to the laws of anatexis, considering a continuous magmal ascent up to the surface, within a single cycle the rock-types turn into more and more basic character as a function of time. In contradiction with the latter processes, the diffusive, or possibly assimilative interaction of the magma and the country rocks shows an increasing tendency.

The ascent of the primary magma of presumably basaltic origin is not contuinous, the breaks are marked with formations of secondary magma chambers and within these further differentional processes – mostly changing and concealing the primary features of the magma – have taken place.

The depth of the secondary magma chambers is generally at 5–25 km, thus these formed mainly within the granitic upper crust. The rhyolitic-ignimbritic volcanism is characterized by formation of so-called tertiary magma chambers, where the volatiles have been transvaporized from the wet environment, causing the further differentiation and dispersion of the magma.

In the course of the subsequent andesitic-rhyolitic volcanism the result of the differentiation is the well-known chemical and trace element change and the lesser known differentiation causes and processes.

In a normal differentiation the magnesium, iron and calcium amount and the Mg/Fe ration decreases, on the other hand the silicon, aluminium and alkaline amount, as well as the oxidation grade and the K/Na ratio increases. The change of the titanium is equivocal. At high temperature and in reductive environment the titanium enriches in the colour silicates, but at low temperature and in oxidative environment in the magnetite and ilmenite (Almuhamedov, A. I. (1967). The latter is presumably the case in the volcanics of the Cserhát Hills.

During differentiation the nickel and chrome content considerably, the cobalt and copper content slightly decreases, while the vanadium, lead and zinc content increases.

The process of differentiation is one of the most debated questions the endogene petrology. Leaving the detailed review of the theories and

their imperfections out of consideration, here are given some discussions on newer aspects of the diffenrentiation.

While the origin of the magma is a linear process and it can be unequivocally explained by the complex mobilizational differentiation (Szádeczky – Kardoss E.), the changes taking place at higher levels are of manifold character. The crystallizational differentiation, the liquation, assimilation, magmamixing and transvaporization are occasionally different, and determine the petrochemical character of the effusive lava, depending on the physical and chemical characteristics of the magma and the wall-rocks.

The transvaporization principally plays a great part in the generally near-surface magma chambers and volcanic vents formed in volatile-rich environments (formation of hypomagmas and volatile containing phenochrysts). In the Cserhát Hills transvaporization has importance near to, or at the surface only (precipitation of montmorillonite-nontronite, calcite and limonite). The low temperature and pressure circumstances of the hypomagmatic volatile intake are suggested by – beside the existing phase features – the low dispersion grade of the volatiles and the formation of separated silica and volatile-rich phases as well. The lacking of volatiles in the phenocrysts proves in the same time the volatile-poor environment of the secondary magma chambers.

Phenomena proving magma-mixing are unknown in the Cserhát volcanics, but several facts suggest *partial* and incomplete melting in the formerly crystallized subvolcanic andesites (bronzitic augite matrix portions in the hyperstenic augite andesites and dacites, as well as resorbed plagioclase inclusions mainly in the plagioclases of the amafic andesites).

The much debated *gravitational crystallization differentiation* theory can be found is several recent works in the basaltic and andesitic magma formation and the relationship between andesitic volcanism and Alpine peridotits as well (Green – Ringwood (1967), Osborn (1969), etc.).

The trace element studies of the andesites (Taylor et al. (1969) have shown the difficulties of basaltic magma-origin theory of the andesites. According to the above mentioned authors' studies, the andesitic formation of the Circumpacific Belt are characterized by small nickel content (30 ppm), low Ni/Co ratio (<1), great vanadium content and small, but variable chrome content. The basalts reveal similar vanadium and scandium, greater nickel, cobalt, chrome content and higher Ni/Co ratio. Thus, by the authors, the andesites cannot be originated from basalts through crystallization differentiation, since in the case of pyroxene segregation the amounts of the octaedric nickel, cobalt, chrome and vanadium would decrease (an impossibility because of the great vanadium content of the andesites), or, provided olivin crystallization it will take majority of the nickel and cobalt content along, while the chrome, vanadium and scandium enriches relatively in the residual melt (a fact contradicts the small chrome content of the andesites). The mag-

netite precipitation also diminishes the vanadium content of the residual melt.

The gravitative changes of the main elements' (except the potassium) content can be derived by magma-mixing and assimilation, but the trace element differences do not bear such an interpretation (e.g. to attain the andesitic nickel content would need a more than a 70% granitic mass admixture to the basaltic melt). Because of the different trace element ratios the andesitic magma can be originated neither by assimilation of deep-sea clays, nor partial melting of the eclogite. According to the above mentioned authors through the origin of the andesites at least two partial melting phases can be supposed.

Taking the temperature characteristics of the earth crust into account, the two-phase partial melting can hardly be explained, and in addition it does not elucidate the vanadium content differences mentioned above. Namely, provided the vanadium to be linked to the early precipitating pyroxenes and magnetite, the vanadium would enrich in the residual crystaline phase, and not in the phase of partial melting.

The lesser cobalt, nickel, chrome and greater vanadium content of the andesites, as compared to that of the basalts can be explained from basaltic magmas in the following ways:

1. From the basaltic melt the early crystallizing (magnesium-rich) pyroxenes precipitate, carriing the great part of the chrome and nickel, and a certain part of the cobalt-content. The vanadium content of the early crystallizing pyroxenes is small, thus the vanadium enriches in the residual melt relatively. According to Borisenko (1967) the iron and vanadium content of the pyroxenes is in close correlation.

2. It is conceivable, mainly at higher levels, a development of trace element compound characteristic to the andesites also by olivine (nickel, cobalt) and cromite precipitation (olivin-containing andesites are known from several occurances).

The precipitation of the magnetite, the another possible vanadium bearing of the andesites is determined by the oxidation grade of the magma (Osborn (1969). In the case of a low Fe_2O_3/FeO ratio the magnetite precipitates at the final phase of the crystallization, but in oxidizing environment it is the first product to crystallize.

In the *SW and Central Cserhát Hills* the bronzitic augite andesites of the first explosion are the least differentiated types and they show a close relation to the basaltic chemism. These can be ranged into the normal gabbro-dioritic magma (tite) type of the Niggli system: their magnesium and iron content is greater, silicon, aluminium and alkaline content is lesser as compared to the andesitic average values, so these are intermediates between the basalts and andesites. Their average chrome and cobalt content is greater, and the nickel content somewhat lesser than the averages given by Vinogradov (1962) to the basalts and by Agiorgitis (1968) to the Pannonian basalts. Consequently while the chemical composition of the bronzitic augite andesite is of intermediate character, its trace element content corresponds to the trace element con-

tent of the basaltic magma originated through the partial melting of the peridotitic upper mantle. This heterogenous feature can be deduced from the presumably olivine-basaltic primary magma too, without gravitational differentiation or manifold selective melting. Namely, by selective migration from the more acidic wall-rocks in the course of the ascent, or occasionally in the secondary magma chamber on the one hand, and to some extent by silicon, aluminium alkalines uptake through the melting of alkaline-alumosilicates of low melting point on the other.

The magma of the first explosion presumably could have staid in the secondary magma chamber for a relatively short time. Possibly secondary magma chamber had not been formed yet, thus not even a reduced gravitational differentiation was possible to exist, although the precipitation of the phenocrystals commenced at the greatest depths in that time (coolest environment).

The trace element composition of the eruptions followed the bronzitic augite andesite phase cannot be explained merely by assimilative differentiation of the magma of bronzitic augite andesite composition. The frequent differences of two order of magnitude in the chrome and nickel content are realizable only by the low gravitational differentiation of the magma, i.e. by the segregation of pyroxenes (and possibly olivine and cromite) of great chrome and nickel, moderate cobalt and small vanadium content. The dry environmental secondary magma chamber warranted the stability of the low redox potential of the magma. The magnetite did not precipitate at the beginning of the crystallization, and the vanadium content increase of the residual melt can be explained in this way.

The gravitational differentiation is proved also by estimations: as compared to the normal mineralogical composition of the bronzitic augite andesite, the pyroxene, proportion of the amafic andesites decreased by 13 weight percent (8% bronzite, 5% augite). The composition of the differentiate obtained through the subtraction of the average chemism of the pyroxenes determined by Fedorov method from average chemism of the bronzitic augite andesite as starting material is in close agreement with the chemism of the amafic andesites. Taking the average trace element contents into consideration, the pyroxenes would contain 200 ppm cobalt, 650 ppm nickel, 2800 ppm chrome and 70 ppm copper. This values – excepted the chrome – agree with the data in the literature. On the basis of the high chrome value cromite precipitation also presumable.

REFERENCES

A g i o r g i t i s, G. (1968): Zur Geochemie einiger seltener Elemente in basaltischen Gesteine. Tschermaks Miner. Petr. Mitt. 12. p. 208.

A h r e n s, L. H. (1954): The lognormal distribution of the elements. Geochim. Cosmochim. Acta. 5. p. 49.

A h r e n s, L. H. (1963): Element distribution in igneous rocks. Geochim. Cosmochim. Acta. 27. p. 929.

A l m u h a m e d o v, A. I. (1967): Behaviour of Ti during differentiation of basaltic magma. Geohimija. (1967) p. 75.

Árkai, P. (1967): Correlation of quantitative petrographic characteristics of pyroxene andesites in the volcanic complex of the Southwestern Cserhát Hills. Ann. Univ. Sci. Budapest. Sec. Geol. 11. p. 87.

Árkai, P. (1968): Correlation of rate of cooling, texture and mineralogical composition in the pyroxene andesite complex of the Cserhát Hills. Acta Geol. Acad. Sci. Hung. 12. p. 11.

Árkai, P. (1968): Fabric and jointing in pyroxene andesites, Cserhát Hills, Northeast Hungary. Ann. Univ. Sci. Budapest. Sec. Geol. 12. p. 3.

Árkai, P. (1970): Petrographical-geochemical study on the Early Tortonian volcanism in the Central and Southwestern Cserhát Hills. Doc. Thesis, Budapest. (in Hungarian)

Boriszenko, L. F. (1967): O korrelacionnoj szvjazi zseleza, vanadija i titana v pirokszenah. Geohimija. (1967) p. 304.

Carr, M. H. – Turekian, K. K. (1961): The geochemistry of cobalt. Geochim. Cosmochim. Acta. 23. p. 9.

Csillagné, T. E. (1963): Different overlying andesites from the Central Mátra Hills. MÁFI Évi Jel. (1963) (in Hungarian)

Fröhlich, F. (1960): Beitrag zur Geochemie des Chroms. Geochim. Cosmochim. Acta. 20. p. 215.

Green, D. H. – Ringwood, A. E. (1967): The genesis of basaltic magmas. Beitr. Miner. Petr. 15.

Hess, H. H. (1949): Chemical composition and optical properties of common clinopyroxenes. Amer. Miner. 34.

Kubovics, I. (1966): Mineralo-petrographic study of the Northeastern and Western Mátra Hills. Cand. Thesis, Budapest (in Hungarian)

Márton, P. – Szalay, E. (1970): Secular changes, polarity epochs and tectonic movements as indicated by paleomagnetic studies of Hungarian rock samples. Pure and Applied Geophysics. 81. p. 151.

Nockolds, S. R. (1966): The behaviour of some elements during fractional crystallization of magma. Geochim. Cosmochim. Acta. 30. p. 267.

Osborn, E. F. (1969): The complementariness of orogenic andesite and alpine peridotite. Geochim. Cosmochim. Acta. 33. p. 307.

Póka, T. (1968): An undifferentiated stratovolcanic marginal facies of the Intra-Carpathian volcanic girdle. (Cserhát Hills, Northeast Hungary) Ann. Univ. Sci. Budapest. Sec. Geol. 12. p. 37.

Ruegg, N. B. (1964): Use of the angle A_1/c in optical determination of the composition of the augite. Amer. Miner. 49.

Simpson, E. S. W. (1954): On the graphical representation of differentiation trends in igneous rocks. Geol. Mag. 16.

Szádeczky – Kardoss, E. (1955): Geochemistry. Budapest. (in Hungarian)

Szádeczky – Kardoss, E. (1968): The structure and evolution of the Earth. Budapest. (in Hungarian)

Szmirnova, N. P. – Neszterenko, G. V. – Almuhamedov, A. I. (1968): O formah nazdenija nikelja i kobalta v osnovnih prodah. Geohimija (1968) p. 411.

Taylor, S. R. – Kaye, M. et al. (1969): Genetic significance of Co, Cr, Ni, Sc and V content of andesites. Geochim. Cosmochim. Acta. 33. p. 275.

Varga, Gy. (1964): The microandesite and its alterations of the Western Mátra Hills. MÁFI Évi Jel. (1964). (in Hungarian)

Vendl, A. (1932): On the pyroxene andesites of the Cserhát Hills. Mat. Term. Tud. Ért. p. 504. (in Hungarian)

Vinogradov, A. P. (1962): Srednie soderzanija himiceskih elementov. Geohimija (1962). p. 555.

РОЛЬ ПРИЛИВНОЙ ДИССИПАЦИИ ЭНЕРГИИ В ТЕРМИЧЕСКОЙ ИСТОРИИ ЛУНЫ

by
B. BODRI
(Geophysical Institute of Loránd Eötvös University Budapest)
(Received: 15th March, 1972)

SUMMARY

The review deals with the role of the tidal heating in the thermal history of the Moon in the light of results from dating measurements of lunar rocks. Formation of Apollo II basalts by partial melting 3.7 billion years ago was probably the result of high initial temperature of the Moon due to the tidal heating. The results of recent computations of evolution of the moon's orbit and the past tidal heating of the Moon due to tidal friction in the interiors of the Earth and the Moon are discussed. The initial lunar orbit should have been much closer to the Earth than at present and its tidal heating was much greater, if the dissipation of tidal energy in the lunar interior was greater than a definite limit. The quantitative relations are illustrated in the from of graphs. The character of the lunar orbit in the past and the rate of tidal dissipation in the lunar interior is evidence in favour of the early magmatic history for the Moon.

До последнего времени наиболее распространенным вариантом термической истории Луны был вариант подробно разработанный Левиным (1963), Левиным и Маевой (1960), а также Urey (1957, 1959, 1960, 1962). Немалый вклад в изучение тепловой истории Луны внесли также McDonald (1959, 1961, 1962, 1963), Fricker (1967), Iriyama и Shimazu (1967).

Этот вариант максимально учитывал процессы формирования и дальнейшего развития Луны как спутника Земли. Эти авторы полагали, что образование Луны относится к началу формирования планетной системы, по расчетам Левина (1966), возраст Луны, приблизительно, на 10^8 лет меньше возраста Земли. Эти авторы считали также, что образование Луны произошло в околоземном рое спутниковых тел. При формировании Земли из различных тел и частиц, их неупругие столкновения приводили к тому, что осколки и обломки этих тел могли оказаться движущимися по эллиптическим орбитам вокруг Земли и образовать, так называемый, околоземной рой. По расчетам Сафронова (1969) наибольшие из этих тел имели около 100 километров в поперечнике. Таким образом, с космогонической точки зрения, наиболее вероятной является гипотеза первоначально „холодной" Луны, которую и принимают во внимание обычно при расчетах тепловой истории Луны. Что касается гипотезы о первоначально „расплавленном" состоянии Луны, на которой основаны тепловые расчеты ряда авторов, например, McDonald (1959, 1961), то против

нее можно выдвинуть очень серьезные космогонические и геофизические возражения (Левин, 1962).

Самый распространенный метод определения температуры Луны основан на решении уравнения теплопроводности. Если в среде есть ненулевой градиент температуры, то в ней происходят процессы переноса тепла, приводящие к выравниванию температуры. Как механизм такого переноса обычно берется обычный механизм теплопроводности в твердых телах. Второй механизм, а именно, конвекция, когда нарушается механическое равновесие тела и происходит не только перенос тепла, но и перенос вещества, для Луны не рассматривают.

Уравнение теплопроводности в случае Луны имеет вид:

$$c_p \varrho \frac{\partial T}{\partial t} = \frac{1}{r^2} \frac{\partial}{\partial r} \left(\varkappa r^2 \frac{\partial T}{\partial r} \right) + F(r, t), \qquad (1)$$

где c_p – теплоемкость вещества Луны, ϱ – его плотность, T – температура, t – время, $\varkappa$ – коэффициент теплопроводности, F – генерация тепла, тепловыделение, r – текущий радиус Луны.

Уравнение (1) составлено в пренебрежении температурными деформациями для сферически-симметричной Луны. При расчетах тепловой истории граничное условие обычно выбирается в виде:

$$T(R_A, t) = 0^\circ \mathrm{C} \qquad (2)$$

для всех моментов времени. Здесь R_A – радиус Луны.

Сложнее задать начальное условие. Под начальным распределением температуры $T(r, 0)$ подразумевается то распределение, которое установилось к концу формирования Луны как небесного тела. Полагают, как я уже говорил выше, что этот процесс длился 10^8 лет (Левин, 1966; Сафронов, 1969). Эта температура определяется следующими основными источниками:

1. Удары падающих тел.
2. Радиогенное тепло.
3. Химические процессы.
4. Сжатие вещества под давлением прибавляющихся сверху слоев.
5. Приливный нагрев.

Очевидно, что вклад каждого из этих источников далеко не равноценен. Сжатие вещества, вероятно, внесет малый вклад в начальную температуру Луны из-за малых давлений внутри Луны. Разогрев из-за ударов падающих тел существенно зависит от принятой гипотезы образования Луны, но он, конечно, намного меньше, чем в случае Земли. Скорее всего, этот источник тоже пренебрежимо мал (Сафронов, 1958). Вклад тепла химических реакций оценить практически представляется невозможным. Влияние на начальную температуру Луны радиоактивных источников тепла зависит почти целиком от их периода

полураспада. Роль короткоживущих изотопов скорее всего окажется несущественной (Birch, 1965; McDonald, 1957).

Из всего вышесказанного видно, с какими большими трудностями сталкивается определение начальной температуры Луны. Однако большинство авторов полагают, что не считая приливного нагрева, наибольший вклад в начальную температуру Луны внес второй источник. Например, Левин и Маева (1960) в своих расчетах брали начальную температуру Луны в виде:

$$T(r,t) = 273 + T(0,\tau)(1 - r^2/R_\Lambda^2), \text{°K} \qquad (3)$$

Здесь $\tau = 2 \cdot 10^8$ лет. Причем, они предполагали, что за время τ тепло выделялось только долгоживущими радиоактивными изотопами. Их вклад в момент $t = 0$ обычно определяется по формуле:

$$F = \bar{\varrho} \sum_{i=1}^{n} Q_i p_i e^{\lambda_i (t^* - t)} = \sum_i F_{i0} e^{-\lambda_i t} \qquad (4)$$

где Q_i — количество тепла, выделяемое 1 г i-го изотопа в 1 сек, p_i — содержание i-го изотопа, $\bar{\varrho}$ — средняя плотность Луны, λ_i — постоянная распада i-го изотопа, $F_{i0} = \bar{\varrho} Q_i p_i e^{\lambda_i t^*}$ — генерация тепла $4{,}5 \cdot 10^9$ лет назад.

Положив $F = \text{const}$ за τ, определяем температуру в центре Луны. В других работах брались другие варианты начальных температур. О влиянии начальных условий на последующее распределение температуры в Луне я расскажу ниже.

Что касается содержания долгоживующих радиоактивных элементов, то вначале оно предполагается постоянным во всем объёме Луны, а числовые значения я привожу в табл. 1. Такое содержание их соответствует примерному содержанию радиоактивных элементов в хондритах. Параметр m в табл. 1 — это параметр, меняющийся от 0 до 5.

Таблица 1

Содержание радиоактивных элементов в хондритах (г/г).

Table I. The concentration of the radioactive elements in chondrits (g/g).

Элементы	Левин	Urey	McDonald
U	$m \cdot 10^{-8}$	$1.14 \cdot 10^{-8}$	$1.1 \cdot 10^{-8}$
Th	$4m \cdot 10^{-8}$	$3.36 \cdot 10^{-8}$	$4.4 \cdot 10^{-8}$
K^{40}	$0.091 \cdot 10^{-6}$	$0.1 \cdot 10^{-6}$	$0.096 \cdot 10^{-6}$

При расчетах тепловой истории Луны учитывается вклад только этих радиоактивных элементов, так как они, во-первых, достаточно широко распространены, во-вторых, выделяют достаточно большую

энергию, в-третьих, их период полураспада $\sim 10^9$ лет, что равно порядку возраста солнечной системы.

Одним из важных вопросов при решении уравнения теплопроводности является также вопрос о значении параметров $\varkappa$, ϱ, c_p. Если их принимать переменными во всем объеме среды, то уравнение (1) не имеет аналитического решения. Для его решения применяются численные методы.

Перейдем к обсуждению результатов решения уравнения теплопроводности для Луны, полученных различными авторами. На рис. 1, 2 представлено распределение температуры по U r e y (1962) для первоначально „холодной" Луны при коэффициенте температуропроводности χ соответственно 0,01 и 0,005. Здесь $\chi = \varkappa/c_p\varrho$. Оценку температуры плавления силикатной смеси в ходе тепловой истории U r e y проводил по формуле:

$$T_H = 1000 + 500\,(1 - r^2/R_\Lambda^2)$$
$$T_K = 1600 + 200\,(1 - r^2/R_\Lambda^2), \text{ где} \qquad (5)$$

T_H и T_K, соответственно, температуры начала и конца плавления, r — текущий радиус Луны.

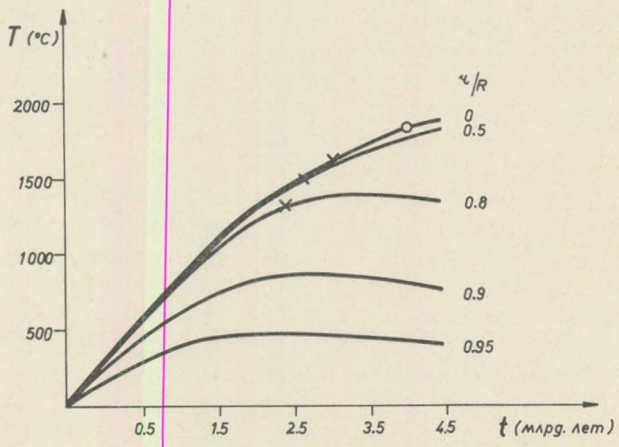

Рис. 1. Распределение температуры для первоначально холодной Луны по расчетам U r e y (1960) при $\chi = 0{,}01$.

Fig. 1. Heating curves for the initially cold moon according to U r e y (1960), $\chi = 0.01$.

Области неполного расплавления отмечены на рисунках крестиками, полного — кружочками. При обоих χ частичное плавление наступает на разных глубинах но приблизительно в одинаковое время $t =$ = 2,5 млрд. лет.

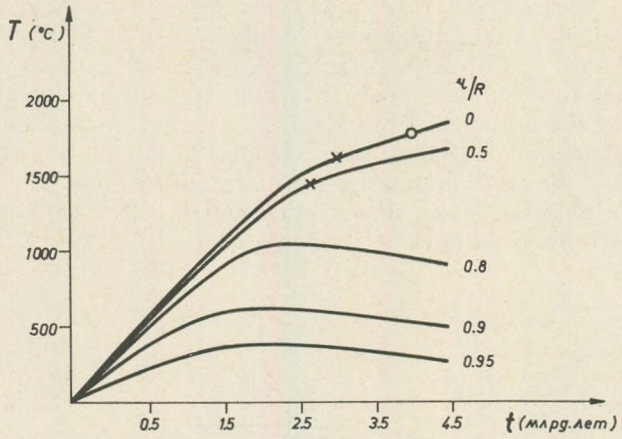

Рис. 2. Распределение температуры для первоначально холодной Луны по расчетам Урея (1960) при $\chi = 0{,}005$.

Fig.2. Heating curves for the initially cold moon according to Urey (1960a), $\chi = 0.005$.

Здесь следует отметить, что с началом плавления в недрах Луны должна была начаться дифференциация вещества по плотности и химическому составу, которая привела бы к началу конвективного переноса тепла и к переносу радиоактивных источников к поверхности Луны. Как известно, окислы радиоактивных элементов являются примесями, снижающими температуры плавления силикатного вещества. Поэтому они попадают в легкие расплавы и вместе с ними выносятся кверху. Попытка учесть эти процессы, которые чрезвычайно сложны и плохо изучены, была сделана Левиным и Маевой (1960), а также McConnell и другими (1967). Если эти процессы действительно происходили в недрах Луны, то, как отмечают эти авторы, после стадии разогревания Луны должна была начаться стадия ее охлаждения. Однако, очевидно, на время начала магматической дифференциации учет этих процессов существенно не повлияет.

McDonald (1959, 1961, 1962a, 1962b) также расчитал несколько вариантов тепловой истории Луны, причем с учетом зависимости теплопроводности от температуры. Его результаты примерно аналогичны результатам Урея.

Наиболее подробный анализ тепловой истории Луны был проведен Левиным и Маевой (1960), Левиным (1963, 1966) и Маевой (1964). Их расчеты основывались на очень разных исходных данных, хотя качественный характер полученных ими результатов был приблизительно одинаков. Во всех расчетах они использовали модель первоначально холодной Луны с равномерным распределением радиоактивных элементов. Ими также учитывалась зависимость теплопро-

водности от температуры. Температуры плавления вещества Луны расчитывались по модифицированной кривой плавления дунита. На рис. 3, 4 представлены результаты их вычислений для двух вариантов начальных данных. Из них видно, что при средней начальной температуре 400—500°К примерно через 1,8—2 млрд. лет большая часть Луны была расплавленной. Твердая кора имела, в зависимости от модели, толщину 300—500 км. Различия в содержании радиоактивных элементов на время расплавления, как выяснилось, почти не влияли, а изменяли лишь толщину коры.

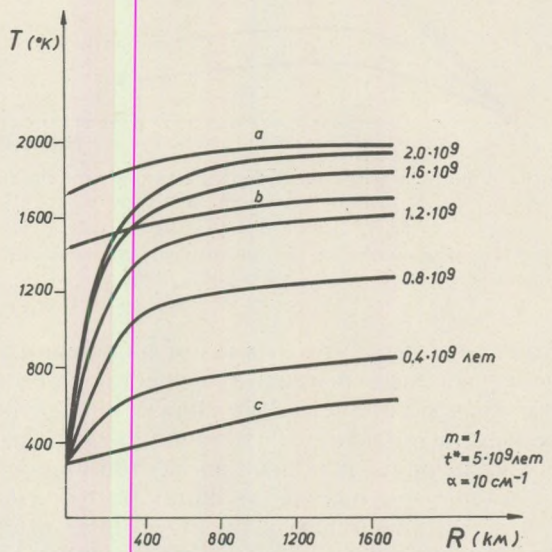

Рис. 3. Распределение температуры внутри Луны на стадии разогревания по расчетам Левина и Маевой (1960) при средней начальной температуре 410°К

Fig. 3. The temperature distribution within the moon at the heating stage for mean initial temperature 410°K Levin and Maeva, 1960).

Таким образом, используя первоначально холодную модель Луны, ряд авторов пришли к примерно одинаковым временам начала дифференциации, 2,5—2 млрд. лет после формирования Луны. Надо сказать, что до последнего времени этот вариант термической истории Луны не вызывал сомнений. Но в связи с определением возраста лунных базальтов потребовалось отодвинуть время начала магматической дифференциации на 1—1,5 млрд. лет в прошлое. В табл. 2 собраны данные по определению возраста камней, привезенных Аполлоном 11 и Аполлоном 12. Химический состав материалов лунной поверхности, а также их возраст от 4,4 до 4,7 млрд. лет, указывает на ранее начало магматической дифференциации в Луне.

Какие возможности изменения термической истории Луны мы имеем? Очевидно, что сильно изменить концентрацию долгоживующих радиоактивных элементов не представляется возможным. Расчеты Маевой (1964) для моделей Луны с приблизительно хондритовым составом радиоактивных элементов при учете переноса радиоактивных источников к поверхности Луны, приведенные в табл. 3, дают современные тепловые потоки через поверхность Луны по порядку совпадающие с теми, которые получены Кротиковым и Троицким (1963) при радиоастрономических наблюдениях Луны на различных волнах. В табл. 3 q — тепловой поток, ε — коэффициент поглощения, m_H — параметр, аналогичный параметру m табл. 1, но после дифференциации радиоактивных элементов в недрах Луны.

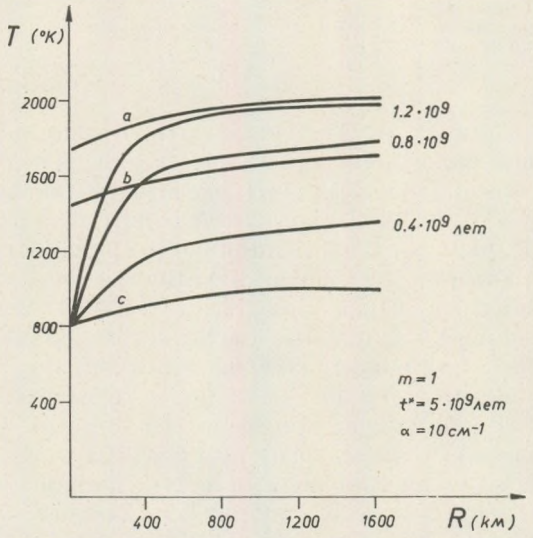

Рис. 4. Распределение температуры внутри Луны на стадии разогревания по расчетам Левина и Маевой (1960) при средней начальной температуре 900°К.

Fig. 4. The temperature distribution within the moon at the heating stage for mean initial temperature 900°K (Levin and Maeva, 1960).

Небольшое же изменение содержания радиоактивных элементов (табл. 1), как показали расчеты Левина и Маевой (1960), на время начала магматической дифференциации практически не влияет.

Зато представляется возможным изменить среднюю начальную температуру Луны путем учета приливной диссипации энергии системы Земля-Луна. Как показали расчеты Маевой (1964), рис. 4, стоит поднять среднюю начальную температуру Луны на 500°, чтобы частичное расплавление началось уже через 0,8—1,2 млрд. лет после завер-

Таблица 2

^{87}Rb – ^{87}Sr возрасты камней, приведенных Аполлоном 11 и Аполлоном 12.

Table 2. ^{87}Rb – ^{87}Sr ages of Apollo 11 and Apollo 12 samples.

Камни	Возраст (млрд. лет)	Камни	Возраст (млрд. лет)
Тип А	3.88[a]	10085 Luny 1	4.45[a]
Тип В	4.7[a]	12013	4.52[b]
Почва	4.59[a]	12002 12051	4.52[c]
Брекчия	4.27[a]	12070	4.37[c]

a – возрасты по Papanastassiou и др. (1970), *b* – возрасты по Albee и др. (1970), *c* – возрасты по Papanastassiou, Wasserburg (1970).
a – Papanastassiou et al. (1970), *b* – Albee et al. (1970), *c* – Papanastassiou and Wasserburg (1970).

шения формирования Луны. Следует сказать, что мысль о возможности значительного приливного нагрева в прошлом была высказана U r e y больше 10 лет назад (1959). Первые расчеты приливной диссипации принадлежат K o p a l (1963). Но в этой работе K o p a l взял слишком формальную модель Луны, состоящей из жидкости с Ньютоновской вязкостью, которая дает максимальный эффект. С его результатами вряд ли можно согласиться. Еще K a u l a (1964) отмечал, что K o p a l сильно завысил радиальные смещения поверхности Луны под действием земного приливообразующего потенциала. При тепловыделении, расчитанном K o p a l, Луна должна была нагреться более, чем на 1000 °K только за счет приливов, что заметно изменило бы ее термическую историю. Кроме того, K o p a l не учел того влияния, которое оказывает диссипация энергии в Луне на изменение ее орбиты.

В данной работе проведен анализ приливного нагрева Луны. При расчетах я пользовался анализом M c D o n a l d (1964) для раз-

Таблица 3

Тепловой поток из недр Луны по Маевой (1964).

Table 3. The heat flow from the interior of the Moon, Maeva (1964).

m_H	0.2				0.8			
ϵ, $см^{-1}$	10		40		10		40	
m	1	2	1	2	1	2	1	2
q кал/см² сек	0.37	0.46	0.35	0.45	0.34	0.44	0.32	0.41

личных моделей Луны, предложенных Harrison (1963) и ряда углов запаздывания. Луну считал сферически-симметричным телом постоянной массы, орбиту ее — Кеплеровским эллипсом, причем пренебрегал наклонностью орбиты Луны к плоскости земного экватора, что довольно упростило расчеты. В разложении приливного потенциала пренебрегал членами порядка выше второго, так как согласно предварительному подсчету, даже второй член разложения составляет не более 2% величины первого. Кроме того, пренебрегал изменением осевого вращения Луны, а считал, что период вращения Луны вокруг оси всегда совпадал с периодом ее обращения вокруг Земли. Это предположение вполне оправдано, так как согласно Парийскому (1960) торможение осевого вращения Луны требует в 10^3-10^4 раз меньших промежутков времени, чем занимает приливная эволюция ее орбиты.

Согласно McDonald (1964), средняя скорость изменения большой полуоси лунной орбиты и ее эксцентриситета выражается следующими формулами:

$$\frac{\overline{da}}{dt}=\frac{2A}{\mu^{1/2}a^{11/2}(1-e^2)^6}\left\{-[(3\cos^2\delta-1)+D]\left[\frac{3}{2}\sin\delta\,e^2+\right.\right.$$
$$+\left(\frac{3}{4}\sin\delta+\frac{3}{4}\sin 2\delta\right)e^4+\left(\frac{3}{32}\sin\delta+\frac{1}{32}\sin 3\delta\right)e^6\Big]+$$
$$+\frac{2}{\pi}q'F(q)\sin 2\delta\left[1+\left(3+\frac{9}{2}\cos\delta\right)e^2+\left(\frac{9}{4}+\frac{9}{4}\cos\delta+\right.\right.$$
$$\left.\left.+\frac{9}{8}\cos 2\delta\right)e^4+\left(\frac{9}{32}\cos\delta+\frac{1}{32}\cos 3\delta\right)e^6\right]\Big\}, \tag{6}$$

$$\frac{\overline{de}}{dt}=\frac{A}{\mu^{1/2}a^{13/2}(1-e^2)^5}\left\{-[(3\cos^2\delta-1)+D]\cdot\left[\frac{3}{2}e\sin\delta+\right.\right.$$
$$+\left(\frac{3}{4}\sin\delta+\frac{3}{4}\sin 2\delta\right)e^3+\left(\frac{3}{32}\sin\delta+\frac{1}{32}\sin 3\delta\right)e^5\Big]+$$
$$+\frac{2}{\pi}F(q)q'\sin 2\delta\left[\left(\frac{5}{2}+3\cos\delta\right)e+\right.$$
$$+\left(\frac{15}{4}+\frac{27}{8}\cos\delta+\frac{9}{8}\cos 2\delta\right)e^3+$$
$$\left.\left.+\left(\frac{9}{32}+\frac{3}{8}\cos\delta+\frac{1}{32}\cos 3\delta\right)e^5\right]\right\}, \text{ где} \tag{7}$$

A и D выражаются формулами:

$$\begin{cases} A = \dfrac{3}{2} GmR_3^5 K_2 \\ D = 2\dfrac{K_{\mathbb{C}2}}{K_2}\left(\dfrac{M}{m}\right)^2\left(\dfrac{R_л}{R_з}\right)^5, \end{cases} \tag{8}$$

где

G — гравитационная постоянная, m — масса Луны, M — масса Земли, $R_л$ — радиус Луны, $R_з$ — радиус Земли, k_2 — число Лява для Земли, $k_{\mathbb{C}2}$ — число Лява для Луны, a — большая полуось лунной орбиты, e — ее эксцентриситет, δ — угол запаздывания наблюдаемого прилива по отношению к статическому приливу, который имел бы место для идеально упругой Земли. Угол запаздывания для Луны, вслед за многими авторами, я считал равным углу запаздывания для Земли. $F(q)$ — эллиптический интеграл первого вида:

$$F(q) = \int_0^{\pi/2} \frac{d\varphi}{(1-q^2\sin^2\varphi)^{1/2}}, \tag{9}$$

где

$$q^2 = (\sin^2\epsilon)/(1+\alpha^2-2\alpha\cos\epsilon), \tag{10}$$

$$q'^2 = 1-q^2,$$

$$\alpha = n/\Omega,$$

причем

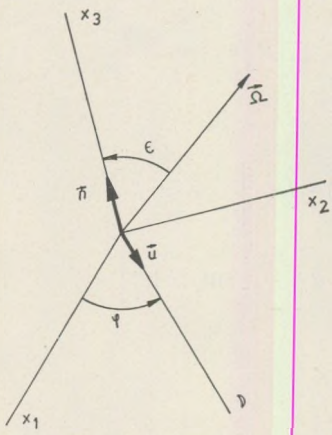

Рис. 5. Координатная система, которая обычно используется для описания движения Луны.
Fig. 5. The Coordinate system used to describe the Moon's motion.

n — угловая скорость обращения Луны по орбите, Ω — скорость углового вращения Земли, $\epsilon = 90° - \beta$, где β — наклон оси вращения Земли к ее экватору, φ — угол между направлением на восходящий узел лунной орбиты и Луной. Координатная система, которая обычно используется для описания движения Луны, представлена на рис. 5, гед $\{x_1, x_2, x_3\}$ — правовинтовая координатная система, причем, $\vec{x}_1$ — направление на восходящий узел лунной орбиты, а $\vec{u}$ — единичный вектор, направленный к Луне.

Срденяя энергия, выделившаяся в Луне, отнесенная к единице массы Луны, выражается формулой:

$$\overline{\frac{dE}{dt}} = -\frac{3e^2 A\,\mu^{1/2}}{2a^{15/2}}[(3\cos^2\delta - 1) + D]\sin\delta. \tag{11}$$

Учет векового замедления вращения Земли производился по формуле Парийского (1960):

$$\frac{d\Omega}{dt} = -\frac{3}{2}\,\frac{K_2 G m^2 R_3^5}{J a^6}\sin 2\delta\,, \qquad (12)$$

где J – момент инерции Земли.

Числовые данные, использовавшиеся при расчетах, представлены в табл. 4.

Таблица 4

Числовые данные, использовавшиеся в данной статье при расчетах

Table 4. Numerical Data used in computations

Обозначения	CGS	Планетарные единицы
G	$6.67 \cdot 10^{-8}$	1
m	$7.35 \cdot 10^{25}$	0.0123
M	$5.977 \cdot 10^{27}$	1
R	$1.738 \cdot 10^{8}$	0.2725
R	$6.378 \cdot 10^{8}$	1
k_2	0.3	0.3
J	$0.487 \cdot 10^{10}$	0.3306
a	$3.84 \cdot 10^{10}$	60.23
e	0.0549	0.0549
n	$2.67 \cdot 10^{-6}$	$4.19 \cdot 10^{-4}$
Ω_0	$7.292 \cdot 10^{-5}$	$5.640 \cdot 10^{-2}$
β	66° 33′	66° 33′
c_p	10^7	$1.61 \cdot 10^{-5}$

Запаздывание максимума приливного выступа по отношению к тому моменту, когда Луна находится в перигее, приводит к уменьшению e и a со временем, то есть к обратному эффекту по сравнению с отклонением приливного горба в Земле от линии центров Земля-Луна. Обычно называют первое запаздывание месячным, а второе – суточным. Если бы не было месячного запаздывания на Луне, то вывод о том, что орбита Луны в прошлом была более круговой, был бы правилен. Но при большой диссипации энергии в Луне ход изменения e со временем может оказаться прямо противоположным. Конечно, если приведенные для компланарной с экватором модели расчеты можно экстраполировать на реальную орбиту Луны.

В данной работе я производил расчеты для различных моделей Луны и нескольких вариантов угла запаздывания. Данные, приведенные в книге Munk and McDonald (1960), по-видимому, подтверждают наличие для Земли в целом угла запаздывания порядка одного – двух градусов. Правда, в статье Парийского (1963) предлагается совершенно иная методика определения угла запазды-

вания, которая дает значительно большие его величины. Но соответствующие данные получены пока только для Европы и Азии, а значения угла запаздывания для Земли в целом по этой методике не определялось.

Первый из расчитанных вариантов — это модель насквозь твердой Луны с углом запаздывания $\delta = 2°.16$ и числом Лява $k_{\ell_2} = 0{,}02$. В этой модели вещество Луны считается довольно жестким, $K = 7{,}38 \cdot 10^{11}$ дин/см^2, где K — твердость. Такая жесткость характерна для твердого вещества мантии Земли, сжатого до гораздо больших давлений, чем вещество Луны. Этот вариант, рис, 6, 7 характеризуется довольно коротким временем приливной эволюции, составляющей около 2 млрд. лет. Наименьшее расстояние между Землей и Луной в начале приливной эволюции составляло около 4 радиусов Земли, что соответствует, по расчетам Р у с к о л (1963), плотной внутренней части околоземного роя. Эксцентриситет орбиты Луны в этом случае несколько возрастает. Нагрев Луны для этого варианта весьма незначителен. Он составляет лишь около 70° за первые $1-3 \cdot 10^6$ лет эволюции при расстоянии наибольшего сближения и резко уменьшается по мере отхода Луны на более удаленные орбиты. За последующие 1—2 млрд. лет Луна нагревается приливами менее, чем на 1°. Такой нагрев Луны не вносит существенных изменений в начальную температуру Луны и уж тем более не влияет заметным образом на время начала магматической дифференциации.

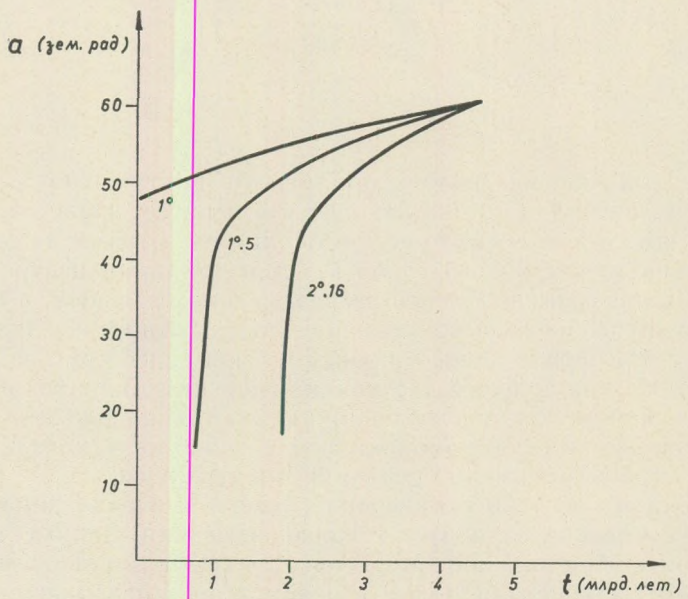

Рис. 6. Изменение расстояния Земля-Луна в прошлом при $k_{\ell_2} = 0{,}02$.
Fig. 6. The past variation of the earth-moon distance for $k_{\ell_2} = 0.02$.

Уменьшая угол запаздывания, мы получаем варианты с более продолжительным временем приливной эволюции, 3,5 млрд. лет для $\delta = 1.5°$ и 4,5 млрд. лет для $\delta = 1°$. Расстояние наибольшего сближения увеличивается, соответственно, до 10 и 46 земных радиусов. Возрастание эксцентриситета со временем делается все более незаметным. Точно так же, убывает и приливный нагрев. При угле запаздывания $\delta = 1.5°$

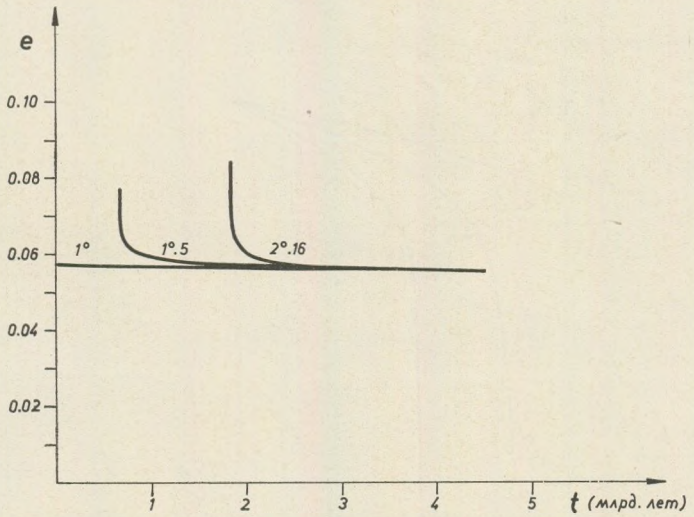

Рис. 7. Изменение эксцентриситета лунной орбиты в прошлом при $k_{(2} = 0{,}02$.
Fig. 7. The past variation of the eccentricity of the moon's orbit for $k_{(2} = 0.02$.

на расстоянии наибольшего сближения нагрев Луны за счет приливов составляет лишь 30° за первые 10° лет, а при угле запаздывания 1° нагрев за время всей эволюции составляет лишь 1°—2°, то есть выделение энергии не превышает современного. Качественный ход кривых изменения температуры Луны не зависит от угла запаздывания. Во всех этих случаях максимальный нагрев приходится на первые $1-3 \cdot 10^6$ лет приливной эволюции, то есть на то время, когда Луна находилась на ближайшем к Земле расстоянии.

Здесь следует заметить, что короткое время приливной эволюции отнюдь не означает подтверждения гипотезы захвата Луны, как полагали многие авторы, например, Urey (1960, 1962), McDonald (1964) и другие. Еще Левин (1962) высказал предположение, что затруднения с малостью шкалы времени приливной эволюции полностью разрешаются, если в расчетах учитывать увеличение угла запаздывания со временем. В самом деле, в Земле, когда она была еще холодной, диссипация энергии должна была быть меньше, чем теперь. Кроме того, роль морских приливов также уменьшалась в прошлое, так как вода лишь постепенно выделялась из недр Земли в ходе их ра-

зогрева. Правда, поведение угла запаздывания Луны во времени могло быть и более сложным в зависимости от ее термической истории. Во всяком случае, введением разумных предположений об изменении угла запаздывания приливов во времени, вероятно, можно затянуть шкалу времени приливной эволюции системы Земля-Луна до возраста этой системы и, возможно, несколько изменить шкалу приливного нагрева.

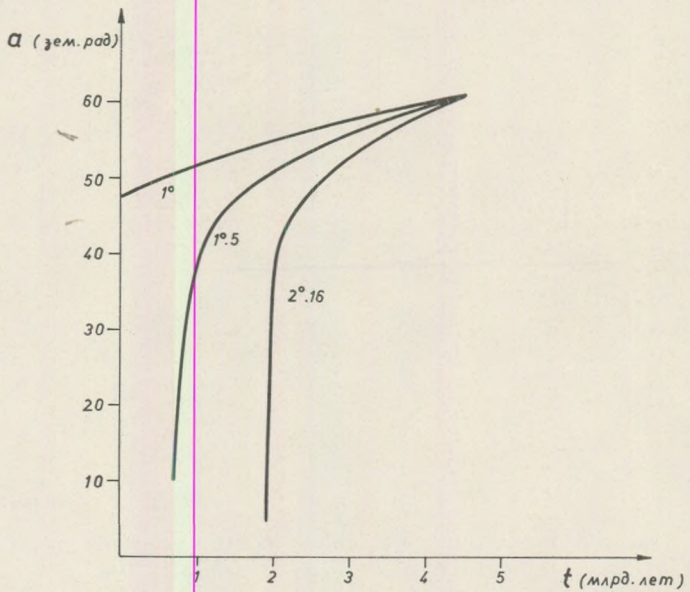

Рис. 8. Изменение расстояния Земля-Луна в прошлом при $k_{\ell_2} = 0{,}0384$.
Fig. 8. The past variation of the earth-moon distance for $k_{\ell_2} = 0.0384$.

Второй вариант расчетов представленный на рис. 8, 9, — это приливная эволюция модели с жидким ядром до половины радиуса и твердой оболочкой. Согласно Harrison (1963), вещество такой Луны при твердости $K = 4 \cdot 10^{11}$, то есть гораздо меньшей, чем в первом варианте, будет иметь число Лява $k_{\ell_2} = 0{,}0384$. Качественный ход кривых изменения элементов орбиты в этом случае сходен с предыдущим вариантом. Однако увеличение эксцентриситета лунной орбиты здесь более существенно, хотя при угле запаздывания $\delta = 1°$ эксцентриситет, как и раньше, почти не изменяется со временем. На изменение большой полуоси орбиты величина угла запаздывания влияет относительно меньше. Оба эти варианта дают обычное увеличение a с t. Единственным изменением является увеличение расстояния наибольшего подхода Луны к Земле. При угле запаздывания $\delta = 2°.16$ оно составляет около 12 радиусов Земли и 48 радиусов Земли при $\delta = 1°$. Приливный нагрев Луны в этом варианте несколько возрастает. При угле запаздывания $\delta = 2°.16$ он составляет около 100° за первые 10^6 лет эволюции.

Для $\delta = 1.5°$ – около 65° за то же время, и для $\delta = 1°$ – нагрев, как и в предыдущем случае, менее 1° за все время эволюции. Точно так же, как и раньше, не изменяется качественный ход кривых приливного нагрева: резкое возрастание температуры в первые $1 - 3 \cdot 10^6$ лет эволюции и практически не увеличивающаяся температура в последующие 4,5 млрд. лет.

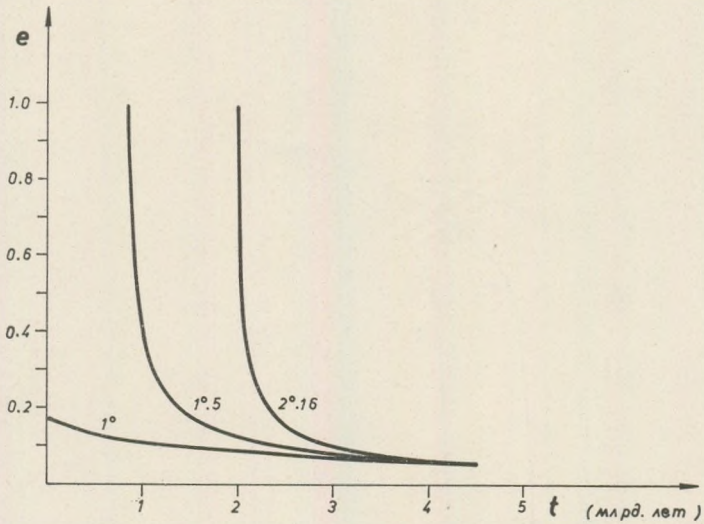

Рис. 9. Изменение эксцентриситета лунной орбиты в прошлом при $k_{\mathfrak{C}_2} = 0{,}0384$.
Fig. 9. The past variation of the eccentricity of the moon's orbit for $k_{\mathfrak{C}_2} = 0.0384$.

Третий и четвертый варианты расчетов, представленные на рис. 10 – 13, – это приливная эволюция моделей Луны со значительно менее твердым веществом, чем в предыдущих случаях. Согласно Harrison (1963), модель Луны с плотностью такой же, как и в двух предыдущих вариантах, $\bar{\varrho} = 3{,}34$ г/см³, то есть такой, какая обычно принимается для лунных пород, но твердостью значительно меньшей, $K = 2 \cdot 10^{11}$ дин/см², имеет число Лява $k_{\mathfrak{C}_2} = 0{,}0701$. Любопытно, что примерно равное число лява имеет модель с жидким ядром до 3/4 радиуса и твердой оболочкой с $K = 7{,}39 \cdot 10^{11}$ дин/см². Приливная эволюция в этом случае качественно не отличается от двух предыдущих. Большая полуось орбиты Луны так же увеличивается со временем, только расстояние наитеснейшего сближения увеличивается в этом случае при $\delta = 2°.16$ до 17 радиусов Земли, и до 14 земных радиусов при $\delta = 1°.5$. Вариант с углом запаздывания 1° не столь интересен, эволюция протекает крайне медленно при любых значениях числа Лява, расстояние наибольшего сближения никогда не делается меньше 48 радиусов Земли, что противоречит гипотезе образования Луны в околоземном рое. Приливный нагрев, независимо от числа Лява, составляет не более

1° – 2° за все время эволюции. Вероятнее всего, что угол запаздывания у Луны, по крайней мере, его среднее значение, было несколько выше.

Но при углах запаздывания 2°.16 и 1.5° Луна была нагрета на 497° и 588° соответственно за первый же 1 млн. лет эволюции, находясь на расстоянии наибольшего сближения. Такой нагрев, как я уже говорил выше, вполне достаточен для того, чтобы коренным образом изменить термическую историю Луны так, чтобы частичное расплавление началось уже 4,5 – 4 млрд. лет назад.

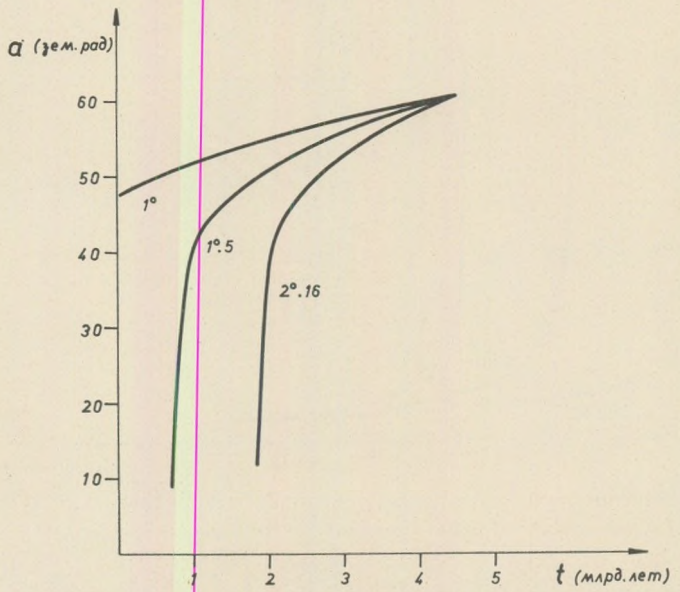

Рис. 10. Изменение расстояния Земля-Луна в прошлом при $k_{\mathfrak{C}_2} = 0{,}0701$.
Fig. 10. The past variation of the earth-moon distance for $k_{\mathfrak{C}_2} = 0.0701$.

Вариант четвертый, рис. 12 – 13, – это модель Луны с плотностью, как и обычно, $\bar{\varrho} = 3{,}34$ г/см³, но средней твердостью $K = 1{,}10^{11}$ дин/см², то есть, по Harrison (1963), числом Лява $k_{\mathfrak{C}_2} = 0{,}1381$, что в пять раз больше, чем для моделей первого варианта. Следует сказать, что модель с твердой оболочкой и жидким ядром более 3/4 радиуса при твердости $K = 7{,}38 \cdot 10^{11}$ дин/см² имеет такое же значение числа Лява. Качественно этот вариант похож на вариант приливной эволюции, расчитанный McDonald (1964) для другой модели Луны. С точки зрения изменения элементов орбиты этот вариант чрезвычайно интересен, так как при $\delta = 2.16°$, например представляет собой, если идти от прошлого к настоящему, резкое приближение Луны к Земле с сильно гиперболической орбиты, совершающееся за время порядка $\sim 10^5$ лет до минимального расстояния 43 земных радиуса, а потом, в течение следующих 2,5 млрд. лет, обычную приливную эволюцию до современ-

ного расстояния. Таким образом, за 2,5 млрд. лет, считая от настоящего к прошлому, Луна находилась на расстоянии, примерно, 200 радиусов от Земли и эксцентриситет ее орбиты был чуть меньше единицы, причем, продолжал увеличиваться.

При угле запаздывания $\delta = 1.5°$ приливная эволюция имеет тот же характер, с тем же расстоянием теснейшего сближения с Землей, лишь отход на гиперболическую орбиту становится более плавным и время приливной эволюции занимает около 3,5 млрд. лет.

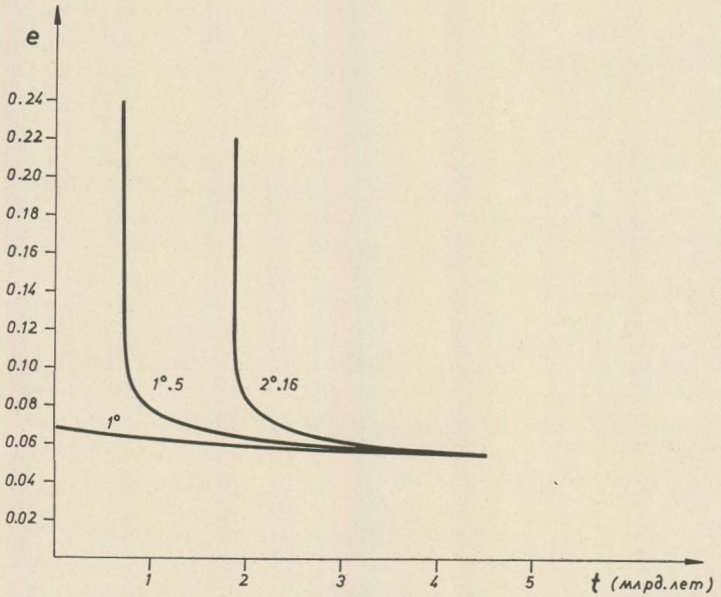

Рис. 11. Изменение эксцентриситета лунной орбиты в прошлом при $k_{\zeta_2} = 0{,}0701$.

Fig. 11. The past variation of the eccentricity of the moon's orbit for $k_{\zeta_2} = 0.0701$.

С точки зрения приливного нагрева этот вариант менее интересен, чем предыдущий. Правда, на минимальном расстоянии приливный нагрев довольно заметен, он составляет 180° при $\delta = 2°.16$ и 120° при $\delta = 1°.5$ за первые 10^6 лет приливной эволюции. Но серьезно изменить термическую истории Луны подобный нагрев, безусловно, не может, да и возник он только из-за наличия у Луны либо протяженного жидкого ядра, либо довольно малой твердости. McDonald (1964) интерпретирует этот вариант, как захват Землей готовой Луны. Но я полагаю, что если рассматривать изменение элементов орбиты и низкий приливный нагрев в совокупности с последними данными о ранней магматической дифференциации в недрах Луны, то приведенные расчеты являются, скорее, доводом против гипотезы захвата, так как

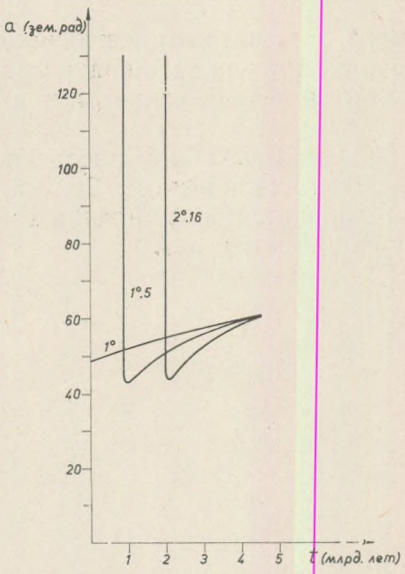

Рис. 12. Изменение расстояния Земля-Луна в прошлом при $k_{\mathbb{C}_2} = 0{,}1381$.

Fig. 12. The past variation of the earth-moon distance for $k_{\mathbb{C}_2} = 0.1381$.

при таком значении средней начальной температуры Луны раннее расплавление ее недр было невозможно.

Из приведенного анализа приливной диссипации энергии в Луне можно заключить, что даже при относительно небольших значениях диссипации энергии в Луне, то есть при угле запаздывания не более 2°, для ряда моделей Луны можно получить приливный нагрев в прошлом значительно изменяющий ее среднюю начальную температуру, а тем самым и термическую историю. Учитывая вклад приливного нагрева в начальную температуру Луны вполне можно согласовать при разумных предположениях о внутреннем строении Луны вычисленное и экспериментально определенное значение времени начала магматической дифференциации. Таким образом, представляется вполне возможным объяснить возрастлунных базальтов более высокой, чем полагали до сих пор, средней начальной температурой Луны, возник-

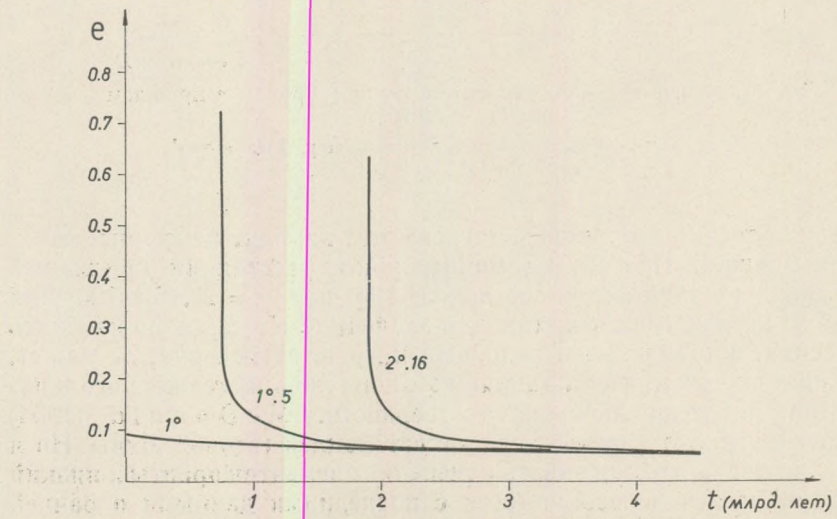

Рис. 13. Изменение эксцентриситета лунной орбиты в прошлом при $k_{\mathbb{C}_2} = 0{,}1381$.

Fig. 13. The past variation of the eccentricity of the moon's orbit for $k_{\mathbb{C}_2} = 0.1381$.

шей в результате диссипации энергии приливов. Кроме того, рассматривая совместно приливный нагрев и экспериментально определенные возрасты лунных базальтов можно выбрать довольно ограниченный класс моделей Луны, которые удовлетворяют обоим условиям вместе. Правда, поднимая значения диссипации энергии, что вполне возмож-

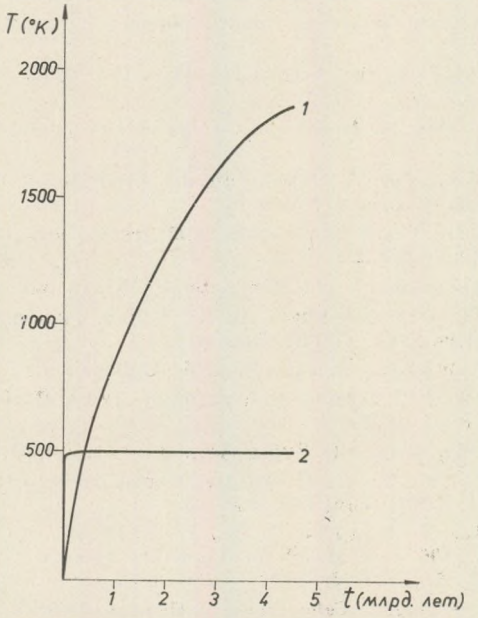

Рис. 14. Сравнение радиоактивного и приливного нагрева Луны.

1 — распределение температуры для первоначально холодной Луны при $\chi = 0{,}01$ и $r/R = 0{,}5$ (Urey, 1960).
2 — приливное нагревание Луны $\delta = 2°$. 16 и $k_2 = 0{,}0701$.

Fig. 14. The comparison of radioactive and tidal heating of the moon.

1 — heating curve for the initially cold mon for $\chi = 0{,}01$ and $r/R = 0{,}5$ according to U r e y (1960).
2 — tidal heating of the moon for $\delta = 2°$, 16 and $k_2 = 0{,}701$.

но, как я уже замечал при обсуждении работы П а р и й с к о г о (1963), можно получить несколько более широкий класс моделей с большей начальной температурой, вызванной диссипацией энергии приливов.

В заключение следовало бы сказать несколько слов о соотношении приливного и радиогенного нагрева. Как видно из рис. 14, последний сравнивается с приливным нагревом уже через $2-3 \cdot 10^8$ лет после начала приливной эволюции и уже через 1 — 2 млрд. лет значительно его превышает. Но на ранних этапах эволюции приливный нагрев, очевидно, вносит более существенный вклад в температуру Луны.

LITERATURE

Albee, A. L., Burnett, D. S., Chodos, A. A., Haines, E. L., Huneke, J. C., Papanastassiou, D. A., Podosek, F. A., Price, G. R., Wasserburg, G. J. (1970): Mineralogic and isotopic investigations on lunar rock 12013. Earth Planet Sci. Lett. Vol. 9.

Birch, F. (1965): Speculations on the Earth's thermal history Bull. Geol. Sci. Am. Vol. 76.

Джеффрис, Г. (1960): Земля, ее происхождение, история и строение. Перев. с англ. Москва.

Fricker, P. E. (1967): On the thermal history of the moon. Journ. Geophys. Res. Vol. 72. N. 10.

Harrison, I. C. (1963): An Analysis of the Lunar Tides. Journ. Geophys. Res. Vol. 68. N. 14.

Iriyama, J., Shimazu, Y. (1967): Internal structure of the Moon in the light of her thermal history. Icarus. Vol. 6. N. 3.

Kaula, W. M. (1964): Tidal dissipation by solid friction and resulting orbital evolution. Revs. Geophys. Vol. 2.

Kopal, Z. (1963): Convection in planetary interiors. Icarus. Vol. I.

Кротиков, В. Д., Троицкий, В. С. (1963): Радиоизлучение и природа Луны. Успехи физ. наук. Том 81. Вып. 4.

Levin, B. JU. (1962): La Physique des Planetés. Université de Liége. p. 39.

Левин, Б. Ю. (1963): О термической истории Луны. В сб. „Новое о Луне". Изд-во АН СССР.

Левин, Б. Ю. (1966): Строение Луны. Астрон. ж. Том 43. Вып. 3.

Левин, Б. Ю., Маева, С. В. (1960): Некоторые расчеты термической истории Луны. Докл. АН СССР. Том. 133. Вып. 3.

McConnell, R. K., McClaine, L. A., Lee, D. W., Aronson, J. R., Allen, R. V., (1967): A Model for Planetary Igneous Differentiation. Revs. Geophys. Vol. 5N. 2.

McDonald, G. J. F. (1959): Calculations on the termal history of the Earth. Journ. Geophys. Res. Vol. 64. N. 11.

McDonald, G. J. F. (1961): The interior of the Moon. Science. Vol. 133.

McDonald, G. J. F. (1962a): On the internal constitution of the inner planets. Journ. Geophys. Res. Vol. 67. N. 7.

McDonald, G. J. F. (1962b): The Moon and its interior. Astronautics. Vol. 7.

McDonald, G. J. F. (1964): Tidal friction. Revs. Geophys. Vol. 2. N. 3.

Маева, С. В. (1964): Некоторые расчеты термической истории Марса и Луны. Докл. АН СССР. Том 159. Вып. 2.

Мельхиор, П. (1968): Земные приливы. Перев. с англ. Москва.

Munk, W. H. McDonald, G. J. F. (1960): The Rotation of the Earth. Cambrige.

Papanastassiou, D. A., Wasserburg, G. J. (1970): Rb-Sr ages from the Ocean of Storms. Earth Planet. Sci. Lett. Vol. 8.

Papanastassiou, D. A., Wasserburg, G. J., Burnett, D. S. (1970): Rb-Sr ages of lunar rocks from Sea of Trankuillity. Earth Planet. Sci. Lett. Vol. 8.

Парийский, Н. Н. (1960): О влиянии земных приливов на вековое замедление вращения Земли. Астрон. ж. Том 37. Вып. 3.

Парийский, Н. Н. (1963): Земные приливы и внеутреннее строение Земли. Изв. АН СССР. Сер. геофиз. Вып. 2.

Рускол, Е. Л. (1963): О происхождении Луны. II. Рост Луны в околоземном спутниковом рое. Астрон. ж. Том 40. Вып. 2.

Сафронов, В. С. (1958): О росте планет земной группы. Вопросы космогонии. Том 6.

Сафронов, В. С. (1969): Эволюция допланетного облака и образование Земли и планет. Москва.

Urey, H. C. (1957): Boundary Conditions for Theories of the Origin of the Solar System. In "Physics and Chemistry of the Earth". N. 2.

Urey, H. C. (1960a): The origin and the nature of the Moon. Endeavour. Vol. 19. N. 87.

Urey, H. C. (1960b): Proc. of the first Int. Space Symp. North-Holland Publ. Comp. Amsterdam. P. 1114.

Urey, H. C. (1962): Origin and history of the Moon. In "Physics and Astronomy of the Moon". Ed. Z. Kopal. Acad. Press.

Urey, H. C., Elasser, W. H., Rochester, M. G. (1959): Note on the internal structure of the Moon. Astrophys. Journ. Vol. 129.

CONTRIBUTION TO THE GEOLOGY OF THE UPPER PALEOZOIC SEDIMENTS AT BAGA GAZRIN (CENTRAL GOBI AIMAK, MONGOLIA)

by
L. BOGNÁR* – A. MINDSZENTY**

(Received: 15th March, 1972)

SUMMARY

Sedimentological observations and general geological considerations made by the authors in 1970 – 71 on the Baga Gazrin Area (Central Gobi Aimak, Mongolia) are presented. On the basis of field- and laboratory work the Paleozoic sedimentary sequence is proved to be of flyschoid type. Graded – bedding, cross bedding, laminite- and turbidite textures were observed on the field. Mineralogical composition and grain size distrubution of the sediments at Baga Gazrin agree with those of the "old greywackes" described by Cummings (1962).

INTRODUCTION

The granite intrusion of Baga Gazrin is situated in the Central Gobi Highland about 60 km NE of Mandal Gobi in the N part of central Gobi Aimak. From the Geological poit of wiew the area concerned is part of the transition zone between the Caledonian and Late Hercinian – Early Mezozoic structures of the Central Mongolian Geanticline and the Mongol – Amur Folded Belt, respectively (Marinov, 15) (Fig. 1.).

The most characteristic feature of this transition zone is – according to Marinov – that the margins of the Caledonian basement, consolidated since Early Paleozoic time, became relatively mobile during the Late Hercyinian – Early Mezozoic development of the neighbouring Mongol – Amur geosyncline, too. On this mobile basement several small basins had formed with sediments generally very similar to those of the real geosynclinal regions: mostly of the molassoid type either continental or marine.

In the S foreland of the mountain 1:5 000-scale ore geological mapping and 1:32,000-scale exploration surveying were carried out in 1970 and 1971. General geological and sedimentological results of this work are presented here.

Previous work

General geological mapping was carried out between 1925 and 1953 by Russian geologists *(1–4)*, ore geological data are available since 1954/55, mainly in Russian exploration reports *(5–6)* In 1965/67 a Mongolian *(7)*, in 1968/69 two collective Mongolo-Hungarian and in 1970/71 two Hungarian teams *(10–11)* worked there. The suggestions of these expeditions concerning the geology of the area could be summarized as follows.

* Department of Mineralogy, L. Eötvös University, Budapest.
** Engineering Centre of the Hungarian Aluminium Corporation, Budapest.

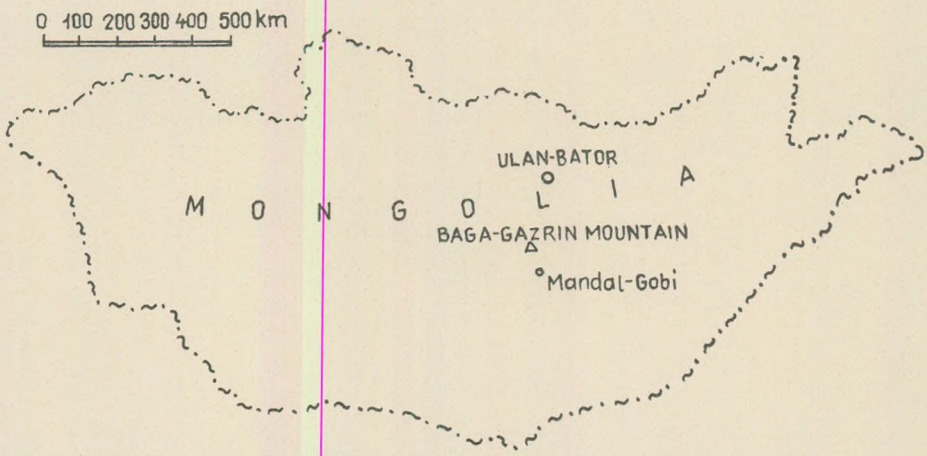

Fig. 1. General Sketch map of Mongolia with the exploration area of the expedition, 1970—71.

The sedimentary sequence surrounding the Baga Gazrin Mountain is of Upper Paleozoic age. According to B u j a n and M á t y á s *(9)*, it would be a geosyncline-type formation, deposited in a long narrow trough in the centre of which the Baga Gazrin granite would have been intruded in early Mesozoic time, in close connection with the geosynclinal development. Post-depositional folding and subsequent faulting took place both in the Paleozoic and the Mesozoic—Cenozoic. As to lithology, the sedimentary sequence seems to consist of fine- to coarse-grained sandstones, shales and conglomerates of various size of pebbles, as suggested by field observations. No paper on microscipic investigations has so far been published except for a few thin section descriptions of the 1969 exploration report by B u j a n and M á t y á s (9).

The lack of valuable fossils makes impossible the refinement of the above age estimation based mostly on petrological considerations. The authors took therefore the general term "Upper Paleozoic" as a valid age for their subsequent, non-stratigraphic, investigations.

Field observations

The authors had the 1 : 32 000-scale set of aerial photographs (1966) at their disposal as a basis for the field work. The well-bedded character of the sedimentary sequence and the consistence of the individual beds over a rather long distance (several km) could be readily proved by the aerial photographs.

1 : 5000 scale mapping was carried out in an area of about 5.5 km^2 immediately in the southern foreground adjacent to the Baga Gazrin Mountain, on the so-called Delger Ula.

On the field the following main rock types could be distinguished:

1. *Shale and mudstone* – dark grey, hard, rigid, mostly of unbedded character. On its light, weathered surface little dark mottles can be occasionally observed ("leopard spotted" variant).
2. *Medium-grained sandstone* – dark, light-grey, yellowishbrown, of medium hardness, bedded or unbedded. The weathered surface is rough, uneven. Within the unbedded-type, lense-shaped, clay pelletic horizons could be identified in some cases.
   The bedding is either of the graded- or of the laminite-type. In the first case it is due to changes in the grain size of the sediment. Wavy or oblique bedding planes, cross-bedding and turbidite textures are common here (Table I. and II.). The individual layers are 0.1 to 2.0 mm in thickness.
   In the laminite-type sandstone the bedding is due to changes in mineralogical composition (enrichment in micas) and/or in colour. The 0.1-mm-thick laminae are mostly parallel and alternate frequently. Wavy surfaces are somewhat less common here.
3. *Coarse-grained feldspar-containing tuffite* – light grey in colour, with characteristic white patches of coarse-grained feldspars in it. They have proved to be characteristic horizons of the sedimentary sequences here.

The whole sequence consists of these shales, fine- and medium-grained sandstones and tuffites, alternating at every 0.5 – 8.0 m. The transition from the medium-grained to the fine-grained laminite-type rock is mainly continuous: there is no discrete boundary between the two members of the sequence. The shale/medium- or coarse-grained sandstone boundary, on its turn, is always discrete.

Microscopic investigations

Sandstones (Paleozoic, Southern Area, surface samples)

These consist of medium-sorted sand-size crystal- and rock fragments cemented by small amounts of interstitial claysize matrix.

The crystal fragments of the sand fraction are predominantly those of quartz and feldspar (see Fig. 2.), subordinated biotite and muscovite with epidote, chlorite, chloritized amphibole, pyroxene, ilmenite, magnetite, zircon, topase, garnet, sphene and crystobalite as accessories. The most frequent feldspars are the plagioclases both of silicic and of intermediary semi-basic character, orthoclase and microcline being somewhat poorer.

The rock fragments are those of granite (graphic granite, aplite), diorite, quartz-porphyry, diorite-porphyry, andesite, diabase, sandstone, shale, sandy shale, fine-grained sandstone and sericitic shale. The effusive fragments are almost always strongly oxidized with a matrix altered into a reddish-brown ferruginous mass. Most of the sedimentary fragments (sandstones) were similarly affected by oxidative cementative pro-

cesses. Conversely, the intrusive and aplitic fragments are generally quite fresh or less altered.

The matrix consisting of clay-size crystal fragments is mostly impregnated by silica and/or iron oxide. Patch-like enrichment of calcite, chlorite, epidote or zeolite (wairakite) can be observed at some places, too.

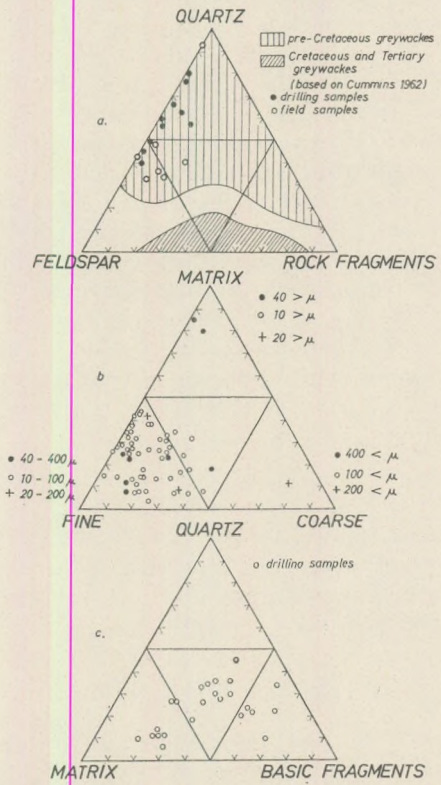

Fig. 2. Mineralogical composition (A, C) and grain-size distribution (B) of the Baga Gazrin sediments.

The almost total absence of matrix can be shown locally. In that case the grains are cemented by a tiny superficial ferruginous "glue" only and the whole phenomenon is accompanied by a decrease in the amount of the effusive fragments: the rock becomes an a r c o s e.

Dia- and epigenic changes in the sediment:

a) silification indicating the recrystallisation of the matrix,

b) formation of sericite and illite by post-depositional decomposition of the clay-size feldspars in the matrix,

c) epidotization, calcitization, zeolitization,

d) tiny (1 – 2 μm) ferruginous coating of the sand-grains indicating post-depositional iron mobilization, formation of small patches of crystalline or amorphous goethite in the matrix.

e) formation of siliceous fissure-fillings with fine-grained or well-crystallized quartz and/or mica.

Roundness – The crystal fragments are angular or – less frequently – subangular in all but a few cases. The rock fragments, however, are more or less rounded for the most part.

Shales (Paleozoic, Southern Area, surface samples). These consist of predominantly clay-size ([10 μm) crystal fragments cemented by a clayey silicic-sericitic matrix, locally with some epidote. Sand-size grains of quartz, plagioclase, opaque minerals, epidote and mica are rare but they could be identified in some cases. The extremely fine crystallites are supposed to be quartz, muscovite and feldspar.

Shales (Paleozoic, Southwestern Area, surface samples). These are quite similar to those of the Southern Area. The only difference is that in the samples of the SW Area (400 – 800 μm) elongated patches of sand-size consisting of sericite and chlorite, were observed. Certain regularity in the position of these patches can frequently be observed: the axes of the ovales have statistically the same orientation. The patches are characterized by a higher grain-size in and by a lower opaque content as compared to the "groundmass". Their quartz grains are of 3 – 4 and their muscovites of 30 – 40 μm size. The transition between the patches and the matrix is continuous.

On the basis of morphological considerations the sericite patches are supposed to be pseudomorphs post-feldspars quartz-mica. Siliceous and fluoritic veinlets are relatively common in the rocks here, mostly with associated goethite.

Dia- and epigenic changes in the sediments:

a) enrichment of epidote and calcite,

b) development of a sericite-patched texture,

c) siliceous-fluoritic impregnation, iron mobilization.

The sand-size feldspar grains deposited together with the clay-size crystal fragments had been disintegrated by post-depositional alteration ultimately into a sericitic-quartzitic aggregate, the grain-size of which agrees with that of the matrix, and so the present sericite-patched texture has developed.

Sandstone (Paleozoic, Delger Ula, borehole samples): 34 samples of the 76-m-deep exploratory drilling (No 32) were investigated in thin section. The mineralogical composition observed was essentially similar to that of the surface samples – with quartz and feldspar as main consitituents. Biotite and muscovite were also identified, although subordinately. In accessorial amounts epidote, chlorite, hornblende, zircon, apatite, cassi-

terite, opaque minerals, fluorite, garnet, calcite and topase were also present. No rock fragment of greater size could be found at all.

The matrix consists mainly of clay-size crystal fragments, of which only quartz, sericite and biotite could be recognized. Chloritic and calcitic cement also occurs and ferruginous impregnation is frequent.

Epigenic changes in the sediment: first of all, sericitization, calcitization, chloritization and somewhat lesser silification took place.

Roundness and texture: The crystal grains are angular or subangular. Oriented texture is rare. The above-mentioned sericite-patched feldspar-pseudomorphs are relatively common.

The mineralogical composition and grain-size distribution of the sandstones are illustrated by diagrams in Fig. 2. It turns out that there is a good agreement partly between the Baga Gazrin sediments and the "greywackes" of Dzulinsky—Walton and partly between the Baga Gazrin sediments and the so-called "old greywacke" class of Cummings by mineralogy and by grain-size distribution, respectively. The latter seems to confirm the supposed Paleozoic age of the sedimentary sequence.

Structure

Folded structural elements

On the Delger Ula the 2 to 8-m-wide outcrops strike more or less parallel, in ENE direction. They dip generally at 15°—30° in SSE direction. At the northern boundary of the granite intrusion the strikes turn first to the NE and than to the N. Having the supplementary eastern and northern aerial photographs adjacent to the Delger Ula the structure could be interpreted as a NE axes gentle anticline open to the W.

Somewhat farther to N and SW off the Baga Gazrin a heavy folding of the sedimentary sequence can be observed. The folds are generally sublinear, they could be interpreted in some cases even as brachyform fold-sequences. The orientation of the fold axes is mainly NE—SW. The one-time strain-conditions — as indicated by the above structural pattern — must have been at least partly tangential. (Fig. 3.).

Faulting

Faulting of the Delger Ula sandstone sequence took place after the folding. The surfaces or the NNE—SSW and EW shear joints are always plane.

The fissures due to dilatational forces are uneven and rough, however. The NS joints are mostly mineralized while in the EW joints the fillings are rare (Fig. 4.).

Relative movements along these fissures and joints could be readily proved by their horizontal component but no sufficient data about eventually vertical movements are available.

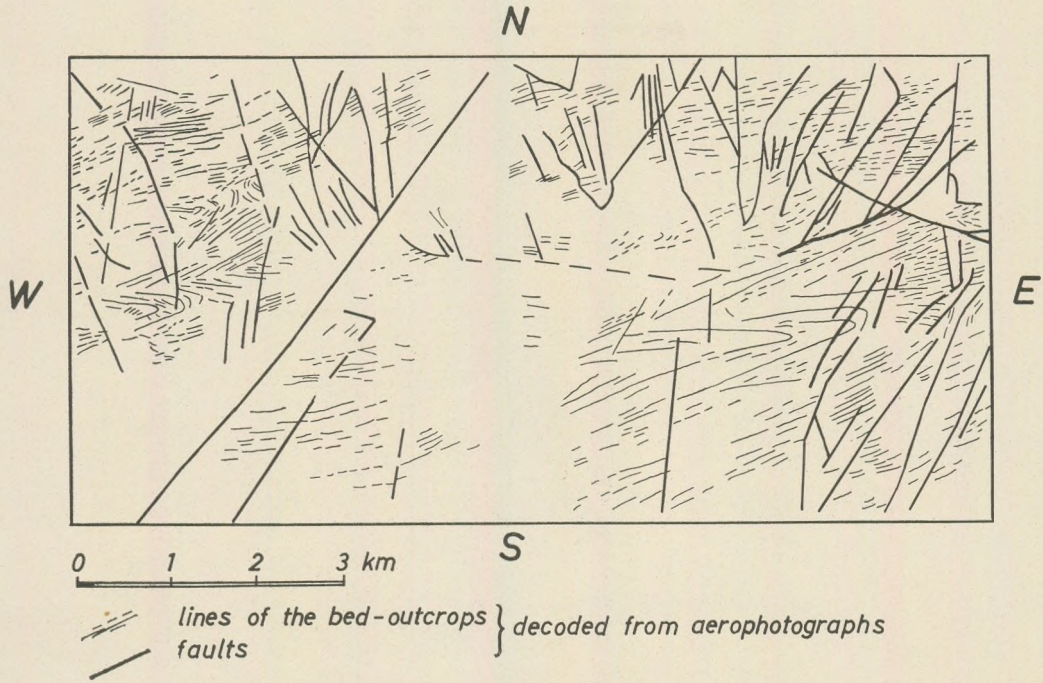

Fig. 3. Non-concentric folded structure in the Baga Gazrin sedimentary complex

Conclusions

The results of the authors, field- and laboratory investigations are summarized as follows:

The mineralogical composition grain-size distribution rhythmical structure (mega- and micro-rhytmus), relative persistence and the quite common laminite- and turbidite-textures suggest that the Baga Gazrin sedimentary rocks must be of the flyschoid type. This is confirmed by the quasi-linear folds indicating contemporaneous tangential movements in the sedimentary basin. The above statements suggest that the Baga Gazrin Upper Paleozoic sequence must have been deposited in one of those molasse-basins formed on the edges of the Central Gobi Highland in the late Paleozoic time in of much higher mobility than mentioned by Marinov et al. (15).

The presence of wairakite in several samples indicates a slight regional metamorphism due to tectonic movements.

Partly in the later phase of the folding and immediately after it the sedimentary sequence underwent a strong shear deformation. The resulting plane-surface joints and fissures are filled by the mineralization (ore veins and aplites) connected with the Baga Gazrin granite intrusion.

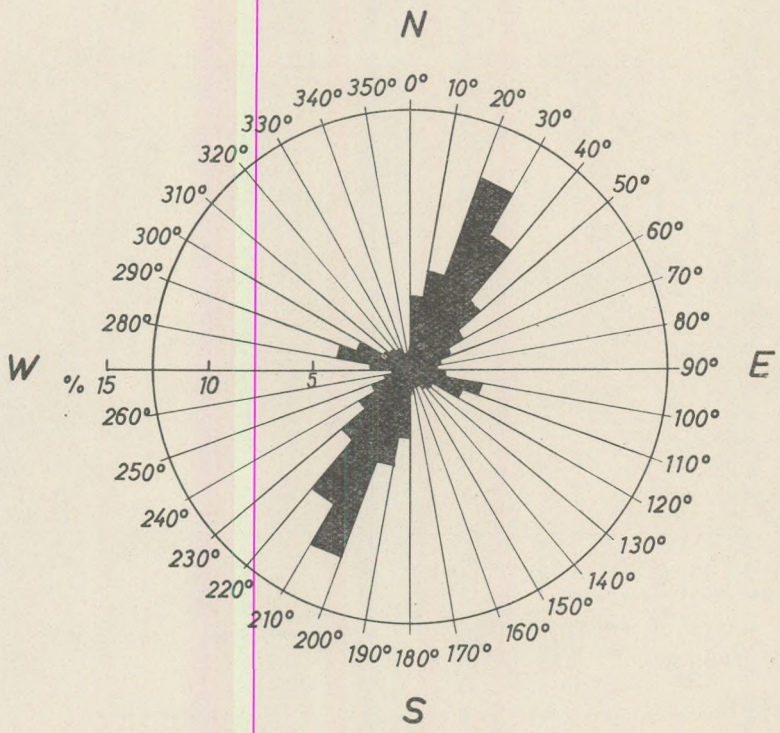

Fig. 4. Frequency distribution of the direction of cleavages

Consequently the granite must have been intruded *after* the folding when the sedimentary rock was already rigid.

The absence of contact-metamorphic alteration of the sandstone also suggest that the granite intruded into a consolidated sediment, the water-content of which had been almost completely lost before.

The obvious need for space of the intrusion resulted in a pulling strain that produced dilatational joints and fissures of always uneven surface. The amount of these is relatively smaller than those formed by shearing in connection with the folding.

After the igneous activity ceased, structural movements of lesser intensity took place, the result of which are the joints and fissures without mineralization. Their frequency is far lesser than that of the others mentioned before.

On the basis of the above considerations the suggestions of the literature concerning the Baga Gazrin Area are to be corrected as follows:

The small-size granitic body of the Baga Gazrin intruded into the flyschoid-type sediments *after* their folding had finished. The intrusion must have coincided not with the so-called geosynclinal (main-folding) but with the *orogenic* (uplift) phase of the development of the neighbouring geosynclinal area.

REFERENCES

Zselubovszkij, J. Sz. (1945): Geologiceskije strojenije i poleznije iskopajemije Centralnoj Chastyi Srednye Gobijskovo Ajmaka, M. N. R. Exploration report.

Makarov, P. A. – Pantjuhina, M. A. (1953): Geologija i poleznije iskopajemije Rajona Bajan Undur Somona i Delger-Han Szomona Undur Hangajskovo i Centralnovo Ajmakov, M. N. R. Expl. report.

Ponomarjova, N. I. – Vojenuskin, Sz. F. (1955): Geologija i poleznije iskopajemije Rajona Burun Ucszsul Somonov Centralnovo Ajmaka M. N. R. Expl. report.

Zosimovskij, N. M. – Kolosov, G. I. (1955): Objasnitelnaja zapiska k podscotu zapasov olova po Baga Gazrinskomu rossipnomu mestorozdeniju v Centralnoj Mongolii. Expl. report.

Ponomarjova, N. I. et al. (1956): Geologiceskoje strojenije Rajonov Delger-Cogtu i Uhtal Somonov, Sredne Gobijskovo Ajmaka M. N. R. Expl. report.

Makarov, V. A. et al. (1956): Geologiceskoje strojenije i poleznije iskopajemije Rajona rabot partii No. 222/223. Expl. report.

Bujan, Cs. et al. (1970): Exploration report on Baga Gazrin Area (1965 – 67).

Bujan, Cs. – Káposzta, J. (1969): Exploration report on tin-ore occurence at Baga Gazrin Csulu.

Bujan, Cs. – Dr. Mátyás, E. (1970): Final exploration report on prospects for occurences of tin-ore in 1965 – 69 at Baga Gazrin Mountain, Central Gobi Aimak.

Vörös, I. (1971): Exploration report of the Hungarian tin-ore prospecting Expedition in 1970.

Vörös, I. (1972): Final exploration report on prospects at Baga Gazrin Area, Central Gobi Aimak.

Ashgirej, F. (1963): Strukturgeologie, Berlin.

Szutyenko, O. D. (1970): Osnovnije certi Stratigrafii. Stratigrafija i tektonika M. N. R. Moskva.

Dzulinski, S. – Walton, E. K. (1965): Sedimentary features of flysch and greywackes. Elsevier, Amsterdam, London, New York.

Marinov, N. D. et al. (1967): Geologiceskije issledovanija M. N. R., Moskva.

TABLE I.

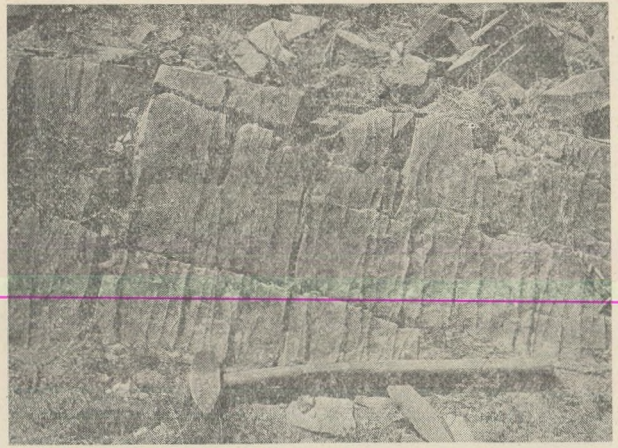

1.

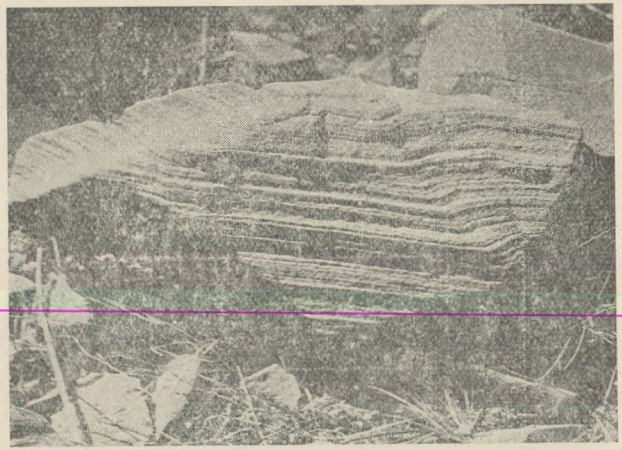

2.

3.

4.

1. Mineralized joints on the bedding plane of medium-grained sandstone, Delger Ula. 2. Fine-grained, laminated-type sandstone, Delger Ula. 3. Light and dark clay-pelletic sandstone, Delger Ula. 4. Turbidite texture on sandstone surface, Degler Ula.

TABLE II.

1.

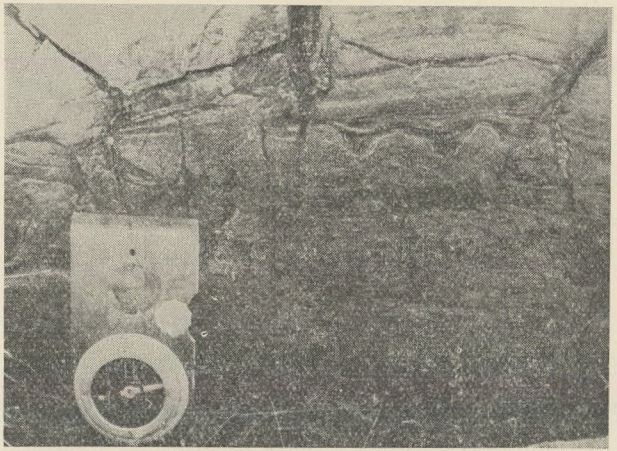

2.

3.

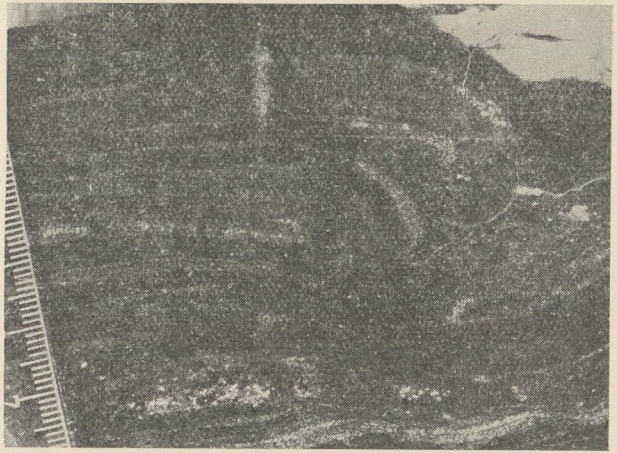

4.

1. Ripple load convolution in medium-grained sandstone, Delger Ula. 2. "Load structures" in medium-grained sandstone, Delger Ula. 3. "Sand-volcano"-type load structures in medium-grained sandstone, Delger Ula. 4. Turbidite-type sandstone (polished surface), Delger Ula.

ПОПЫТКА ОПРЕДЕЛЕНИЯ КРАЕВЫХ ЗНАЧЕНИЙ МЕСТОПОЛОЖЕНИЯ СРЕДНЕГО ЭНЕРГЕТИЧЕСКОГО УРОВНЯ ПО ВЫСОТЕ

М. М. ЧАСАР

(Кафедра метеорологии Университета им. Л. Этвеша, Будапешт)
(Поступила: 30. 3. 1972)

SUMMARY

In characterizing the climate of an area, particular role is ascribed to the daily, monthly or annual sums of the individual elements. The vertical distributions and statistical parameters of the individual elements of weather have been of particular importance for the investigations of the spatial and time structure of the climatic elements. An important information is obtained for the global review of the conditions of movement on the basic of the averages of the so-called integrated characteristics. In this paper the position and changes of the mean energetic level are examined as a function of vertical stability. In the final part of the paper the variation of the mean energetic level in dependence on the changes of the internal, potential, latent and kinetic energies is demonstrated.

В последние 15—20 лет значительно увеличился объём специальной литературы, касающейся результатов по определению структурных особенностей метеорологических элементов и полученных от них величин. Выяснилось, что некоторые элементы, принимая во внимание их пространственную и временную структуру, имеют характерные значения. Такие результаты статистической обработки обращают внимание специалиста на внутренние структурные особенности атмосферы, не безразлично, значит, открытие и диагностические изучение причинных взаимосвязей установленных таким образом особенностей. Результаты исследований необходимы для усовершенствования методов, применяемых при количественных прогнозах и для использования в метеорологии результатов измерений, производимых с помощью искусственных спутников, но определение их является основным и в других областях метеорологии.

При изучении атмосферных процессов в целях выбора граничных условий и установления функциональных зависимостей уже и раньше обратили особое внимание, например, на уровень ведущего потока, на уровень без дивергенции, на максимальное и минимальное значение вертикальных восходящих потоков и на краевые значения других производных величин. Одновременно с этим для глобального обзора условий движения атмосферных потоков определили и их средние значения.

Распределение этих параметров по вертикали даёт нужную информацию, в первую очередь, для определения места и управляющего характера атмосферных процессов.

В литературе энергетики атмосферных процессов считаются значительными результатами выводы, относящиеся к среднему энергетическому уровню, сделанные в книге Е. П. Борисенкова, вышедшей из печати в 1960 г. Одновременно с выделением этого уровня, Борисенков дал и его характеристику, и этим содействовал более глубокому познанию процессов, происходящих в тропосфере. С точки зрения энергетических взаимовлияний может представлять интерес изучение этого характерного уровня в зависимости от вертикальной устойчивости и связывание его изменений с погодными явлениями и энергетическими изменениями.

Потенциальная энергия единицы массы на высоте z следующая:

$$P = gz \tag{1}$$

а внутренняя энергия её определяется уравнением

$$I = c_v T\,, \tag{2}$$

где g – ускорение силы тяжести, T – температура на уровня z, c_v – удельная теплоёмкость при постоянном объёме.

Потенциальную и внутреннюю энергию элементарного объёма можно выразить так:

$$dP = gzdm \tag{3}$$

$$dI = jc_v Tdm \tag{4}$$

Потенциальная и внутренняя энергия единичного столба атмосферы, расположенного между уровнями с давлением p_1 и p_2 равняется:

$$P = \int_{z_1}^{z_2} gzdm \tag{5}$$

$$I = jc_v \int_{z_1}^{z_2} Tdm \tag{6}$$

где $j = 1/A$, – механический эквивалент теплоты. Используя уравнение статики и уравнение состояния газов, уравнения (5) и (6) будут иметь следующих вид:

$$P = \int_{p_2}^{p_1} zdp \tag{7}$$

$$I = \frac{jc_v}{g} \int_{p_2}^{p_1} Tdp \tag{8}$$

Если проинтегрируем уравнение (7) по частям, тогда потенциальная энергия единичного столба атмосферы, расположенного между уровнями с давлением p_1 и p_2 будет:

$$P = p_1 z_1 - p_2 z_2 + \frac{R}{g} \int_{p_2}^{p_1} T dp \tag{9}$$

Сложив (8) и (9), получим сумму потенциальной и внутренней энергии атмосферного столба, которая в специальной литературе часто называется „полной потенциальной энергией":

$$P + I = p_1 z_1 - p_2 z_2 + \frac{R}{g} \int_{p_2}^{p_1} T dp + \frac{jc_v}{g} \int_{p_2}^{p_1} T dp \tag{10}$$

Сложив последние два слагаемых правой части в формуле (10), получим следующий результат·

$$P + I = p_1 z_1 - p_2 z_2 + \frac{jc_p}{g} \int_{p_2}^{p_1} T dp \tag{11}$$

На поверхности Земли $z_1 = 0$, а на верхней границе атмосферы $p_2 = 0$. Отсюда полная потенциальная энергия столба атмосферы, простирающегося от поверхности Земли до верхней границы атмосферы (для бесконечного столба атмосферы) равняется

$$P + I = \frac{jc_p}{g} \int_{p_2}^{p_1} T dp \tag{12}$$

Соотношение внутренней энергии и потенциальной

$$\frac{I}{P} = \frac{jc_v}{R} = \frac{1}{\varkappa - 1} = 2{,}5 \tag{13a}$$

или

$$\frac{P}{I} = \frac{AR}{c_v} = 0{,}4 \tag{13b}$$

Если при нормальных атмосферных условиях определим отношение внутренней и потенциальной энергии единицы массы, и результаты нанесем на такую систему координат, по абсциссе которой измеряются частные I/P, а по ординате — давление, тогда мы получим кривую, соответствующую приведенной на рис. 1. На диаграмме видно, что значение частного I/P приблизительно около уровня 400 мб равно 2,5.

Из уравнения (11) является очевидным, что значение I/P равняется 2,5 и в том случае, если $p_1z_1 - p_2z_2 = 0$. Следовательно, в атмосфере должен существовать такой уровень, для которого выполняется условие $p_1z_1 - p_2z_2 = 0$. Е. П. Борисенков этот уровень назвал средним

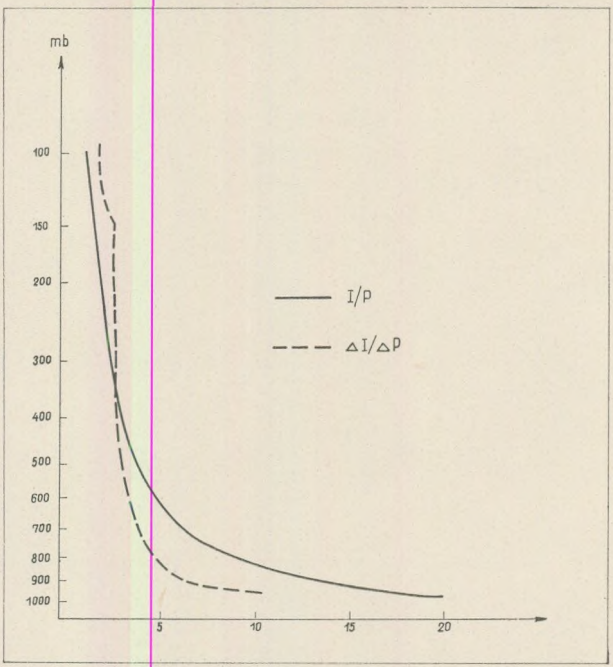

Рис. 1. Связь между потенциальной и внутренней энергией на различных уровнях по Борисенкову

энергетическим уровнем и обозначил его буквой Z, а его величину определил следующей формулой:

$$Z = \frac{RT}{g} \tag{14}$$

Изучая особенности среднего энергетического уровня Е. П. Борисенков указал на то, что функция $\Psi = pz$ достигает максимума вблизи этого уровня. В ранее написанной статье (1972) нами была сделана попытка определения максимума функции $\Psi = pz$, и оказалась, что при политропной атмосфере эта высота совпадает с высотой среднего энергетического уровня. Было изучено также, где располагается максимальное значение функции $\Psi = pz$ при однородной, при изотермической и при адиабатической атмосфере. Нами было получено, что при начальных условиях p_0, T_0 (давление и температура на поверхности Земли) функция $\Psi = pz$ достигает своего максимума при изотермической атмосфере на возможно самом высоком уровне, а при однород-

ной атмосфере — на возможно самом низком уровне. Взяв за основу ежемесячные температуры за промежуток времени в десять лет, было определено годовое изменение этой функции для некоторых европейских городов, и установлено, что в её амплитуде и годовом изменении отражается степень континентального или океанического влияния, играющего роль в формировании климата некоторых городов, областей.

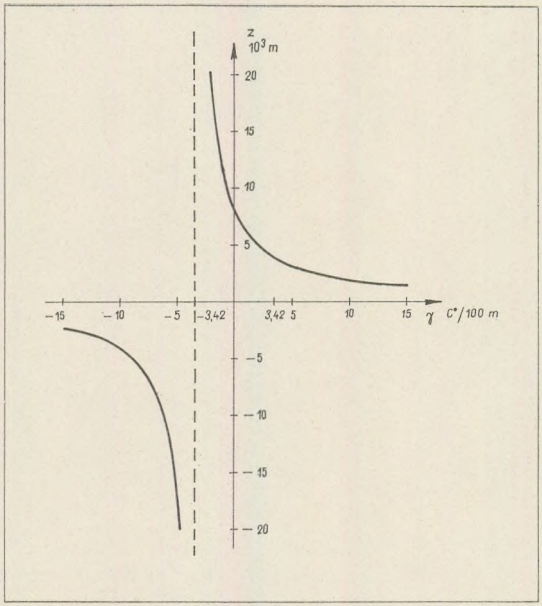

Рис. 2. Кривая функции $Z = \dfrac{RT_0}{g+R\gamma}$ в системе координат (γ, z)

В связи с вышеуказанными результатами представляется интересным определение высоты среднего энергетического уровня в зависимости от градиента температуры, а также определение этого уровня на возможно наименьшей и наибольшей высоте при одинаковых начальных значениях p_0, T_0 на поверхности Земли и предполагаемых постоянных градиентах температуры.

Если в уравнении (14) на место T написать выражение $T_0 - \gamma z$, то получим:

$$Z = \frac{R(T_0 - \gamma z)}{g} \quad \text{или} \quad Z = \frac{RT_0}{g+R\gamma} \tag{15}$$

Проанализируем функцию Z в зависимости от градиента температуры. Пусть на поверхности Земли $T_0 = 273°$, тогда при различных значениях γ на распределение Z получим кривую, приведенную на рис. 2. Исключим из нашего анализа значения градиента $\gamma > g/R = 3{,}42°/100$

м, поскольку при таких значениях градиента плотность атмосферы с высотой возрастала бы, что приводило бы к немедленному её перемешиванию. Из рис. 2. видно, что при $\gamma = \infty$ атмосфера суживалась бы до бесконечно малой величины и её средний энергетический уровень находился бы на поверхности Земли. Давление среднего энергетического уровня тоже можно определить в зависимости от градиента температуры, если исходить из формулы политропной атмосферы и в уравнении $T = T_0 - \gamma z$ на место z поставить $z = Z$, выражение для определения высоты среднего энергетического уровня:

$$p = p_0 \left(\frac{T}{T_0} \right)^{\frac{g}{R\gamma}} = p_0 \left(\frac{T}{T + \gamma z} \right)^{\frac{g}{R\gamma}} \tag{16}$$

Если на место Z впишем формулу среднего энергетического уровня, то получим следующее:

$$p_{cp} = p_0 \left(\frac{T}{T + \frac{\gamma R T}{g}} \right)^{\frac{g}{R\gamma}} = p_0 \left(\frac{Tg}{Tg + R\gamma T} \right)^{\frac{g}{R\gamma}} \tag{17}$$

где p_{cp} обозначает давление среднего энергетического уровня. Сократив на T, p_{cp} будет иметь следующий простой вид:

$$p_{cp} = p_0 \left(\frac{g}{g + R\gamma} \right)^{\frac{g}{R\gamma}} \tag{18}$$

Из уравнения (18) сразу видно, что давление среднего энергетического уровня можно определить в зависимости от приповерхностных данных и градиента температуры. Из уравнения (18) следует и то, что при стабильной атмосфере давление среднего энергетического уровня меньше, чем при больших значениях градиентов температуры.

Из рис. 2. видно, что функция $Z = \frac{RT_0}{g + R\gamma}$ при значении $\gamma = -\frac{g}{R}$ имеет перерыв. Если продифференцируем выражение среднего энергетического уровня по γ, тогда при значении $Z' = 0$ функция Z имеет крайнее значение.

Исходя из уравнения:

$$Z = \frac{RT_0}{g + R\gamma}$$

её производная:

$$Z' = -\frac{R^2 T_0}{(g + R\gamma)^2} \tag{19}$$

$Z' = 0$, если $\gamma = \infty$,

а при значении $\gamma = -\frac{g}{R}$

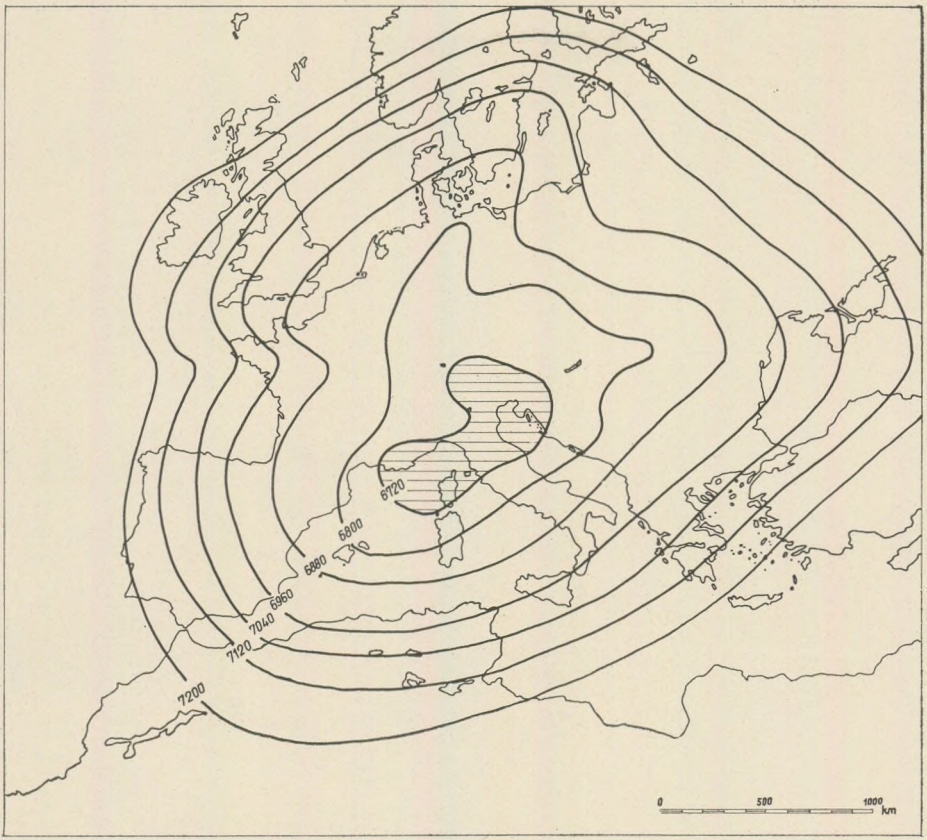

Рис. 3. Площадное распределение среднего энергетического уровня в 00 часов 18 ноября 1966 г.

$Z' = \infty$, то есть тангенс угла касательной к кривой функции $Z = \frac{RT_0}{g + R\gamma}$ при значении $\gamma = -\frac{g}{R}$ является бесконечным.

Но при реальной атмосфере изменение функции Z необходимо исследовать только в интервале от $\gamma = 0$ до $\gamma = \frac{g}{R}$. Внутри этого интервала функция Z достигает сваего максимума при $\gamma = 0$, а своего минимума – при $\gamma = \frac{g}{R}$, что является эквивалентным тому определению, по которому максимальное значение среднего энергетического уровня можно определить при изотермической атмосфере, а минимальное значение – при однородной атмосфере.

В заключительной части данной статьи, прослеживая развитие генуэского циклона, показывается местоположение среднего энергети-

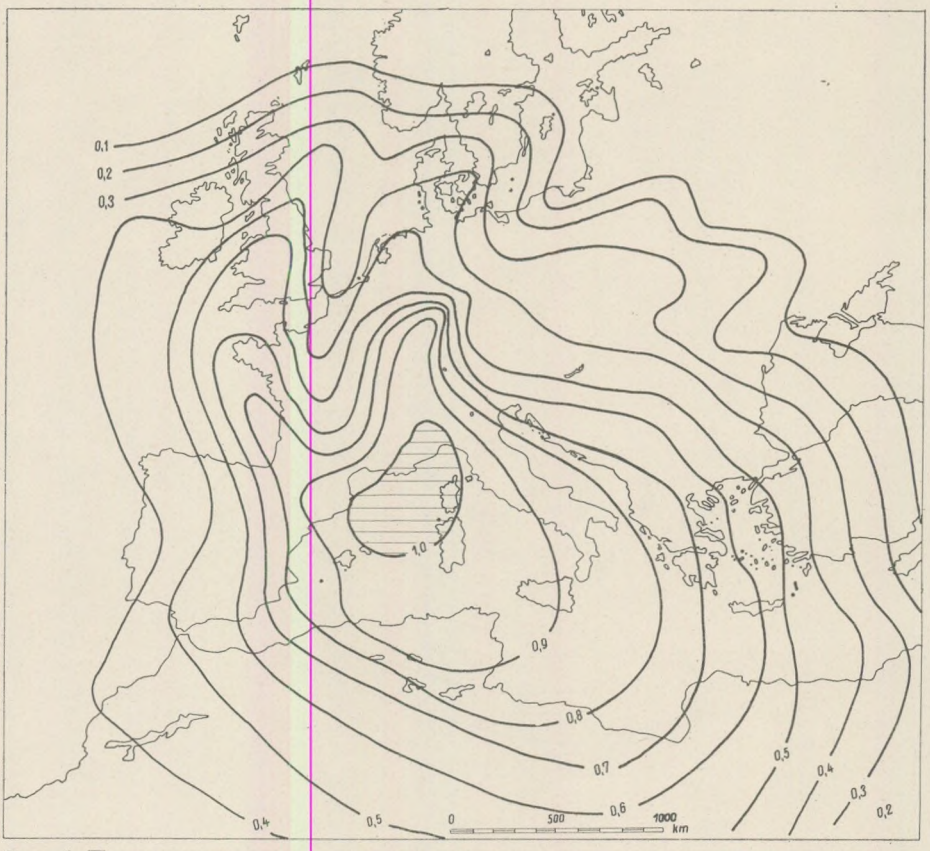

Рис. 4. Площадное распределение средних вертикальных градиентов температуры в 00 часов 18 ноября 1966 г.

ческого уровня (рис. 3.), территориальное распределение среднего вертикального градиента температуры и локальных энергетических изменений. Приведенные значения определены между поверхностью Земли и поверхностью 100 мб.

Из сравнения карт 4 и 5 видно, что Z имеет минимальное значение там, где средний градиент температуры атмосферного столба большой. Получили бы более реальную картину, если бы вместо поверхности 100 мб выбрали бы высоту тропопаузы, поскольку в результате более раннего анализа было установлено, что между высотами среднего энергетического уровня и тропопаузы существует кореляционная связь, коэффициент которой примерно равен 0,6 (1971).

Из сравнения карт 5, 6 и 7 в первую очередь хотелось бы указать на связь, существующую между локальными изменениями высоты среднего энергетического уровня и запасов энергии атмосферы. Из карт видно, что увеличение высоты среднего энергетического уровня

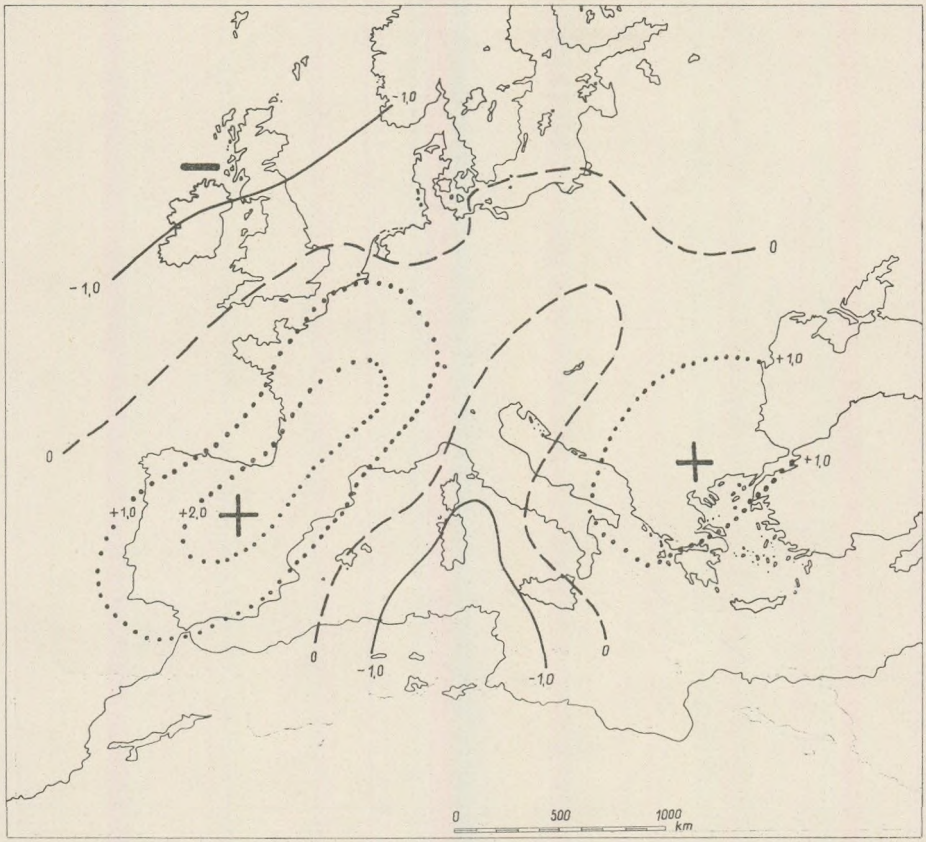

Рис. 5. Локальное изменение полной потенциальной энергии $\Sigma(P+I+L)$ в период 12 часов 18 ноября 1966 г. (в милливатт/см^2)

со путствуется увеличением кинетической энергии и уменьшением суммы потенциальной, внутренне-ой и скрытой энергий.

Надо отметить, что по такому упрашенному изображению превращения энергии мы еще не получим представление о величине той полезной потенциальной энергии, которая имеется над данной территорией для превращения в кинетическую энергию. Полезная потенциальная энергия по определению Лоренца (1955) это разница между полной потенциальной энергией фактического состояния и полной потенциальной энергией такого состояния, которого достигла бы атмосфера при адиабатическом перераспределении масс после того, что давление изентропных поверхностей приняло бы, так называемое, референциальное состояние.

Именно поэтому сумма полной потенциальной энергии сама по себе еще не достаточно хороший параметр для охарактеризования пре-

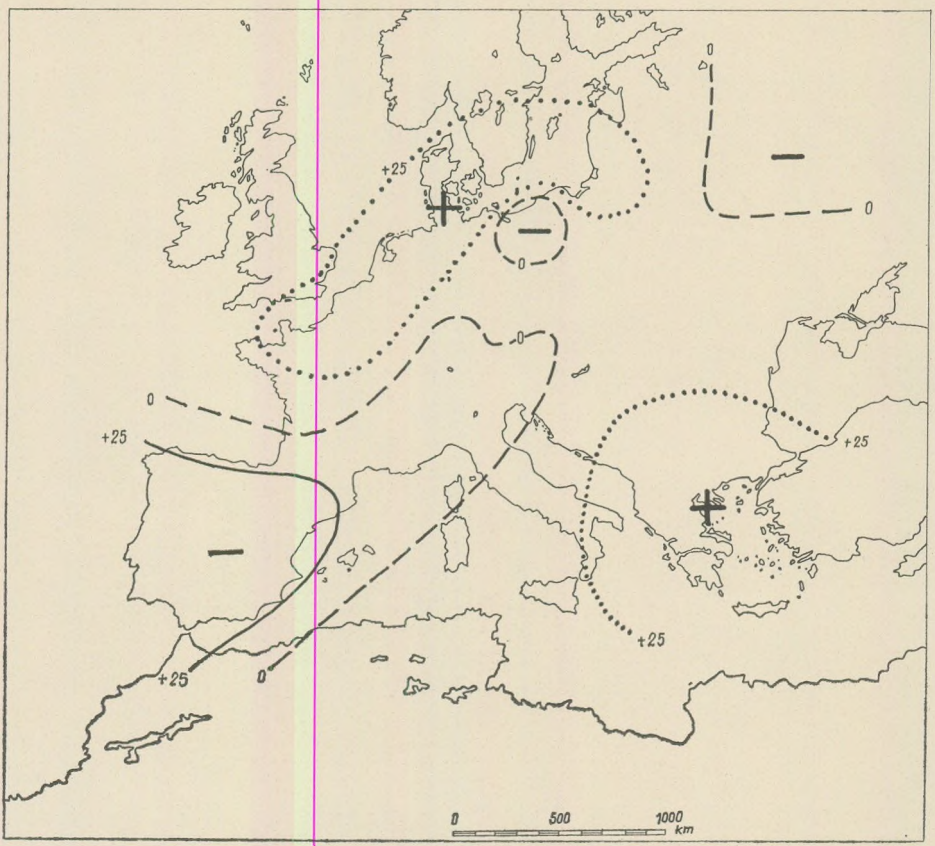

Рис. 6. Локальное изменение кинетической энергии в период 12 часов 17 ноября 1966 г. – 00 часов 18 ноября 1966 г. (в милливатт/см²)

вращения в кинетическую энергию. По точной формуле (Дуттон — Джонсон (1967), Смис (1969)] генерацию полезной потенциальной энергии надо искать в кореляции между диабатическими процессами и коэффициентом влияния, а превращение в кинетическую энергию регулируется варианциями вертикального движения холодных и теплых воздушных потоков. На изменение полезной энергии в ограниченном интервале в значительной мере влияют процессы горизонтального и вертикального перемещения масс; ими только тогда можно пренебречь, если процессы превращения энергии будем исследовать целиком для всей массы атмосферы.

Лоренц (1955) уже в первой своей работе, связанной с понятием полезной потенциальной энергии отметил, что в тех случаях, когда увеличиваются оба вида энергии неизбежно захватываются и адиабатические процессы; таким образом, мы получаем объяснение и

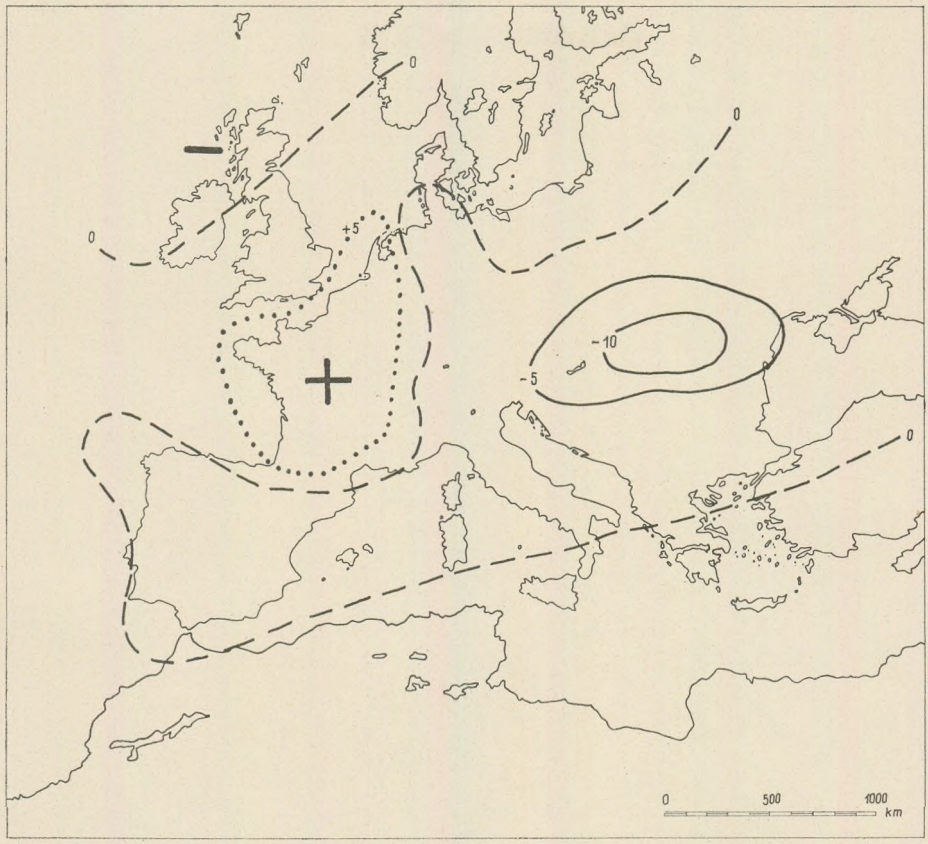

Рис. 7. Локальное изменение среднего энергетического уровня в период 12 часов 17 ноября 1966 г – 00 часов 18 ноября 1966 г.

для тех случаев когда уменьшение полной потенциальной энергии не сопровождалось однозначно увеличением кинетической энергии.

Значит, средний энергетический уровень, по существу не является пригодным показателем для отображения запасов полной энергии. Значение запасов полной энергии все равно не является информацией относительно дальнейшего развития атмосферных процессов, немного больше узнаем из величины полезной потенциальной энергии, для которой значение среднего энергетического уровня оказалось подходящим первым показателем. Если в каком-то мгновенном состоянии атмосфера сильно отклонена от состояния равновесия, тогда полезная потенциальная энергия достигает большой величины, а средний энергетический уровень расположен низко. Именно поэтому кажется целесообразным связывать средний энергетический уровень с энтропией которая достигает своего максимума при статически установившемся состоянии равновесия атмосферы.

Е. П. Борисеков в своих исследованиях показал, что на среднем энергетическом уровне термогидродинамические уровнения и полученное из них уравнение вихря скорости можно применять в упрощенной форме, а агеострофическое отклонение ветра является функцией только от адвекции температуры, поэтому стоит подумать о попытке прогнозирования этого уровня, что возможно дало бы больше информации о развитии погодных изменений синоптического масштаба, чем прогнозное значение некоторых изобарических поверхностей.

ЛИТЕРАТУРА

Борисенков, Е. П. (1960): Вопросы энергетики атмосферных процессов. Гидрометеоиздат, Ленинград.

Császár M. M. (1972): Kísérlet a $\psi = pz$ függvény maximumának kijelölésére (в рукописи).

Császár M. M. (1971): Some Statistical and Energetical Properties of the Average Energetical Level. Időjárás, 75.

Lorenz, E. N. (1955): Available Potential Energy an the Maintenance of the General Circulation. Tellus, 7. No. 2.

Dutton, I. A. – Johnson, D. R. (1967): The Theory of Available Potential Energy and a Variational Approach to Atmospheric Energetics. Advaces in Geophysics. V. 12.

Smith, P. I. (1969): A computational study of the energetics of a limited region of the atmosphere. Tellus. Vol. 21.

INVESTIGATIONS ON THE TERRITORIAL DISTRIBUTION OF THE GLOBAL RADIATION OVER HUNGARY

by
Z. DOBOSI
(Department of Meteorology, L. Eötvös University, Budapest)
(Received: 31st March, 1972)

РЕЗЮМЕ

Рассматриваются некоторые проблемы глобальной радиации при помощи уравнений регрессий между глобальной радиацией и продолжительностью инсоляции. Автор считает применение дневных суммарных излучений более выгодным по сравнению с рассчетами, основывающимися на месячных суммарных величинах. Он доказывает существование в Венгрии сигнификантных расхождений между регрессионными констатами, полученными для разилчных станций, и на этом основании он применяет региональные уравнения. Он продемонстрирует распределение излучений, вычисленных путем применения региональных уравнений и сопоставляет его с ранее опубликованной картой распределения излучений, вычисленного с помощью стандартного уравнения.

Global radiation is the sum of both direct and diffuse solar radiation reaching the horizontal surface of the Earth. The fraction of this energy absorbed by soil surface is transformed into heat energy necessary for warming up the soil and air and vaporizing the water released by the soil into the atmosphere. In the final analysis, this is what controls the climate and keeps in operation the mechanism of weather.

To investigate its territorial distribution, several reasonably-distributed stations are necessary. Radiation recording instruments, however, operate at a small number of stations. Moreover the series of observations available are so short that the conclusions deduceable therefrom only, are still insufficient for climatic purpuses.

Extrapolation in space and time of the data of radiation measuring stations is made possible by the close relationship existing between duration of sunshine and global radiation. Good examples elucidating the characterization of the closeness of this relationship are furnished, in addition to the author's earlier results (1), by the readings taken during the period of 1958 – 1965 at the seven stations listed below. During that period simultaneous observations of global radiation and sunshine duration were conducted at these stations. The coefficients of correlation between the daily sums of these elements are shown in Table I.

All the values of the tabulation are far higher than the maximum random value pertaining to the $P = 0.01\%$ level. In other words, the correlation coefficients differ significantly from zero.

Table I

Coefficients of correlation between the daily sums of sunshine duration and global (radiation 1958—1965.)

	Budapest	Pécs	Békés-csaba	Debrecen	Keszthely	Siófok	Szeged
I.	0.82	0.47	0.77	0.80	0.81	0.80	0.86
II.	0.87	0.62	0.78	0.90	0.84	0.87	0.90
III.	0.89	0.67	0.88	0.90	0.87	0.84	0.91
IV.	0.90	0.71	0.91	0.88	0.90	0.86	0.94
V.	0.91	0.76	0.90	0.88	0.92	0.89	0.95
VI.	0.86	0.92	0.92	0.87	0.92	0.88	0.94
VII.	0.90	0.91	0.85	0.74	0.89	0.85	0.90
VIII.	0.99	0.92	0.83	0.77	0.86	0.84	0.92
IX.	0.86	0.93	0.84	0.82	0.88	0.89	0.92
X.	0.90	0.89	0.86	0.88	0.90	0.87	0.88
XI.	0.83	0.86	0.83	0.90	0.88	0.88	0.90
XII.	0.79	0.87	0.83	0.82	0.81	0.85	0.87

Almost unprecedented in climatic investigations is the close correlation warranting the linearity of the stochastic relationship existing between the two elements.

Since sunshine duration records have been available since a much earlier date and for a much greater number of stations, the resulting linear regression equations have enable the author to extrapolate Hungary's global radiation data both in space and time.

Let us discuss hereafter two problems connected with the regression equations expressing the stochastic relationship between the elements under consideration.

The objective being climate-oriented, the author's aim is to give on the basis of the available eight-years readings of global radiation an estimate of daily averages of global radiation for 30 or 50 years, i.e. for such a long period over which sunshine duration records are available.

A question that may now arise is whether the regression equations to rely upon in calculating monthly averages are to be preferentially the ones calculated from the daily sums of global radiation and sunshine duration or those calculated from the monthly sums of the same two elements ? The question can be answered with a view to the fact that the two kinds of regression lines intersect each other in the point representing the 1958—1965 averages of the two elements. Accordingly, the closer one approches to the point of intersection defined by the averages, the smaller the difference of global radiation calculated ot the basis of the two lines; in other words, the less the divergenczy of the data yielded by the two different methods. The angle between the two lines is low indeed, as the difference of the directional tangents is small. And since the averages of sunshine duration of the years 1958—1965 are close to the 1901—1950 figures, the global radiation values calculated by the two methods differ

rather little, e.g. by less than 0.2% in case of Budapest. Hence the application of both methods are equally justified.

The author believes the application of the regression equations of daily basis to be more reasonable at present, as calculations in this case rely on about 300 pairs of values, as opposed to the lo pairs of monthly values obtainable. For, in case of utilization of a greater number of daily sums the result is les influenced by single incidental errors.

The other problem the writer has sought to tackle here is faced when the regression equations obtained for the various stations are compared. Of course, these figures will differ from one another. It is desirable to examine if the divergencies between them or their constants, respectively, are significant. The values of the directional tangents of the regression lines and their standard deviations are shown in Table II.

Table II

Constants a of the regression equation $G = aN+b$ and σ_a values of the standard deviations of a

		I	II	III	IV	V	VI	VII	VIII	IX	X	XI	XII
Budapest	a	14.4	19.9	26.8	28.3	31.0	30.2	29.1	26.0	24.7	21.7	16.6	12.8
	σ_a	0.5	0.6	0.7	0.8	0.7	1.0	0.8	0.8	0.8	0.6	0.6	0.5
Debrecen	a	15.7	22.3	29.4	30.8	30.9	31.8	24.9	28.7	30.0	22.9	18.5	15.4
	σ_a	0.8	0.7	0.9	1.1	1.1	1.1	1.4	1.4	1.3	0.7	0.5	0.6
Keszthely	a	16.5	21.7	28.2	31.6	33.6	33.2	31.6	29.7	29.9	24.1	20.3	16.1
	σ_a	0.8	0.9	1.0	1.0	0.9	0.9	1.0	1.0	1.0	0.7	0.7	0.7
Siófok	a	16.4	21.4	27.9	29.2	31.0	29.7	28.6	27.8	28.6	22.2	19.6	15.6
	σ_a	0.8	0.8	1.1	1.1	1.0	1.0	1.1	1.1	0.9	0.8	0.6	0.6
Szeged	a	15.4	20.1	26.5	28.7	28.8	27.4	25.0	25.6	25.5	18.6	16.6	13.8
	σ_a	0.6	0.7	0.8	0.7	0.6	0.7	0.7	0.7	0.6	0.6	0.5	0.5
Békés-csaba	a	13.9	19.3	25.8	28.6	28.7	28.9	26.6	25.5	24.3	19.3	18.0	13.4
	σ_a	0.7	1.0	0.9	0.9	0.9	0.9	1.0	1.0	1.0	0.7	0.7	0.5
Pécs	a	15.3	19.5	24.9	32.2	34.4	30.6	30.9	30.6	27.8	21.7	17.4	16.1
	σ_a	1.1	1.0	0.5	1.1	0.9	0.9	0.8	0.8	0.7	0.7	0.6	0.5

In equation

$$G = a\,N+b$$

G means global radiation in cal cm^{-2} day^{-1} units, N the sunshine duration in hours.

As evident from the table II, in some cases the differences of the values of a are usually less than their standard deviations, or the double of these. Accordingly, one might say that their differences are not significant. On this ground, as was shown in an earlier paper (2), one standard equation can be established for the entire country.

Examining the data with closer scrutiny, one becomes convinced that the rules of significance must not be applied mechanically, unless running the risk of committing a so-called type II statistical error, ie.

ignoring the significance of slight, but significant, differenes which are inherent in Nature and not due to a statistical hazard.

Nota bene, the differences of constants a show mostly the same sign. For instance, all but three data of Budapest are greater than those of Budapest and the Keszthely data are in all months above the Budapest figures, whereas their differences in several months are less than the double of their standard deviations, and so on.

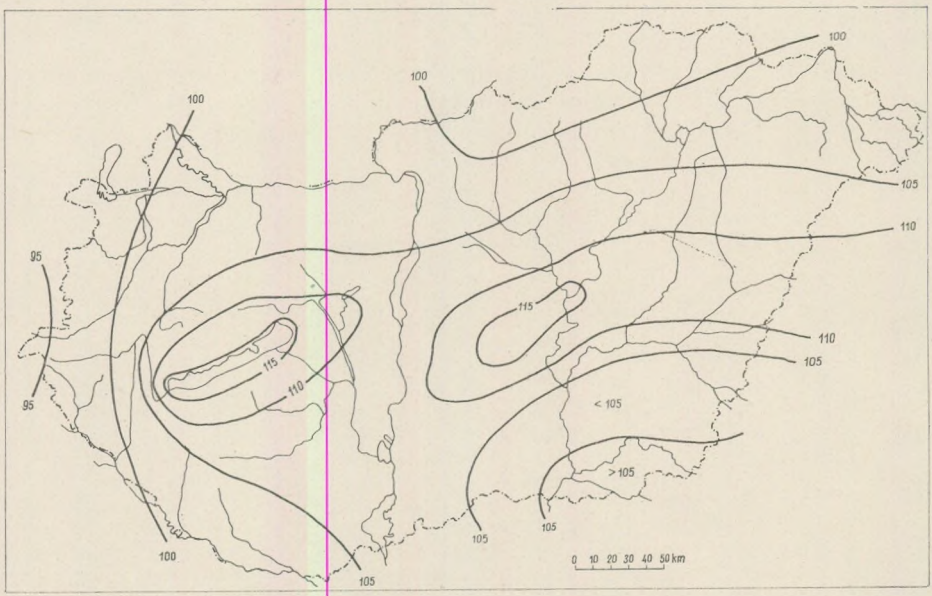

Fig. 1. Distribution of the annual sum total of global radiation on the basis of regional regressions. Cal cm^{-2} $year^{-1}$. 1901 – 1950.

It was by starting from these considerations and assuming the equation of each station to be significantly different from the rest and applying regional regression equations, that the author has calculated the 50-year averages of global radiation. Relying in the avilability of seven stations, the author has divided the country into the same number of regions – using Bacsó's climatic classification (3) in defining the boundaries of his regions – and he has applied for all the sunshine duration measuring stations of each region the regional equations assumed to be valid for the given region. In this way, the territorial distribution of global radiation has been determined for the entire territory of Hungary (Fig. 1.).

The map published herewith shows the distribution of the annual sums calculated on the basis of monthly averages. It compares best with the distribution calculated on the basis of the standard equation (Fig. 2.).

The difference between the two distributions can be summarized as follows.

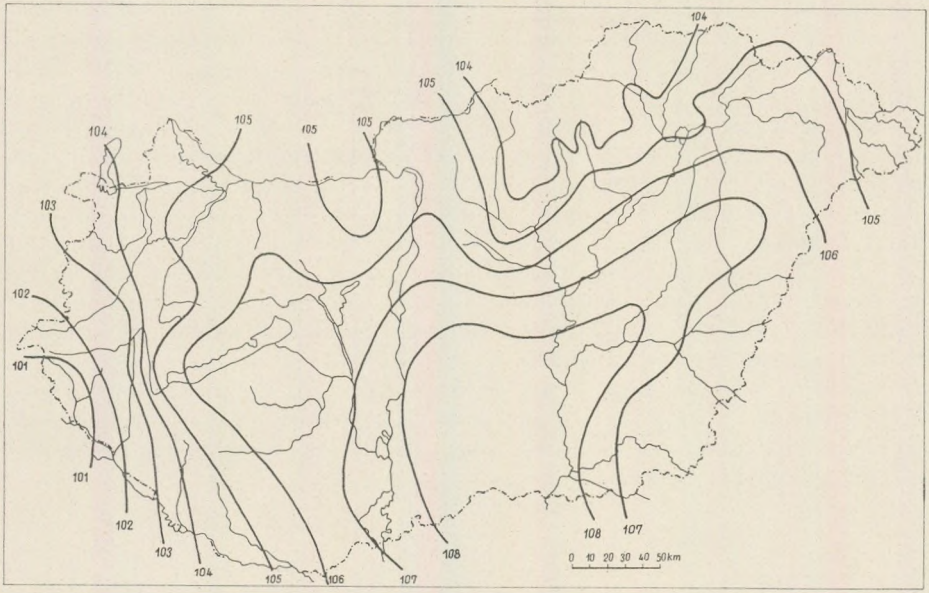

Fig. 2. Distribution of the annual sum total of global radiation on the basis of standard regression. Cal cm^{-2} $year^{-1}$. 1901 – 1950.

1. The distribution pattern based upon the regional equations (Fig. 1.) is characterized by more distinct contrasts, the territorial divergencies of radiation being more remarkable than the distribution obtained with the aid of the standard equation (Fig. 2.). The basis of calculation, the territorial distribution of sunshine duration obtained for the period of 1901 – 1950, has been the same in the cases of both types of distribution. Consequently, the differences are due to the new kind of application of the regression method. The territorial differences of the distribution obtained with the standard equation varied between 101 and 108 Cal cm^{-2} $year^{-1}$. The regional method yielded values varying between 98 and 113 Cal cm^{-2} $year^{-1}$.The territorial mean has been the same with both methods being close to 106 Cal cm^{-2} $year^{-1}$. Let us conclude then that the standard equation, whose constants are furnished by the mean value of the constants of the regional equations, will fade the spatial divergencies, leaving the average unchanged.

The other difference consists in the distribution itself. Fig. 2 has located the maximum, 108 Cal cm^{-2} $year^{-1}$, in the southern half of the Great Hungarian Plain. In Fig. 1. two maxima can be recognized: one in the vicinity of Kecskemét, the second at Lake Balaton, both with a value of 113 Cal cm^{-2} $year^{-1}$. The maximum in the central Great Hungarian Plain is due the basin effect that is manifested in the case of other elements such as clouds, precipitation, etc. as well. The Lake Balaton maximum is believed to be of particular importance, being presumably due to double

causes. On the one hand, it seems to be of dynamical origin, for the prevailing NW winds getting over the crest of the Bakony bring about an effect resembling that of the foehn. The second reason may be the skies less abundant in cumulus on account of the reduced ascendent current above the water surface which is less liable to warming up during sunshine. This phenomenon is not reflected by the available information on cloudiness — a fact seemingly due to the lower sensitivity of estimate-based observations. The data of precipitations, however, do indicate Lake Balaton's shortage of precipitations as opposed to its neighbourhood (4). The regional map inserted into this paper shows a decrease of the global radiation sums towards the southern mergin of the Great Hungarian Plain. The reason for this is believed to consist in the presumably different structure of cloudiness. The cumulus-type clouds which attains in radiation a higher degree largely responsible for this behaviour of global radiation. Because of its higher sensitivity, radiation measurements do indicate this phenomenon otherwise unreflected by the less sensitive, estimate-based cloudobservations.

REFERENCES

D o b o s i, Z. (1957): A napfénytartam és a globális sugárzás összefüggése Magyarországon. (Relationship between the sunshine duration and global radiation in Hungary). Időjárás 61. p. 357.

D o b o s i, Z. (1959): A globális sugárzás területi eloszlása Magyarországon. (Territorial distribution of global radiation in Hungary), Időjárás 63. p. 82.

B a c s ó, N. (1959): Magyarország Éghajlata. (The climate of Hungary). Akad. Kiadó. Budapest.

Magyarország Éghajlati Atlasza (1960): (Climatic Atlas of Hungary). Akadémiai Kiadó. Budapest.

HOURLY VALUES OF THE RADIATION BALANCE IN THE SUMMER HALF-YEAR

by
L. FELMÉRY

(Department of Meteorology, L. Eötvös University, Budapest)
(Received: 28th March, 1972)

РЕЗЮМЕ

В работе рассматриваются часовые, дневные и месячные величины радиационного баланса, полученные для летних месяцев при помощи коротковолнового баланса, определенного по серии результатов измерений, проведенных на станции Мартонвашар-Эрдёхат на протяжении двадцати лет. Для вычислений был использован метод, разработанный В. П. Гагуой (V. P. Gagua).

The energy exchange, the heat balance of the earth's surface, and of the near-surface air layers depend above all on the radiation balance of the terrestrial surface. This is expressed by the fact that in the well-known basic equation of the heat balance on the left-hand side only the radiation balance is generally represented. On the right-hand side of the above equation however there are different components of the heat balance, the heat-conductions to the ground and to the air and the heat consumption for evaporation. In this way the radiation balance has a basic importance for the investigations of the heat balance. This component, and its daily and yearly variations are useful in the interpretations of the daily and yearly cycles of temperature, humidity, and other elements of meteorology, moreover, they allow some weather forecasts concerning potential frosts fogs etc.

Investigating the radiation balance there are the following objects to be reached: dot-like or areal distribution. In both relations it was Dobosi [1, 2] who carried out pioneering work in this country. According to the reference [1] the radiation balance was determined on the basis of the global radiation data measured at the Martonvásár–Erdőhát station ($\varphi = 47° 21'$) in the period of 1953–1955, the other components were calculated. The results obtained in this way made possible to investigate the yearly course of the radiation balance. Using the abovementioned results of Dobosi it was possible to determine not only the radiation balance but all of the other components of the heat balance for Budapest, which was done by Bacsó [3]. In this study the yearly value of the radiation balance was 42,2 Kcal/cm^2. year. Later on Felméry also made an attempt at calculating the radiation balance for Budapest. This atempt was reported as a numerical example of Budyko's met-

hod, and it was published as a textbook for teaching [4]. In this latter study a slightly greater value was obtained (50 Kcal) for the radiation balance because the time interval of negative radiation balance in the winter months was found to be shorter, and its absolute value was smaller. The areal distribution of the radiation balance in Hungary have been in two papers. Dobosi [2] gave distribution of the yearly values, Major, GY., and Tárkányi, Zs. [5] calculated the monthly distributions, and presented them in 12 maps. The map on the yearly distribution showed good agreement with the reference [2].

The above results have a common feature, as the data were obtained in indirect way, and they were not based on direct balance measurements. The determinations were made in the following manner. The radiation balance was specified for different components, and these were determined in terms of the meterological elements with suitable long-range sets of measurement. Following this procedure a climatological interpretation of the balance values can be performed. As arule none of the components was measured directly. Because of this the global radiation is calculated on the basis of its correlation with the insolation duration. The determination of the albedo for the given terrestrial surfaces is based either on literature data or on short-range measurement sets. For determining effective radiation, several empirical formulae are available. These formulae involve the temperature of the active surface as well as air temperature, humidity and cloudiness. The indirect determination methods have certain advantages: the possibility to use long-range measurement sets and accordingly the climatological interpretation. There are other opinions to take into account. The world wide network of actinometry is not suitable developed (there are about 200 balance measuring stations distributed in a rather irregular way, most of them are in the temperate zone of the northern hemisphere with a measuring period of seven-ten years only). For this reason, the indirect methods of determination of the radiation balance will be needed for a long time.

Naturally, the indirect and combined methods are pregnant with errors, and they are unsuitable to determine the radiation balances of shorter periods, e.g. a few hours or days. For this reason, in the last 15-year period a method was developed to determine the total radiation balance on the basis of the short-wave balance. For this method, data based on a network global radiation measurements are available: moreover, the density of this network is greater, the measuring period connecting it is longer than in the case of the above-mentioned balance measurements. The total radiation balance R can be written in the following form:

$$R = R_r - R_h \tag{1}$$

$$R_r = Q\,(1 - A) \tag{2}$$

where Q denotes global radiation, A is the albedo of the terrestrial surface, R_h is the long-wave balance or effective radiation, R_r is the short-

wave balance or the net solar radiation. According to the investigations [6, 7, 8, 9, 10, 11, 12, 13, 14, 15, 16] there are suitable strong linear connections between factors R and Q, and R and R_r as well, which may be given by the following regression equations:

$$R = aQ - b \tag{3}$$

$$R = cR_r - d\,. \tag{4}$$

The constants a, b, c and d have been determined by different authors with the results shown in Table 1 (let us remark that most of the data in Table 1 have derived from the temperate zone corresponding to the summer half-year).

The relationship between factors R and R_r is much stronger than in case of R and Q. It is quite natural because the feature of the surface influencing strongly the absorbed radiation is taken into consideration in

Table I

Measuring stations	a	b	Authors
Hamburg	0.60	15 cal/cm² day	Fleischer, R., 1954
Ames (USA)	0.75	21 cal/cm² day	Shaw, R., 1956
Soviet Union middle latitudes	0.55	14 cal/cm² day	Pavlov, A. V., 1962
Wageningen	0.79	27 cal/cm² day	Scholte-Ubing, 1959
Hawaii	0.72	28 cal/cm² day	Chang, Jen-Hu, 1961
Genoa			
spring	0.48	32 cal/cm² day	
summer	0.59	63 cal/cm² day	Bossolasco, 1962
autumn	1.31	97 cal/cm² day	
Ibadan and Dakar	0.61	28 cal/cm² day	Davies, 1966
	c	d	
Nebraska	0.80	4.5 cal/cm² hour	Lettau, H.—Davidson, B., 1957
Rothamsted (clear sky)	0.82	5.9 cal/cm² hour	Monteith, J.—Szeicz, G., 1961
Karadag	0.85	0.07 cal/cm² min	Baraskova, E. P., 1961
Jakutsk, Sverdlovsk, Kiev, Odessa	0.83	0.05 cal/cm² min	Baraskova, E. P., 1961
Humid territories	0.90	0.9 Kcal/cm² month	Berljand, T. G. and
Dry territories	0.70	1.4 Kcal/cm² month	Muhenberg, V. V., 1963
Soviet Union, middle latitudes, northward slopes, steeper than 10°	0.70	33 cal/cm² day	
southward slopes, steeper than 10°	0.70	29 cal/cm² day	Golubova, T. I., 1967

factor R_r trough the albedo. In the winter half-year surfaces with long-lasting snow-cover show a poor relationship between factors R and R_r.

Data in Table 1 have been taken from comparatively short sets of measurements. Therefore it is noteworthy to take into account specially the study written by V. P. G a g u a [16]. In this paper the analysis of the relationship between factors R and R_r was made using the numerous data accumulated since the International Geophysical Year (IGY). Data of 17 stations from different climatic zones from the pole to the equator were analysed in the above-mentioned study. Even the shortest measuring period among them lasted at least for two years. It is necessary to report G a g u a' s method and results to set up from the m e a s u r e d values of the short-wave balance, the hourly, daily and monthly values of the radiation balance for a station of Hungary.

The correlation graphs for the months of January, April, July and October for all of the 17 stations were produced by G a g u a. The average monthly sums per hour of factor R were plotted against the same hourly values of factor R_r along the vertical and horizontal axes, respectively. An exact linear correlation was found for every months and for all of the stations available in the territory between the equator and the latitude of $40°\varphi$. The same linear correlation was found for stations at higher latitudes for the summer half-year only.

Table 2 shows the moderate variations of the constants c. The average is $c = 0.87$. This is the reason why the angle of inclination is 41° for the line of average condition. Constant d is equal to the value of radiation balance at sunrise or sunset, varying between 3 – 6 cal/cm² hour. In Fig. 1. data of 12 stations can be seen. Most of the stations are at the middle

Table 2

Stations	c				d cal/cm² hour			
	I	IV	VII	X	I	IV	VII	X
Resolute, Can.	–	–	0.81	–	–	–	– 3	–
Dixon	–	–	0.78	–	–	–	– 3	–
Jakutsk	–	0.81	0.81	0.84	–	3	4	2
Leningrad	–	0.90	0.90	0.93	–	3	4	2
Omsk	–	0.84	0.84	0.87	–	4	4	2
Odessa	0.90	0.84	0.84	0.87	3	3	4	4
Karadag	0.84	0.87	0.78	0.84	3	4	4	4
Toronto	0.78	0.81	0.81	0.84	3	4	4	4
Vladivostok	–	0.87	0.93	0.90	–	4	2	4
Tbilisi	0.81	0.87	0.87	0.84	3	3	4	3
Genoa	–	0.81	0.93	0.93	–	3	5	4
Chardzhou, USSR	0.90	0.90	0.93	0.87	3	4	6	4
Buenos Aires	0.78	0.81	0.81	0.87	2	3	4	4
Pilar	0.90	0.93	0.97	0.97	4	3	4	3
Hanoi	0.90	0.90	0.97	0.97	3	3	3	2
San Salvador	0.87	0.90	0.87	0.87	5	4	3	3
Yangambi	0.84	0.84	0.84	0.84	3	3	3	3

and low latitudes. From the stations at high latitudes only summer half-year values were taken for plotting.

The graph proves the existence of a linear relationship between factors R and R_r. If the values of constants c and d are known and the measured values of the shortwave radiation balance R_r, are available the hourly sums of the total radiation balance R can be determined. For the regression analysis the values of both R_r and the average monthly sums per hour of R were used. Accordingly the above-mentioned correla-

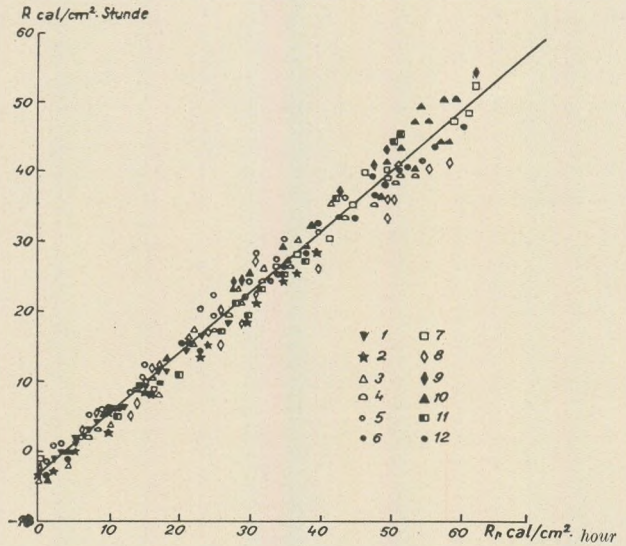

Fig. 1. Relationship between the radiation balance, and the average monthly sums per hour of the absorbed radiation (after GAGUA)

1 — Resolute, 2 — Yakutsk, 3 — Voyeykovo, 4 Toronto, 5 — Vladivostok, 6 — Tbilisi, 7 — Chardzhou, 8 — Buenos Aires, 9 — Hanoi, 10 — San Salvador, 11 — Kinshasa, 12 — Yangambi.

tion is true for the conditions of the average cloudiness. In Fig. 1. the conditions of clear sky or total cloudiness would be granted if the straight line with the directional tangent of 0.87 was moved away parallel to itself downwards or upwards, respectively. Consequently, in case of medium cloudiness, a given value of R_r corresponds to a smaller value of R, than in case of overcast sky. In this way the constant d can be used in two senses. It may give the variation of regres sion depending on the latitudes for medium cloudiness. On the other hand the constant d may define the dependence of the regression equation on the degree of the cloudiness for a given place. This dependence would be necessary, if the virtual hourly values of the radiation balance instead of its average monthly values were to be determined.

To determine the radiation balance around the clock it is necessary to have the nightly values, too. Value of factor R is negative at night (excluding the summer polar "day period" in the polar regions), and it equals to the long-wave radiation balance. In the comprehensive work mentioned above [16] the analysis showed that the average monthly sums per hours of night of the radiation balance are practically unvaried in the period from sunset to sunrise in the different climatic zones. This is generally true even for single nights as verified by the author's own measurements (performed by the S c h e n k-type balance-meter). In this way knowing value of factor R at the time of sunrise (or at sunset) it can be used as a first approximation for the hours of nights, too. Assuming $Q = 0$ or rather $R_r = 0$, and using Eq. (4) the value of R is determined by constant d. In this manner it is possible to make the average monthly sums per hour of the radiation balance for whole days from the equator to the high latitudes.

To use allow a wide use of his method G a g u a has generalized the values of the constant d form Table 2. for the climatic zones.

Table 3

Climatic zones	d cal/cm^2 hour			
	Warm season	Dry season	Humid season	Year
Polar and subpolar	2			
Temperate	4			
Subtropical				
a) continental		6	4	
b) Mediterranean		5	3	
c) monsoonal		4	3	
Tropical				
a) desert				8
b) semiarid		7	5	
c) savannah				
dry		6	4	
humid		5	3	
Equatorial monsoon		4	3	
Equatorial				3

The procedure of calculations is the following: let us select the value of the constant d according to the climatic zone and the season from Table 3. As a following step let us determine the average hourly value of factor R connecting with the measured value of factor R_r using the suitable line of constant d from Fig. 2. Let us take the radiation balance to be approcimately constant in the period from sunset to sunrise and its value to correspond quantitavely to the constant of d.

Estimating properly the approximate procedure for the hours of night let us examine for some stations the average monthly sums per hour at midnight (11^{30} p.m. – 0^{30} a.m.) of the radiation balance calculated by the method of B e r l j a n d, M. E. The result can be seen in the following list.

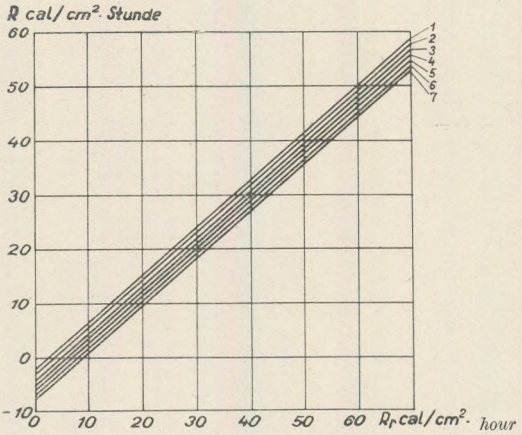

Fig. 2. Graph for the determination of the hourly values of the radiation balance (after Gagua)

1. d = 2 cal/cm² hour;
2. d = 3 cal/cm² hour; ... 7. d = 8 cal/cm² hour.

Table 4

Stations	R(at midnight) cal/cm² hour			
	I	IV	V	X
Verkhoyansk	–1	–2	–2	–2
Helsinki	–1	–3	–4	–3
Hamburg	–1	–2	–2	–3
Budapest	–2	–4	–4	–3
Genoa	–5	–3	–5	–4
Dakar	–7	–6	–5	–5
Aden	–4	–5	–5	–5
Yangambi	–3	–3	–3	–3

Considering the absolute values of the effective radiation the highest average values occur in the dry territories of the tropical and subtropical zones (Dakar, Aden). In the winter half-year of the temperate zone the lowest values can be found in those territiories where relatively low surface and air temperatures are connected with high humidity and plenty of cloudiness (Hamburg). The absolute peak value was measured in the Arabian Desert near Aswan at midnight with clear sky, and it attained – 9 cal/cm² hour.

Table 5

Months \ Hours	4–5	5–6	6–7	7–8	8–9	9–10	10–11	11–12	12–13	13–14	14–15	15–16	16–17	17–18	18–19	19–20
April	–	0.17	0.17	0.15	0.15	0.14	0.14	0.14	0.14	0.14	0.15	0.15	0.16	0.19	0.21	–
May	0.18	0.16	0.16	0.15	0.15	0.15	0.15	0.15	0.15	0.15	0.15	0.15	0.17	0.17	0.19	0.20
June	0.20	0.18	0.17	0.17	0.17	0.17	0.17	0.18	0.18	0.17	0.18	0.19	0.18	0.19	0.21	0.22
July	0.24	0.22	0.21	0.20	0.19	0.18	0.18	0.18	0.18	0.18	0.19	0.20	0.20	0.21	0.22	0.24
August	0.23	0.21	0.20	0.20	0.20	0.20	0.19	0.19	0.19	0.19	0.19	0.20	0.20	0.21	0.22	0.23
September ..	–	0.23	0.22	0.20	0.20	0.20	0.19	0.19	0.19	0.20	0.20	0.20	0.21	0.23	0.24	–

Table 6

Months \ Hours	0–1	1–2	2–3	3–4	4–5	5–6	6–7	7–8	8–9	9–10	10–11	11–12	12–13	13–14
April	–4.0	–4.0	–4.0	–4.0	–4.0	–3.4	0.7	9.2	17.6	24.7	29.1	30.8	30.8	28.3
May	–4.0	–4.0	–4.0	–4.0	–3.9	–0.6	6.9	15.1	23.8	29.1	32.4	34.5	33.7	31.4
June	–4.0	–4.0	–4.0	–4.0	–3.2	1.6	10.5	16.9	25.3	31.7	35.5	36.4	35.8	33.4
July	–4.0	–4.0	–4.0	–4.0	–3.4	0.4	7.5	16.3	24.4	28.9	34.2	36.1	36.2	34.1
August	–4.0	–4.0	–4.0	–4.0	–3.9	–2.5	3.7	12.8	20.7	27.1	32.2	33.1	31.8	30.4
September	–4.0	–4.0	–4.0	–4.0	–4.0	–3.7	–0.5	6.0	14.1	20.4	25.0	26.7	25.9	23.6

	14–15	15–16	16–17	17–18	18–19	19–20	20–21	21–22	22–23	23–24	Daily amounts cal/cm² day
April	23.3	17.6	11.2	4.4	–1.3	–4.0	–4.0	–4.0	–4.0	–4.0	183.0
May	27.2	21.9	15.6	8.5	1.3	–2.7	–4.0	–4 0	–4.0	–4.0	242.2
June	29.1	24.1	18.6	11.9	3.6	–1.1	–4.0	–4.0	–4.0	–4.0	278.1
July	29.6	24.6	18.1	11.0	2.4	–2.0	–4.0	–4.0	–4.0	–4.0	266.4
August	26.3	20.5	14.6	7.4	–0.1	–3.3	–4.0	–4.0	–4.0	–4.0	218.8
September	18.9	10.4	5.7	0.5	–3.1	–4.0	–4.0	–4.0	–4.0	–4.0	129.9

The procedure detailed above has the following global value: the classified values of the radiation balance from the different climatic zones can be directly compared with one another, the applied procedure being equivalent.

A 20-year series of the average monthly sums per hour as well as the daily and monthly amounts of the global radiation measured in the Meteorological Laboratory of the Eötvös University at Martonvásár – Erdőhát are available. The hourly amounts of the average measured albedo for the summer half-year are also known based on a few years' series (Table 5).

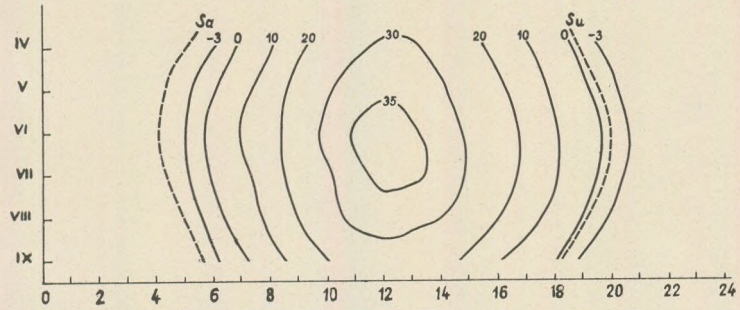

Fig. 3. Isopleths of the daily and half-year variations of the radiation balance at the station of Erdőhát.

Accordingly, using Eq. (2) the sets of data of the short-wave balance can be determined.

Let us suppose that the station at Martonvásár – Erdőhát represents an areal-average, with a view to the climate of Hungary and to the geographical situation of this station. The uncultivated soil of this station is always kept bare, so it can be considered as a reference surface compared with surfaces changing in every season. On the basis of all these facts our aim was convenient, namely to investigate the pointlike radiation balance using the national direct measurements at the Erdőhát station, assuming its representativeness.

Table 6. contains the average monthly sums per hour (cal/cm^2 hour) and per day (cal/cm^2 day), of the radiation balance based on 20-year average sets. In Fig. 3. the isopleths have also been drawn on the basis of the above-mentioned data. In this figure the times of the sunrise, and the sunset (L. M. T.) have also been presented with dashed lines. The maximum hourly value is 36,4 cal between 11 a. m. and 12 a. m. of June. The absolute maximum value is 46 cal between 12 a. m. and 1 p. m. of July 1952. Isopleths with 35 cal surround a three-hour period (10 a. m. – 1 p. m.) in June, and a two-hour period (11 a. m. – 1 p. m.) in July. In the different months the maxima appear between 11 a. m. and 12 a. m. alike, excluding its occurence between 12 a. m. and 1 p. m. in July. The closed isopleth of 30 cal is appearing in April, however, it does not concern Sep-

tember. Naturally, there are values greater than 30 cal of September in the different years. This fact is somewhat surprising because the middle month of the spring, April is generally compared with the middle month of autumn, October. Concerning the radiation balance, September is not equivalent to April. The other isopleths parallel to the curves of the sunrise and sunset, being open in our figure. They are certainly closed in the corresponding winter months half-year. However, we have no proper data for the winter half-year because of the following: there are no albedo measurements, and applicability of the method is limited.

Table 7

	April	May	June	July	August	September
1951	6 693	6 791	7 957	7 957	6 509	2 128
1952	4 153	5 503	10 103	10 985	8 504	4 113
1953	7 187	8 492	9 419	9 856	7 507	4 610
1954	5 513	8 726	8 708	7 665	7 908	4 214
1955	6 110	8 964	8 049	7 022	5 967	3 635
1956	5 698	7 438	7 544	7 993	7 132	4 774
1957	4 765	4 819	11 034	8 287	7 444	3 979
1958	6 145	11 499	7 904	9 776	8 851	4 715
1959	6 410	9 082	8 100	8 016	6 277	4 210
1960	4 861	6 132	7 212	6 342	5 897	2 580
1961	6 426	7 419	8 871	8 571	7 538	4 424
1962	4 762	7 111	7 676	7 117	6 758	3 278
1963	4 303	5 636	7 129	6 987	6 032	3 812
1964	5 697	6 737	7 594	8 694	6 309	4 068
1965	3 907	6 726	7 904	8 317	6 068	3 621
1966	4 667	7 737	7 797	7 316	5 852	3 642
1967	5 456	7 869	9 131	8 614	6 980	3 491
1968	5 525	6 938	8 006	7 699	5 402	3 242
1969	6 132	8 130	7 793	8 590	5 562	4 090
1970	5 280	7 737	8 940	7 935	6 437	4 745
mean	5 485	7 474	8 343	8 187	6 747	3 869

In Table 7 the original time-series of the radiation balance may arouse some interest. Data in this table are based on a 20-year set obtained for the six months of the summer half-year in cal/cm^2 month values.

Averaged for 20 years the maximum is 8,3 Kcal in June. The value of 8,1 Kcal in July comes close to the above-mentioned value. In our set the peak value is 11.5 Kcal in May 1958, and the minimum value for the summer half-year is 2.1 Kcal in September 1951.

Concerning the data reported here, one fact should be taken into consideration: the estimation of the error is based on the literature data because of the lack of a direct balance-meter. According to reference [16], there is an excellent agreement between the values calculated by the above-mentioned method and the measured values of the average monthly

data. The relative errors of the calculated hourly and daily values are smaller than 10 – 15 per cent of the measured values.

Let us emphasize finally that the data reported in this study may enhance just a modest progress in the investigation of the national radiation balance. Actually, the direct measurements have been restricted indeed to the short-wave component of the radiation balance.

REFERENCES

Dobosi Z. (1957): Vizsgálatok egy hazai talajfelszín sugárzási mérlegéről. Időjárás 61. évf. 260 – 265 p.

Dobosi Z. (1963): A sugárzási mérleg eloszlása Magyarországon. A Kárpátok hatása az időjárásra c. kötetben Akadémiai Kiadó, Budapest. 267 – 271 p.

Bacsó N. (1959): Magyarország éghajlata. Akadémiai Kiadó, Budapest.

Dobosi Z. – Felméry L. (1971): Klimatológia. 490 p. Tankönyvkiadó, Budapest.

Major Gy. – Tárkányi Zs. (1969): A számított sugárzási egyenleg területi eloszlása Magyarországon. Időjárás 73. évf. 81 – 85 p.

Fleischer, R. (1954): Der Jahresgang der Strahlungsbilanz und ihrer Komponenten. Annalen der Meteorologie. H. 11/12. 1953/54.

Shaw, R. (1956): A Comparison of Solar Radiation and Net Radiation. Bull. Am. Met. Soc., Vol. 37. 205 – 206 p.

Павлов, А. В. (1962): Расчетный способ определения радиационного баланса по суммарной радиации. Изв. АН СССР, сер. геогр. № 6.

Davies, J. A. (1967): A Note on the Relationship Between Net Radiation and Solar Radiation. Q. J. Roy. Met. Soc., Vol. 93. 109 – 115 p.

Bossolasco. M. (1965): Ricerche sulla radiazione solare. Contributi dell'Inst. G. e. G. dell'Univ. di Genova. N. 3. Roma.

Lettau, H. – Davidson, B. (1957): Exploring the Atmosphere's First Mile. Pergamon Press, London.

Monteith, J. – Szeicz, G. (1961): The radiation balance of bare soil and vegetation Q. J. Roy. Met. Soc., Vol. 87. 159 – 170 p.

Барашкова, Е. П. (1961): Радиационный баланс Карадага. Актинометрия и атмосферная оптика. Гидрометизд. Ленинград.

Барашкова, Е. П. (1961): Радиационный режим СССР. Гидрометизд. Ленинград.

Берлянд, Т. Г. – Мухенберг, В. В. (1963): Роль поглощенной радиации в формировании радиационного баланса. Трубы Г.Г.О. 139. Гидрометизд. Ленинград.

Гагуа, В. П. (1968): Методика косвенного определения часовых величин радиационного баланса. Трубы Г.Г.О. 233. Гидрометизд. Ленинград.

THE ORIGIN OF THE JURASSIC FAUNAL PROVINCES AND THE MEDITERRANEAN PLATE TECTONICS

by
B. GÉCZY
(Institute of Paleontology, Eötvös University, Budapest)
(Received: 1st March, 1972)

РЕЗЮМЕ

Сформирование и разделение фаунапровинций нижней-юры связаны с географическим разделением, причиненным тектоническими движениями, и это разделение вызвало широкое приспособление и развитие Аммоноидов.

Первичная медитерранская фаунапровинция вследствие раскрывания Тетхис, постепенно разделялась на три части·

1. южный, карбонатный граничный комплекс
2. средний, океанский район
3. северный граничный комплекс, с большим содержанием терригенного материала.

Южный граничный комплекс-это территория с малым количеством отложений, сформировавшаяся из бывшего карбонатного платформа, после его раздробления и потопа. Разнородный рельеф морского дна создал экологические камеры, способствующие специализации Аммонитов. С точки зрения количественного и качественного состава, фауна южного граничного комплекса является самой богатой. Об аммонитной фауне средней части раскрывающегося океана из за последующей двойной селекции, мы относительно мало знаем. На близкорасположенном к устойчивой европейской пластине северном граничном комплексе, который характеризуется быстрым потопом и отложением значительного количества терригенного вещества, медитерранские обвиквистичные и Северозападно-Европейские породы присутствуют примерно в равных количествах. Северозападно-европейская фаунапровинция образовалась в мелком море, которое покрывало большую часть устойчивой европейской пластины. Трансгрессия может быть отнесена к эустатическому изменению уровня моря, связанному с образованием средних океанских хребтов. С усилением трансгрессии оказались под уровнем моря и те районы, которые раньше обеспечивали расход обломковой материи, и на обеих граничных комплексах океанское влияние стало доминирующим.

В Венгрии горы Баконь первоначально принадлежали к карбонатной платформе южной границы Тетхиса, а горы Виллань и Мечек принадлежали к северному комплексу, взятому в более широком смысле. Настоящее, обратное распределение является результатом горизонтального движения более мелких пластин, расположенных между устойчивыми африканской и европейской пластинами.

Introduction

It was more than a century ago that the Mediterranean and "Central European" faunal provinces were separated by N e u m a y r (1871, p. 521) on the basis of the high frequency or sparsity of the phylloceratids and lytoceratids. The distribution of the Lower Jurassic ammonites of the

two provinces was discussed by Donovan (1967) in detail. Donovan included Spain, Morocco, Algeria, Sicily, Italy and Greece into the Mediterranean realm, and the Carpathians and Hungary into the Alpine regime. NW Europe corresponding to the Central European faunal province includes England, the Low Countries, Denmark, Southern Sweden and the extra-Alpine territories of France and Germany. The Mediterranean-Alpine province is equivalent of the mobil belt, while the Central-European province corresponds to the stable Europe tectonically. The recent faunistical results and the plate tectonic concept complete and modify Donovan's synthesis.

Arkell (1956, p. 607.) considered the Lower Jurassic ammonite faunas to be universal. However, by the synthesis of Donovan (loc. cit. p. 127.) beside unrestricted genera, there are certain forms occuring only in the south, certain ones appearing only in the north. On the basis of his data the percentage distribution of genera is as follows:

Stages	Northern	Unrestricted	Southern
Toarcian	7%	76%	17%
Pliensbachian	23%	26%	51%
Sinemurian	28%	35%	37%
Hettangian	—	40%	60%

This synthesis shows the faunal profusion and the independence of the southern faunal province up to the Toarcian. But whether the southern faunal province is undivided remains a question.

The further studies need quantitative examinations based upon specimen numbers. In this way the sources of error caused by sparse occurence of certain ammonites can be eliminated. Since the organisms in question are not sessile, some specimen might fossilize in exotic realm, but these mark rather dispersion than real areal distribution. On the other hand the rare species occuring sparsely in both provinces will remain a matter of other consideration.

The fauna

Arkell (loc. cit. p. 190.) considered the Bakony Mountains in Hungary the one of the world's richest areas for Liassic ammonites. The undisturbed stratification accompanied to great faunal profusion provided particularly suitable conditions for quantitative examinations. The quantitative distribution of the Sinemurian, Pliensbachian and Toarcian ammonite faunas collected from ammonitico rosso and Hierlatz limestone facies is established on more than 31.000 specimen. The result is reviewed by superfamilies, according to Schindewolf's (1960–68) classification.

a) *Phylloceratacеae*

Some genera (e. g. *Schystophylloceras, Paradasyceras)* of this most characteristic Mediterranean superfamily derived from Lower Triassic ancestors can be found even in the Hettangian ammonitico rosso of the Eastern Alps and Eastern Carpathians. The Hettangian strata of the Bakony Mountains yielded no ammonite faunas so far. Here the first representatives *(Geyeroceras)* of the family Phylloceratidae appear in the basal Lower Sinemurian, and the first juraphyllitids *(Juraphyllites)* occur in the basal Upper Sinemurian. The genus *Phylloceras* together with *Partschiceras* appears at the lower boundary of the Upper Sinemurian. D o n o v a n (1967, p. 114.) took into account gradual east to west spreading of the phylloceratids. The early appearance of genera in the Bakony Mountains confirms this assumption. From the representatives of the specialized Phylloceratacеans the galaticeratids occured in the lower part of the Lower Pliensbachian, the harpophylloceratids and the meneghiniceratids in the middle part of the Lower Pliensbachian and the calliphylloceratids at the Sinemurian/Pliensbachian boundary respectively.

The single large *Paradasyceras* specimen was collected from the basal Upper Sinemurian, hence this genus lived longer in the Bakony Mountains as in the southern and northern areas.

The Phylloceratacean genera *Phylloceras* and *Calliphylloceras* are frequent in the Lower Jurassic continually. *Partschiceras* is especially characteristic in the Carixian, sporadic in the Middle Domerian, very rare in the Upper Domerian, but in the Toarcian is absent. The flourishing period of the juraphyllitids is in the Upper Carixian Davoei Zone. From this time they decreased in both specimen and species number, and at the top of the Middle Domerian disappeared without leaving any descendants. Similar is the case with *Harpophylloceras* and *Meneghiniceras*, genera having lower frequency than that of the Juraphyllites.

The lack of tragophylloceratids in the Mediterranean areas was emphasized by D o n o v a n too, though single specimen was found in the Fleckenmergel facies of the NW Carpathians (G é c z y 1959). This Central European zonal-index genus is unknown in the Bakony Mountains.

b) *Lytoceratidae*

This another characteristic superfamily of the Mediterranean faunal province occurs in the Lower Jurassic of the Bakony Mountains in great specimen number and diversity. The early (Lower Sinemurian, Bucklandi Zone) appearance of the genera *Tragolytoceras* and *Adnethiceras* as well as the greater species-number of the family Pleuracanthidae restricted excusively to Mediterranean areas are of special interest. The first representatives of the genus *Lytoceras* can be sporadically found as early as basal Upper Sinemurian, and from the Lower Pliensbachian onwards they are common. The northern Alpine and Bakony Mountains occurence of many species of the genus *Holcolytoceras* originally designated from the

Ibex Zone of the Central European faunal province (Württemberg), as well as the survival of the species *H. quadrijugum* (R o s e m b e r g 1909) into the Davoei Zone suggests Mediterranean origin for this group. The genus *Aegolytoceras* appears in the Bakony Mountains in the Lower Pliensbachian (Jamesoni Zone), and the species *Aegolytoceras? fuggeri* (G e y e r 1893) is especially characteristic to the Davoei Zone. The audaxlytoceratids are most frequent in the middle part (Davoei and Stokesi Zones) of the Pliensbachian, and disappear in the Spinatum Zone.

The Lytoceratacean invasion due to the Toarcian transgression led in the NW European faunal province to development of special forms (*Trachylytoceras*, *Pleurolytoceras*, etc.). The majority of these forms is hitherto unknown in the Bakony Mountains.

c) *Psiloceratacea*

The earliest Ammonitina firstly adopted epipelagic habit appear within the Psiloceratacea, superfamily had been arised from the presumably bathypelagic Phylloceratacean (or Lytoceratacean). The Psiloceratacean appeared at the beginning of the Jurassic transgression, namely at the Triassic/Jurassic boundary (T o z e r 1971, p. 565.). The shallow-water conditions facilitated their distribution during the Hettangian, therefore it is clear that their majority was originally ubiquitous.

The subfamily Schlotheimiinae is excusively represented in the Bakony Mountains by the genus *Angulaticeras* restricting to the Upper Sinemurian. The world-wide genus *Metophioceras* can be found also in the Bakony Mountains, on the other hand the large coroniceratids characteristic to the NW European faunal province are absent. The occurence of the genera *Eparietites* and *Aegasteroceras* supports the opinion of D o n o v a n (1967, p. 118.), who indicated wide-spread paleogeographic distribution to these genera. The Obtusum Zone occurence of the new subspecies of *Protechioceras formosum* (F u c i n i 1902) previously known only from Italy elucidates the Mediterranean origin of Echioceratidae, a subfamily flourishing in the NW European area. The family Oxynoticeratidae is represented in the Bakony Mountains mainly by the genus *Paroxynoticeras*, the probable Mediterranean counterpart of the genus *Oxynoticeras* flourished in NW Europe.

In the Bakony Mountains the Cymbitidae is too sporadic in occurence to conclude anything for the evolution centre of this family.

The genera *Bifericeras*, *Ophideroceras* and *Hemimicroceras* of the family Polymorphitidae are hitherto unknown in the Bakony Mountains. The genus *Eoderoceras* is very rare, but the genera *Microderoceras*, *Hyperderoceras*, *Epideroceras*, *Apoderoceras*, *Tetraspidoceras* and *Metaderoceras* are more common. The lack of genera *Pimelites*, *Diaphorites* and *Kondiloceras* suggests more southerly Mediterranean restriction of these forms. Of the genus *Phricodoceras* the wide vertical range is striking. While the genus in NW Europe is characteristic to the Jamesoni Zone, in the Bakony Mountains it persists in the whole Carixian. On the other hand the deri-

vation of *Phricodoceras* from the Lower Sinemurian *Adnethiceras* (c.f. Wiedmann 1970, p. 1002.) has no paleontological evidence at all. The vertical range of the *Coeloceras* s. l. is similar to that of the genus *Phricodoceras*. In NW European areas the *Coeloceras* is restricted to the Jamesoni Zone, but in the Préalps Medians, in Asia Minor and in the Bakony Mountains the first coeloceratids (i.e. *C. oosteri* Hug 1899) appeared as early as the Raricostatum Zone, and existed more advancely in all of the Carixian zones. The species ranged by Pinna and Levi–Setti (1971, p. 60–72.) into the genera *Aveyroniceras* and *Reynesoceras*, are, together with numerous prodactylioceratids, characteristic to the Davoei Zone. The afore mentioned species are separable from the *Reynesoceras* s. str., a genus characteristic to the Margaritatus Zone. The lower part of the Stokesi Zone yielded several specimen of *Porodactylioceras? psiloceroides* (Fucini 1905). Consequently this species can be rather the last representative of the prodactylioceratids than the transient to the Dactylioceratidae. In the Bakony Mountains the Mediterranean species of the Dactylioceratidae are dominant. Modern explanation of the paleogeographical connections of this family is given by Pinna and Levi – Setti (1971).

The genera *Tropidoceras* and *Gemmellaroceras* are very common in the Bakony Mountains. Additionally the genera *Polymorphites*, *Platypleuroceras* and *Uptonia* occur subordinately. The genus *Dayiceras* characteristic in the Western Mediterranean and England is unknown in the Bakony Mountains. Apart from *Vicininodiceras* all genera of the family Liparoceratidae is present in the Bakony Mountains, but neither of these genera is common or characteristic to any strata. The sporadic occurence of *Oistoceras* is remarkable, because the Amaltheidae presumably derived from these forms. On the basis of the Bakony Mountains occurence of the most primitive *Amaltheus* (*A. bifurcus* Howarth 1959) it is not improbable the Mediterranean origin if this family too. This family migrated into the more favourable epicontinental area presumably from this region. Otherwise the NW European origin of this family was accompanied with widespread distribution without any success in the densely-populated Mediterranean realm. Nevertheless the almost total absence of the genera *Amaltheus* and *Pleuroceras* is the most striking feature of the fauna-rich Domerian beds of the Bakony Mountains.

d) *Hildoceratacеae*

The Mediterranean origin of this superfamily is supported not only by its high frequency, but its early (Upper Sinemurian, Fischer 1971) appearance in the Mediterranean area. In the Bakony Mountains the earliest *Protogrammoceras* is yielded from the topmost Jamesoni Zone, and the genus flourished in the Stokesi Zone. The genus *Eofuciniceras* was restricted to the Ibex and Davoei Zones, on the other hand the more frequent and abundant genus *Fuciniceras* was dominant in both the Davoei and Stokesi Zones. The first proarieticeratids occured in the lower part of the Stokesi Zone, and the flourishing of the mere *Arieticeras*

can be restricted to the Margaritatus Zone. *Emaciaticeras* can be sparsely found in the Spinatum Zone.

The Mediterranean feature of the Bakony Mountains Toarcian faunas is determined partly by the high frequency of *Mercaticeras* and partly by the marked absence of grammoceratids. Southerly (in the Mecsek Mountains) and easterly (in Transsylvania, c.f. P a t r u l i u s – P o p a 1971, p. 135; P r e d a 1971, p, 430) to the Bakony Mountains the *Grammoceras* and *Pseudogrammoceras* species are very common, but, in contrast to the Bakony Mountains, in a facies of rich in terrigenous material!

The ubiquitous genera *(Hildoceras, Harpoceras, Polyplectus,* etc.) of the superfamily Hildocerataceae are common also in the Bakony Mountains.

e) *Hammatocerataceae*

This superfamily equally comprising Mediterranean, NW European and ubiquitous genera unites the most developed Lower Jurassic ammonites. The Mediterranean character of the Bakony Moutains fauna is reasonable from the high frequency of the genera *Frechiella* and *Erycites*, as well as the *Dumortieria* species restricted to the Mediterranean realm.

Fauna and facies

The Lower Jurassic ammonites of the Pannonian basin and surrounding areas occur in the following litho- or biofacies types:

1. Carbonate rocks free of terrigenous material:
   a) Ammonitico rosso,
   b) Hierlatz limestone,
2. Carbonate rocks rich in terrigenous material:
   a) Fleckenmergel.

The carbonate rocks free of terrigenous material are characterized by reduction of the sequences on the one hand, and quick temporal and spatial alteration of litho- and biofacies on the other. The dominant biofacies are the predominantly red, nodular calcilutite, the ammonitico rosso limestone and its varieties. The occurence of Hierlatz-type calcarenite is more subordinate.

The carbonate rocks rich in terrigenous material are ranged into the type Fleckenmergel (Allgäu Beds) characterized by great thickness and facies monotony.

The ammonite faunas of the two main carbonate rock-types are different.

1. In the rocks free of terrigenous material the Mediterranean forms are predominant, namely either the families Phylloceratidae, Juraphyllitidae and Lytoceratidae, or other Mediterranean groups, e.g. *Paroxynoticeras, Protogrammoceras* and *Fuciniceras* as well as

specialized coeloceratids and erycitids. Ubiquitous forms are subordianete and strictly NW European species are rare or absent.

2. In the rocks rich in terrigenous material the proportion of Mediterranean, ubiquitous and NW European species is simliar.

In order to demonstrate the different faunal content, the distribution of 170 Pliensbachian ammonite species, collected from the Bakony Mountains ammonitico rosso and 202 ammonite species of the Bavarian Alps' Fleckenmergel studied by Schröder (1927) is given below. Schröder's data refer to the fauna of the whole Lower Jurassic sequence.

	Ammonitico rosso limestone	Fleckenmergel
Mediterranean	77%	38%
Ubiquitous	11%	29%
NW European	9%	22%
Endemic, etc.	3%	11%

If the ammonites had been benthonic, the difference of deposits would directly elucidate the dissimilarity of the faunal content. But the nekto-planktonic ammonites are clearly independent of the nature of the bottom (Hahn 1971, p. 524).

The difference between the Mediterranean and Central or NW European faunal province was explained by Neumayr (1871, p. 524) and Donovan (1967, p. 130) finally with temperature variation. But the temperature data (20 – 22.5 C°) based on oxigen isotopic studies of the two (ammonitico rosso and Fleckenmergel) Mediterranean facies are identical (Fabricius 1967, p. 214). Consequently *within* the Mediterranean realm the faunal differentiation is unexplicable on the basis of temperature variation.

The specialization of certain ammonite groups in the shallowly overflown NW European area can be interpreted by food and possibly temperature changes (Hallam 1967, p. 214). On the other hand the carbonate rocks rich in terrigenous material in the Mediterranean area had undoubtedly greater organic matter supply from land masses, while the fauna here just poorer comparing with that of the carbonate rocks free of terrigenous material. The faunal content of the Mediterranean areas suggests normal salinity sea-water according to Hallam too.

In separation of Mediterranean and Central European faunal provinces the depth-differences has a part in some respect. The phylloceratids and lytoceratids were considered even by Haug (1911, p. 938) as bathyal organisms living in the deepest troughs of the geosynclinal axis. The deeper-water habit of the phylloceratids and lytoceratids is evidenced by increasing proportional number going from shallow to deeper water sediments (Géczy 1958, p. 127) on the one hand, and the more resis-

ting inner shell structure (Westermann 1971, p. 34) on the other. Within the Mediterranean realm the lack or scarcity of phylloceratids and lytoceratids is reasonable on the submarine topographic highs. On the other hand on these swells not NW European, but markedly Mediterranean faunas can be found. The quantitative examinations carried out by Fischer (1971, p. 116) are especially remarkable in this respect. The classical fauna of Monte Cetona is of markedly Mediterranean character, despite of the low proportion of the phylloceratids and lytoceratids.

The deposition depth of the carbonate rocks free or rich in terrigenous material is in dispute. Hallam (1971a, p. 141) regards the ammonitico rosso limestone and both the ammonitico rosso marls and Fleckenmergel as deposited in smaller and greater depth respectively. It is more likely, however, that the different types of the ammonitico rosso limestone were deposited in different depth.

The carbonate rocks free or rich in terrigenous material certainly indicate two different paleogeographical units. These two units in Hungary can be easily separated. In the NW portion of the Pannonian basin (i. e. Bakony and Gerecse Mountains) the Jurassic is represented only by rocks of free in terrigenous material. In the Mecsek and Villány Mountains situated in the south, terrigenous material rich rocks (coal measures of Gresten type and Fleckenmergel) occure exclusively (Fülöp 1971, p. 32). In the Carpathians of Roumania (Eastern Carpathians, Southern Carpathians, Apuseni Mountains) the rocks rich in terrigenous material are characteristic, while the red "Adneth type" limestones corresponding to ammonitico rosso occur solely as small, isolated "olistoliths" within the Transsylvanian Nappe of the Eastern Carpathians (Patrulius–Popa 1971, p. 131).

In the Great Fatra area of the Northern Carpathians the Fleckenmergel is characteristic to the northern, while the Adneth limestones to the central part, with contact of the two types (Mišik – Rakus 1964, pp. 174–175).

In the Alpine regions the rocks of free and rich in terrigenous material are associated. But the explanation of the depositional depth of the two main lithofacies types is greatly encumbered because of the complicated tectonics. According to the Alpine geologists the terrigenous material of the Fleckenmergel was originated partly from the Bohemian Forest massif or from its westerly prolongation, the "Windelician Land", and partly from the lands proceeded from the breaking up of these landmasses (Hölder 1964, pp. 359–72). The source area of the terrigenous material of the Fleckenmergel was certainly in close connection with the Variscan stable Northern Europe.

The Lower Jurassic rocks free of terrigenous material can be detected southerly in Western Greece, in the Southern Alps, in the Apennines and in Sicily (Bernoulli and Jenkyns 1970, p. 516). Bernoulli and Peters pointed out (1970, p. 619) that the "paleotectonic evolution" of the Bakony and Gerecse Mountains is very similar to that of the Trento Zone in the Southern Alps, the Umbrian Apennines and

Western Sicily. Presumably these areas originally belonged to the vast continuous carbonate platform bordering the *southern* margin of the Tethys (Laubscher 1970, p. 815). The differentiation and the following superimposition and juxtaposition of the two paleogeographical unites can be explained by plate tectonic movements.

Facies and tectonics

On the area under consideration the opening of the Tethys was initiated by constant submergence of the continental crust. The sedimentation keeping pace with the submergence led to shallow-water deposition of great thickness. The carbonate platform including originally the Bakony Mountains formed in the Triassic in this way. The lowland of the stable Europe was overflown by the transgression commenced at the Triassic/Jurassic boundary, bringing a new faunal province about. The transgression accompanied practically the whole Jurassic is related to eustatic sea-level rise due to the elevation of middle-oceanic ridges (c.f. Hallam 1969, Brookfield 1970). On the basis of the facies-connection existed in the lowermost Jurassic the middle-oceanic ridges of that time were outside the Alpine–Carpathian area.

The alterations within the Mediterranean realm are unexplicable merely by the Jurassic transgression. The Mediterranean realm was not completed with the newly formed epicontinental shallow-water seas, but with the sinking area developed along the northern margin of the Tethys, i.e. along the southern border of the stable Europe. The subsidence of this area is more intensive than the result of eustatic sea-level changes could be. In the Mecsek Mountains the total thickness of the Gresten facies s. l. and the overlying Fleckenmergel is estimated to 3500 m (Nagy 1971, p. 159) and 2600 m (Fülöp 1971, p. 32) respectively. On the northern margin the subsidence was equated by great terrigenous material supply. On the other hand at the southern carbonate platform this was not the case.

If only the biogenic sedimentation of the carbonate platform had ceased in the earliest Jurassic, it would be explained by sea-level changes. Some sea-level changes accompaniing with light and temperature decrease yield unfavourable conditions for the reef-building organisms. But on the southern areas crustal movements unrelated to sea-level changes can be recognized during the subsidence of the northern marginal area. These tectonic movements are of dilatational character and resulted in the breaking up of the carbonate platform. More or less parallel to the border of the platform relatively narrow basins and submarine highs, locally associated with seamounts and islands were formed (Bernoulli 1967, Jenkyns 1970, Bernoulli and Renz 1970, Hallam 1971b). The tectonic mevements are indicated by the appearance of abruptly opening fissures, "oceanic" facies and synsediment breccias (c.f. Wiedenmayer 1963, Aubouin 1964, Castellarin 1966, Garrison-Fischer 1969, Jurgan 1969, Trümpy 1971,

Schöll – Wendt 1971, Wendt 1971, etc.). These movements can be faunistically dated.

The synsediement tectonic movements and the reduction of sedimentation, i.e. the formation of "starving basin", began to exist in the Eastern Alps as early as the Late Triassic (Schlager 1969). The ammonitico rosso facies in both the Eastern Alps and the Eastern Carpathians in some places is characteristic even in the Hettangian. This segment, therefore, has broken away probably earlier from the carbonate platform. The first traces of ammonitico rosso sedimentation can be detected in the Bakony Mountains in the Lower Sinemurian, and the earliest fissures formed before the Late Sinemurian sedimentation (Konda 1970, p. 234.). Consequently the Bakony segment separated form the carbonate platform later as compared to the westerly and easterly lying areas, but much earlier than the segments situated southerly. In Western Greece the southern margin of the Tethys started to breaking up in the Middle Liassic (Bernoulli – Renz 1970, p. 591), but in Sicily in the Toarcian only (Jenkyns – Torrrens 1971 p. 95). Consequently the disintegration of the carbonate platform most likely took place heterochronously. In the course of the periodical disinteg-

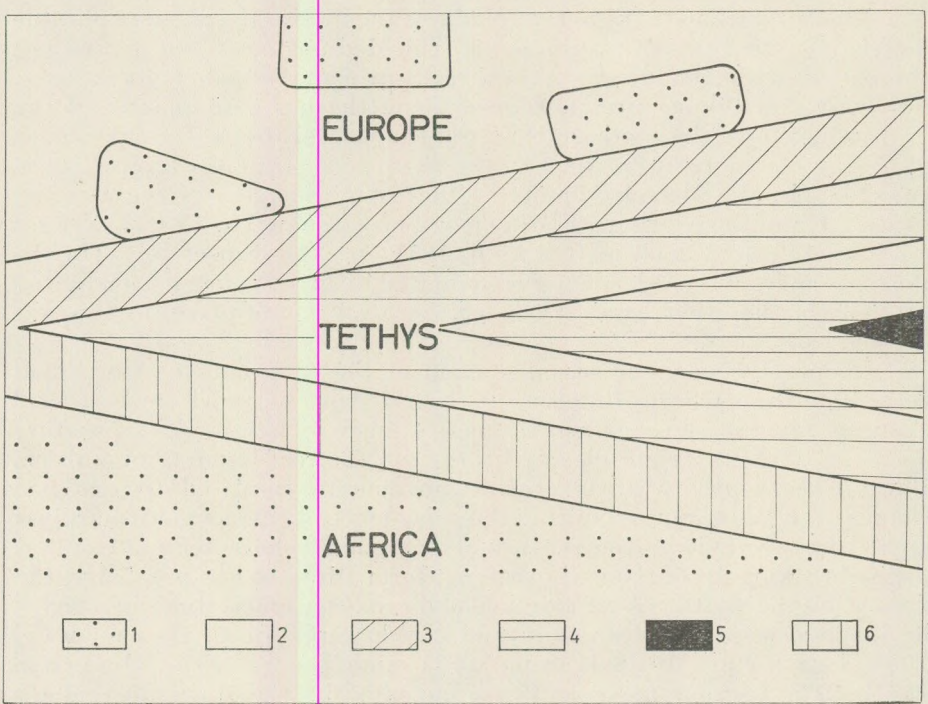

Fig. 1. The relationships of the NW European (white) and Mediterranean (hatched) provinces, and the original tectonic units.

(1 = lands; 2 = epicontinental shallow-water sea; 3 = northern marginal depression; 4 = oceanic sea floor; 5 = middle-oceanic ridge; 6 = southern carbonate marginal complex)

ration the certain units drifted gradually away from the African plate. Then these subsiding units came increasingly under oceanic influence.

The breaking up of the former carbonate platform as well as the development and permanent subsidence of the structure built up by basins and swells can be due to the controversy of the upper, brittle, and the lower plastic, capable to creep parts of the lithosphere (S t e w a r t 1971, B o t t 1971).

According to L a u b s c h e r ' s large-scale synthesis (1969, 1971), during the closure of the Tethys in the Jurassic the northern and southern complexes separated by the opening ocean came into superimposition with coincident distruction of the original (ofiolitic) bottom. In the course of horizontal movements succeeded the the shifting, certain parts of the northern margin moved southward, and subsequently the Dinarides moved in westward direction. The Mecsek Mountains – adopting L a u b s c h e r' s hypothesis to the mountains of the Pannonian basin – originally belonged to the northern marginal depression of the Tethys. The originally northerly situated Villány Mountains was most likely a smaller portion of the epicontinental area. The two mountains were moved to the present situation by a relatively later, clockwise horizontal movement. It is the solution of the apparent contradiction raised from the present proximity of the pelagic Jurassic sediments of the Bakony Mountains (G é c z y 1961, p. 544) and the contemporary sedimentary basin profusely accumulating clastic material in the Mecsek Mountains.

Tectonics and evolution

The flourishing of Ammonoids in the Jurassic is due to a coincidence of several facts.

1. *The favourable genetic capability* of the Phylloceratáceae with a past of 20 million years permitted this subfamily not only to survive, but also to make manifold further development.
2. The total extinction of Ceratitina lineages at the end of the Triassic presented a *disappearance of competition* in paleobiological point of view.
3. The Lower Jurassic transgression (W i e d m a n n 1970, p. 965) and the oceanicity presented favourable *ecologic niches* providing an opportunity to the manifold adaptation and specialization.

From the lowermost Jurassic onwards the number of ammonite groups increased parallel with the enlarging environmental possibilities. The breaking up of the southern margin of the Tethys and the bottom disintegration into submarine swells and troughs made way to the radiative adaptation of bathypelagic Phylloceratidae probably lived even formerly in deeper waters, or to the differentation of the Mediterranean faunas. The increasing oceanic influence consolidating the environmental circumstances (salt content, temperature) promoted the slow and far-reaching evolutionary processes. On the other hand the southern margin

was probably the development area of ammonite groups wich invaded the shallow-water, diversified, but respecting to the full amount of ammonites more unfavourable NW European realm.

The other consequence of the paleogeographical differentiation was the areally different vertical range, i.e. the heterochronism of certain ammonite groups. Recently several good example furnishes (F i s c h e r 1971, p. 122; G u e x 1971, p. 240) the earlier or later appearance of given forms within certain faunal province, or in different parts of the same province. These forms obviously developed in smaller ecologic niches and became widespread either under the necessity of inner forces (e.g. overpopulation) or by the change of previously specialized external circumstances into universal. The Lower Toarcian world-wide radiation of the Hildoceratinae is most probably in connection with the latter. On the other hand the ecologic niches must have provided relict areas for some groups of declining tendency, resulting in this way their survival for some times.

In contradiction to the ammonite evolution promoting effect of the opening of the Tethys, the paleotectonic movements affected disadvantageously to the remaining. Certain parts of the marginal areas coming increasingly under oceanic influence subsided already in the Early, but especially in the Middle Jurassic into a depth where the calcareous shells were either in part, or as a whole destroyed by subsolution effects. The

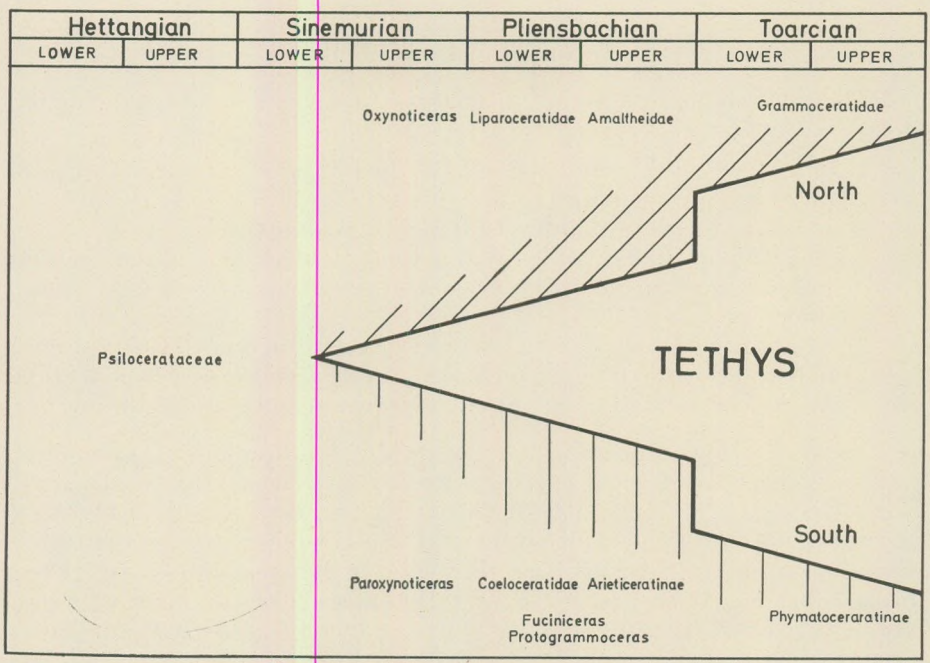

Fig. 2. Separation of Ammonite-faunas in the Lower-Jurassic

oceanic bottom probably was beneath the lysocline as well as the even deeper compensation depth. Consequently the records of the ammonite evolution disappeared tracelessly on increasingly broadering areas immediately after the death of the animals. During the closure of the Tethys the oceanic bottom was subducted, obliterating mostly the traces furnish information on the organisms of the above watermasses. The groups of hitherto unknown genealogy and the cryptogenetic forms probably evolved in this oceanic regions. The groups suddenly appeared in the NW European faunal province were considered by N e u m a y r (1878, p. 57) as of Mediterranean origin. The missing link within the Mediterranean realm was probably restricted to the middle-oceanic areas.

S z á d e c z k y K. E. (1971, p. 89) and J a r d i n e – M c K e n z i e (1972, p. 20) and others suggested relationship between plate tectonic movements and evolution. In the case of the Lower Jurassic ammonite evolution the plate tectonic movements took a prominent part by the enlarging of favourable possibilities.

Conclusions

The origin and disintegration of the Lower Jurassic faunal provinces, which enhanced the wide accomodation and evolution of ammonites is related to the paleogeographical differentiation arised from plate tectonic movements.

The Mediterranean faunal province progressively disintegrated into three part as a result of the opening of the Tethys

1. Southern, carbonate marginal complex (with ammonitico rosso and Hierlatz limestone),
2. Central, oceanic area,
3. Northern, continental marginal complex (Gresten and Fleckenmergel facies).

The southern marginal complex is a sediment-starving area developed from the breaking up and submergence of the former carbonate platform. Its pronounced submarine relief raised favourable ecologic niches for the specialization of the ammonites. The Mediterranean fauna of the southern marginal complex is the richest both in quantitative and qualitative points of view. The ammonite faunas of the central part of the opening ocean are relatively unknown because of the subsequent twofold selection (subsolution of shells and then the destruction of the oceanic bottom). The faunas of the northern marginal complex situated near to the stable Europe and characterized by rapid subsidence and great terrigenous sedimentation are constituted in nearly equal proportion by Mediterranean, ubiquitous and NW European species.

The NW European faunal province developed through the marine overflow of the major part of the stable Europe due to eustatic sea-level changes relating to the elevation of the middle oceanic ridges. In the course of the increasing transgression the source area of the clastic mate-

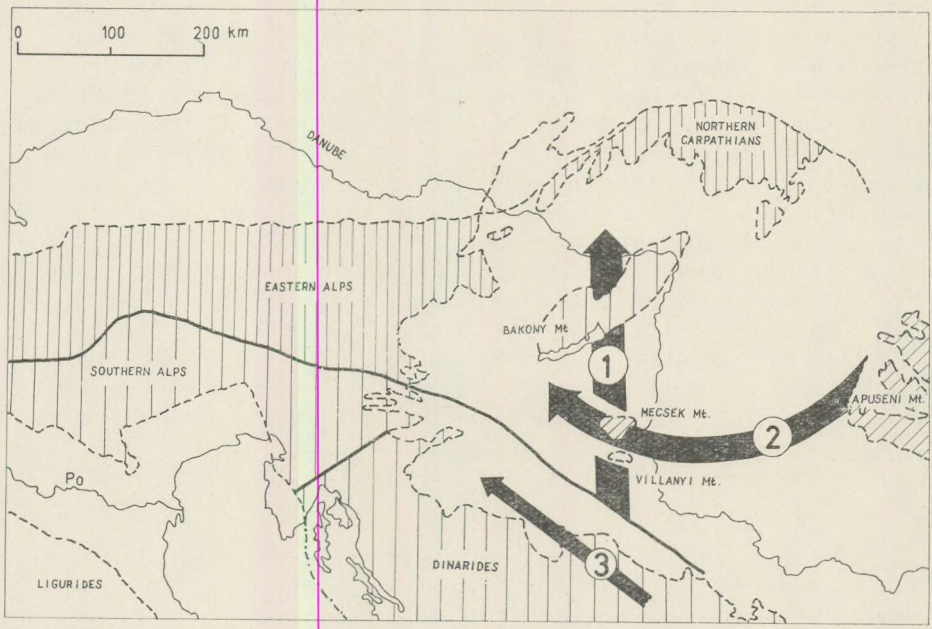

Fig. 3. The present position of the former palaeogeographical units after the closure of the Tethys and horizontal displacements of smaller segments situated between the African and European plates. Numbers indicate the chronological oder of the displacements (Simplified and completed after Laubscher 1971).

rial was also overflown by the sea, and both the northern and southern marginal complexes came under oceanic influence.

In Hungary the Hungarian Central Mountains belonged originally to the carbonate platform of the southern margin of the Tethys. On the other hand the Mecsek and Villány Mountains were parts of the northern marginal complex s.l. The recent inverse position have been arised from subsequent horizontal displacements of smaller segments situated between the stable African and European plates.

REFERENCES

Arkell, W. J. (1956): Jurassic geology of the world. Edinburgh, London. p. 1–806.

Aubouin, J. (1964): Réflexions sur le facies "ammonitico rosso". Bull. Soc. géol. France 7. ser., 6. Paris. p. 475–501.

Bernoulli, D. (1967): Probleme der Sedimentation im Jura Westgreichenlands und des zentralen Apennin. Verhandl. Naturf. Ges. Basel. 78. p. 35–54.

Bernoulli, D. – Renz, O. (1970): Jurassic carbonate facies and new ammonite faunas from Western Greece. Ecl. Geol. Helv. 63. Basel. p. 573–607.

Bott, M. H. P. (1971): Evolution of young continental margins and formation of shelf basins. Tectonophysics. 11,5. Amsterdam. p. 319–327.

Castellarin, A. (1966): Filoni sedimentari nel Giurese di Loppio. Giorn. Geol. 33., 1965. Bologna. p. 527–546.

Donovan, D. T. (1967): The geographical distribution of Lower Jurassic ammonites in Europe and adjacent areas. In: Aspects of Tethyan Biogeography; Syst. Ass. Publ. No. 7. London. p. 111 – 134.

Fabricius, F., Friedrichsen, H., Jakobshagen, V. (1970): Zur Methodik der Paläotemperatur Ermittlung in Obertias und Lias der Alpen und benachbarter Mediterran-Gebiete. Verh. Geol. B.-A. 1970. Wien. p. 583 – 593.

Fischer, R. (1971): Die Coeloceratinen (Ammonoidea) des Monte Cetona (Prov. Siena). Geol. Palaeont. 5. Marburg. p. 93 – 129.

Fülöp J. (1971): Les formation jurassiques de la Hongrie. Ann. Inst. Geol. Hung. 54/2. Budapest. p. 31 – 63.

Garrison, R. E., Fischer, A. G. (1969): Deep-water limestones and radiolarites of the Alpine Jurassic. SEPM Spec. Publ. No. 14. p. 20 – 56.

Géczy B. (1958): Quantitative Auswertung jurassischer Cephalopoden von Csernye. Földt. Közl. 88. Budapest. p. 125 – 127. (in Hungarian with German abstr.)

Géczy B. (1959): Tragophylloceras vadászi (Lóczy, 1915) emend. nov. aus der Klippenzone der NW Karpaten. Geol. Prace 16. Bratislava p. 183 – 7.

Géczy B. (1961): Die jurassische Schichtenreiche des Tűzköves-Grabens von Bakonycsernye. Ann. Inst. Geol. Hung. 49. Budapest. p. 507 – 567.

Guex, J. (1971): Sur la classification des Dactylioceratidae (Ammonoidea) du Toarcien. Ecl. Geol. Helv. 64, Bale. p. 225 – 243.

Hahn, W. (1971): Die Tulitidae S. Buckman, Sphaeroceratidae S. Buckman und Clydoniceratidae S. Buckman (Ammonoidea) des Bathoniums (Brauner Jura Epsilon) im südwestdeutschen Jura. Jh. geol. Landesamt Baden-Württ. 13, Freiburg. p. 55 – 122.

Hallam, A. (1967): Sedimentology and palaeogeographic significance of certain red limestones and associated beds in the Lias of the Alpine region. Scott. J. Geol., 3. p. 195 – 220.

Hallam, A. (1969): Faunal realms and facies in the Jurassic. Palaeontology, 12. London. p. 1 – 18.

Hallam, A. (1969): Tectonism and eustasy in the Jurassic. Earth – Sci. Rev. 5. Amsterdam. p. 45 – 68.

Hallam, A. (1971a): Provinciality in Jurassic faunas in relation to facies and palaeogeography. In: Faunal provinces in space and time. Geol. J. Spec. Iss. No. 4. Liverpool p. 129 – 152.

Hallam, A. (1971b): Mesozoic geology and the opening of North Atlantic. J. Geol. 79. Chicago. p. 129 – 157.

Haug, E. (1911): Traité de géologie. Edit. Colin. Paris. p. 1 – 2024.

Hölder, H. (1964):: Jura. Handbuch d. startigr. Ged. IV. Stuttgart. p. 1 – 603.

Jardine, N. – McKenzie, D. (1972): Continental drift and the dispersal and evolution of organisms. Nature. 235. New York. p. 20 – 24.

Jenkyns, H. C. (1970): Growth and disintegration of a carbonate platform. N. Jb. Geol. Paläont. Mh. Stuttgart. p. 325 – 344.

Jenkyns, H. C. – Torrens, H. S. (1971): Palaeogeographic evolution of Jurassic seamounts in Western Sicily. Ann. Inst. Geol. Hung. 54/2. Budapest. p. 91 – 104.

Jurgan, H. (1969): Sedimentologie des Lias der Berchtesgadener Kalkalpen. Geol. Rundschau. 58. Stuttgart. p. 464 – 501.

Konda, J. (1970): Lithologische und Fazies-Untersuchung der Jura-Ablagerungen des Bakony-Gebirges. Ann. Inst. Geol. Hung. 50. Budapest. p. 161-260.

Laubscher, H. P. (1969): Mountain building. Tectonophysics. 7. Amsterdam p. 551 – 563.

Laubscher, H. P. (1971): Das Alpen-Dinariden-Problem und die Palinspastik der südlichen Tethys. Geol. Rundschau. 60. Stuttgart. p. 813 – 833.

Mišik, M. – Rakus, M. (1964): Bemerkungen zu räumliche Beziehungen des Lias und zur Paläogeographie des Mesozoikum in der Grossen Fatra. Sborn. Geol. Vied Rad ZK. Zvazok 1. Bratislava. p. 157-184.

Nagy, E. (1971): Der unterliassische Schichtenkomplex von Grestener Fazies im Mecsek-Gebirge (Ungarn). Ann. Ist. Geol. Hung. 54. Budapest. p. 155–159

Neumayr, M. (1871): Jurastudien II. Jb. k. k. geol. Reichsanst. 21. Wien. p. 451–536.

Neumayr, M. (1878): Ueber unvermittelt auftretende Cephalopodentypen im Jura Mitteleuropa's. Jb. k.k. geol. Reichsanst. 28. Wien. p. 38–81.

Patrulius, D. – Popa, E. (1971): Lower and Middle Jurassic ammonite zones in the Roumanian Carpathians. Ann. Inst. Geol. Hung. 54. Budapest. p. 131–149.

Pinna, G. – Levi-Setti, F. (1971): I Dactylioceratidae della provincia Mediterranea (Cephalopoda, Ammonoidea). Mem. Soc. Ital. Sci. Nat. 19. Milano. p. 49–136.

Preda, I. (1971): Der Lias des Padurea Craiului. Ann. Inst. Geol. Hung. 54. Budapest. p. 429–432.

Schindewolf, O. H. (1961–68): Studien zur Stammesgeschichte der Ammoniten. I–VII. Abhandl. Akad. Wiss. Literat. Mainz, Math-nat. Kl. Wiesbaden. p. 1–901.

Schlager, W. (1969): Das Zusammenwirken von Sedimentation und Bruchtektonik in der triadischen Hallstätterkalken der Ostalpen. Geol. Rundschau. 59. Stuttgart. p. 289–308.

Schöll, W. U. – Wendt, J. (1971): Obertriadische und jurassische Spatenfüllungen im Steinernen Meer. N. Jb. Geol. Paläont. Abh. 139. Stuttgart. p. 82–98.

Schröder, J. (1927): Die Ammoniten der jurassischen Fleckenmergel in den bayrischen Alpen. Palaeontographica 68. Stuttgart. p. 111–232.

Stewart, J. H. (1971): Basin and range structure: A system of horst and grabens produced by deep seated extension. Geol. Soc. Amer. Bull. 82. Boulder. p. 1019–1044.

Szádeczky-Kardoss, E. (1971): Mechanism of the new global tectonics and its relations to the evolution of the Earth and life. Geonómia és Bányászat. 4. Budapest p. 3–89. (in Hungarian with English abstr.)

Tozer, E. T. (1971): One, two or three connecting links between Triassic and Jurassic Ammonoids. Nature, 232. New York. p. 565.

Trümpy, R. (1971): Stratigraphy in mountain belts. Quart. J. Geol. Soc. London. 126. p. 293–318.

Wendt, J. (1971): Genese und Fauna submariner sedimetärer Spaltenfüllungen im Mediterranen Jura. Palaeontographica, 136. A. Stuttgart. p. 121–192.

Westermann, G. E. G. (1971): Form, structure and function of shell and siphuncle in coiled mesozoic ammonoids. Life Sci. Contr. R. Ont. Mus. 78. Toronto. p. 1–39.

Wiedenmayer, F. (1963): Obere Trias bis mittleren Lias zwischen Saltrio und Tremona (Lombardischen Alpen) – Die Wechselbeziehungen zwischen Stratigraphie, Sedimentologie und syngenetische Tektonik. Ecl. Geol. Helv. 56. Basel. p. 529–640.

Wiedmann, J. (1970): Über den Ursprung der Neoammonoiden – Das Problem einer Typogenese. Ecl. Geol. Helv. 63. Basel. p. 923–1020.

AN ALGORITHM FOR AUTOMATIC SEISMIC REFLECTION PICKING

by
I. KÉSMÁRKY
Geophysical Prospecting Company of the Hungarian Oil and Gas Trust, Budapest
(Received: 10th March, 1972)

SUMMARY

The object of this paper is to present a new mathematical model of reflection picking based on the tehory of Markov-chains. The corresponding computer program, the flow chart of which is also given, seeks for regularly positioned local maxima and classifies the elementary reflections on the basis of their average amplitude. Elementary reflections are defined as at least 7 local maxima on neighbouring traces in a predefined neighbourhood of a straight line.

The usefulness of the method is demonstrated on a synthetic seismogram. The results of the present method and those of the P a u l s o n – M e r d l e r's method are also compared.

Introduction

One of the ambitions of the fundamental research done in the field of digital processing of seismic data is to draw the computer into the interpretation. It involves that besides the now existing and currently applied algorithms for corrections, filtering, stacking, velocity determinations etc. interpretation oriented routines have to be developed. One of the most important among these routines is the automatic reflection picking. If the reflection picking could be automated the interpretation would become faster and the subjective errors may also be decreased.

The picking techiques, reported in the literature are based on cross-correlation (Massé, 1955; B a r a n o v and Picou, 1964) or on the lateral continuity of positive maxima (P a u l s o n and M e r d l e r, 1968).

The governing idea of the latter is the fitting of a straight line through local maxima of three neighbouring traces, using he method of the least squares. The time instant, where the straight line intersects the fourth trace, together with an allowed error interval $\pm \Delta$ defines an interval where the local maxima of the fourth trace should lie. If a maximum is really found in the interval the process can be similarly continued, normally from the left to the right. In the P a u l s o n – M e r d l e r's method three peaks form a reflection element.

Main ideas of the reflection picking

Reflections may be detected by the following criteria:

phase continuity,
increased energy level,
identical (or very similar) frequency content and wavelet shape.

In practice, however, the energy level peak may be so small that it has no significant diagnostic value. We shall also leave out of consideration of the last property of a reflection event. Phase continuity will be taken into account, only. This simplification seems justified because analogue interpretation is also based on the regular alignment of peaks. Thus we considered our main task to recognize the arrival of coherent energy and tracing the reflection elements through possible crossings and branchings of the individual reflection axes.

The picking operation is subdivided into two steps as follows.

1. We try to recognize and store all coherent events which can be observed on a seismogram or on a seismic section. These events may be reflections but are not necessarily those. That is this part of the algorithm extracts all information which may be useful.

2. In this step we classify the events in order to select those which can be qualified as reflections at a reasonable probability level. The selection is based on the numerical values of some parameters (e.g. length of the reflection element, expressed in the number of traces and the average amplitude). If the actual values of the parameters are smaller than a prefixed threshold the event is discarded.

In accordance with the above mentioned considerations the following specifications were used. Those events are accepted as reflections which can be traced through six or more channels. The numerical value is tentatively suggested, it may be specified otherwise or used as a parameter.

Instead of using all data in a chosen part of a section (or a seismogram) we used the positive maxima, only.

The picking of the axes of the reflections were modelled by a M a r k o v-chain. This point needs some further clarification. Let us assume that the interpreter starts with a peak on the left-hand side trace of a seismogram. Taking into consideration of the positions of the peaks on neighbouring traces he chooses first a direction and then tries to locate more peaks in this direction, along a nearly straight line. If the series of peaks can not be continued in this direction he goes back to a branching point or, possibly, even to the starting point. From the new starting point he tries to find an other series of peaks in other directions.

By the definition of M a r k o v-chains there are M_{11}, M_{21}, M_{22}, ... M_{kl} positions which are constructed by the elements of the neighbouring traces and a conditional probability, p (kl/ij) may be ordered to all M_{ij} positions, which characterizes the probability of stepping from the position M_{ij} to the position M_{kl}. The number of nonzero probabilities is

restricted (See Fig. 1.). Nonzero probabilities are regulated by the following rules:

1. From the i-th trace we could step to the (i+1)-th trace, only.

2. Probability is nonzero in the intersection of a selected angle-domain (the angle is δ) and of a zone between two parallel lines, which are not necessarily perpendicular to the traces. The width of this skewed

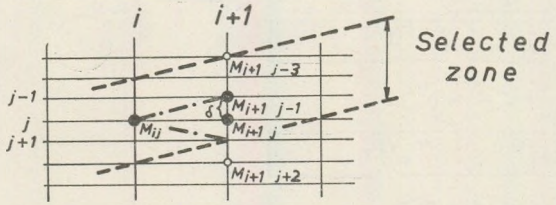

$$p(i+1\ \ j-1\,|\,ij) \neq 0 \qquad p(i+1\ \ j-2\,|\,ij) \neq 0$$
$$p(i+1\ \ j\,|\,ij) \neq 0 \qquad p(i+1\ \ j-3\,|\,ij) \neq 0$$

Fig. 1. The determination of transitional probabilities in M a r k o v -chains

zone is specified later. Probabilities in the allowed zone are proportional to the amplitudes and the sum of the transitional probabilities is equal to 1. This requirement has got a role in making the computation time shorter and corresponds to the assumption that a reflection axis goes through the greatest amplitudes.

A reflection element is found by point to point steps. The first two points are picked deterministically and denotes the slope of the zone between the parallel straight lines. The width of the zone may be 7 or 8 ms. Then we try to continue the M a r k o v-chain from the second point, i. e. we try to find a peak on the third trace in the allowed zone and angle-domain. This involves the investigation of 3 to 5 deterministic slopes within the allowed region. (See Fig. 2.) When there is only one local maximum in the allowed interval of the next trace the transitional probability is necessarily 1.

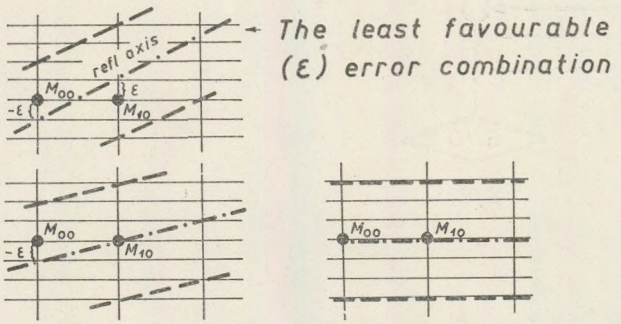

Fig. 2. The schematic diagram of allowed error combinations

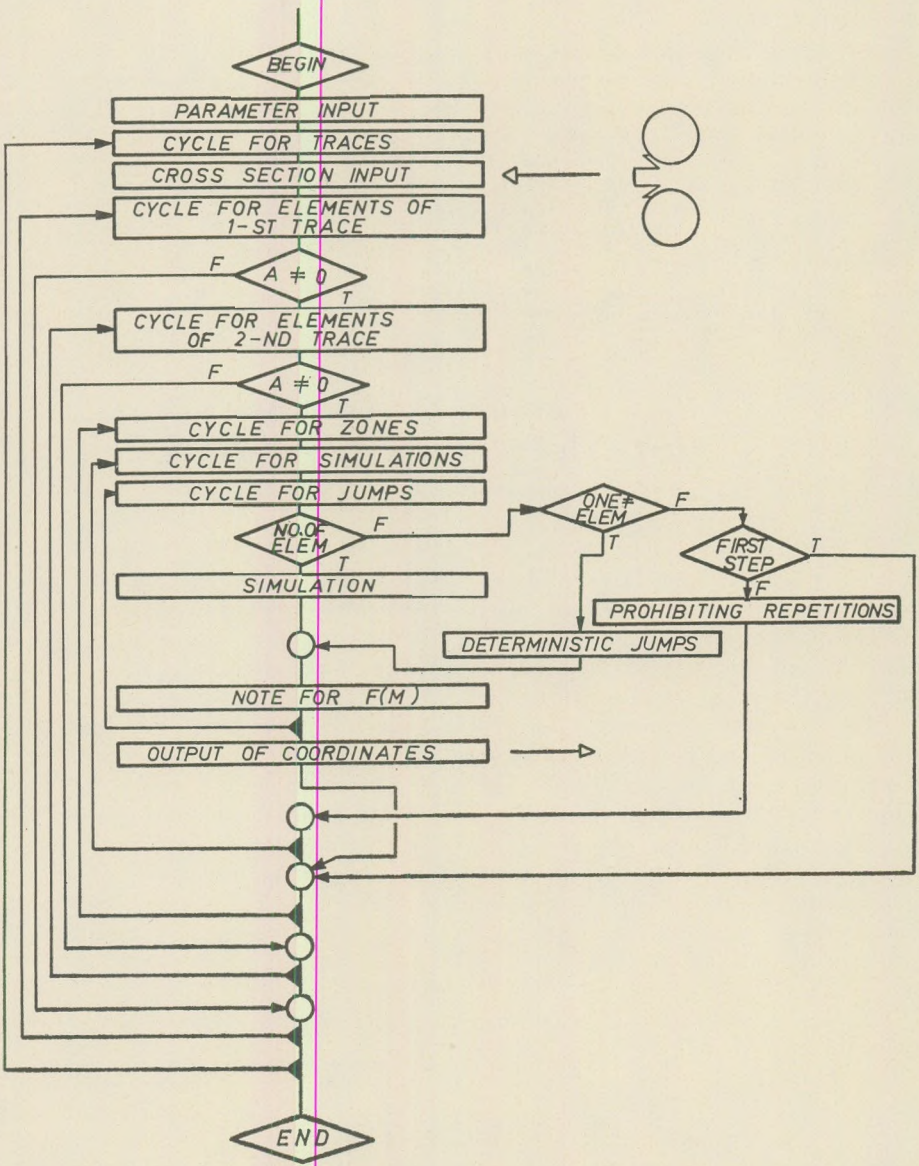

Fig. 3. A simplified flow chart of the reflection picking program based on the M a r k o v-chain model

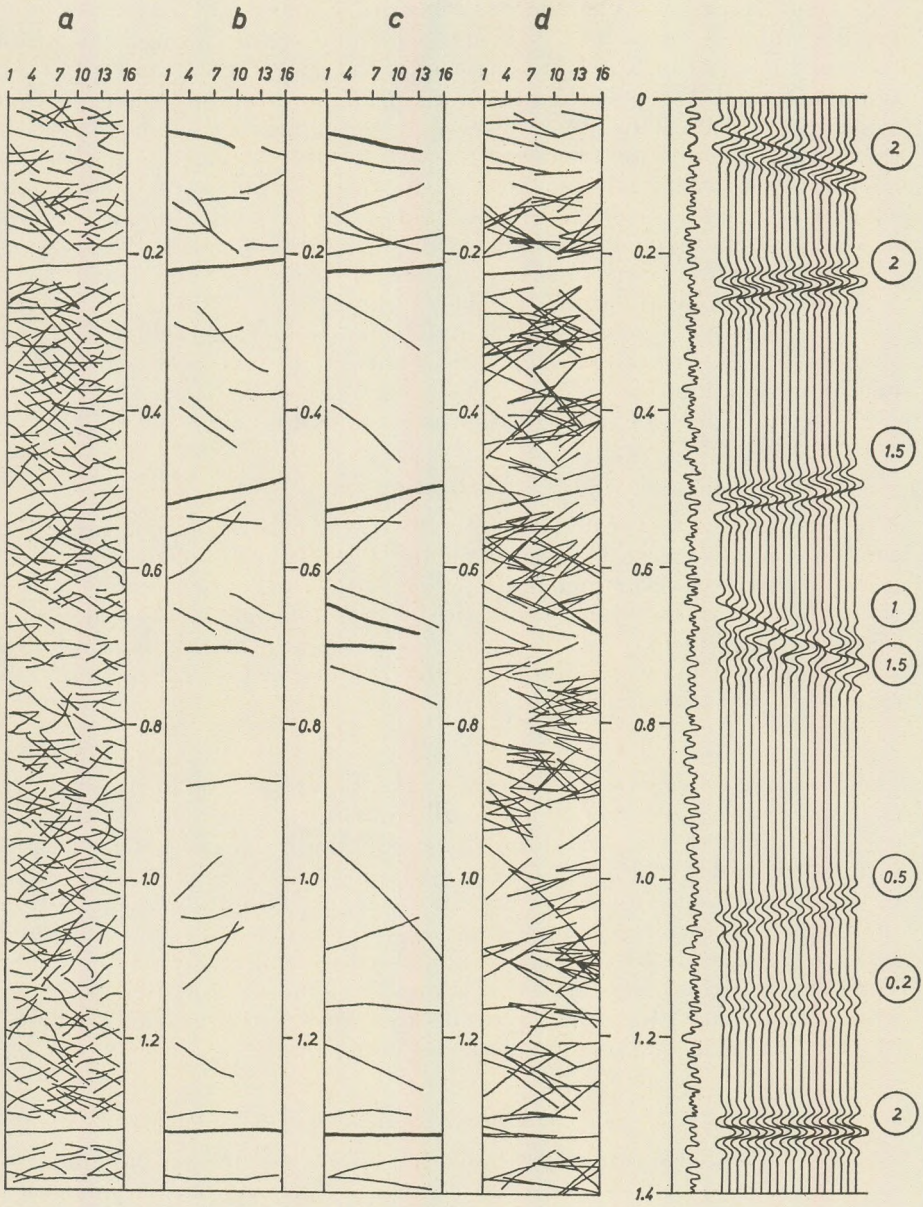

Fig. 4. Comparison of two reflection picking methods. On the right hand side the noise free seismogram is shown. One of the 16 different noise realisation is depicted on the left-hand side of the synthetic seismogram

a) The original reflection elements obtained by the Paulson-Merdler method
b) Classified elements of the Paulson-Merdler's method
c) Classified reflection elements of the output of the Markov-chain model
d) Original elements of the Markov-chain model

To all M a r k o v-chains, consisting of the found and within the given limits regularly placed local maxima, which also goes through the predetermined number of traces (in our case through 7 traces), an $F(M)$ function is assigned. We used the sum of the peak amplitudes of the concerned elements as $F(M)$. This function serves as a diagnostic tool in the classification of the reflection element. The whole process terminates sooner if no chains, which arrived to terminal positions, can be repeated again. This confinement means that if one quasi-coherent event (chain) is found in a zone no more event is looked for here.

The program starts to search reflections on every third trace. Later on it may be made a variable of the routine.

If we define similar M a r k o v-chains, connecting elementary reflections with nearly equal slopes, the horizon can be followed through one or two bad traces.

The flow chart of the algorithm is given as Fig. 3.

Application

The process was tested on a 16-channel synthetic seismogram. As a comparison the method described by P a u l s o n and M e r d l e r (1969) was also programmed and applied to the same seismogram. Reflection axes were allocated deterministically with different slopes and various signal-to-noise ratios. The trace length was 1.4 sec, the sampling interval 2 ms. The wavelets were modelled by eighth degree Hermit polynomials, truncated by Gaussian tapers:

$$w(t) = H_8(t)\, e^{-(0.06t)^2}$$

The peak frequency of the wavelet is 48 Hz. Band-limited (20 Hz – 100 Hz) Gaussian white noise was added to all traces.

The input of the compared processes, the rough and the classified results are shown in Fig. 4. The comparison of the two methods can not be considered decisive because a great number of Δ, ε and σ combinations should be investigated before drawing final conclusions, on one hand, and the results of this particular model are very similar, on the other. The Markov-chain model, however, seems to be more perceptive especially when reflections with small amplitudes are concerned. It may be explained by the fact that in the model the reflection axes are strictly straight lines.

Acknowledgements

The author would like to thank the OKGT Seismic Department for the support and help extended on him while carrying out the investigations reported in this paper.

REFERENCES

K. V. P a u l s o n, S. C. M e r d l e r, (1968): Automatic seismic reflection picking Geophysics, Vol. 33 No. 3.

J. A. S r e j g y e r, (1965): Monte Carlo módszerek, (Monte Carlo methods) Tankönyvkiadó.

POLE-AND-ZERO DESIGN OF RECURSIVE FILTERS

by
A. MESKÓ
(Dept. of Geophysics, L. Eötvös University BUDAPEST)

(Received: 10th March, 1972)

SUMMARY

A new iterative method of recursive filter design is reported. It can be used to approximate any given transfer function provided that the phase response is zero. The method is based upon the relationship between the frequency response and the location of poles and zeros on the z-plane. The desired function is approached successively by adjusting the pole radii and the normalizing factor. The procedure is fast, easy to control and gave better approximations than those known from the literature.

Applications are illustrated by three practical examples.

Introduction

The possible applications of recursive filters in processing of geophysical data heve been repeatedly discussed in the literature. (S h a n k s, 1967, M o o n e y, 1968, A g u i l e r a et al., 1970).

Recursive filters, however, do not appear to have been widely used in routine processing. It may be partly explained by the extended use of the Cooley-Tukey algorithm which has made discrete Fourier transformation and thus filtering in the frequency domain very efficient. An other factor, on the other hand, may be the lack of simple enough procedures for designing recursive filters. Several papers describe algorithms for constructing various kinds of recursive filters but most of them involve the solution of systems of linear equations (e.g. S h a n k s, 1967, A g u i l e r a et al., 1970) and possibly even the computation of the complex roots of high order polynomials.

It is not yet clear how many terms are to be used in the numerator and denominator of the z-transform, describing the transfer properties of recursive filters, because in some cases fewer terms gave better approximations (e.g. A g u i l e r a et al, 1970 p. 252). The computation of the complex roots of high order polynomials must also be done by some numerical approximation technique and the stability and the convergence of the solutions is also far from being understood, in particular cases encountered in processing of geophysical data. Both methods are far too sophisticated to be easily controlled and both are obviously time consuming.

A new method is reported in this paper which can be used to construct recursive filters with any given amplitude characteristic and zero phase

response. The method is based upon the relationship between the frequeny response and the location of poles and zeros on the z-plane. It approaches the desired function by successive approximations. In due course of each step the location of poles (or that of the zeros) are appropriately modified to bring the actual response closer to the desired. The efficiency of the method is demonstrated by construction of recursive band-pass filters and a smoothing filter.

Groundwork

Many excellent texts provide introduction to the theory of recursive digital filters: Archambeau and Flinn, 1965, Holz and Leondes, 1966, Kaiser, 1966, Rader and Gold, 1967, Shanks, 1967, Mooney, 1968, Pelladini et al., 1969, to name but a few. Therefore it seems enough to give here only a brief summary of the theory and emphasize those points of the recursive filter design which will be made use of in the forthcoming derivations.

Let us denote the time series to be filtered, i.e. the input to the filter by

$$x_k \quad (k = 0, 1, \ldots)$$

and the output sequence by y_l $(l = 0, 1, 2, \ldots)$.

The output of a general digital filter is given by the formula

$$y_l = \sum_{i=0}^{n} a_i x_{l-i} + \sum_{i=0}^{m} a_{-i} x_{l+i} + \sum_{i=0}^{q} b_i y_{l-i} \tag{1}$$

i. e. the filter uses for the computation of one output value

a) the weighted average of past input values (first sum),
b) the weighted average of future input values (second sum)
c) the weighted average of past output values (third sum).

Convolution filters, whose output depends only on the input may contain the first two sums. One-sided realizable convolution filters, a subclass of the previous type of filters, use the first sum, only. The purely regressive filters, on the other hand, use the third sum i.e. the recursive or feedback terms, alone.

Taking the z-transform of equation (1) we obtain

$$Y(z) = X(z)\left[\sum_{i=0}^{n} a_i z^i + \sum_{i=0}^{m} a_{-i} z^{-i}\right] + Y(z) \sum_{i=1}^{q} b_i z^i ,$$

or

$$Y(z) = \frac{\sum_{i=0}^{n} a_i z^i + \sum_{i=0}^{m} a_{-i} z^{-i}}{1 - \sum_{i=1}^{q} b_i z^i} X(z) . \tag{2}$$

If we confine our investigations to filters with realizable convolution parts the filtering process simplifies to

$$y_l = \sum_{i=0}^{n} a_i x_{l-i} + \sum_{i=1}^{q} b_i y_{l-i} . \tag{3}$$

and the tranfer function also becomes simpler. Let us introduce some denotions, defined as below

$$A(z) = \sum_{i=0}^{n} a_i z^i \tag{4}$$

and

$$B(z) = 1 - \sum_{i=1}^{q} b_i z^i , \tag{5}$$

then

$$Y(z) = S(z)\, X(z) \tag{6}$$

where

$$S(z) = \frac{A(z)}{B(z)} . \tag{7}$$

The well known relationship between the z-transform and discrete Fourier transform offers a way for determining the transfer function of the filter as a function of the dimensionless frequency $f' = f\tau$ (where f is the frequency and τ is the sampling period).

Substituting $\exp(-j2\pi f')$ for z we obtain

$$S(f') = \frac{\sum_i a_i e^{-ij2\pi f'}}{1 - \sum_i b_i e^{-ij2\pi f'}} . \tag{8}$$

The problem of filter design consists of giving appropriate values to the a_i and b_i coefficients so as to achieve good approximation of some desired frequency response $S^*(f')$.

Let us suppose in the followings that the desired filter is a zero phase response filter. The phase characteristic of a recursive filter, arc $\{S(f')\}$ can not be identically zero. There exist, however, procedures which can make the phase shift of a tandem of two resursive filters identically zero. One of the techniques, described by a number of authors (e.g. Archambeau and Flinn, 1965, Shanks, 1967, Mooney, 1968) cosists of passing the input through the filter with the response $S(z)$ and then passing its output through the revese time filter with the response $S(z^{-1})$. If the frequency response of the basic filter is $S(f')$ then the response of the combination of the direct and inverse time filters will be $|S(f')|^2$ with zero phase shift. If we use this technique the coefficients a_i and b_i in formula (8) should be determined in such a way that $|S(f')|^2$ be a good approximation to $S^*(f')$.

The transfer function $S(z)$ of the recursive filter, defined by equation (4), (5) and (6) can always be written in terms of the poles z_{pi} $(i = 1, 2, \ldots)$ and zeros z_{0i} $(i = 1, 2, \ldots)$ of the complex function $S(z)$. As it is known, the poles are the the roots of the denominator $B(z)$ and the zeros are the roots of the numerator $A(z)$. If we could properly locate the poles and zeros the remaining of the process would be straightforward. The ceoffi-cients of the polynomials $A(z)$ and $B(z)$ are unambigously determined by the roots and simple routines can be easily written for computing these coefficients from the roots of the polynomials.

In most cases we have to use a scaling factor k in order to normalize the frequency response. The scale factor does not effect either the location of the zeros or that of the poles, because a polynomial $kP(z)$ obviously possesses the same roots as the polynomial $P(z)$. Normalization should be done in the following manner. Let us suppose that the coefficients determined by the roots are a_i^* $(i = 0, 1, 2, \ldots)$ and b_i^* $(i = 0, 1, 2, \ldots)$. The denominator and numerator is divided by b_0 in order to make the first term in the numerator a one. Then the frequency response is determined by equation (8) and the proper scale factor k is assigned. The coefficients of the numerator are multiplied now by the factor k, i. e.

$$b_i = \frac{b_i^*}{b_0^*} \qquad (i = 0, 1, 2, \ldots)$$

and

$$a_i = k\frac{a_i^*}{b_0^*} \qquad (i = 0, 1, 2, \ldots).$$

In selecting poles and zeros two constraints must be imposed:

(*a*) The poles and zeros must be either real or they must appear in complex conjugate pairs. This requirement is necessary in order to yield real values for the coefficients a_i and b_i.

(*b*) The poles must lie outside of the unit circle in order to produce a stable filter.

Let us consider the simplest possible example by placing one real zero and one real pole, denoted by z_0 and z_p respectively. The transfer function of this real pole and zero pair filter is

$$S(z) = k\frac{z - z_0}{z - z_p}.$$

The frequency response becomes

$$S(f') = k\frac{e^{-j2\pi f'} - z_0}{e^{-j2\pi f'} - z_p} = k\frac{\cos 2\pi f' - z_0 - j\sin 2\pi f'}{\cos 2\pi f' - z_p - j\sin 2\pi f'}, \tag{10}$$

and the square of the amplitude characteristic is

$$S(f') = \frac{1 - 2z_0\cos 2\pi f' + z_0^2}{1 - 2z_p\cos 2\pi f' + z_p^2}. \tag{11}$$

It is clearly seen from the expression (11) that both the denominator and the numerator monotonously increase as the frequency f' increases from zero to the Nyquist frequency $f'_N = 0.5$. If z_p and z_0 are close enough the ratio is approximately 1.0 in the whole Nyquist interval, but a small neighbourhood of the zero frequency. For $f' = 0$ the equation (11) gives

$$S(f' = 0) = k^2 \frac{(1-z_0)^2}{(1-z_p)^2} .$$

If $z_0 = 1$, the filter removes the zero frequency component and attenuates the very low frequencies but passes through most frequencies with very little amplitude distortion. An example of this zero frequency notch filter is shown in S h a n k s (1967, p. 38). If, on the other hand, $z_0 > z_p > 1$, the filter enhance the zero frequency and the very low frequencies though apparently passes through other frequencies as well. Let us suppose, however, that $z_0 = 1.2$, $z_p = 1.02$ and $k = 0.1$. The recursive filter with these parameters will still pass the zero frequency and its close neighbourhood, because

$$S(f' = 0) = 0.1^2 \frac{(1-1.2)^2}{(1-1.02)^2} = 1$$

but it will severely attenuate any other frequencies because $|S(f')|^2 \approx 0.01$ if f' is not near to zero.

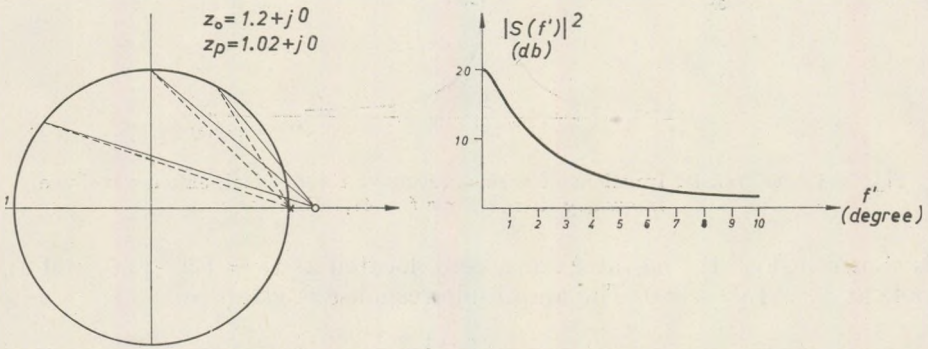

Fig. 1. A simple recursive filter for enhancing the zero frequency. On the lefthand side the zero and pole positions and the graphical visualisation of the amplitude response is shown. On the righthand siede the (nonnormalized) power transfer function is depicted

The z-plane can be used to make a rapid graphical evaluation of the amplitude response of a filter the poles and zeros of which are known. Some examples are given in S h a n k s's paper (1967: Fig. 2, 3, 4 and 6), illustrating various notch filters. A zero frequency enhancing filter, which is the simplest of the kind of filters the forthcoming algorithm is based on,

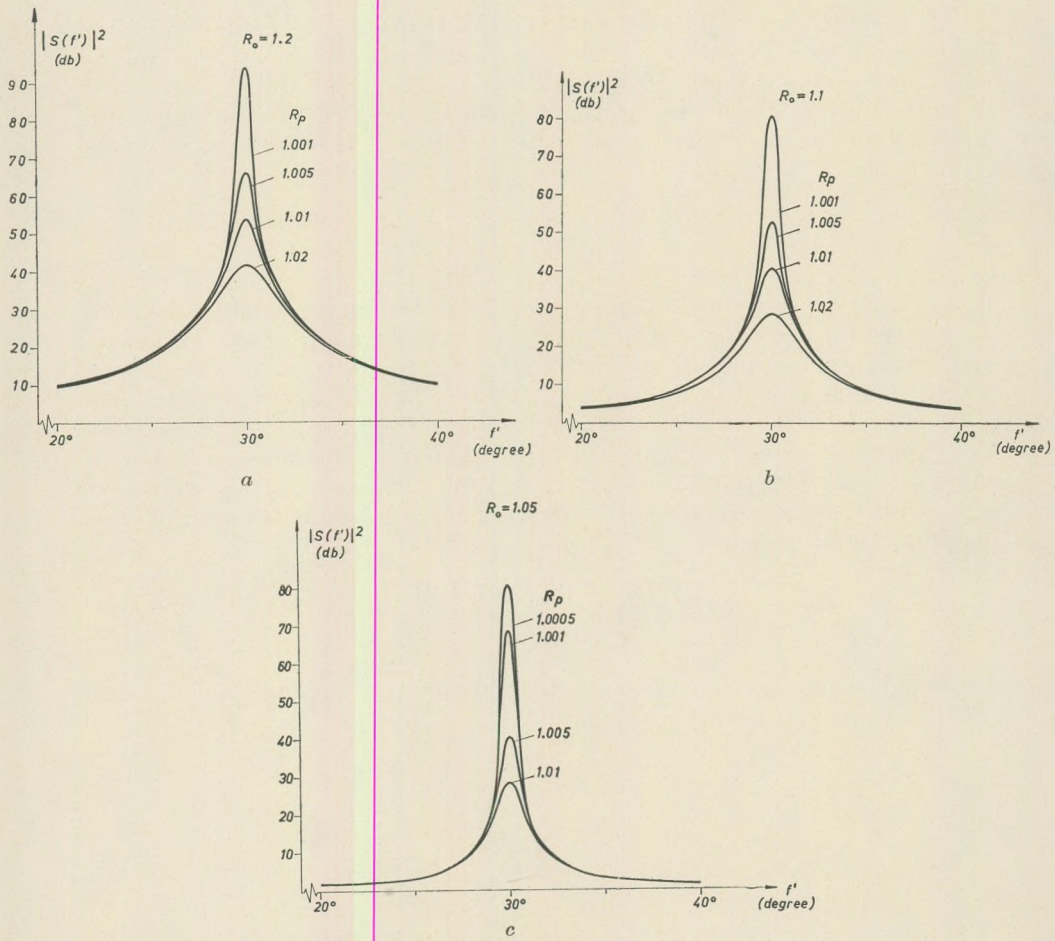

Fig. 2. Power transfer functions of various recursive filters which enhance a single frequency (if $\tau = 2$ ms $f = 41{,}4$ Hz).

is shown in Fig. 1. The filter has a zero, located at $z_0 = 1.2 + \mathrm{j}0.0$, and a pole at $z_p = 1.02 + j0.0$. The amplitude response is given by

$$S(z) = \frac{z - 1.2}{z - 1.02},$$

$$\left(z = \exp\left(-2\pi j f'\right)\right).$$

Values of z for which $|z| = 1.0$ correspond to values of real frequency. The point $z = 1.0 + j0.0$ corresponds to zero frequency $f' = 0$, the point $z = -1.0 + j0.0$ corresponds to the Nyquist frequency $f'_N = 0.5$. Frequencies linearly distributed between zero and 0.5 correspond to points on the unit circle linearly distributed between zero and π radians (or between

angles 0° and 180°). A given frequency, f'_0 determines a point P, on the unit circle. The length of the line which connects the pole and P gives the absolute value of the numerator of $S(z)$, while the length of the line connecting the zero and P gives the absolute value of the denominator. The amplitude response at the frequency f'_0 is the ratio of the length of the first line to the length of the second line. For $f' = 0$ the ratio is 10, but it rapidly decreases and stays close to 1.0 throughout the whole Nyquist interval. The square of the amplitude characteristic is 100 for $f' = 0$ and it decreases even more rapidly and remains close to 1.0. The square of the normalized characteristic is plotted in the same Fig. on a logarithmic scale (normalizing factor is $k = 0.1$).

We can design filters to echance any particular frequency by locating two poles z_p and $\bar{z}_p$ and two zeros z_0 and $\bar{z}_0$ along two lines associated with that frequency f' and $-f'$ The relation.

$$|z_0| > |z_p| > 1$$

must hold. The degree of the enhancement depends on the ratio $(|z_0| - 1)$ to $(|z_p| - 1)$. Figures 2*a*, 2*b* and 2*c* give some examples. Poles and zeros were located at $\pm 30°$, which corresponds to 41,3 Hz if $\tau = 2$ ms. Various pole and zero radii were used and the squares of the (non-normalized) amplitude responses were plotted on a logarithmic scale against the di-

Table 1

The logarithm of the power transfer function vs. dimensionless frequency (measured in degrees) for some pole radii, R_p ($R_0 = 1.05$)

f' \ R_p	1.0005	1.001	1.005	1.01
20	1.52	1.52	1.44	1.32
21	1.66	1.66	1.58	1.46
22	1.86	1.86	1.78	1.66
23	2.16	2.14	2.06	1.92
24	2.58	2.56	2.48	2.32
25	3.22	3.22	3.12	2.96
26	4.32	4.30	4.20	3.98
27	6.30	6.28	6.14	5.82
28	10.26	10.26	10.02	9.42
29	19.76	19.72	19.00	17.16
30	80.44	68.40	40.40	28.32
31	19.76	19.72	19.00	17.16
32	10.26	10.26	10.02	9.42
33	6.29	6.28	6.14	5.82
34	4.32	4.30	4.20	3.98
35	3.22	3.22	3.12	2.94
36	2.56	2.56	2.46	2.32
37	2.14	2.14	2.06	1.92
38	1.86	1.84	1.76	1.64
39	1.66	1.64	1.56	1.46
40	1.50	1.50	1 42	1.32

Table 2

The logarithm of the power transfer function (in db) vs. dimensionless frequency (measured in degrees) for some pole radii, R_p ($R_0 = 1.1$ in all cases)

f' \ R_p	1.001	1.005	1.01	1.02
20	4.02	3.94	3.84	3.58
21	4.48	4.40	4.28	4.00
22	5.06	4.98	4.86	4.56
23	5.88	5.78	5.66	5.32
24	6.98	6.90	6.74	6.34
25	8.56	8.46	8.28	7.80
26	10.88	10.76	10.54	9.88
27	14.42	14.28	13.96	12.94
28	20.26	20.02	19.44	17.52
29	31.48	30.76	28.90	23.98
30	80.90	52.90	40.82	28.68
31	31.46	30.74	28.90	23.98
32	20.26	20.02	19.42	17.50
33	14.42	14.26	13.94	12.92
34	10.86	10.74	10.52	9.86
35	8.54	8.44	8.26	7.76
36	6.96	6.86	6.72	6.32
37	5.84	5.76	5.62	5.28
38	5.02	4.94	4.84	4.52
39	4.42	4.36	4.24	3.96
40	3.98	3.90	3.78	3.54

mensionless frequency, measured now in degrees (1 degree corresponds to 1.44 Hz if $\tau = 2$ ms).

If the radius of the zeros, R_0 is held fixed the enhancement at 30° depends on the pole radius R_p, only, and obviously is given by

$$\frac{(R_0-1)^2}{(R_p-1)^2}.$$

The closer are the poles to the unit circle, the greater is the enhancement. We should like to call attention to one feature of the curves, presented in Fig. 2. The responses outside of a $\pm 3°$ neighbourhood of the peak are almost independent of the pole radii, at least until $R_0 = 1.2$ and $1.00 < R_p < 1$. It involves that though the variation of the pole position significantly modifies the value of the peak and influences its close neighbourhood, it does not change but slightly the outer parts. This statement may also be checked by Tables I., II. and III. containing numerical values of the logarithm of the power transfer function for some R_p positions This observation is a crucial point of the algorithm for constructing filters with given frequency responses.

Table 3

The logarithm of the power transfer function (in db) vs. dimensionless frequency (measured in degrees) for some pole radii, R_p ($R_0 = 1.2$ in all cases)

f' \ R_p	1.001	1.005	1.01	1.02
20	9.98	9.90	9.80	9.54
21	10.96	10.88	10.78	10.50
22	12.18	12.10	11.98	11.68
23	13.70	13.62	13.50	13.14
24	15.62	15.54	15.40	15.00
25	18.10	18.00	17.82	17.34
26	21.36	21.24	21.02	20.36
27	25.84	25.70	25.38	24.36
28	32.50	32.26	31 68	29.76
29	44.28	43.56	41.70	36.78
30	93.90	65.90	53.82	41.70
31	44.26	43.54	41.68	36.78
32	32.46	32.22	31.64	29.72
33	25.80	25.64	25.34	24.30
34	21.30	21.18	20.96	20.30
35	18.02	17.92	17.74	17.24
36	15.52	15.44	15.28	14.88
37	13.58	13.50	13.38	13.02
38	12.04	11.96	11.84	11.54
39	10.80	10.72	10.62	10.34
40	9.80	9.72	9.62	9.36

The algorithm for recursive filter design

The basic element of the design procedure is the quadruplet (z_0, $\bar{z}_0$, z_p, $\bar{z}_p$). The logarithm of the transfer function associated with the direct and time reversed application of the recursive filter, determined by the quadruplet or the logarithm of the squared amplitude characteristic (or the logarithm of the power transfer) of the direct filter will be denoted by $g(\alpha, \alpha_0, R_0, R_p)$, i.e.

$$g(\alpha, \alpha_0, R_0, R_p) = 2 \log \left| \frac{(z-z_0)(z-\bar{z}_0)}{(z-z_p)(z-\bar{z}_p)} \right|, \tag{12}$$

where $z = \exp(-jf \; 2\pi \; f') = \exp(-j\alpha), \quad -180° < \alpha < 180°$

$$z_0 = \exp(-j\alpha_0),$$

$$z_p = \exp(-j\alpha_p).$$

The transfer function of a recursive filter containing n quadruplets and a normalizing factor K is given by

$$S(z) = K \prod_{i=1}^{n} \frac{(z-z_{0i})(z-\bar{z}_{0i})}{(z-z_{pi})(z-\bar{z}_{pi})}$$

and the logarithm of the power transfer becomes a sum of the contributions of the individual quadruplets as follows

$$\log |S(f')|^2 = \sum_{i=1}^{n} 2 \log \left| \frac{(z-z_{0i})\,(z-\bar{z}_{0i})}{(z-z_{pi})\,(z-\bar{z}_{pi})} \right| + 2 \log K =$$

$$= \sum_{i=1}^{n} g(\alpha, \alpha_{0i}, R_{0i}, R_{pi}) + C \qquad (13)$$

where $C = 2 \log K$.

In order to achieve a good approximation of a given function $A(f') = 2\log |S^*(f')|$, where $S^*(f')$ is the power transfer function of a zero phase filter, one can manipulate with the parameters n (number of quadruplets), α_{0i}, R_{0i}, R_{pi} and K. We may start with an initial set of the parameters, compute the corresponding transfer and then modify the parameters in such a way that the second approximation be closer to $A(f')$ than the previous. A method which would adjust all the parameters at the same time is apparently difficult to handle, though it might lead to faster convergence and better approximations. Therefore we did not change the α_{0i} and R_{0i} values and concentrated our attention to the investigation what could be achieved if R_{pi} and K are properly adjusted in each step. Results proved to be satisfactory in most cases showing that this approach is justified.

M o o n e y (1967) described a method for constructing band reject and band pass recursive filters and summarized the "thumb-rules" of locating poles. The present method goes one step forward. Instead of placing poles essentially by trial and error the algorithm computes the new pole positions.

The computational steps of the algorithm are as follows.

Preparations

The bandwidth of $A\ (f')$ is expressed in degrees (e.g. if the filter passes the 20 Hz – 30 frequency band and the sampling interval is 2 ms the lower and upper cut-offs will be at 14,4° and 21,6°, respectively). Pole and zero directions i.e. the α_{0i}-s are taken at regular intervals $\Delta\alpha$. In all of the investigated cases $\Delta\alpha = 3°$ proved to be sufficient.

The zeros are assigned a constant radius (e.g. $R_{0i} = 1.2$).

The initial set of pole radii is assigned.

Normalizing factor is not dealt with in this step (or it is assumed that $K = 1$).

Step 1.

The transfer of the individual quadruplets with the given parameters and the sum (13) is computed. The peak values of the individual quadruplets are stored for further use. Let us denote these peaks by p_i.

The normalizing factor is determined by the requirement that

$$\sum_{k=k_1}^{k_2} [A(\alpha_k) - \log|S(f')|^2]^2 = \min . \tag{14}$$

where α_{k1} and α_{k2} are the limits of the frequency band over which good approximation is essential. Introducing the notation $D(\alpha_k)$ for

$$A(\alpha_k) - \sum_{i=1}^{n} g(\alpha_k, \alpha_{0i}, R_{0i}, R_{pi})$$

(14) can be rewritten as

$$\sum_{k=k_1}^{k_n} [D(\alpha_k) - C]^2 = \min ,$$

from which follows that

$$C = \frac{\sum_k D(\alpha_k)}{k_n - k_1 + 1} . \tag{15}$$

All parameters of the first approximation having been determined the transfer log $|S_1(f')|^2$ can be computed and plotted. (See e.g. curve 1 of Fig. 3.)

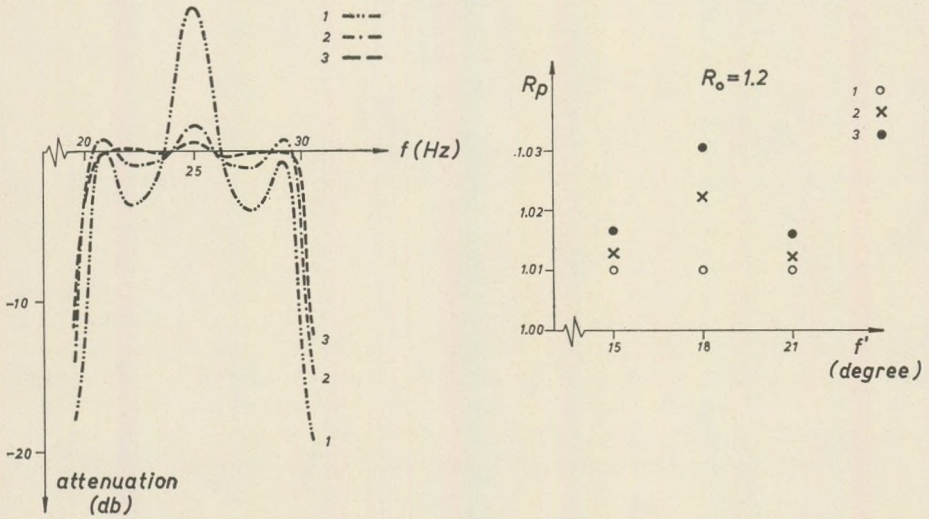

Fig. 3. Construction of a narrow band-pass filter. Curves 1, 2 and 3 show the results of the successive iterations in the pass-band (20 Hz – 30 Hz)

Step 2: Adjustment of pole positions

The first approximation gives a curve which oscillates around the $A(f')$. Peaks occour at pole and zero diections i.e. at α_i ($i = 1,2, \ldots,n$), troughs about at $\alpha_i + 1/2\Delta\alpha (i = 1, 2, \ldots, n-1)$. As it has been pointed out in the previous section the radius R_{pk} of a pole influences significantly its small neighbourhood, only (about $\pm 3°$ if R_0 and R_{pk} are within certain limits). Thus by decreasing the radius of the k-th pole, R_{pk} and consequently diminishing the peak, p_k of the individual quadruplet, the corresponding peak at α_k on the composite curve will also be diminished but the change will not significantly alter the shape of the other parts of the composite curve. By changing all the poles each value of $\log|S_1(f')^2|$ including those at the troughs, will decrease but the amplitude of the oscillations will also be damped. It proved to be a save practice to change R_{pk} according to the requirement

$$p_k^{(1)} - p_k^{(2)} = D(\alpha_{0k}) - \frac{1}{2}\left[D\left(\alpha_{0k} + \frac{\Delta\alpha}{2}\right) + D\left(\alpha_{0k} + \frac{\Delta\alpha}{2}\right)\right], \qquad (16)$$

i. e the modification of an individual peak is equal to the difference between the corresponding peak and the average of two neighbouring troughs on the composite curve. It assures that troughs and peaks remain at the same places and pole radii in the next approximation should be decreased again.

Step 1. and 2. are repeated until the approximation is satisfactory or a limit, set for the maximum number of approximations is reached. If the procedure fails to give acceptable results the number of quadruplets or the spacing, $\Delta\alpha$ or the initial set of pole radii should be changed.

Applications

The algorithm described in the previous section has been thoroughly checked by several filter design. Some representative examples are given below.

a) *Narrow band-pass filter*

Figures 3 and 4 show the construction of a filter which passes the 20 Hz – 30 Hz frequency band. The sampling distance is equal to 2 ms, therefore poles and zeros were placed at $\pm 15°$, $\pm 18°$ and $\pm 21°$. The third iteration gave satisfactory approximation. The difference between the highest peak and the deepest trough is less than 0.8 db. The results of consecutive approximations are shown at the lefthand side of Fig. 3. while pole positions are depicted at the righthand side of the same figure. This figure shows the frequency band of interest, only, Figure 4. gives the whole power transfer function.

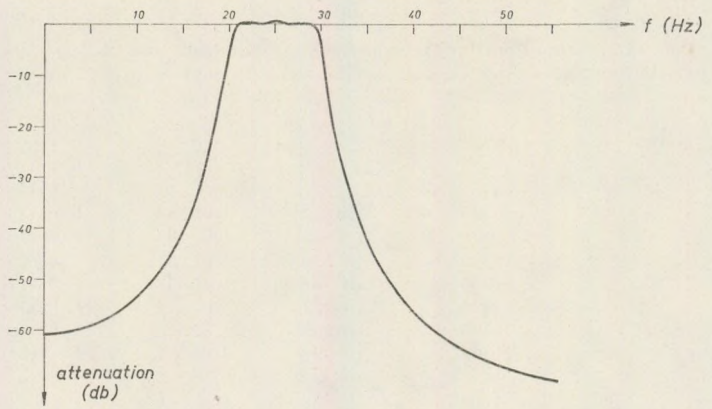

Fig. 4. The power transfer function of the narrow band-pass recursive filter, obtained in the third approximation

b) *Wide band-pass filter*

Figure 5. and 6. illustrate the construction of a filter which passes the 25 Hz – 50 Hz frequency band. Poles and zeros were placed between 18° and 36° and the conjugate poles and zeros between −18° and −26° at

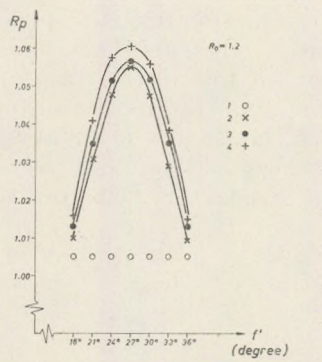

Fig. 5. Construction of a wide band-pass filter. The pole positions in the successive iterative steps 1, 2, 3 and 4 are shown. The pass-band is 25 Hz – 50 Hz and $\tau = 2$ ms therefore poles and zeros were taken between 18° and 36°.

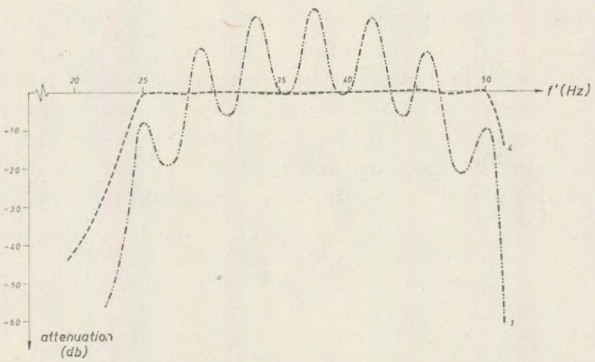

Fig. 6. The power tranfer function of the wide band-pass recursive filter obtained in the first and the fourth approximations

regular 3° intervals. Figure 5. shows the pole radii for the four iterations. Table IV. lists the numerical values. The first and fourth approximations of the band-pass filter are shown in Fig. 6. The results of the two inter-

Table 4

Pole radii in the iterative steps of the approximation of a 25 Hz – 50 Hz band-pass filter vs. pole direction, α_p (in degrees), $\tau = 2$ ms

α_p step No	1	2	3	4
18	1.005	1.0102	1.01288	1.01549
21	1.005	1.0307	1.0346	1.04056
24	1.005	1.0480	1.0513	1.05715
27	1.005	1.0555	1.0565	1.06047
30	1.005	1.0477	1.05172	1.05550
33	1.005	1.0289	1.03510	1.03820
36	1.005	1.0092	1.01307	1.01408

mediate approximations were not plotted in order to make the picture clear. The difference between the highest peak and the deepest trough is 1.22 db.

c) *Shaping filter*

The transfer of the filter is now a smoothly varying function of the frequency. (See Fig. 8 broken line.) The peak is at about 55 Hz and the frequency band of interest, i.e. the part, where attenuation is not less than -40 db lies about between 40 Hz and 70 Hz. If $\tau = 2$ ms the peak frequency corresponds to 40°. In the first approximation 9 quadruplets were used, placed between 28° and 52° at regular 3° intervals. The quadruplets thus covered the part, where exact approximation of the transfer is essential. It turned out, however, in the first step of the first iteration that two of the quadruplets, placed at the ends of the set are superfluous and in the next approximation 7 quadruplets between 31° and 49° were used, only. The third approximation proved to be satisfactory. The results

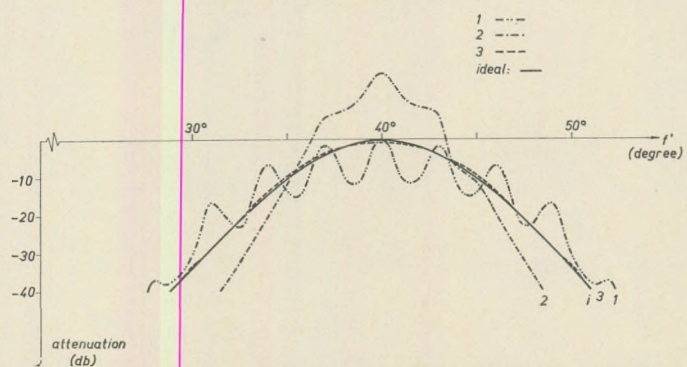

Fig. 7. Construction of a recursive shaping filter. Power transfer functions obtained in the first, second and third iterative steps are shown over the frequency band where attenuation is between 0 db and -40 db

of the successive approximations over the frequency band 40 Hz – 70 Hz are shown in Fig. 7, while the behaviour of the original shaping filter and its third approximation over the range 0 Hz – 120 Hz can be compared in Fig. 8.

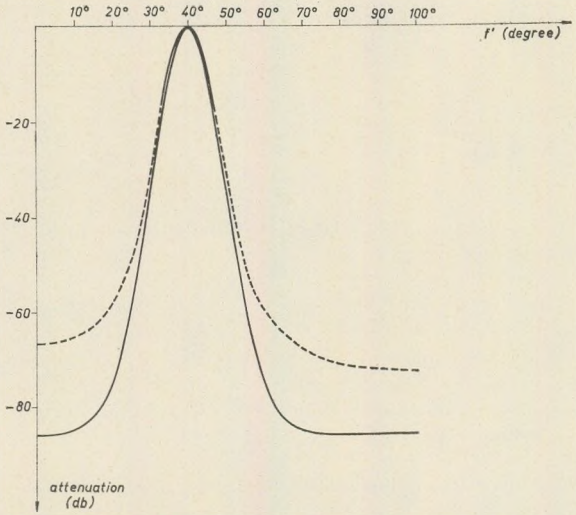

Fig. 8. Power transfer function of the recursive shaping filter (solid line) and the power transfer what it approximates (broken line)

The approach is apparently very good and there is no need to bring it closer to the original where attenuation is more than −40 db. The maximum deviation in the range between 40 Hz and 70 Hz is less than 1.0 db.

Conclusions

The algorithm for recursive filter design, reported in this paper has several advantages over those, described in the literature. Its simplicity makes the computation fast and easy to handle and to control in due course of the iterative steps. Experimentation with the algorithm (including the examples shown in Figs. 4 through 8) proved that a 3° spacing is sufficient in most cases in contrast with M o o n e y's examples who used 1/2°, 1° and 2° spacings. Moreover, better approximations to the "ideal" transfers have been easily arrived at by the present algorithm than by those, known from the literature: e.g. S h a n k s, (1967) Fig. 9, M o o n e y, (1968) Fig. 3 and 4 or A g u i l e r et al, (1970) Fig. 1 and 3.

Manipulations with the other parameters, e.g. with R_{0i} or α_{0i}, α_{pi} may result in further improvements but considering the goodness of fit and the fast convergence of the present method it hardly seems probable that a more sophisticated algorithm would very often be necessary except for some special type of filter.

Acknowledgement

The author is greatly indebted to his colleague Mr. I. Szulyovszky who wrote the computer programs for the practical realization of the successive iterations and supervised the computation of several recursive filters, including those presented in this paper.

REFERENCES

Aguilera, R., Debremaecker, J., Cl., Hernandez, D., (1970):. Design of recursive filters .
Geophysics, Vol. 35, No. 2, p. 247 – 253.

Archambeau, C., Flinn, E., (1965): Automated analysis of seismic radiation for source characteristics.
Proc. I. E. E. E., Vol. 53, p. 1876 – 1884.

Holz, H., Leondes, C. T., (1966): The sythesis of recursive digital filters.
Jour. ACM, Vol, 13, No. 2, p. 262 – 280.

Mooney, H. M., (1968): Pole-and-zero design of digital filters.
Geophysics, Vol. 33, No. 2, p. 354 – 360.

Pelladini, F. et al., (1969): Synthèse des filters digitaux avec contre-réaction dans le domaine des fréquences.
Mitteilungen AGEN, Nr. 9, p. 30 – 40.

Shanks, J. L., (1967): Recursion filters for digital processing.
Geophysics, Vol. 32, No. 1, p. 33 – 51.

BEITRAG ZUR METHODIK DER AUFSAMMLUNG VON MIKROFOSSILIEN: MIKROFAUNA AUS GASTROPODEN

von
M. MONOSTORI

(Lehrstuhl für Paläontologie, L. Eötvös, Budapest)
(Universität Budapest)
(Eingegangen am 25. 2. 1972)

SUMMARY

According to the author's investigations, a microfauna recovered from gastropod shells provides, on account of its good preservations state, an excellent material for fundamental monographic elaborations. At the same time, with adequately careful approaches, it may be suitable for an accurate identification of facies and communities. It may thus provide a basis for comparisons in analyzing rather poorly preserved and more or less mixed materials recovered from rocks (drill cores). Accordingly, the understanding of the ecology of both the gastropods and the microfauna can be mutually enhanced. In case of gastropods removed from their habitat, the environment, in which they may have lived, can be identified. In addition, information on the original nature of the sediment, heavily distorted as it often is by diagenesis, may be obtained.

Einige Probleme der Mikrofaunenuntersuchungen

In der Brauchbarkeit der paläontologischen Ergebnisse spielt der Erhaltungszustand der untersuchten Fauna eine wichtige Rolle. Im Falle der Mikrofauna gilt das besonders für die Ostracoden. Auf der Schale sind hier solche morphologischen Merkmale für die Bestimmung wichtig, sie man nur bei gut erhalten gebliebenen Formen auf befriedigende Weise zu studieren bekommt.

Die im Gestein eingeschlossenen Ostracoden-Überreste – die wegen der Zerstörungsfaktoren, die diese Fossilien vor der endgültigen Ablagerung angreifen können, nur einen von vorherein geringen Teil der originalen Fauna ausmachen – konnten während der Diagenese, aber auch danach bis zur Gegenwart, zahlreiche Verformungen erlitten haben. Die Auflösungswirkung verschiedener chemischer Agenten und auch die damit in entgegengesetzter Richtung wirkende Substanzablagerung (z.B. Kalkausscheidung) konnten einen weiteren – und es ist keine Übertreibung zu behaupten, dass wiederum den grösseren – Teil der Fossilien zugrunde gerichtet haben.

Neben der Frage des Erhaltungszustandes taucht ein anderes, mindestens ebenso wichtiges Problem auf, dass nicht nur die Ostracoden-Untersuchungen, sondern auch den ganzen Bereich der Mikropaläontologie betrifft. Diese Frage hängt mit dem Charakter der Sedimentation zusammen. Die modernen Meeresforschungen haben eindeutige Beweise

darüber geleifert, dass das Sediment vor seiner endgültigen Ablagerung sich wiederholt umhäufen kann. Diese Umhäufung betrifft die Fauna und zwar insbesondere die Mikrofauna, die wegen ihrer Kleinwüchsigkeit leicht vom jeweiligen Ablagerungsort weggetrieben wird.

Die moderne Paläontologie kann sich nicht einfach mit der Bestimmung des Alters der Schichten begnügen. Mindestens genauso wichtige, ja eventuell sogar bedeutendere Aufgabe ist für sie die Rekonstruierung der ehemaligen Fazies, des Meeresmediums. Die Paläontologie wendet den paläoökologischen, paläogeographischen Untersuchungen immer grössere Aufmerksamkeit zu. Das ist selbsverständlich, denn die meisten nutzbaren sedimentären Bodenschätze an gewisse Fazies gebunden sind.

Die modernste Untersuchungsmethode ist die Biozönosen-Analyse, selbstverständlich versucht man dieses Verfahren auch in der Mikropaläontologie anzuwenden. Es gelingt jedoch nicht immer, die Ergebnisse der im gegenwärtigen Milieu ausgeführten Analysen mit den Angaben über die geologische Vergangenheit in Einklang zu bringen. Eine der Hauptgründe dafür besteht in der bereits erwähnten mehrmaligen Umhäufung. Diese hat eine Homogenisierung der Mikrofauna in kleineren oder grösseren Räumen zur Folge. Es vermischen sich Gemeinschaften, die nebeneinander oder zeitlich übereinander lebten. Daher scheint es so, dass aus der Mikrofauna nur mit grösster Behutsamkeit auf die Verhältnisse geschlussfolgert werden kann, die einst im Bildungsraum des Gesteins existierten.

Gastropodengehäuse: eine spezielle Fundstätte von gut erhaltener Mikrofauna

Nach all diesen Erwägungen müssen wir die Frage stellen: gibt es überhaupt eine solche Stelle, wo die ehemalige Mikrofauna besser als der Durchschnitt sowohl angesichts ihres Erhaltungszustandes als auch ihrer Zusammensetzung konserviert ist?

Solche Stellen sind allerdings nicht so schwer zu finden, nur hat man diese für die Mikrofaunen-Analysen wenig ausgenutzt. E. Szőts hat kleinwüchsige eozäne Mollusken und embryonale Molluskenschalen aus der Füllmasse von Gastropodengehäusen geschlämmt (L. Strausz, 1970). Diese Gastropodengehäuse enthalten natürlich auch eine reiche Mikrofauna.

Vorteile der aus Gastropodengehäusen stammenden Mikrofauna

Was is denn von der Gastropodengehäusen vom Gesichtspunkt des vorher Gesagten zu erwarten?

1. Die Schalen der unlängst verstorbenen Formen werden nach Einschwemmung durch das Gastropodengehäuse vor mechanischen Beschädigungen geschützt. Es bleibt auch ein Teil der

äusserst dünnschaligen embryonalen Formen erhalten, was auch die Onthogenese der einzelnen Gruppen in klares Licht stellen kann.

2. Das Gastropodengehäuse verhindert oder wenigstens erschwert die Zirkulation der mineralisierenden Lösungen. Das Sediment bleibt oft in suboriginalem Zustand erhalten, die Formen weisen z.T. einen, den rezenten ähnlichen Zustand auf.
3. Auf die Frage der Erhaltung der ehemaligen Gemeinschaft (Biozönose) müssen wir schon eine vorsichtigere Antwort geben. Allerdings verringert die gute Erhaltung wesentlich einen der Störungsfaktoren: die selektive Zerstörung. Damit man mit einer, der ursprünglichen nahestehenden Mikrofaunengemeinschaft rechnen kann, sind zwei Bedingungen unentbehrlich:

a) die eine Vorbedingung besteht darin, dass die Gastropodenschale an solcher Stelle verschlammt werden muss, wo eine reiche Mikrofauna lebt;

b) die andere wesentliche Vorbedingung ist, solche Verhältnisse zu haben, unter welchen das Sediment nicht leicht aus der verschlammten Gastropodenschale ausgewaschen werden kann.

Ein einwandfreies Ergebnis darf nicht einmal in disem Falle erwarten. Infolge der Bewegungen des Sedimentes können auch früher verstorbene, unterschiedlichen Charakter aufweisende, eventuell aus anderen Gebieten stammende Mikrofaunenelemente zugemischt werden. Im Oberflächensediment, mit welchem die Schalen verschlammt sind, haben trotzdem die Schalen der *in situ* gelebten und unlängst verstorbenen Mikroorganismen den grössten Prozentanteil.

Eine weitere Schwierigkeit besteht auch darin, dass aus einer Gastropode man nur selten eine so grosse Menge von Mikrofossilien herausgewinnen kann, die für eine quantitative Analyse ausreicht. Beim Vorhandensein von vielen Gastropoden kommt es jedoch – wie auch den vorliegenden Untersuchungen zu entnehmen ist – zu neueren Überlappungen. Das Biotop der einzelnen Gastropodenpopulation war in der Regel unterschiedlich von dem der Mikrofaunen-Gemeinschaften. Das Biotop einer gegebenen Gastropode kann von den Biotopen von mehreren Mikrofaunen-Gemeinschaften überdeckt werden. Also, wenn man die Füllmasse von mehreren Gastropoden-Individuen zusammen prüft, so kann sich wieder gewisse Vermischung ergeben.

Es ist sehr wichtig diese Störungsfaktoren bei den Unterschungen zu berücksichtigen. Allerdings bedeutet das jedoch nicht, dass diese Untersuchungen überflüssing sind.

Die Hypothesen im Lichte der Fakten

Derartige Untersuchungen führte der Verfasser des vorliegenden Aufsatzes an Octracoden durch, die durch Schlämmanalyse aus den Gastropoden von zwei ungarischen Mittelmiozän-Komplexen (Dudar und Gánt) gewinnen wurden (M. Monostori, 1972a, 1972b).

Wenn im Laufe der Untersuchung genügendes Material zur Verfügung stand, wurden die Ostracoden aus den zu einer Art gehörenden Gehäusen, bei wenigerem Material jedoch aus den zu einer Gattung gehörenden Gehäusen gewonnen.

In letzterem Falle ist natürlich, im Laufe der ökologischen Schlussfolgerungen mit grösseren Überdeckungen zu rechnen.

Diese Untersuchungen haben die vorangehend erwähnten Erwartungen vollkommen berechtigt.

1. Der Erhaltungszustand des untersuchten Materials war weitgehend besser, als jener der aus Gesteinsproben abschlämmbaren Fossilien. Also die Gastropoden hatten einen guten Schutz gegen nachträgliche mechanische Effekte gewährleistet.
   Eine Korrelationsbeziehung mag zwischen der äusseren Gestalt des Gastropodengehäuses und dem Erhaltungszustand der Mikrofauna bestehen: in einem Raum mit agitiertem Wassermedium haben die mit breiter Mündung und wenigen Windungen versehenen Formen (z.B. *Velates)* die Mikrofossilien nicht so gut geschützt, wie die Gastropoden von turmförmigem Gehäuse (z.B. Cerithien). Bei den ersteren Formen kann sich die Füllmasse leicht, sogar mehrmals, abschlämmen.

2. Die beiden Fundorten lieferen ein gutes Beispiel dafür, dass die diagenetischen Prozesse innerhalb des Gastropodengehäuses oft beschränkt wurden. Die Füllmasse besteht sehr häufig aus Lockersedimenten – Kalksand, Kalkschlamm, sanding-toniger Kalkschlamm – oder aus nur leicht zementierten Sediment, während das einschliessende Gestein in vielen Fällen schwer zu schlämmen ist und eine spärliche und schlecht erhaltene Ostracoden-Fauna führt.

(Hier sei es bemerkt, dass in manchen Fällen die Füllmasse im Gegenteil noch besser diagenisiert als das einschliessende Gestein ist. Solche Gastropodenfunde sind natürlich zu unserem Zweck nicht geeignet.)

3. Die für die Erhaltung der Biozönose unentbehrlichen Bedingungen waren bei den *Velates* des – aus grobkörnigem Kalksand entstandenen – Kalkmergels von Dudar nicht vorhanden. Hier konnte die Ostracoden-Fauna nicht zu reich gewesen sein, daneben konnte wegen der äusseren Gestalt des Gehäuses mehrmaliges Ein- und Ausswaschen stattgefunden haben. Daher ist die Zusammensetzung der Ostracoden-Fauna hier von ziemlich eventuellem Charakter. Trotzdem wird die Untersuchung durch die einigen, gut erhaltenen Formen berechtigt, da aus dem einschliessenden Gestein keine Ostracode zum Vorschein gekommen ist.

   Im Laufe der speziellen Untersuchung eines, aus den Gehäusen von anderen Gastropoden-Gattungen *(Natica)* oder Arten *(Cerithium subcorvinum Opph., Campanile sp., Tympanotonos calcaratus (Brongn.), T. hungaricus (Zitt.), T. rozlozsniki*

Szőts, Faunus fornensis (Zitt.), Cantharus brongniarti (d'Orb.)). gewonnenen Materiales kam eine Ostracoden-Fauna von guter Erhaltung zum Vorschein, die sehr charakteristische Unterschiede in ihren quantitativen Verhältnissen aufgewisen hat (Auftreten in varierendem Prozentsatz von Formen, die nur aus Wasser von normalem Salzgehalt und von solchen, die hauptsächlich aus Brackwassermedium bekannt sind; Mengenverhältnis der ornamentierten Formen zu den glattschaligen usw.).

Diese Mikrofaunen scheinen die Biotop-Verhältnisse der einzelnen Gastropoden-Arten bzw. -Gattungen gut zu charakterisieren. Aufgrund der Untersuchungen lassen sich stark gegliederte küstennahe Meeresteile (Buchten, Lagunen) von stellenweise schwankendem Salzgehalt und mit veränderlichen hydrodynamischen Verhältnissen erkennen. In diesem Rahmen haben die verschiedenen Gastropoden-Arten verschiedene Stellen bevorzugt, was durch die quantitative Analyse der Mikrofossilien gut illustriert wird.

Nicht unbedingt ist jedoch das erhaltene Ergebnis für die ursprünglichen Bildungsverhältnisse der die Gastropoden einschliessenden Schichten in den gegebenen Gebietteilen charakteristisch. Die Füllmasse der Gastropoden — besonders bei den in stärker agitiertem Wasser abgelagerten Sedimenten — kann verschieden sein, was sogar mit unbewaffnetem Auge erkennbar ist (die eingeschwemmten Gastropodenschalen aufbewahren das Sediement eines anderen Beckenteiles: des ehemaligen Biotops). Also diese Untersuchungsmethode dürfte sich auch dafür eignen, um festzustellen, ob irgendwelche Gastropode ein fremdes Element im gegebenen Milieu ist oder nicht.

Schlussfolgerungen

1. Aufgrund der erhaltenen Ergebnisse scheint es zweckmässig zu sein, die Füllmasse der Gastropoden von — hauptsächlich tertiären — Schichtenfolgen, die eine verhältnismässig reiche Gastropoden-Fauna führen, abzuschlämmen und die dadurch gewonnene Mikrofauna zu untersuchen.
2. Die monographische Bearbeitung der herausgewonnenen Mikrofauna gibt eine gute Vergleichsbasis für die Bearbeitung von gleichalten aber schlechter erhaltenen Bohrmaterialien.
3. Man kann Angaben über die ursprünglichen Mikrofaunen-Gemeinschaften und deren ökologischen Verhältnisse (die Grösse der Vermischung bzw. Überdeckung nimmt in Abhängigkeit davon zu, ob man die Mikrofossilien aus einem einzigen Gastropoden-Exemplar, oder aus mehreren Exemplaren einer und derselben Art, oder aus mehreren Exemplaren von mehreren Arten der gleichen Gattung, oder aus mehreren Exemplaren von verschiedenen Gastro-

poden-Gattungen aus dem gleichen Fundort gewinnt) erhalten. Diese Abgaben können eine gute Vergleichsbasis für die Untersuchung der aus Bohrungen stammenden Mikrofaunen, deren Zusammensetzung unbedingt mehr gemischt ist, liefern.

LITERATUR

Monostori, M. (1972a): Dudari eocén Ostracodák facies értékelése (Fazies-Auswertung der eozänen Ostracoden von Dudar), Őslénytani Viták, 20.

Monostori, M. (1972b): A gánti eocén Ostracodák facies értékelése (Fazies-Auswertung der eozänen Ostracoden von Gánt). Őslénytani Viták, 20.

Strausz, L. (1970): Über Kleinmollusken aus dem Eozän von Dudar, II. [Földtani Közlöny, 100. pp. 66–76, (p. 66)].

FAZIESUNTERSUCHUNGEN DER UNTERPANNONISCHEN ABLAGERUNGEN VON TINNYE UND ALSÓTOLD

von
I. ORSOVAI
(Lehrstuhl für Angewandte und Ingenieurgeologie, L. Eötvös Universität, Budapest)

(Eingegangen am 28. 3. 1972)

SUMMARY

In the lagoonal facies of the basin-marginal deposits of the Lower Pannonian Substage an assemblage of peculiar small-size fossils (Orygoceras, Papyrotheca, Baglivia, etc.) can be found. As a result of frequent, post-sedimentary redepositions, the ostracods and small-size molluscs have been preserved in most of the cases just in the mouths of larger Melanopsis specimens. Beside the close resemblance of the mollusc faunae there are considerable divergencies in the ostracod faunae of different localities.

Einleitung

Die besondere Faunengemeinschaft der Lagunenfazies des unteren Pannons ist vor allem aus dem Territorium von Jugoslawien (Markuseveč, Vrabče, Ripaňj) bekannt, aber sie kommt an einigen Lokalitäten auch in Rumänien vor. Das von der Literatur bekannte reichste Fundort, Szócsán (13), kann überhaupt nicht ausgewertet werden (Sammlung von Viktor Aradi). Auf dem Territorium Ungarns, ist ausser dem, heutzutage nicht mehr zugängigen Eigel'schen Brunnen von Kőbánya eine reiche Fauna aus der Umgebung von Sopron (21, 22, 23, 24), Eger (6) und Tinnye (4, 8, 11, 12) beschrieben worden, aber einzelne Faunenelemente kommen auch an anderen Lokalitäten vor. Der vorliegende Aufsatz enthält die Untersuchungsergebnisse über die bisher noch nicht bearbeiteten Fauna der Lokalität Alsótold im Cserhát-Gebirge.

Die Fossilien der Fundorte bei Tinnye wurden von I. Lőrenthey bearbeitet (11). Die von ihm besprochene Faunenliste enthielt Fossilien von verschiedenen Lokalitäten, was später zu gewissen Missverständnissen führte. Als seine Arbeit veröffentlicht wurde, waren in Ungarn 75% der Fauna – 81 Arten – allein aus Tinnye bekannt. Lőrenthey's klassischer Irrtum bezüglich des Vorkommens von autochtonen pannonischen Foraminiferen (15) war z.T. dadurch bedingt, dass die Allochtonie der in die pannonischen Ablagerungen von Tinnye eingewaschenen Faunenelemente nicht erkannt war.

In den Jahren 1919–1920 sammelte I. Ferenczi im Laufe der geologischen Aufnahme die Fauna der einzelnen kleinen Fundorte gesondert ein. Die von ihm gesammelten Fossilien wurden von I. Mez-

nerics mit ihrer eigenen Sammlung ergänzt und bearbeitet (8). Ihr gelang es, die reiche Faunenliste Lőrentheys mit neun Arten zu ergänzen, von denen sich fünf als Neuarten erwiesen.

In diesem Aufsatz wird die Fauna der zeitweise in Anspruch genommenen Sandgrube nördlich von Tinnye (der alte Aufschluss Vásárhelyi's) an Hand der Sammlungen von 1967–1970 besprochen. Die reiche Ostracoden-Fauna des Fundortes wird zum ersten Mal bearbeitet.

Geologische Charakterisierung der Fundorte

I. Tinnye. In der Sandgrube, die ganz unregelmässig für die Sandgewinnung benutzt wird, sind die präpliozänen Ablagerungen nicht erschlossen. In der unterpannonischen Schichtenfolge lassen sich die Lagerungsverhältnisse der verschiedenen Schichten und ihre Beziehungen zueinander wegen Rutschungen nur in kleinen Flecken studieren.

1. Man kann einen grobsandigen, kreuzgeschichteten Gesteinstyp mit grosswüchsigen Bruchstücken von Melanopsis und Gastropodengehäusen unterscheiden, der sich in einer Aufeinanderfolge mehrmals wiederholt. Es sind die Steinkerne der Mündung der Melanopsis-Gehäuse, die die unversehrte, kleinwüchsige Mollusken- und Ostracoden-Fauna enthalten. Mit dieser Beschaffenheit stimmt Tinnye mit den Lokalitäten von ähnlicher Fazies überein.

Granulometrische Zusammensetzung des einschliessenden Gesteins:

1,4 mm <	5%
1,00–1,4 mm	3%
0,63–1,00 mm	9%
0,32–0,63 mm	21%
0,20–0,32 mm	36%
0,10–0,20 mm	17%
0,06–0,10 mm	6%
0,06 mm >	3%

Der $CaCO_3$-Gehalt ist 8%, was sich aus den Mollusken-Fragmenten ergibt.

Die granulometrische Zusammensetzung des sandigen Tones, der aus den Mündungen der Melanopsis ausgewaschen wurde, ist die folgende:

0,32–0,63 mm	5%
0,20–0,32 mm	10%
0,10–0,20 mm	14%
0,06–0,10 mm	31%
0,06 mm >	40%

Der $CaCO_3$-Gehalt ist 68%, der Grossteil des Gesteins besteht aus feinen Mollusken-Fragmenten und vollständigen Fossilindividuen.

Das Gestein hat sich in der Nähe des Küstenrandes gebildet. Darauf weisen die im grobklastischen Material häufig vorkommenden Gerölle

(Quarzit und Dolomit!), die zerbrochenen Gastropoden-Gehäuse und die abgerollten Melanopsis hin.

2. Es lässt sich eine lithologisch nicht deutlich fassbare Bildung unterscheiden, die aus Tiefbohrungen und Tagesaufschlüssen unter dem Namen „unterpannonischer weisser Mergel" bekannt ist, aber mit ihrem Habitus von Tinnye sich als lockerer, staubiger Kalkschlamm erweist. Nach den Angaben der Literatur und des Aufschlusses von Alsótold dürfte diese das originale Gestein der Orygoceras-Faunengemeinschaft sein. In Tinnye beinhaltet sie zwar einige Mollusken-Arten des Steinkernes von Melanopsis-Gehäusen, dennoch ist ihre ausserordentlich spärliche Ostracoden-Fauna unterschiedlich und die auch übrigens seltenen, aber charakteristischen Gattungen Orygoceras, Papyrotheca und Baglivia fehlen vollkommen. Es ist wahrscheinlich, dass das Sediment sich in einer ± geschlossenen Lagune ablagerte, wohin die feinen Brüchstücke der in der aktiven Brandungszone zerbrochenen Mollusken-Gehäuse schwebend eingeführt wurden. Granulometrische Zusammensetzung des „weissen Mergels":

0,32 mm	3%
0,20 – 0,32 mm	6%
0,10 – 0,20 mm	44%
0,06 – 0,10 mm	35%
0,06 mm >	12%

$CaCO_3$-Gehalt = 95%.

Das Alter der Lokalität Tinnye dürfte aufgund der spärlichen Congeria partschi Čžjžek und der durch häufige juvenilen Individuen vertretenen Congeria ornithopsis Brus. dem mitteren-oberen Horizont der unterpannonischen Unterstufe entsprechen.

Bemerkungen zu einigen Arten:

a) *Baglivia sp.*

Bis jetzt war diese Form von der Lokalität Tinnye unbekannt. Bei den Gastropoden ist der devolute („korkzieherförmige") Gehäusebau selten, nur bei einigen Gattungen zu beobachten. Unter den unterpannonischen Fossilien sind die Arten der Gattung Baglivia (B r u s i n a 1902) durch einen devoluten Gehäusebau charakterisiert.

L ő r e n t h e y (1895) beschrieb Baglivia spinata (9) aus Szekszárd von Kőbánya hat er Baglivia bythinellaformis n.sp. ohne ausführlichere Beschreibung und Abbildung erwähnt.

H o e r n e s (1897) hat die Art Hydrobia (Liobaikalia ?) sopronensis von der Umgebung von Zemendorf beschrieben. Es hat sich jedoch herausgestellt, dass diese mit L ő r e n t h e y's Form von Kőbánya identisch ist.

Was die in Tinnye vorgefundenen, zwei unvollständigen Exemplare betrifft, so stimmen diese nur mit ihrem devoluten Gehäusebau mit den

angeführten Arten überein, ihre Grösse ist aber das Mehrfache der Dimensionen der letzteren. Ausserdem besteht noch der Unterschied darin, dass in der Nähe des Apex der devolute Charakter weniger ausgeprägt ist, während unsere Exemplare bereits beim Apex ausgesprochen devolut sind. In Tinnye kamen zwei unvollständige Exemplare zum Vorschein, das eine ist durch den Apex und eine vollständige Windung, das andere durch den Apex und eine Halbwindung vertreten.

b) *Orygoceras*

Bezüglich der von Kittl (1886) als Creseis Fuchsi beschriebenen Pteropoden-Art kam Lőrenthey 1903 zur Erkenntnis (12), dass sie mit Orygoceras corniculum Brusina (1892) identisch war. In der unterpannonischen Beckenrandfazies ist die ziemlich weit verbreitet, Brusina (1892) hat ausserdem die Arten O. filocinctum, O. cultratum und in 1902 noch O. fistula und O. scolecostomum beschrieben. Die Orygoceras-Gehäuse von Tinnye sind unvollständig erhalten geblieben; unter den mehrere hundert Exemplaren ist kein unversehrtes bis auf Species genau bestimmbares Exemplar angetroffen worden. Vom Gehäuse sind im allgemeinen der Nucleus und der sich daran anschliessende Gehäuseteil unversehrt geblieben, die Umgebung der Mündung ist zugrunde gegangen. Aus den erhalten gebliebenen Teilen können die von Lőrenthey erwähnten drei Arten; O. filocinctum, O. culturatum, O. fuchsi (=O. corniculum) identifiziert werden.

c) *Papyrotheca*

Lőrenthey (1893) fand in Tinnye eine bis dahin unbekannte Gastropode, die „... obwohl der Succinea sehr nahekommt, trotzdem soviel selbständig mit ihren unterschiedlichen Eigenschaften ist, dass sie als eine neue Gattung anzunehmen ist“ (10). Bald danach publizierte Brusina die Beschreibung eines aus Ripaňj stammenden neun Fossils unter dem Namen Papyrotheca mirabilis, das dem aus Tinnye beschriebenen Art Lőrenthey's gleich war. Brusina rechnete die neue Gattung aufgrund einer unsicheren Annahme zu den Limnaea. Die Gehäusewand wurde nämlich für so dünn gehalten, dass die Existenz des bei den Succineen vor handenen Mündungsdeckels ausgeschlossen wurde. In der Tat steht Papyrotheca in Verwandschaft mit der Gattung Succinea.

In der von Lőrenthey (1895) auf das erste Mal veröffentlichten Faunenliste von Tinnye figuriert die Art Succinea gracilis n.sp., mit welcher der Verfasser die Art Papyrotheca mirabilis vergleicht und die grosse morphologische Ähnlichkeit feststellt. In seiner 1902 erschienenen, z.T. auch Material aus Tinnye beinhaltenden Arbeit (11) rechnete er auch Succinea gracilis zur Gattung Papyrotheca.

I. Vitális (1938) fand in den fossilreichen unterpannonischen Gesteinen der Umgebung von Sopron eine grosse Anzahl von Exemplaren, die der Papyrotheca-Succinea-Gattung angehören. Aufgrund der Samm-

lungen aus der Lokalität Tinnye und einer Vergleichung stellt er fest: 1. zwischen mirabilis Brus. und gracilis Lör. besteht ein generischer Unterschied; 2. mirabilis gehört zur Papyrotheca-Gattung, gracilis zur Gattung Succinea.

Nach der Meinung des Verfassers des vorliegenden Aufsatzes gehören die beiden Arten zur gleichen Gattung und die zwischen den beiden bestehenden morphologischen Unterschiede werden durch die Einreihung in verschiedene Arten zum Ausdruck gebracht. Von den zwei Arten steht P. gracilis wirklich den Succineen näher, aber P. mirabilis kann keineswegs zur Succinea-Gattung gerechnet werden, daher werden die beiden Arten als Vertreter der Papyrotheca-Gattung betrachtet.

c/1. *Papyrotheca mirabilis Brus.*

Länge 5,5 mm, Breite 1,9 mm. In orientierter Position kommt die rechte Gehäusewand geradlinig mit der linksseitigen in Berührung und der Kontakt ist mit dem eingerollten Teil nicht überdeckt. Einrollungsgrad: anderthalb Windungen. Aus Tinnye sind ein vollständiges und sechs unvollständige Exemplare zum Vorschein gekommen.

c/2. *Papyrotheca gracilis (Lőr.)*

Länge 6,2 mm, Breite 0,8 mm. Schlankere Form als P. mirabilis. In orientierter Position berührt sich die rechte Seite des Gehäuses eine parallele Linie entlang mit der linken Seite und der Kontakt ist z. T. durch die Windung überdeckt. Einrollungsgrad: 2–3 Windungen. Ein einziges vollständiges Exemplar wurde in Tinnye angetroffen.

II. Alsótold. Die Lokalität wird 1937 von I. Sándor erwähnt (6). Er hält sie für eine terrigene und irrtümlich für eine Süsswasser-Ausbildung. Auch J. Noszky gibt Hinweise auf die gegliederte Becken von Cserhátszentiván und Alsótold. Die grösste Bedeutung der Lokalität besteht darin, dass sie ein wichtiges georgraphisches Verbindungsglied zwischen den Orygoceras-Faunengemeinschaften von Tinnye–Budapest–Kőbánya und von Ostoros bei Eger (6) ist.

Das Fundort liegt 300 m S von der Ortschaft Alsótold, SW von der Strasse nach Kozárd. Das Gestein, das die Fauna enthält, ist „unterpannonischer weisser Mergel". Ein Unterschied von den anderen Fundorten von gleichen Alter und gleicher Fazies besteht darin, dass die aus den Mündungen von grossen Melanopsis herausgewonnenen kleinwüchsigen Fossilien mit denen des einschliessenden Gesteins übereinstimmen. Ein weiterer Unterschied von der Lokalität Tinnye ist einerseits, dass der Grobsand vollkommen fehlt und die Melanopsis-Gehäuse kaum abgerollt sind; andererseits, dass es sehr fein zerkleinerte Mollusken-Fragmente reichlich verhanden sind und ca. 80 bis 90% des Schlämmungsrückstandes ausmachen.

Granulometrische Zusammensetzung des Gesteins:

0,32 – 0,63 mm	1%
0,20 – 0,32 mm	2%
0,10 – 0,20 mm	48%
0,06 – 0,10 mm	39%
0,06 mm >	10%

Kalkgehalt ($CaCO_3$) = 91%.

Eine charakteristische Beschaffenheit der Lokalität stellen die vielen durchsichtigen Kieselschwammnadeln, dar, wobei sowohl Triaxone als auch Tetraxone vorkommen. Diese zwei Schwammnadeltypen sind fremde Faunenelemente im Pannon. Für ihre Herkunft bestehen zwei Hypothesen:

1. Im unteren Pannon konnten die in einem, noch teilweise geschlossenen Becken weiterlebenden, euryhalinen Schwämme in einem Wasser, dessen Salzgehalt höher als pliohalin war, immer noch am Leben gelbieben sein. Gegen diese Hypothese spricht die Tatsache, dass die restlichen Elemente der Fauna nicht auf einen höheren Salzgehalt hindeuten, obwohl sarmatische Ostracoden-Relikte vorhanden sind.

2. Wahrscheinlicher ist die Annahme, dass diese Formen aus dem nahe gelegenen karpatischen Schlier umgelagert wurden. Das wird dadurch unterstützt, dass im Schlier viele Schwammnadeln vorhanden sind und der Rückstand des pannonischen Tones nach Behandlung mit Salzsäure mit dem Lösungsrückstand des Schliers übereinstimmt. Es ist zu vermuten, dass es sich um eine selektive Umhäufung handelt, wobei die kalkigen Skelette aufgelöst wurden, da der Schlier in der Umgebung der Lokalität an anderen Mikrofossilien (Mikrofauna) reich ist, während in den Pannonbildungen kein karpatisches Fossil, nicht einmal in Form von Fragmenten, angetroffen werden kann.

Das Alter der Lokalität – ähnlich wie in Tinnye – ist an Hand der Congeria partschi Czjzek und Congeria ornithopsis Brus. mit dem mittleren-oberen Horizont der unterpannonischen Unterstufe identifizierbar.

In ihrer Artenzusammensetzung sind die Mollusken der Fauna von Ostoros und Tinnye sehr ähnlich, der auffallendste Unterschied besteht im völligen Fehlen von Papyritheca. Orygoceras sind in grösserer Individuenzahl als in Tinnye vorhanden, aber durch unvollständige Exemplare vertreten.

Das Fehlen von gröberem Sediment und die geringere Abrollung weisen darauf hin, dass die Energie der Wasserbewegung nicht bedeutend war, dagegen deuten die häufigen Mollusken-Fragmente auf eine Brandungszone hin. Allerdings ist es wahrscheinlich, dass die Mollusken nicht in situ zerbrochen, sondern vom Strand in die etwas tieferen Beckenteile, weiter von der Küste hineingetragen wurden. Im beckennahen Festland-Milieu war der helvetische Schlier an der Oberfläche am weitesten verbreitet, die unterpannonischen Ablagerungen wurden durch die Abtragung dieses Gesteins geliefert. Die kleinen lokalen Sedimentationsbecken standen stets mit der pannonischen Binnensee in Verbindung, da auf-

grund der Fauna kein Salzgehalt-Unterschied nachweisbar ist. Die Ostracoden weichen dagegen wesentlich von denjenigen der Lokalität von Tinnye ab, was darauf zurückzuführen ist, dass Tinnye vorwiegend eine Strandfazies darstellt (mit Ausnahme des weissen staubigen Kalkschlammes, der eine Lagunenablagerung ist), während Alsótold eine lagunäre Ausbildung ist.

Unsere Meinung ist im Einklang mit den Feststelungen von K. Tóth (19), dass die Ostracoden-Fauna dem ebenfalls in lagunärer Fazies azusgebildeten Congeria Čžjžeki-Horizont des SO-Vorlandes des Vértes ähnlich ist.

Tabelle I

Liste der Ostracoden

	1	2	3
Amplocypris munita Zal.	+	–	–
Amplocypris pannonica Zal.	–	–	+
Amplocypris elegans (Méh.)	+	–	+
Amplocypris sinuosa Zal.	+	–	–
Amplocypris sp.	+	–	+
Hungarocypris sieberi (Méh.)	+	+	–
Hungarocypris sieberi nodosa (Méh.)	+	+	–
Hungarocypris pannonica Zal.	+	–	–
Candona rostrata Brady-Norm.	–	–	+
Candona paralella G. W. Müll.	–	–	+
Cyprideis pannonica (Méh.)	–	+	+
Cyprideis pannonica tuberculata (Méh.)	–	+	+
Cyprideis heterostigma obesa (Reuss)	–	–	+
Cyprideis sulcata Zal.	–	+	–
Cypris inaequalis Sieber	–	–	+
Darwinula stevensoni Brady-Norm.	–	–	+
Hemicytheria hungarica (Méh.)	+	+	+
Hemicytheria lőrentheyi (Méh).	+	+	+
Hemicytheria ampullata (Méh.)	+	+	–
Erpetocypris reticulata Zal.	–	–	+
Loxoconcha rhombovalis Pokorný	+	+	+
Loxoconcha mülleri (Méh.)	–	–	+
Leptocythere egregia (Méh.)	–	–	+
Leptocythere andrusovi (Livental)	–	+	–
Leptocythere olivina (Livental)	+	–	–

1 = Tinye; 2 = Alsótold; 3 = Ostoros (nach Jankovich, 1969)

Bemerkungen zur Verbreitung der Ostracoden

Die Mollusken geben das gleiche Alter für alle andere Aufschlüsse an, auch die Fazies ist ähnlich; daher ist auffallend, dass nur 30% der Gattungen an allen drei Fundorten, 40% nur an zwei Fundorten 30% nur an einem einzigen Fundort vorhanden sind. 11% der Arten kommen an drei Fundorten, 27% zwei und 55% an einem einzigen Fundort vor.

Leider können die Überreste von Pflanzen, welche diewichtigsten ökologischen Bedürfnisse der Ostracoden befriedigt haben sollten, nicht

nachgewiesen werden. Weder die granulometrische Zusammensetzung, noch der Karbonatgehalt weisen einen Zusammenhang mit der Verbreitung der einzelnen Arten auf.

Tabelle II

Verbreitung der Ostracoden

	1	2
Amplocypris munita Zal.	22%	–
Amplocypris sinuosa Zal.	9%	–
Amplocypris elegans (Méh.)	4%	–
Hungarocypris sieberi (Méh.)	24%	8%
Hungarocypris sieberi nodosa (Méh.)	21%	3%
Hungarocypris pannonica Zal.	15%	–
Cyprideis pannonica Zal.	–	65%
Cyprideis pannonica tuberculata (Méh.)	–	6%
Cyprideis sulcata Zal.	–	4%
Hemicytheria lörentheyi (Méh.)	2%	6%
Hemicytheria hungarica (Méh.)	2%	5%
Hemicytheria ampullata (Méh.)	0.5%	1%
Loxoconcha rhombovalis Pokorný	1%	1%
Leptocythere olivina (Livental)	0,5%	–
Leptocythere andrusovi (Livental)	–	0.5%
Erpetocypris reptans Baird	–	0.5%

1 = Tinye; 2 = Alsótold.

In Tinnye sind Hungarocypris sieberi und eine von ihrer Unterarten, H. s. nodosa, am häufigsten und liefern insgesamt 45% der Fauna. Häufig ist noch Amplocypris munita mit 22% und Hungarocypris pannonica mit 15%. In Tinnye fehlt die Gattung Cyprideis, was merkwürdig ist, denn es handelt sich um eine häufige Form der unterpannonischen Unterstufe, die in den gleichalten Bildungen der Umgebung verbreitet ist.

In Alsótold ist Cyprideis pannonica, mit 65%, am weitesten verbreitet. Die anderen Arten sind in beinahe gleicher Zahl vorhanden. Die Gattung Amplocypris fehlt, Hungarocypris ist in kleinerer Zahl, 11%, vertreten. Die gemeinsamen Arten sind verhältnismässig selten. Wenn man die Verbreitung im Rahmen einer höheren systematischen Einheit prüft, so ist die Superfamilie Cypridacea, mit 95%, für Tinnye, die Superfamilie Cytheracea, mit 89%, hauptsächlich für Alsótold charakteristisch.

LITERATUR

Bartha, F. (1971): A magyarországi pannon biosztratigráfiai vizsgálata (Biostratigraphische Untersuchungen des ungarischen Pannons) in: A magyarországi pannonkori képződmények kutatásai (Forschungen im Bereich der Pannon-Bildung in Ungarn). pp. 9–172.

Brusina (1882): Orygoceras eine neue Gastropoden-Gattungen der Melanopsiden-Mergel Dalmatien. Beitr. z. Paläont. Öst. Ung. II. Bd. p. 33.

Brusina (1893): Papyrotheca a new genus of gastropoda form the pontic stepps of Serbia. The Conchiologist Vol. II. p. 7.

Hantken, M. (1887): Tinnyea Vásárhelyii. Egy új csiganem és új faj a Congeria rétegekből (Eine neue Gastropoden-Gattung und neue Art ais den Congerien-Schichten). Földtani Közlöny XVII.

Jámbor, Á. (1967): Budapest környéki neogén képződmények ősföldrajzi vizsgálata (Paläogeographische Untersuchung der Neogenablagerungen der Umgebung von Budapest). Földtani Intézet Évi Jelentése 1967-ről pp. 135 – 142.

Jankovich, I. (1969): Alsópannon fauna Ostorosról (Unterpannonische Fauna von Ostoros). Földtani Közlöny XCIX. pp. 81 – 90.

Méhes, Gy. (1907 – 1908): Adatok Magyarország pliocén Ostracodáinak ismeretéhez (Beitrag zur Kenntnis der pliozänen Ostracoden Ungarns). Földtani Közlöny.

Mezneries, I. (1930): Az Uny – Tinnye vidéki fiatal harmadkorú üledékek földtani és őslénytani viszonyai (Geologische und paläontologische Verhältnisse der jungtertiären Ablagerungen der Umgebung von Uny-Tinnye). Bölcsészdoktori Értekezés pp. 14 – 21.

Lőrenthey, I. (1895): Neuere Daten zur Kenntniss der oberpontischen Fauna von Szegszárd. Természetrajzi Füzetek Vol. XVIII. pp. 316 – 326.

Lőrenthey, I. (1895): Néhány észrevétel a Papyrothecáról (Einige Bemerkungen zu Papyrotheca). Földtani Közlöny XXV. pp. 237 – 241.

Lőrenthey, I. (1902): Die pannonische Fauna von Budapest. Paleontographica Bd. 48. Stuttgart.

Lőrenthey, I. (1903): Néhány megjegyzés az Orygoceras fuchsi Kittl sp.-ről (Einige Bemerkungen zu Orygoceras fuchsi Kittl sp.). Földtani Közlöny XXXIII. pp. 470 – 471.

Lőrenthey, I. (1903): A szarmata és pannóniai képződményeket áthidaló rétegeknek egy classicus lelethelye Magyarországon (Eine klassische Lokalität der das Sarmat und Pannon überbrückenden Schichten in Ungarn). Földtani Közlöny XXXIII. pp. 60 – 62.

Lőrenthey, I. (1905): Érdekesebb kővületek előfordulásáról Tinnye és Budapest környékén (Interessantere Fossilfunde in Tinnye und in der Umgebung von Budapest). Földtani Közlöny XXXV.

Lőrenthey, I. (1900): Foraminiferen der Pannonischen Stufe Ungarns. Neuen Jahrb. für Min. pp. 99 – 107.

Sándor, I. (1932): A Cserhát szarmáciai és pontusi pannóniai üledékei (Die Sarmat- und Pont-Pannon-Ablagerungen des Cserhát). Bölcsészdoktori Értekezés Mezőtúr pp. 25 – 28.

Strausz, L. (1941): Melanopsisok változákonysága (Die Veränderlichkeit der Melanopsis). Földtani Közlöny LXXI. pp. 135 – 146.

Strausz, L. (1941): A dunántúli pannon szintezése (Stratigraphische Horizontierung des transdanubischen Pannons). Földtani Közlöny LXXI. pp. 220 – 235.

Tóth, K. (1971): A Vértes délkeleti előterének pannon képződményei (Pannon-Ablagerungen des SO-Vorlandes des Vértes) in: A magyarországi pannonkori képződmények kutatásai (Forschungen im Bereich des Pannons in Ungarn). pp. 345 – 361. Treatise on invertebrate Paleontology „Q" Ostracoda. Univ. of Kansas 1961.

Vitális, I. (1936): Orygocerasok a Sopron-vidéki alsópontusi üledékekben s elterjedésük hazánkban és a környező országokban (Die Vertreter von Orygoceras in den pontischen Ablagerungen der Umgebung von Sopron und ihre Verbreitung in Ungarn und den Nachbarländern). MTA Mat. és Term. tud. Értesítője LIV. pp. 626 – 643.

Vitális, I. (1937): A soproni Virágvölgy fossilis Bagliviái és kortársaik (Fossile Baglivien ind ihre Zeitgenossen im Virágvölgy bei Sopron). MTA III. oszt. 1937. ápr. 26-i ülés. pp. 672 – 686.

Vitális, I. (1938): Papyrotheca mirabilis és Succinea gracilis (Papyrotheca mirabilis und Succinea gracilis). MTA Mat. és Term. tud. Értesítője LVII. pp. 778 – 787.

Vitális, I. (1951): Sopron környékének szarmáciai és pannoniai-pontusi üledékei és kövületei (Sarmatische und pannon-pontische Ablagerungen und Fossilien in der Umgebung von Sopron). Földtani Intézet Évkönyve pp. 37 – 69.

Zalányi, B. (1929): Morpho-systematische Studien über fossile Muschelkrebse. Geol. Hung. ser. Pal. 5. pp. 1 – 152.

Zalányi, B. (1944): Magyarországi neogén Ostracodák (Die neogenen Ostracoden von Ungarn). Geol. Hung. ser. Pal. 21. pp. 1 – 184.

TAFELERKLAERUNGEN

Tafel I

1. Baglivia sp. Tinnye
   Vergrösserung: 9×
2. Schwammnadeln. Tinnye
   Vergrösserung: 30×
3. Papyrotheca mirabilis Brus. Tinnye
   Vergrösserung: 20×
4. Papyrotheca gracilis (Lőr.). Tinnye
   Vergrösserung: 13×

5 – 8. Veränderung des Seitenumrisses der Art Hungarocypris sieberi im Laufe der Ontogenese
   Vergrösserung: 20×

9. Orygoceras filocinctum Brus. Tinnye
   Vergrösserung: 25×
10. Orygoceras cfr. cultratum Brus. Alsótold
    Vergrösserung: 25×
11. Orygoceras cfr. fuchsi (Kittl). Tinnye
    Vegrösserung: 25×

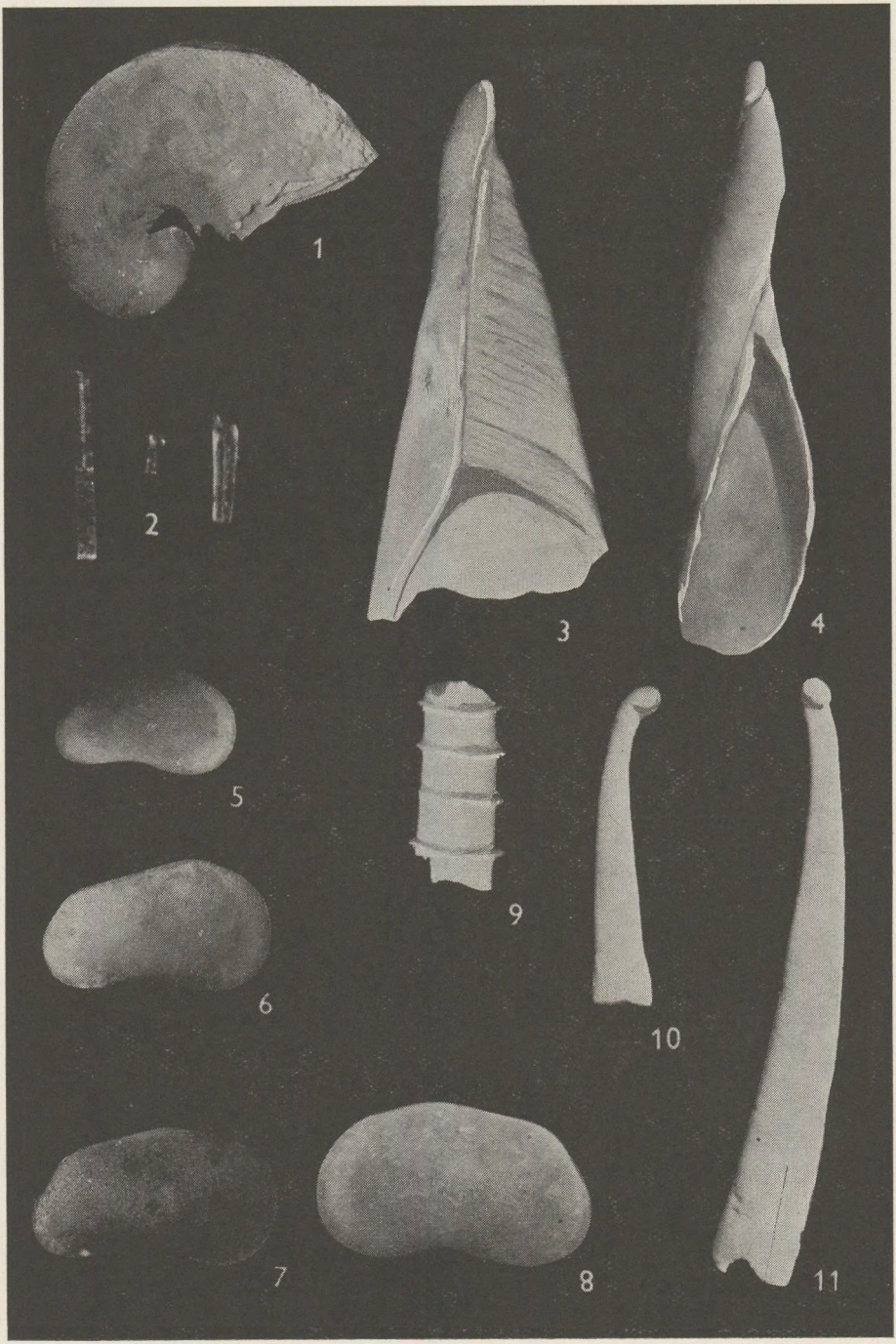
1
2
3
4
5
6
7
8
9
10
11

Tafel II

1. Amplocypris munita Zal. Tinnye
   Vergrösserung: 20×
2. Amplocypris munita Zal. Tinnye
   Vergrösserung: 15×
3. Amplocypris elegans (Méh.). Tinnye
   Vergrösserung: 15×
4. Hungarocypris pannonica Zal. Tinnye
   Vergrösserung: 25×
5. Hungarocypris sieberi (Méh.). Tinnye
   Vergrösserung: 25×
6. Cyprideis pannonica (Méh.). Alsótold
   Vergrösserung: 25×
7. Cyprideis sulcata Zal. Alsótold
   Vergrösserung: 25×
8. Leptocythere andrusovi (Livental). Alsótold
   Vergrösserung: 50×
9. Hemicytheria ampullata (Méh.). Tinnye
   Vergrösserung: 30×
10. Hemicytheria hungarica (Méh.). Alsótold
    Vergrösserung: 20×
11. Hemicytheria hungarica (Méh.). Tinnye
    Vegrösserung: 30×
12. Hemicytheria lőrentheyi (Méh.). Tinnye
    Vergrösserung: 40×
13. Hemicytheria lőrentheyi (Méh.). Alsótold
    Vergrösserung: 40×
14. Amplocypris sinuosa Zal. Tinnye
    Vergrösserung: 15×
15. Loxoconcha rhombovalis Pokorny. Tinnye
    Vergrösserung: 50×
16. Loxoconcha sp. Tinnye
    Vergrösserung: 50×

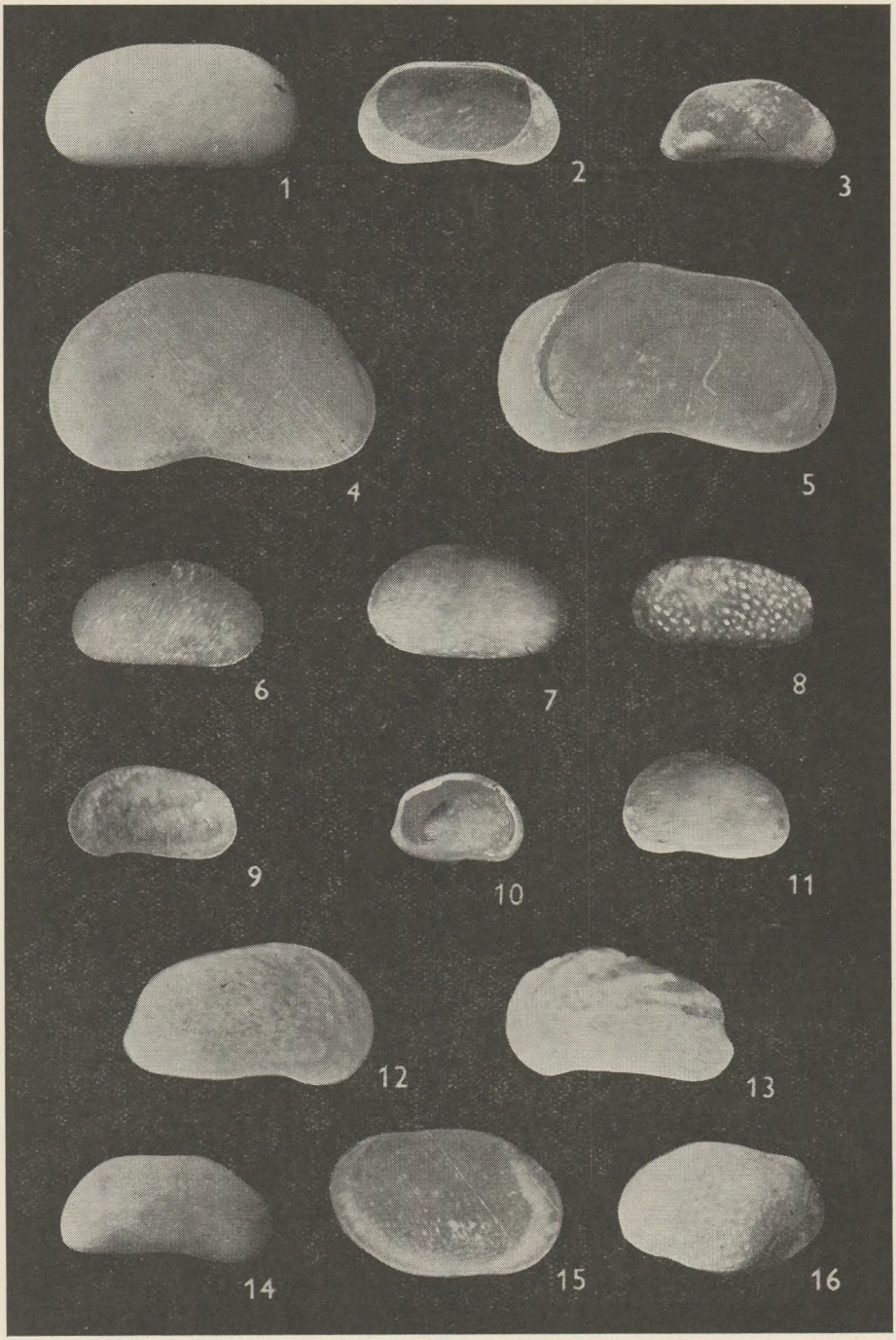
1
2
3
4
5
6
7
8
9
10
11
12
13
14
15
16

GEOCHEMICAL INVESTIGATIONS OF SEDIMENTARY ROCKS FROM THE VICINITY OF FELSŐPETÉNY

by
É. PÉCSI–DONÁTH
Department of Petrography and Geochemistry L. Eötvös University, Budapest

(Received: 31st March, 1972)

ZUSAMMENFASSUNG

Aufgrund der petrographisch-geochemischen Untersuchungen von feuerfesten Tonen aus der Umgebung von Felsőpetény lässt sich Folgendes feststellen: Das Material des Sandsteins stammt z. T. aus metamorphen zum geringen Teil aus magmatischen (granitischen) Abtragungsgebieten. Die profilmässig durchgeführten (Profile I, II, III) Untersuchungen haben der Verfasserin ermöglicht nachzuweisen, dass die triadischen und oligozänen Formationen unter verschiedenen Verhältnissen entstanden sein konnten. Die industrielle Qualität der feuerfesten Tonlinsen variiert in Abhängigkeit von den durch die Verfasserin nachgewiesenen fünf Tontypen. Das Gebiet ist an Spurenelementen arm. Die Menge der Spurenelemente verändert sich je nach der Lithologie des Gesteins. Der Spurenelementgehalt nimmt in der Reihenfolge Kalkmergel → Tonmergel → Ton [Tone von gemischtem Tonmineralgehalt → karbonatführende Tone → limonitführende Tone → fast reinen Kaolinit enthaltende Tone → Sandstein und Konglomerat ab.

It was in connection with the complex petrographical-geochemical-volcanological investigations of the Cserhát Mountains that the sedimentary petrographical and geochemical analyses of the refractory clays of the vicinity of Felsőpetény were also carried out.

The Felsőpetény refractory clay deposit falls geographically to the territory of one of the faultblocks (horsts) of the Danube's left bank: the Romhány horst (Fig. 1). With a view to its geological structure, this can be taken to be the last outpost of the Transdanubian Central Mountains range.

It was investigated geologically by such reputed scientists of the last century as Stache (1866) and Hauer (1870) and subsequently by J. Noszky Sen. (1939, 1941), E. Vadász (1910), L. Bartkó (1948), L. Majzon (1952), B. Jantsky (1952), Gy. Varjú (1955) and É. V.-Ákos (1964).

In addition to the above, recent results of detailed investigations of the Felsőpetény refractory clays were reported by B. Gabona (1969), G. Venczel (1969), F. Kneifel (1970) and M. Horváth (1971). The industrial significance of the deposit was evaluated in a multi-Mining Unit of the National Enterprise for Ore and Mineral Mining (1971).

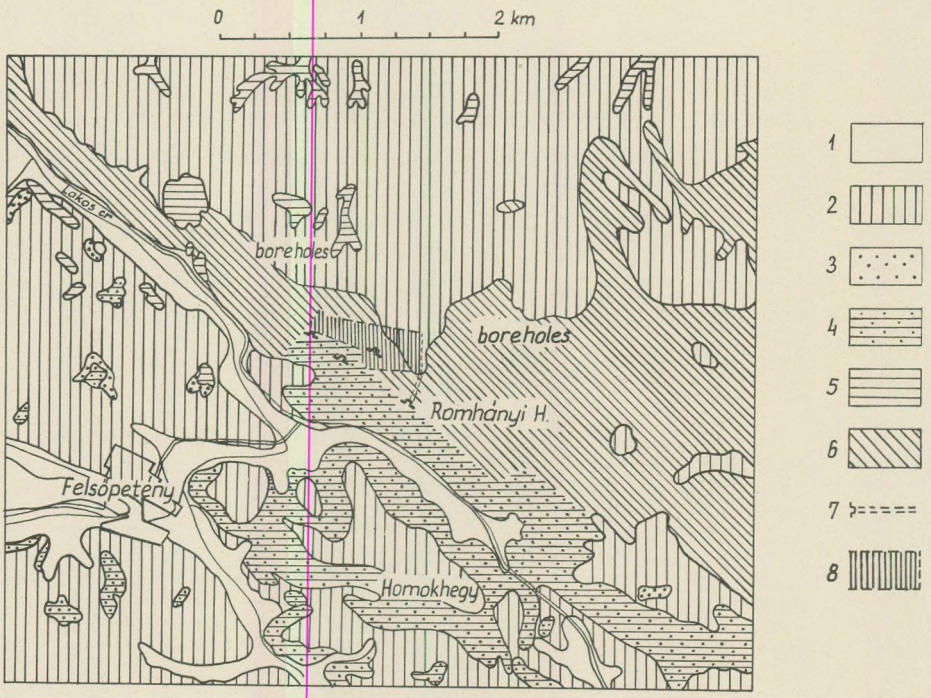

Fig. 1. Geological map of the Romhány horst

1. Alluvium (Holocene); 2. Loess (Pleistocene); 3. Limonitic gravels (Lower Miocene); 4. Sandstones and schlier (Upper Oligocene); 5. Kiscell Clay (Middle Oligocene); 6. Sandstone (Lower Oligocene); 7. Adit; 8. Area with resources stripped off; (Compiled in the Pilisvörösvár Mining Unit of the National Enterprise for Ore and Mineral Mining)

As shown by different authors, early and recent, the refractory clay beds of the area are enclosed within Lower Oligocene sandstones underlain by Upper Triassic, Norian, Dachsteinkalk (in some places Eocene Lithothamnium limestones have also been cut by drilling) and overlain by Pleistocene or Holocene sediments, respectively.

The author's investigations were aimed at determining the geochemical distribution of trace elements. In addition, the quality of the clay minerals (by means of derivatograph) and, the lithology of the sandstones and limestones as well as their trace element distribution were investigated.

In the vicinity of Felsőpetény – Romhány both sandstones and refractory clays repeat themselves several times within the Lower Oligocene sequence, which made troublesome the correct identification of the formations. To eliminate this and to provide a basis for the real evaluation of the data as well as to shed light upon the distribution of the trace elements at different depths, the author has analysed mineralogico-petrographically and geochemically the materials of the 23 holes drilled by the National Enterprise for Ore and Mineral Mining and she has processed

them along three main strike directions (Fig. 2), too. (I. NW–SE trending northern profile: Boreholes 212, 215, 233, 225, 244, 297; II. NW–SE trending southern profile: Boreholes 275, 269, 272, 263, 328, 315: III. NE–SW trending profile: Boreholes 247, 245, 240, 299, 310, 328.) Beside processing in detail the materials of Boreholes 344 and 339 and Boreholes 341 and 342, situated a little farther away from the area, the author has extended her investigations to the partly processed materials of Boreholes 292, 286, 291, 293, 296, 298, 301 and 283 as well.

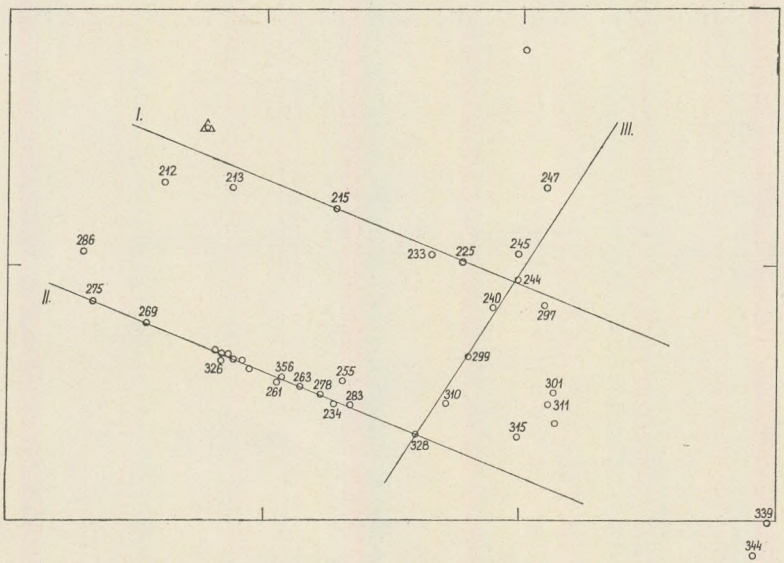

Fig. 2. Distribution of the investigated boreholes by profiles

The analyses for trace elements were performed with the aid of a quartz spectrograph Q–24 designed by J. Nagy-Balogh, staff engineer of the Department. A quantitative evaluation of informative nature was done with the use of a series of synthetic standards, with the aid of a combination of concentration and "*Y*" scales. The geometric mean of the "minimum and maximum" averages used in the Hungarian Geological Institute has been considered to be the average value, whereas the enrichment factor (*ef*) has been the ratio of the average of an element as referred to the average given by Vinogradov for sediments.

The *X*-ray analyses were performed by L. Bognár with the *X*-ray diffractometer of the Department of Mineralogy, L. Eötvös University.

Geology of the Area

Fig. 3 shows as type one of the vertically elaborated boreholes of Felsőpetény. The Triassic limestones are locally followed by Eocene limestones, overlain by calcareous marls, marls and, occasionally, clay-marls as representatives of the Oligocene. These are followed by an alternation of sandstones (conglomerates) and refractory clays overlain by Pleistocene-Holocene formations as final members of the sequence.

The oldest member is Upper Triassic limestone characterizable by an erosion surface on which the Eocene sedimentary sequence rests with a sharp unconformity, being locally confined just to isolated spots.

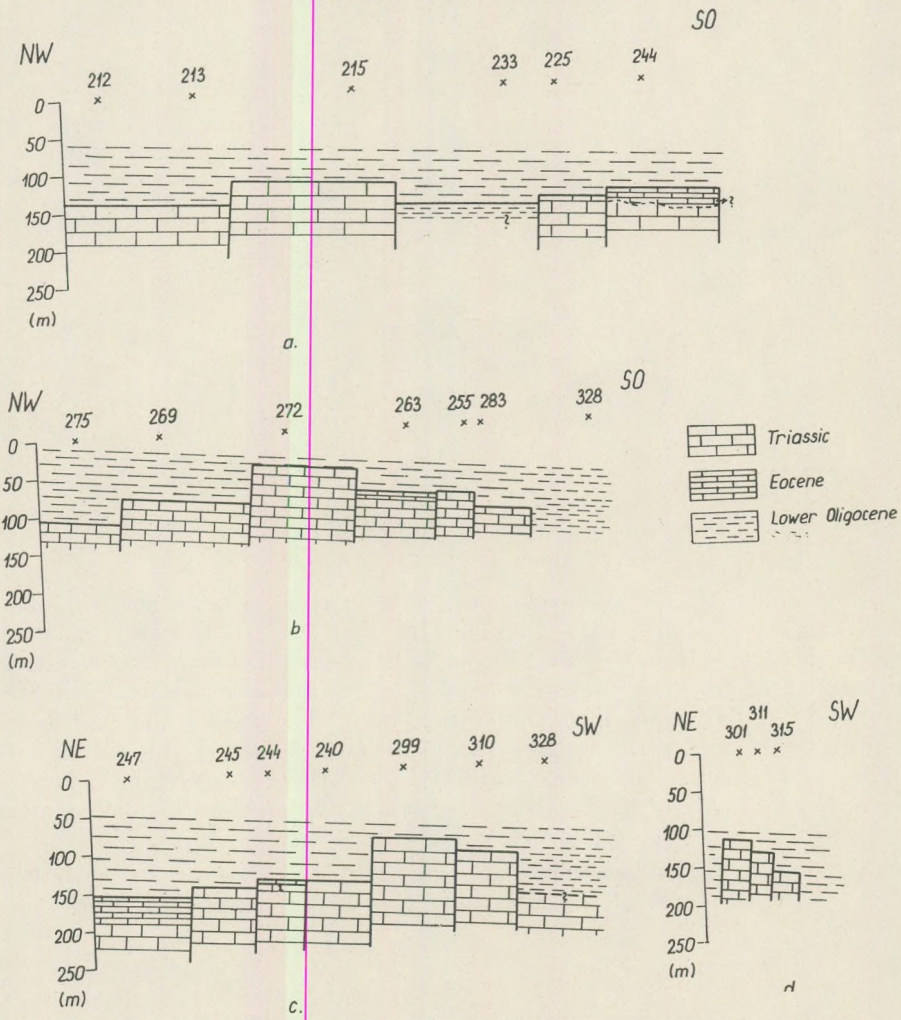

Fig. 4. Sketch of the relative positions of the Triassic limestone blocks

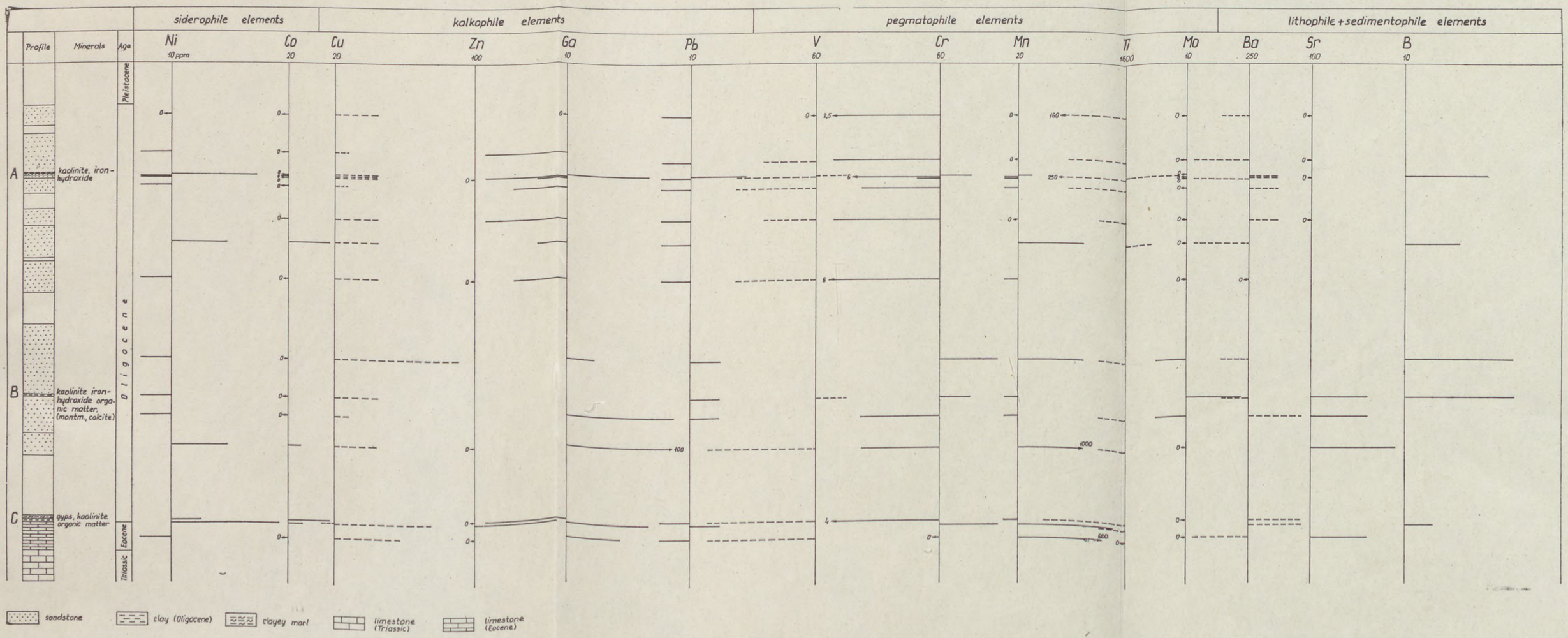

Fig. 3. Lithological log of Borehole Felsőpetény 263 showing the clay mineralization and trace element concentration data

The block-faulting of the area is indicated by the fact that along the two neighbouring sections the Triassic sediments lie at different depths, i. e. in the southern section of NW—SE direction (II) they are of higher position than in the others (I, III). On the basis of the depth data of the Triassic limestones the topography the area is supposed to have had in the Triassic period has been sketched (Fig. 4).

According to É. V. - Á k o s, the geohistorical evolution of the Lower Oligocene formations can be summarized as follows: after the Early Oligocene transgression (represented by the ingression sandstones of Horizon $C/1$ and the clays of Horizon C) the area slowly emerged. Thereafter, a new transgression took place, as indicated by about 50 m of sandstone, to be followed again by an emergence. In the resulting lagoon of some 500 m in diametre a comparatively thick sequence of sandy clays and palustrial and fluviatile sediments (sands of Horizon $B/1$ and clays of Horizon B) were deposited. The overlying sandstones of about 40 m thickness indicate the transgression again (Horizons $A/1$ and A).

The Lower Oligocene sandstone sequence, $C/1$, overlies the Triassic and the Eocene, respectively, the transition to $B/1$ being often continuous.

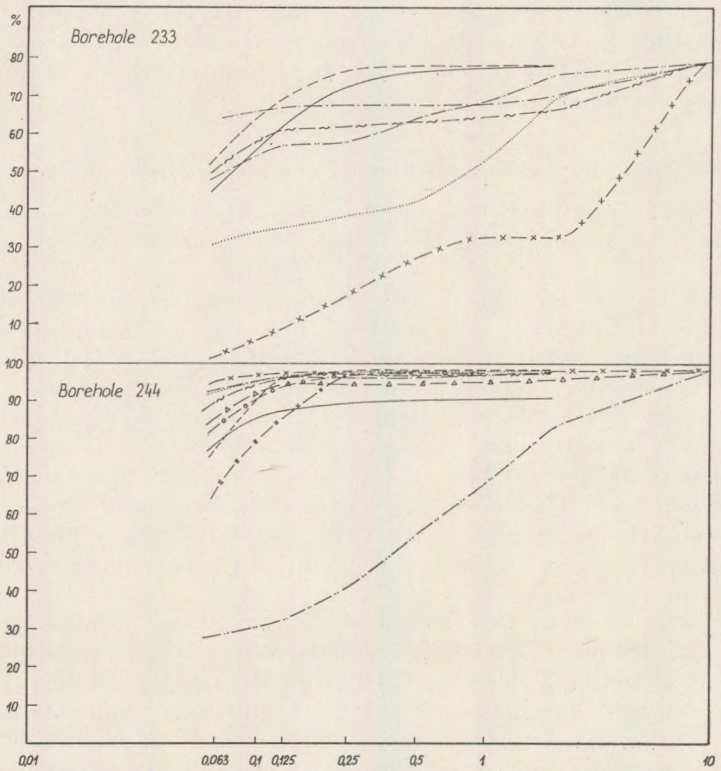

Fig. 5. Grain size distribution curves (Boreholes 233, 244)

In the somewhat thicker section of NW–SE direction (I) interbedded marls and clay- marls are also frequent in the basal member of the sandstone sequence.

The sandstone sequence $B/1$ of varying thickness, 20 to 40 m, interrupted by clay lenses in many places, is often of siltstone facies. It is $B/1$ that contains the commercial refractory clay bodies. In some places, the clays form lenses separated from the sandstones by a sharp boundary or by the change of grain size. The transition is less frequently continuous; the less so, an alternation of thin sandstone and refrectory clay can occasionally be observed.

The sandstone sequence $A/1$ in the investigated area was found to be thicker (10–60 m) than in the area discussed by É. V.-Á k o s. Its thickness decreases along the southern section of NW–SE direction (II). A frequent alternation of sandstone and clay lenses can be observed within the sequence.

The grain size distribution of the single boreholes relates to a varied compositions (Fig. 5). For instance, Sample 21 of Borehole 233 was found to be a sandstone of mixed grain size composition, similarly to Sample 16. In this borehole, sandstones and clays repeat themselves several times, as reflected by the grain size distribution curve. Only three samples (8, 10, 19) show higher clay content. In other cases the samples from different depths of Borehole 244, have similar grain size composition, except for the Pleistocene ones (Fig. 5).

Mineralogical Composition of the Lower Oligocene

Clay-marls contained: kaolinite, illite, hydromuscovite, some montmorillonite as well as varying quantities of organic matter, pyrite and calcite.

In addition to the quartz, calcareous marls contained some illite, kaolinite, montmorillonite and calcite. The derivatograph showed the presence of pyrite, some organic matter and limonite. The calcareous marls, in the neighbourhood of the limestone, contain illite and some kaolinite; in many cases, montmorillonite is also detectable.

Although cut through by several boreholes, conglomerates are nevertheless of local development. In some places, they grade into coarse-grained sandstones. They show a varying grain size composition, consisting of rounded quartz grains, the finer fraction being represented by (limonitic) clays indicating sedimentation in an oxidative environment (terrestrial origin).

In accordance with the results of É. V.-Á k o s and F. K n e i f e l, the author's micromineralogical analyses have shown the sandstones of the investigated area to be constituted predominantly by heavy minerals of metamorphic origin. The material of sandstone originates in smaller measure from an igneous (granitic) source area. Components of volcanic origin, indicating the Upper Eocene andesitic tuffs, occur just sporadically (Table I).

Micromineralogical analyses of sandstones Table I

	A	B	C	D	Nm
212/13	limonite	garnet limonite biotite (bleached too)	limonite magnetite tourmaline biotite muscovite	magnetite muscovite biotite tourmaline pyrite	quartz calcite chlorite (1 – 2) limonite
215/9	biotite muscovite	garnet magnetite	chlorite tourmaline bleached biotite (greenish)	quartz tourmaline pyrite muscovite limonite calcite fossil	quartz chlorite (1 – 2)
233/10	limonite tourmaline biotite muscovite (1 – 2)	zircon fragment muscovite biotite limonite tourmaline magnetite (1 – 2)	limonite bleached biotite muscovite (1 – 2)	limonite coated quartz tourmaline garnet-muscovite (1 – 2)	quartz chlorite calcite (1 – 2)
244/4	limonite muscovite	muscovite limonite tourmaline garnet	biotite plate tourmaline chlorite muscovite limonite sericite	chlorite quartz-grained limonite pseudomorphs limonitic concretions muscovite sericite	chlorite quartz garnet muscovite (1 – 2) tourmaline biotite flakes (1 – 2)
269/11	limonite (1 – 2 grains)	limonite garnet chlorite	tourmaline limonite zircon	muscovite garnet tourmaline sericitic slightly limonitic concretions	quartz calcite (1 – 2) muscovite

Micromineralogical analyses of sandstones Table I

	A	B	C	D	Nm
328/14	limonite biotite zircon fragment quartz	magnetite limonite sericite concretions biotite hematite	limonite magnetite muscovite biotite sericite con- cretions	mica sericite concr. quartz chlorite tourmaline limonite	quartz calcite limonite (1 – 2)
341/9	limonite dotted with quartz grains limonite dotted with musco- vite grains	limonite some magnetite quartz biotite muscovite	limonite some biotite muscovite limonite coated quartz and musco- vite	quartz with limonite on the surface muscovite limonite (1 – 2)	quartz limonite (1 – 2)
342/5	tourmaline garnet chlorite magnetite limonite sericite	biotite garnet limonite chlorite	magnetite sericite muscovite biotite tourmaline	muscovite quartz magnetite tourmaline limonite	quartz muscovite chlorite calcite

The mineralogical composition of the refractory clays has also been determined by derivatographic and X-ray diffraction analyses. As it is shown in the micromineralogical results obtained for the residue of washing of the refractory clays assigned to the A, B and C Horizons within the Lower Oligocene sandstone sequence, the material should be derived partly from metamorphic, partly from igneous areas. 5 main types of refractory clays have been distinguished: (*a*) type characterized by the predominance of kaolinite; (*b*) type of mixed clay mineralization; (*c*) overwhelmingly kaolinitic type accompanied mainly by calcite; (*d*) type of mixed clay mineralization with pyrite and organic matter; (*e*) type characterized by the predominance of kaolinite and iron hydroxide (Fig. 6.). The vertical distribution of the clay mineral types can be characterized as follows: In Horizon C mainly types (*d*) and (*e*), and occasionally (*c*) are represented. In Horizon B mainly types (*b*) and (*a*), in Horizon A primarily types (*a*) and (*b*) are predominant.

According to DTA results obtained for the lower than 0.063 mm fraction of some samples, the finer fraction is characterized by the appearance beside the clay minerals, of hydromuscovite and, occasionally, limonite and calcite as well; whereas the ratio of the organic substances

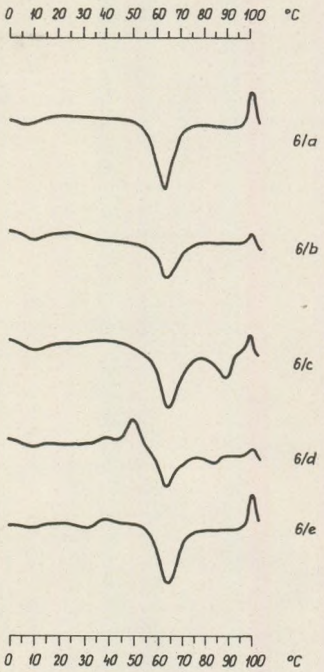

Fig. 6. DTA curves of the main types of refractory clays:

(a) type characterized by the predominance of kaolinite, *(b)* type of mixed clay mineralization, *(c)* overwhelmingly kaolinitic type accompanied mainly by calcite, *(d)* type of mixed clay mineralization with pyrite and organic matter, *(e)* type characterized by the predominance of kaolinite and iron hydroxide

is very reduced. However, both the mixed and the < 0.063 mm grain fractions show essentially the same clay mineral content (Table II).

Also the clay mineral content shows a characteristic distribution by profiles. The material recovered from the boreholes of the profile of NW – SE direction is rather kaolinitic with some pyrite and organic matter (type (*d*)). In the territory of this profile and in its vicinity mainly refractory clays of type (*c*) were formed in a relatively more reductive, probably palustrial environment, at more acidic pH (Horizon *C*).

In this area, a considerable part of the clay lenses of Horizon *B* is kaolinite with which, similarly to Horizon *C*, some pyrite and organic matter are associated. In the southern profile of the same strike type (*b*) is predominant. In addition, Horizon *C* is characterized here, by the richness of carbonates. In the uppermost refractory clay lenses or beds of the southern profile the kaolinite is the predominant constituent again.

In Horizon *C* of the profile of NE–SW direction the predominant kaolinite is accompanied by some pyrite and organic matter. On the basis of the considerable iron hydroxide content of the predominant clay minerals the sediments of the higher strata, however, could have been deposited in a more oxidative environment and they could have later been introduced into an environment of this kind, respectively.

The *X*-ray analyses showed that the examined refractory clays contain beside kaolinite, some pyrite, muscovite and quartz, as well. In cer-

Table II

Derivatographic analyses of mixed grain fractions and below 0.063 mm in diametre

Borehole 212 4—4/a	Composition of clay minerals of mixed grain size	Composition of the 0.063 mm fraction
	kaolinite, (very little) muscovite	kaolinite, iron hydroxide
6.	limonite, some organic matter	kaolinite, pyrite
7.	kaolinite, some hydromuscovite	kaolinite, some hydromuscovite
13.	illite, organic matter, pyrite, limonite	kaolinite, illite, gypsum, pyrite, hydromuscovite
23.	kaolinite, limonite, hydromuscovite, some organic matter	kaolinite, hydromuscovite, hydromuscovite, iron hydroxide
272.		
1.	illite, kaolinite, hydromuscovite, limonite	kaolinite, illite, iron hydroxide
3.	kaolinite, illite, limonite, hydromuscovite	kaolinite, illite, hydromuscovite
4.	kaolinite, illite, hydromuscovite, limonite	kaolinite, illite, hydromuscovite
6.	kaolinite, illite, hydromuscovite	kaolinite, illite, hydromuscovite
9.	kaolinite, quartz, limonite, illite	kaolinite, hydromuscovite, calcite
272/10	kaolinite, hydromuscovite, limonite (illite)	kaolinite, iron hydroxide, illite hydromuscovite
269/2	kaolinite, limonite, some organic matter	kaolinite, pyrite, iron hydroxide
12.	gypsum, organic matter, pyrite, kaolinite	pyrite, organic matter, hydromuscovite

tain cases feldspar, dickite and nacrite could be identified, too. The relatively high quantity of goethite, occurring locally, seems to indicate rather oxidative conditions of sedimentation.

Dickite and nacrite also suggest the possibility of post-sedimentary hydrothermal action (?).

The lateral variation of the clay mineralization has allowed the author to conclude that in the course of the Early Oligocene sedimentation different conditions should have prevailed in the investigated area.

Geochemical investigations

The average values of the trace elements in the Triassic limestones are shown in Table III. On the basis of the enrichment factor (ef), Ag, As, and Sr show some enrichment [ef = 6.4 (Ag); 6.9 (As); 1.1 (Zn); 1.3 (Sr)]. The Ag and As could be determined only in a few samples, hence the average. The variation of the trace elements along the three profiles can be summarized as follows.

i) Along the southern profile of NW—SE direction the As content is high (ef = 8.5) as compared to V i n o g r a d o v's average As contents of sedimentary rocks. This value, however, refers to the

Table III

Averages of trace elements and their distribution by profiles in Triassic limestones

		Total		Profile I		Profile II		Profile III	
		average	ef	average	ef	average	ef	average	ef
Siderophile	Co	10.43	0.52	5.6	0.28	11.2	0.56	5.6	0.28
	Ni	19.48	0.21	14.5	0.15	24.8	0.26	7.2	0.08
Calcophile	Cu	28.74	0.50	42.6	0.75	31.4	0.55	16.1	0.28
	Ag	0.64	6.40	0.5	5	–	–	–	–
	Cd	–	–	–	–	–	–	–	–
	Hg	–	–	–	–	–	–	–	–
	As	39.24	6.95	56.5	8.56	71.5	10.83	–	–
	Sb	–	–	–	–	–	–	–	–
	Bi	–	–	–	–	–	–	–	–
	Te	–	–	–	–	–	–	–	–
	Zn	88.31	1.10	70.7	0.88	221.4	2.77	35.3	0.44
	Ga	3.30	0.11	6.1	0.20	3.1	0.10	1.2	0.04
	Ge	–	–	–	–	–	–	–	–
	In	–	–	–	–	–	–	–	–
	Sn	1.18	0.12	–	–	4.4	0.44	–	–
	Tl	–	–	–	–	–	–	–	–
	Pb	8.13	0.41	6	0.30	8.8	0.44	6	0.30
Pegmatophile	Sc	–	–	–	–	–	–	–	–
	V	14.43	0.11	8.5	0.07	7.1	0.05	–	–
	Cr	13.46	0.13	4.9	0.05	11.3	0.11	7.8	0.08
	Mn	333.9	0.50	547.5	0.82	364	0.54	515	0.77
	Ti	261.9	0.06	152.1	0.03	176	0.04	37.9	0.01
	Y	–	–	–	–	–	–	–	–
	Zr	–	–	–	–	–	–	–	–
	Nb	–	–	–	–	–	–	–	–
	Mo	0.31	0.16	–	–	2.6	1.30	–	–
	Ta	–	–	–	–	–	–	–	–
	W	–	–	–	–	–	–	–	–
Lithophile	Li	–	–	–	–	–	–	–	–
	Be	–	–	–	–	–	–	–	–
	Ba	355.2	0.44	335	0.42	224	0.28	238.7	0.30
	Sr	591.1	1.31	351.2	0.78	500	1.11	443.7	0.99
Sedimentophile	B	15.78	0.16	10	0.10	10	0.10	10	0.10

ef = enrichment factor

As contents of the Triassic member of one borehole. In the same profile the value of Ag (ef = 0.7) and Zn (ef = 0.8) were higher than the others.

ii) Along the northern profile of NW–SE direction, As was similarly abundant as in the former (ef = 10.8), but no Ag was observed. Zn (ef = 22.8) showed a striking concentration peak, while Sn and Mo, found just in one sample of this profile, were relatively enriched (ef = 1.3) as compared to the sedimentary average.

iii) As shown by the trace element content of the two profiles of NW–SE direction, the Triassic rocks of the Boreholes 215 and 272 of rather high hypsometric position are richer in trace elements than those uncovered by the other boreholes. (For a more detailed evaluation of the Triassic limestones, see the paper by J. Rózsavölgyi in this same fascicle.)

Out of the trace elements of the clay-marls, Co, Ni, Ag, As, Zn, Pb, Cr, Sn, Mn, Mo and Sr are present in quantities higher or nearly the same than the sedimentary average. The increase of the concentration of trace elements may have been enhanced by the deposition of placers caused by transgression and possibly by subsequent hydrothermal solutions. Sr can replace the Ca of the carbonate, Cr seems to be contained in the clay minerals, mainly the common illite of the marls. The somewhat higher B content of the clay-marls suggests a marine, sedimentary origin (Table IVa). In the marls the elements Co, Ni, Cu, Ag, As, Zn, Sn, Pb, Cr, Mn, Mo and Sr are enriched, particularly with regard to the other rock types. Here again, the substitution of Ca for Sr seems to be the case, Mo can be fixed by the clay minerals of the marls. Co, Ni, Cu and Zn may be considered a result of subsequent hydrothermal effects as well (?) (Table IVb).

Although the marls and clay-marls contain certain elements of higher concentrations, they cannot be called trace element concentrators.

Out of the trace elements of the calcareous marls, Co (ef = 1.7), Ni, Cu, As, Zn, Pb, V, Mn, Mo and Li are present in considerable amounts, Sr shows a slight enrichment. Cr and V are fixed in illite, Zn and Cu seem to derive from post-sedimentary dissolution. The enrichment of Co and Ni shows certain correlation with the organic matter (Table V). The calcareous marls show minor concentration peaks for almost all of the trace elements.

The conglomerates are characterized by the poorness of trace elements. None of the trace elements has an enrichment factor attaining the value of 1. With regard to the rest of the trace elements, Sr, Mn and Ti show values close to 1 (Table VI).

Let us summarize now the results of the analysis for trace elements of the Lower Oligocene sandstone sequence. The psammitic formations of the investigated area contain relatively few trace elements and even these are present each in a low concentration. The psammitic rocks of the

Table IV

Averages of trace elements and their distribution by profiles in clay-marls and marls

a) **Clay-marl**

		Total		Profile I		Profile II		Profile III	
		average	ef	average	ef	ave-rage	ef	ave-rage	ef
Siderophile	Co	42.78	2.14	40.7	2.04	16	0.80	38.4	1.92
	Ni	108.44	1.14	102.7	1.08	40	0.42	94.7	1.00
Calcophile	Cu	46.76	0.82	49.8	0.87	40	0.70	42.7	0.75
	Ag	0.14	1.41	0.02	0.20	–	–	–	–
	Cd	–	–	–	–	–	–	–	–
	Hg	–	–	–	–	–	–	–	–
	As	72.60	11.00	77.5	11.74	–	–	60.4	9.15
	Sb	–	–	–	–	–	–	–	–
	Bi	–	–	–	–	–	–	–	–
	Te	–	–	–	–	–	–	–	–
	Zn	125.5	1.57	133.3	1.67	100	1.25	118.5	1.48
	Ga	16.07	0.53	19.6	0.65	10	0.33	14.7	0.49
	Ge	–	–	–	–	–	–	–	–
	In	–	–	–	–	–	–	–	–
	Sn	8.76	0.88	10.5	1.05	–	–	9	0.90
	Tl	–	–	–	–	–	–	–	–
	Pb	23.02	1.15	25	1.25	16	0.80	17,4	0.87
Pegmatophile	Sc	–	–	–	–	–	–	–	–
	V	111.9	0.86	124.7	0.96	60	0.46	101.4	0.78
	Cr	121.14	1.21	136.7	1.37	160	1.60	135	1.35
	Mn	1805	2.69	2246	3.35	100	0.15	1730.3	2.58
	Ti	2497	0.55	3352.9	0.75	1000	0.22	2857.1	0.63
	Y	–	–	–	–	–	–	–	–
	Zr	–	–	–	–	–	–	–	–
	Nb	–	–	–	–	–	–	–	–
	Mo	15.55	7.78	5.2	2.60	–	–	24.6	12.3
	Ta	–	–	–	–	–	–	–	–
	W	–	–	–	–	–	–	–	–
Lithophile	Li	–	–	–	–	–	–	–	–
	Be	–	–	–	–	–	–	–	–
	Ba	667.9	0.83	430	0.64	160	0.20	1072.1	1.34
	Sr	417.6	0.93	391.1	0.87	100	0.22	586.4	1.30
Sedimentophile	B	62.7	0.63	77.3	0.77	40	0.40	62.5	0.63

Table IV

Averages of trace elements and b) **marl** their distribution by profiles in clay-marls and marls

Marl

		Total		Profile I.		Profile II.		Profile III.	
		average	ef	average	ef	average	ef	average	ef
Siderophile	Co	60.36	3.02	55.2	2.76			42.3	2.115
	Ni	152.9	1.33	160	1.68			112.2	1.181
Calcophile	Cu	63.15	1.11	43	0.75			94.2	1.65
	Ag	0.22	2.24	0.4	4			–	–
	Cd	–	–	–	–			–	–
	Hg	–	–	–	–			–	–
	As	97.19	14.73	129.7	19.65			85.5	12.95
	Sb	–	–	–	–			–	–
	Bi	–	–	–	–			–	–
	Te	–	–	–	–			–	–
	Zn	162	2.03	203.5	2.54			120.3	1.50
	Ga	21.88	0.73	41	1.37			–	–
	Ge	–	–	–	–			–	–
	In	–	–	–	–			–	–
	Sn	10.67	1.07	16	1.6			7.8	0.78
	Tl	–	–	–	–			–	–
	Pb	32.16	1.61	48.3	2.42			40.1	2.01
Pegmatophile	Sc	–	–	–	–			–	–
	V	119.05	0.92	184	1.42			122.8	0.94
	Cr	122.5	1.23	172	1.72			162.8	1.63
	Mn	1128.4	1.68	2940	4.39			490.8	0.73
	Ti	2938	0.65	4800	1.07			2371.4	0.53
	Y	–	–	–	–			–	–
	Zr	–	–	–	–			–	–
	Nb	–	–	–	–			–	–
	Mo	22.8	11.40	2.6	1.30			28.2	14.10
	Ta	–	–	–	–			–	–
	W	–	–	–	–			–	–
Litophile	Li	–	–	–	–			–	–
	Be	–	–	–	–			–	–
	Ba	394.8	0.50	480	0.60			311.4	0.39
	Sr	655.5	1.46	830	1.84			700	1.56
Sedimentophile	B	71.6	0.72	152	1.52			69.2	0.69

Table V

Averages of trace elements and their distribution by profiles in calcareous marls

		Total	
		average	ef
Siderophile	Co	94.20	4.71
	Ni	153.12	1.61
Calcophile	Cu	65	1.14
	Ag	–	–
	Cd	–	–
	Hg	–	–
	As	56.57	8.57
	Sb	–	–
	Bi	–	–
	Te	–	–
	Zn	134.2	1.68
	Ga	11.45	0.38
	Ge	–	–
	In	–	–
	Sn	6.5	0.65
	Tl	–	–
	Pb	22.88	1.14
Pegmatophile	Sc	–	–
	V	156.4	1.20
	Cr	86.37	0.86
	Mn	4214.5	6.29
	Ti	2750	0.61
	Y	–	–
	Zr	–	–
	Nb	–	–
	Mo	3.53	1.77
	Ta	–	–
	W	–	–
Lithophile	Li	141.4	2.36
	Be	–	–
	Ba	518.7	0.65
	Sr	787.5	1.75
Sedimentophile	B	40	0.40

Table VI

Averages of trace elements and their distribution by profiles in conglomerates

		Total		Profile I		Profile II		Profile III	
		average	ef	average	ef	average	ef	average	ef
Siderophile	Co	14.85	0.74			6.1	0.06	18.6	0.20
	Ni	12.51	0.13			22.7	0.40	35	0.61
Calcophile	Cu	19.71	0.34			–	–	–	–
	Ag	–	–			–	–	–	–
	Cd	–	–			–	–	–	–
	Hg	–	–			–	–	–	–
	As	54.87	8.31			–	–	–	–
	Sb	–	–			–	–	–	–
	Bi	–	–			–	–	–	–
	Te	–	–			–	–	–	–
	Zn	64.16	0.81			70.7	0.88	81.6	1.02
	Ga	3.60	0.12			3	0.10	10.3	0.34
	Ge	–	–			–	–	–	–
	In	–	–			–	–	–	–
	Sn	–	–			–	–	–	–
	Tl	–	–			–	–	–	–
	Pb	7.51	0.38			7	0.09	6	0.30
Pegmatophile	Sc	–	–			–	–	–	–
	V	13.32	0.10			14.5	0.11	17	0.13
	Cr	14.92	0.15			17.5	0.18	20.6	0.21
	Mn	27.17	0.04			16.7	0.02	15.6	0.02
	Ti	620.6	0.14			600	0.13	3466.6	0.77
	Y	–	–			–	–	–	–
	Zr	–	–			–	–	–	–
	Nb	–	–			–	–	–	–
	Mo	–	–			–		–	–
	Ta	–	–			–	–	–	–
	W	–	–			–	–	–	–
Lithophile	Li	–	–			–	–	–	–
	Be	–	–			–	–	–	–
	Ba	130.9	0.16			115	0.14	300	0.38
	Sr	76.69	0.17			70.7	0.16	100	0.22
Sedimentophile	B	10.11	0.10			11.5	0.12	10	0.10

southern profile of NW–SE direction are somewhat richer in trace elements than in the case of the northern profile. As, Zn and Ag can be shown to be present in equal amounts in the sandstones of all of the profiles. Their concentration is approximately the same as the Vinogradov average of sedimentary rocks (ef = 1). Li appears in one or two sandstone samples of a few boreholes, Be shows similar behaviour just in one sandstone sample of the northern profile. Nb was found in a single sandstone sample of the profile of NE–SW direction. Zn is an element of overall distribution Mo and Sn are relatively frequent, but their concentrations are low.

The quantitative distribution of the trace elements indicates that the psammitic materials of the area derive from a granitic area, at least partly.

The concentration of B is generally low in the psammitic rocks showing its mainly terrestrial origin. Similarly Ga is of higher quantity (60 ppm) in the sandstone of some boreholes of the NW–SE section, and it is twice higher in average than in the average of the sedimentary rocks (Table VII).

The Co, Ni, Cu etc. are enriched in the sandstone as compared to Turekian-Wedepohl's average. The twice higher average of Co shows alluvial origin.

The trace element content of sandstones does not reflect the independence of É. V.-Á k o s' genetical groups *A*/1, *B*/1 and *C*/1. This reflects the fact that the source area did not change substantially during the regressions that followed the transgression.

Being poor in trace elements, the sandstones contain in some cases somewhat higher quantities of Ba, Sr, Ti, Mn, P. Zn and Cu–a manifestation of the diversified genetic conditions of the sandstones.

In order to find out the relationship between the enrichment of trace elements and grain size, the author determined also the trace element content of the 0.05–0.002 mm fraction and averaged the obtained results. As shown by a comparison with the trace element content of the original samples, Co, Ba and V are associated with grain sizes exceeding 0.05 mm. Within the 0.05–0.002 mm size fraction V (Ni) is enriched in the larger fraction, B, Pb and Zn are in the medium fraction, Ti, Cr and Cu, Mn in the smaller one. The afore-mentioned enrichment seems to be connected, at least in part, with the distribution of the heavy minerals, according to fractions (Table VIII).

The clay lenses of the Lower Oligocene sequence in the vicinity of Romhány-Felsőpetény show a diversified trace element assemblage, they can be considered as concentrators of trace elements as compared to the other formations (Fig. 3). Regarding the trace element content of the pelitic rocks along the profile, it can be concluded, that the calcareous clays of relatively little volume recovered from the boreholes of the northern profile of NW–SE direction are richest in trace elements. All the examined elements but Ga and Ba show concentrations exceeding the Vinogradov averages. In the clays containing relatively great quantities

Table VII

Averages of trace elements and their distribution by profiles in sandstones

		Total		Profile I		Profile II		Profile III	
		average	ef	average	ef	average	ef	average	ef
Siderophile	Co	16.26	0.813	16	0.80	11.3	0.57	19.4	0.97
	Ni	16.67	0.185	22	0.23	11.6	0.12	17.1	0.19
Calcophile	Cu	34.74	0.609	43	0.75	33.3	0.59	36.7	0.64
	Ag	0.44	4.43	0.4	4.00	0.3	3.00	0.3	3.00
	Cd	–	–	–	–	–		–	–
	Hg	–	–	–	–	–	–	–	–
	As	41.43	6.277	59.7	9.05	46	6.97	62.1	9.41
	Sb	–	–	–	–	–	–	–	–
	Bi	–	–	–	–	–	–	–	–
	Te	–	–	–	–	–	–	–	–
	Zn	78.58	0.982	90.1	1.13	78.5	0.98	86.9	1.10
	Ga	5.58	0.186	13	0.43	5.5	0.18	4.7	0.16
	Ge	–	–	–	–	–	–	–	–
	In	–	–	–	–	–	–	–	–
	Sn	3.80	0.280	3.5	0.35	2.5	0.25	3.7	0.37
	Tl	–	–	–	–	–	–	–	–
	Pb	9.57	0.478	8.9	0.46	11	0.55	10.5	0.53
Pegmatophile	Sc	–	–	–	–	–	–	–	–
	V	29.95	0.230	40.5	0.31	29	0.22	28.8	0.22
	Cr	30.71	0.307	40.2	0.40	34.1	0.34	31.1	0.31
	Mn	192.2	0.286	332.4	0.50	178.8	0.27	2.946	0.44
	Ti	969.9	0.215	1131	0.25	982.1	0.22	1032.8	0.23
	Y	–	–	–	–	–	–	–	–
	Zr	127.6	0.623	215.6	1.08	115.4	0.58	108.2	0.54
	Nb	55.68	2.784	–	–	–	–	108.2	5.41
	Mo	2.03	1.015	3.3	1.65	1.2	0.60	1.8	0.90
	Ta	–	–	–	–	–	–	–	–
	W	–	–	–	–	–	–	–	–
Lithophile	Li	77.99	1.299	60.8	1.01	46	0.77	61.3	30.65
	Be	8.85	2.950	–	–	18.3	6.10	16.9	5.63
	Ba	216	0.208	302.5	0.38	199.8	0.25	292.9	0.37
	Sr	132.7	0.294	189.8	0.42	88.6	0.20	180.8	0.40
Sedimentophile	B	13.77	0.137	15.8	0.16	13.6	0.14	15.4	0.15

Table VIII

Analyses of materials of the 0.05 to 0.002 mm grain fraction for trace elements

	Co	Ni	B	Sr	Cu	Zn	Ga	Pb	Ti	V	Cr	Mn
0.05 – 0.02 mm	–	61	8	102	10	212	0.9	13	496	35	101	3
0.02 – 0.01 mm	–	67	10	129	8	297	0.6	16	529	33	116	2
0.01 – 0.005 mm	–	43	10	92	10	287	1.2	25	410	31	107	2
0.005 – 0.002 mm	–	59	8	112	18	202	0.8	17	373	44	103	2
0.002 mm >	2	10	8	207	18	192	0.8	15	589	38	127	39

of pyrite and organic matter Co, Cu, Pb, Zn, Cr and V are subidentical with the Vinogradov average of sedimentary rocks, though in some cases they may attain a double enrichment. The kaolinitic refractory clays, which are most widely distributed in the area, are poor in trace elements, only Zn, Pb and Cr exceed a little the sedimentary average (Table IX a – e).

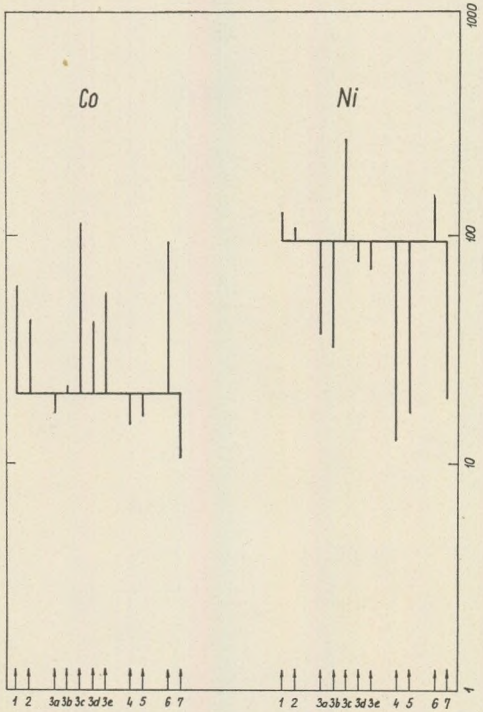

Fig. 7. Distribution of trace elements and Vinogradov averages of the particular rock types
I. Siderophile elements: Co, Ni

1. Marl; 2. Clay-marl; 3. Refractory clay types: *(a)* characterized by the predominance of kaolinite, *(b)* of mixed clay mineralization, *(c)* overwhelmingly kaolinitic, accompanied mainly by calcite, *(d)* of mixed clay mineralization accompanied mainly by pyrite and organic matter, *(e)* characterized by the predominance of kaolinite and iron hydroxide; 4. Conglomerate; 5. Breccia; 6. Sandstone; 7. Calcareous marl

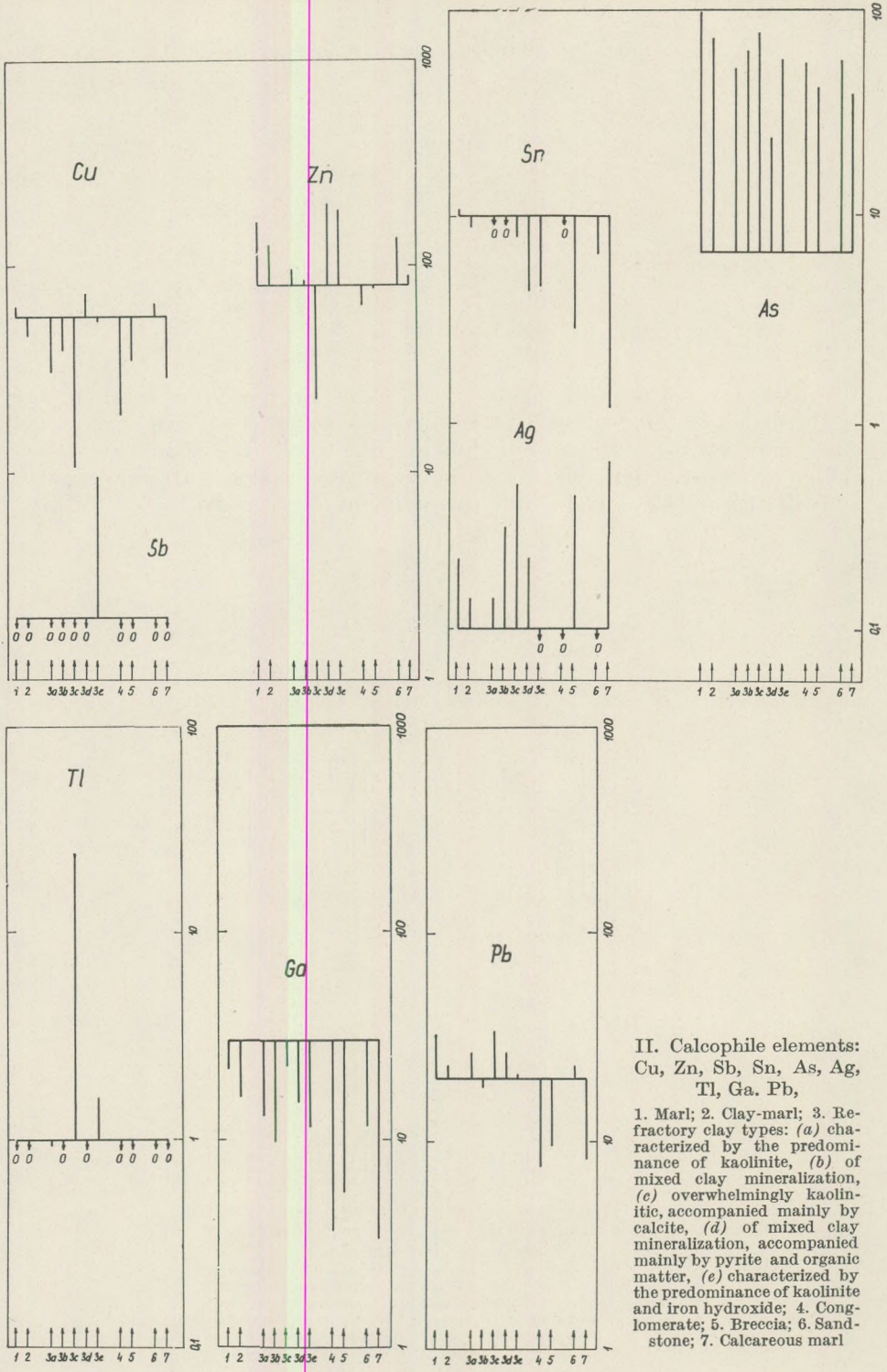

II. Calcophile elements: Cu, Zn, Sb, Sn, As, Ag, Tl, Ga. Pb,

1. Marl; 2. Clay-marl; 3. Refractory clay types: *(a)* characterized by the predominance of kaolinite, *(b)* of mixed clay mineralization, *(c)* overwhelmingly kaolinitic, accompanied mainly by calcite, *(d)* of mixed clay mineralization, accompanied mainly by pyrite and organic matter, *(e)* characterized by the predominance of kaolinite and iron hydroxide; 4. Conglomerate; 5. Breccia; 6. Sandstone; 7. Calcareous marl

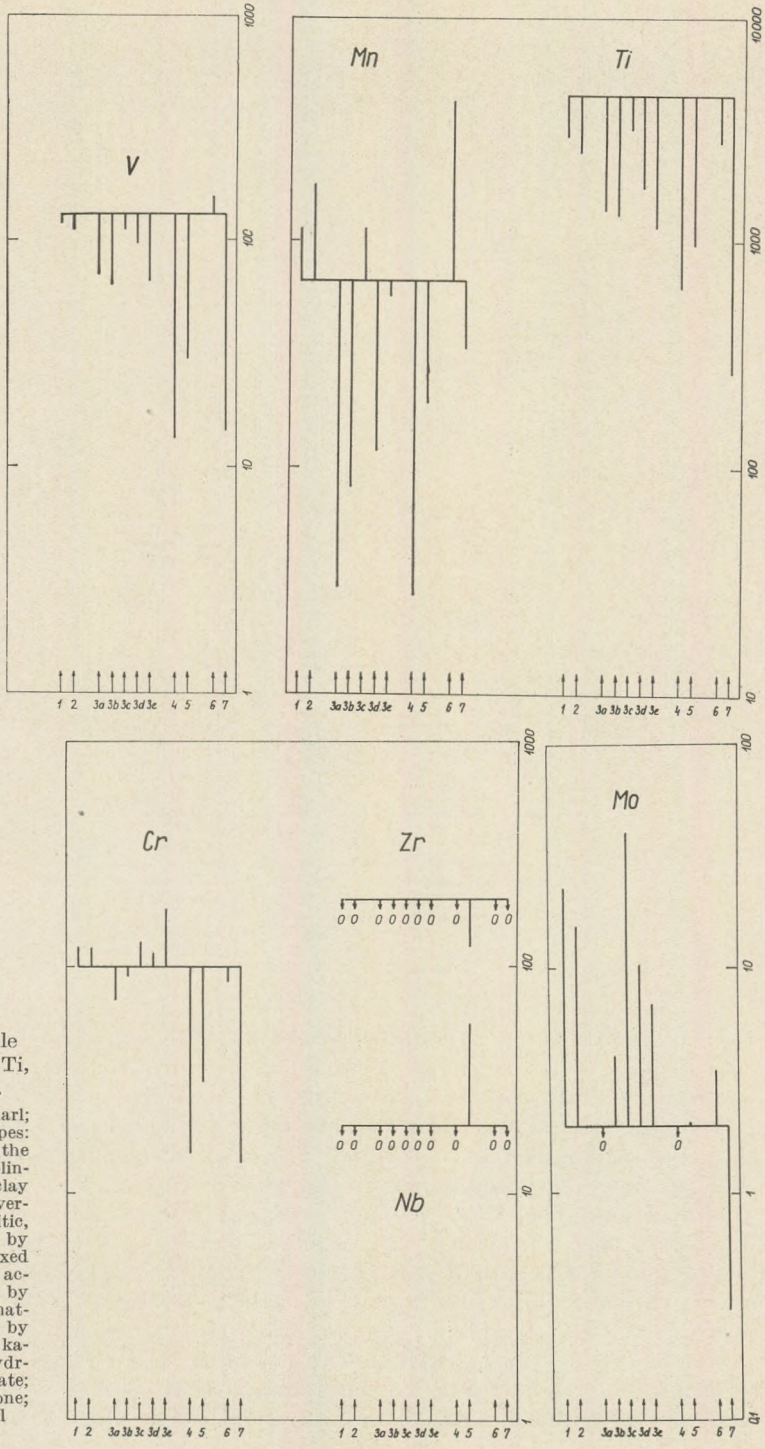

III. Pegmatophile elements: V, Mn, Ti, Cr, Zr, Nb, Mo.

1. Marl; 2. Clay-marl; 3. Refractory clay types: *(a)* characterized by the predominance of kaolinite, *(b)* of mixed clay mineralization, *(c)* overwhelmingly kaolinitic, accompanied mainly by calcite, *(d)* of mixed clay mineralization, accompanied mainly by pyrite and organic matter, *(e)* characterized by the predominance of kaolinite and iron hydroxide; 4. Conglomerate; 5. Breccia; 6. Sandstone; 7. Calcareous marl

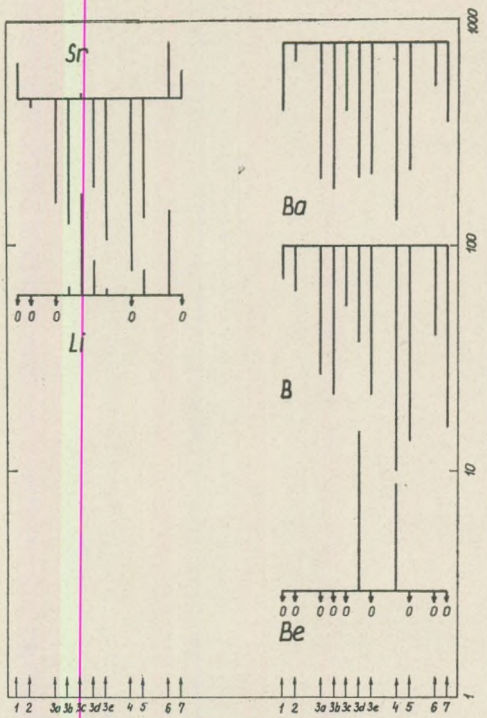

IV. Lithophile and sedimentophile elements: Sr, Li, Ba, Be, B.

1. Marl; 2. Clay-marl; 3. Refractory clay types: *(a)* characterized by the predominance of kaolinite, *(b)* of mixed clay mineralization, *(c)* overwhelmingly kaolinitic, accompanied mainly by calcite, *(d)* of mixed clay mineralization, accompanied mainly by pyrite and organic matter, *(e)* characterized by the predominance of kaolinite and iron hydroxide; 4. Conglomerate; 5. Breccia; 6. Sandstone; 7. Calcareous marl

In the southern profile of NW–SE direction no remarkable concentration of trace elements could be observed. The pyritic-organic components proved to be the most significant concentrators in which Co, Ni, Cu, Zn, Pb, Cr, Mo and Ba locally attained twice the Vinogradov average.

On the basis of the trace element concentrations the 5 characteristic clay types can be well distinguished. The greatest number and the highest concentrations of these elements are present in the clays of mixed clay mineralization. The trace element content decreases in the following succession: type of mixed clay mineralization → overwhelmingly kaolinitic type accompanied by calcite → type characterized by the predominance of kaolinite and iron hydroxide and type of mixed clay mineralization with pyrite and organic matter, respectively → type characterized by the predominance of kaolinite.

Figures 7. I–IV. indicate the averages of the trace elements as calculated from the analyses of the individual rock types according to the

Table IX

Averages of trace elements and their distribution by profiles in clays

a) **Refractory clay type characterized by the predominance of kaolinite**

		Total		Profile I		Profile II		Profile III	
		average	ef	average	ef	average	ef	average	ef
Siderophile	Co	16.86	0.843	–	–	12.07	0.60	12.9	0.65
	Ni	36.81	0.387	40	0.42	26.2	0.28	24.4	0.26
Calcophile	Cu	30.31	0.531	40	0.70	42.1	0.74	24.4	0.43
	Ag	0.14	1.40	–	–	–	–	–	–
	Cd	–	–	–	–	–	–	–	–
	Hg	–	–	–	–	–	–	–	–
	As	51.91	7.865	–	–	–	–	–	–
	Sb	–	–	–	–	–	–	–	–
	Bi	–	–	–	–	–	–	–	–
	Te	–	–	–	–	–	–	–	–
	Zn	96.07	1.20	100	1.25	100.7	1.26	89.4	1.12
	Ga	12.92	0.43	40	1.33	15.4	0.51	14.2	0.47
	Ge	–	–	–	–	–	–	–	–
	In	–	–	–	–	–	–	–	–
	Sn	–	–	–	–	–	–	–	–
	Tl	0.94	0.94	–	–	–	–	–	–
	Pb	26.53	1.326	25	1.25	36 2	1.81	23.6	1.18
Pegmatophile	Sc	–	–	–	–	–	–	–	–
	V	70.59	0.543	100	0.77	74.6	0.57	68	0.52
	Cr	71.89	0.718	100	1.00	111.7	1.12	80	0.80
	Mn	29.44	0.043	25	0.04	39.7	0.06	17.8	0.03
	Ti	1371.57	0.304	4000	0.89	1573.3	0.35	1060	0.24
	Y	–	–	–	–	–	–	–	–
	Zr	–	–	–	–	–	–	–	–
	Nb	–	–	–	–	–	–	–	–
	Mo	–	–	–	–	–	–	–	–
	Ta	–	–	–	–	–	–	–	–
	W	–	–	–	–	–	–	–	–
Lithophile	Li	–	–	–	–	–	–	–	–
	Be	–	–	–	–	–	–	–	
	Ba	200.26	0.25	400	0.50	196	0.26	142	0.18
	Sr	153.6	0.341	100	0.22	220	0.49	123	0.27
Sedimentophile	B	26.86	0.268	40	0.40	42.5	0.43	25.6	0.26

Table IX

Averages of trace elements and their distribution by profiles in clays

b) **Refractory clay type of mixed clay mineralization**

		Total		Profile I		Profile II		Profile III	
		average	ef	average	ef	average	ef	average	ef
Siderophile	Co	21.58	1.079	12.02	0.601	50.6	2.53	–	–
	Ni	32.09	0.337	22.1	0.232	32.4	0.341	15	0.157
Calcophile	Cu	39.18	0.687	66.6	1.168	53.2	0.93	39	0.68
	Ag	0.31	3.1	–	–	–	–	0.3	3.00
	Cd	–	–	–	–	–	–	–	
	Hg	–	–	–	–	–	–	–	–
	As	63.57	9.631	–	–	–	–	–	–
	Sb	–	–	–	–	–	–	–	–
	Bi	–	–	–	–	–	–	–	–
	Te	–	–	–	–	–	–	–	–
	Zn	84.51	1.056	125	1.56	102.9	1.288	81.6	1.02
	Ga	9.83	0.327	17.8	0.59	14.4	0.48	8.6	0.28
	Ge	–	–	–	–	–	–	–	–
	In	–	–	–	–	–	–	–	–
	Sn	–	–	–	–	–	–	–	–
	Tl	–	–	–	–	–	–	–	–
	Pb	18.34	0.917	10.6	0.53	23.2	1.16	12.8	0.64
Pegmatophile	Sc	–	–	–	–	–	–	–	–
	V	62.75	0.482	86.6	0.66	68	0.523	71.7	0.55
	Cr	90.25	0.902	111.6	112	1.12	126.6	1.26	1.26
	Mn	81.42	0.121	35.5	0.052	153.4	0.243	17	0.02
	Ti	1303.15	0.289	1033.3	0.229	1952	0.433	1333.3	0.29
	Y	–	–	–	–	–	–	–	–
	Zr	–	–	–	–	–	–	–	–
	Nb	–	–	–	–	–	–	–	–
	Mo	4.13	2.065	10.4	5.20	–	–	–	–
	Ta	–	–	–	–	–	–	–	–
	W	–	–	–	–	–	–	–	–
Lithophile	Li	64.87	1.081	–	–	–	–	–	–
	Be	–	–	–	–	–	–	–	–
	Ba	180.5	0.225	205	0.25	172	0.21	123.3	0.154
	Sr	125.6	0.279	160	0.355	130	0.28	100	0.222
Sedimentophile	B	21.92	0.219	27.8	0.278	32.4	0.32	27	0.270

Table IX

Averages of trace elements and their distribution by profiles in clays

c) **Overwhelmingly kaolinitic refractory clay type accompanied mainly by calcite**

		Total		Profile I		Profile II		Profile III	
		average	ef	average	ef	average	ef	average	ef
Siderophile	Co	113.94	5.697	25	1.25	45	2.25	16	0.80
	Ni	271.52	2.858	60	0.631	120	1.263	58	0.611
Calcophile	Cu	107.35	1.883	100	1.754	75	1.315	40	0.701
	Ag	0.50	5.00	–	–	–	–	–	–
	Cd	–	–	–	–	–	–	–	–
	Hg	–	–	–	–	–	–	–	–
	As	77.60	11.575	–	–	–	–	–	–
	Sb	–	–	–	–	–	–	–	–
	Bi	–	–	–	–	–	–	–	–
	Te	–	–	–	–	–	–	–	–
	Zn	22.73	0.284	160	2.00	227.5	2.843	100	1.25
	Ga	25.14	0.838	60	2.00	26.5	0.883	11	0.366
	Ge	–	–	–	–	–	–	–	–
	In	–	–	–	–	–	–	–	–
	Sn	7.97	0.797	–	–	12.4	1.24	–	–
	Tl	24.24	24.24	–	–	–	–	–	–
	Pb	33.47	1.674	16	0.80	34	1.70	17.5	0.87
Pegmatophile	Sc	–	–	–	–	–	–	–	–
	V	110	0.846	100	0.769	145	1.115	80	0.615
	Cr	128.82	1.288	160	1,60	137.5	1.37	110	1.10
	Mn	1123.3	1.676	400	0.697	941	1.40	160	0.238
	Ti	3174,11	0.705	2500	0.655	3375	0.75	2050	0.455
	Y	–	–	–	–	–	–	–	–
	Zr	–	–	–	–	–	–	–	–
	Nb	–	–	–	–	–	–	–	–
	Mo	40.47	20.23	16	8.00	30	15	–	–
	Ta	–	–	–	–	–	–	–	–
	W	–	–	–	–	–	–	–	–
Lithophile	Li	168	2.80	–	–	200	3.33	–	–
	Be	–	–	–	–	–	–	–	–
	Ba	394.70	0.493	250	0.312	352.5	0.44	250	0.312
	Sr	460.58	1.023	250	0.555	600	1.33	130	0.228
Sedimentophile	B	53.82	0.538	60	0.600	61.2	0.61	35	0.35

Table IX

Averages of trace elements and their distribution by profiles in clays

d) **Refractory clay type-of mixed clay mineralization with pyrite and organic matter beside the predominant clay minerals**

		Total		Profile I		Profile II		Profile III	
		average	ef	average	ef	average	ef	average	ef
Siderophile	Co	41.77	2.088	40	2.00	39.3	1.965	52.7	2.635
	Ni	77.73	0.818	16	0.168	63.3	0.66	102.9	1.08
Calcophile	Cu	72.81	1.277	16	0.280	76.3	1.339	95	1.666
	Ag	0.219	2.190	–	–	–	–	–	–
	Cd	–	–	–	–	–	–	–	–
	Hg	–	–	–	–	–	–	–	–
	As	24.10	3.651	–	–	–	–	–	–
	Sb	–	–	–	–	–	–	–	–
	Bi	–	–	–	–	–	–	–	–
	Te	–	–	–	–	–	–	–	–
	Zn	200.5	2.506	–	–	166.9	2.086	156.3	1.953
	Ga	14.98	0.499	2.5	0.083	16.7	0.556	15.3	0.510
	Ge	–	–	–	–	–	–	–	–
	In	–	–	–	–	–	–	–	–
	Sn	4.350	0.435	–	–	–	–	6.8	0.680
	Tl	–	–	–	–	–	–	–	–
	Pb	26.45	1.322	6	0.300	33.9	1.695	23.8	1.19
Pegmatophile	Sc	–	–	–	–	–	–	–	–
	V	96.27	0.740	10	0.076	98	0.753	105.4	0.810
	Cr	113.86	1.138	4	0.040	130	1.30	126.3	1.263
	Mn	119	0.177	16	0.023	52.8	0.078	285.1	0.425
	Ti	1737.72	0.386	400	0.088	1680	0.373	2054.5	0.456
	Y	–	–	–	–	–	–	–	–
	Zr	–	–	–	–	–	–	–	–
	Nb	–	–	–	–	–	–	–	–
	Mo	10.25	5.125	–	–	–	–	21.8	10.9
	Ta	–	–	–	–	–	–	–	–
	W	–	–	–	–	–	–	–	–
Lithophile	Li	85.28	1.421	–	–	–	–	–	–
	Be	15.08	5.020	–	–	–	–	–	–
	Ba	201.6	0.252	600	0.750	156	0.195	1105.4	1.381
	Sr	182.27	0.405	100	0.222	100	0.222	356.3	0.791
Sedimentophile	B	37.15	0.371	10	0.100	33.1	0.331	44.6	0.446

Table IX

Averages of trace elements and their distribution by profiles in clays

e) **Refractory clay type characterized by the predominance of kaolinite and iron hydroxide**

		Total		Profile I		Profile II		Profile III	
		average	ef	average	ef	average	ef	average	ef
Siderophile	Co	55.41	2.77	66.1	3.31	23.7	1.19	30.4	1.52
	Ni	70.70	0.744	57.1	0.60	73.4	0.77	77.4	0.81
Calcophile	Cu	55.90	0.98	79.5	1.39	58	1.02	57.1	1.00
	Ag	–	–	–	–	–	–	–	–
	Cd	–	–	–	–	–	–	–	–
	Hg	–	–	–	–	–	–	–	–
	As	56.57	8.57	–	–	–	–	–	–
	Sb	9.48	4.74	–	–	–	–	–	–
	Bi	–	–	–	–	–	–	–	–
	Te	–	–	–	–	–	–	–	–
	Zn	186.1	2.32	178.1	2.23	89.4	1.12	155,5	1.94
	Ga	11.41	0.39	17.1	0.57	14.2	0.47	11.9	0.40
	Ge	–	–	–	–	–	–	–	–
	In	–	–	–	–	–	–	–	–
	Sn	4.58	0.45	–	–	7.1	0.71	–	–
	Tl	1.58	1.58	–	–	–	–	–	–
	Pb	20.82	1.04	11.4	0.57	28.4	1.42	27.5	1.38
Pegmatophile	Sc	–	–	–	–	–	–	–	–
	V	65,5	0.50	81.8	0.63	60	0.46	60	0.46
	Cr	179.1	1.79	100	1.00	104	1.04	97.1	0.97
	Mn	567.8	0.84	240,7	0.36	172	0.26	339.4	0.61
	Ti	1159.5	0.25	1054.5	0.23	1360	0.30	1385,7	0.31
	Y	–	–	–	–	–	–	–	–
	Zr	–	–	–	–	–	–	–	–
	Nb	–	–	–	–	–	–	–	–
	Mo	6.88	3.44	8.2	4.10	–	–	–	–
	Ta	–	–	–	–	–	–	–	–
	W	–	–	–	–	–	–	–	–
Lithophile	Li	63.25	1.05	–	–	–	–	–	–
	Be	–	–	–	–	–	–	–	–
	Ba	208.7	0.27	192.7	0.24	130	0.16	160	0.20
	Sr	105.7	0.23	119.1	0.04	89.4	0.20	100	0.22
Sedimentophile	B	22.07	0.22	21.1	0.21	35	0.35	32.4	0.32

geochemical classification of elements. The straight line is the average given by Vinogradov for sedimentary rocks. The aim of this representation is to show which element in what rock type attains a concentration higher than the average given for sedimentary rocks. The following conclusions can be drawn:

1. The number of the trace elements is relatively low and they exceed the sedimentary average in few formations and to a small extent.

2 Of the siderophile elements, Ni is enriched in the calcareous clays.

3. Of the calcophile elements, Ag and Ga sometimes show over-average values in the clays, marls and clay-marls; Cu does so in the pyritic-carbonaceous clays, whereas the figure of Zn is higher than the average in almost all rock types.

4. Of the pegmatophile elements Mo and Cr are observed to be enriched in the marls and clay-marls; Mn in certain clay types and V (a little) in the calcareous marls and clays.

5. Of the lithophile-sedimentophile elements, Li (as shown by 1 or 2 data), Sr and, sometimes, Ba show slight concetration peaks in marls, calcareous marls and caly-marls.

REFERENCES

Á k o s, É. (1964): A Romhányi-rög kőzettani és földtani vizsgálata (Petrographical and geological investigations of the Romhány block). Manuscript.

B a r t k ó, L. (1948): Előzetes jelentés a Romhány környékén végzett földtani kutatásokról (Preliminary report on the geological investigations carried out in the vicinity of Romhány). Jelentés a Jövedéki Mélykutatás 1947/48. évi munkálatairól. pp. 149–156.

Érc- és Ásványbányászati Vállalat Pilisvörösvári Üzemegységének jelentése (Report of the Pilisvörösvár Mining Unit of the National Enterprise for the Ore and Mineral Mining. Manuscript. 1971.

G a b o n a, B. (1969): A felsőpetényi fúrásszelvény agyagásványainak geokémiai vizsgálata (Geochemical analysis of the clay minerals recovered from the borehole of Felsőpetény). Manuscript.

H a l á s z, A.–D e m e t e r, L. (1921): Hazai tűzálló agyag, különös tekintettel a petényi agyagokra (The refractory clays of Hungary with special regard to the clay of Petény). Manuscript. BKI.

H a n t k e n, M. (1870): A kiscelli tályag elterjedéséről Nógrád-megyében (On the distribution of the Kiscell Clay in Nógrád county). Magyarhoni Földtani Társ. Munkálatai V. Budapest.

H a u e r, K. (1870): Geologische Übersichtskarte d. österr. – ung. Monarchie Blatt VII. J. d. k. k. geol. R. A. Wien.

H o r v á t h, M. (1971): A kaolinit Co-, Ni-, Sr- és V- megkötőképességének vizsgálata (Investigation of the capacity of kaolinite of fixing Co, Ni, Sr and V). Manuscript.

J a n t s k y, B. (1952): A Bánk, Felsőpetény és Szendehely környékén előforduló tűzállóagyagok (Refractory clays in the vicinity of Bánk, Felsőpetény and Szendehely). Földtani Intézet Évi jelentése 1949-ről. pp. 47–58.

K a s z a n i t z k y, F. (1956): Az alsóoligocén (hárshegyi) homokkő ásvány-kőzettani vizsgálata (Mineralogical and petrographical analyses of the Lower Oligocene (Hárshegy sandstones). Földtani Közlöny, 86, pp. 247–256.

Kneifel, F. (1970): Felsőpeténvi sziallitok ásványos alkata és településviszonyai (Mineralogy and structural condition of the Felsőpetény siallites). Manuscript.

Koch, A. (1877): A dunai trachytcsoport jobbparti részének földtani leírása (Geological description of the right-bank part of the Danube trachyte group). MTA Math. és Term. Tud. Oszt. Kiadványa, Budapest. p. 298.

Liffa A. (1942): Néhány geológiailag megvizsgált hazai kaolin és tűzállóagyag előfordulás (About some geologically investigated Hungarian kaoline and refractory clay deposits). Magyar Állami Földtani Intézet Évi Jelentése az 1936 – 38. évről pp. 1125 – 1144.

Majzon L. (1952): Adatok Romhány és Ipolyszög környékének földtanához (Contribution to the geology of the vicinity of Romhány and Ipolyszög). Magyar Állami Földtani Intézet Évi Jelentése az 1938. évről. pp. 19 – 30.

Noszky J. Sr. (1939): A Duna-balparti hegyrögök környezetének geológiai viszonyai (Geological conditions of the region of the horsts on the left bank of the Danube). Földtani Intézet Évi Jelentése 1933 – 35-ről. pp. 473 – 501.

Noszky J. Sr. (1941): Adatok az Északi- és Középső-Cserhát geológiai felépítéséhez (Contribution to the geology of the northern and central Cserhát Hills). Magyar Állami Földtani Intézet Évi Jelentése 1936 – 38-ról. pp. 531 – 545.

Noszky J. Sr. (1943): Felsőoligocén stratigráphiánk problémái (Problems of Hungary's Upper Oligocene stratigraphy). Földtani Közlöny, 35. pp. 87 – 207.

Stache, G.- (1866): Die geologischen Verhältnisse der Umgebung von Waitzen in Ungarn. Jahrbuch d. k. k. geol. R. A. Wien p. 306.

Szádeczky – Kardoss, E. (1935): Adatok a görgetési határ kérdéséhez (Contribution to the probleme of the rolling limit). Földtani Közlöny, 65.

Turekian, K. K. – Wedepohl, K. H. (1961): Distribution of the elements in some major units of the Earth's crust. Bull. Geol. Soc. Amer. 72. No 2.

Vadász, E. (1910): A Duna-balparti idősebb hegyrögök föld- és őslénytani viszonyai (Geological and paleontological conditions of the blocks on the left bank of the Danube). Magyar Állami Földtani Intézet Évkönyve 18. pp. 109 – 173.

Varju, Gy. (1949): A Romhányi-rög területén levő (bánkpetényi) tüzállóagyag-előfordulás (The Bánkpetény refractory clay deposit in the territory of the Romhány horst). Magyar Földtani Intézeti Évi Jelentése 1955 – 56-ról. pp. 361 – 373.

Varjú, Gy. (1955): Összefoglaló földtani jelentés és készletszámítás a Romhányi-rög tűzállóagyag előfordulásairól (An account summarizing the geology and the estimation of the reserves of refractory clays of the deposits of the Romhány horst). Manuscript.

Venczel, G. (1969): A különböző agyagásványok és az agyagos kőzetek nehézfém-megkötő képességének vizsgálata (Examination of the capacity of various clay minerals and clay rocks of fixing heavy metals). Manuscript.

Vendl, A. (1932): A kiscelli agyag (The Kiscell Clay). Földtani Intézet Évkönyve, 29. pp. 93 – 152.

Vinogradov, A. P. (1962): Szrednyije szoderzsányija himicseszkih elementov glavnüh tipah izverzsennüh gornüh porod zemnoj korü. Geohimija. 7.

Vitális, I. (1941): Jelentés a hazai tűzállóagyag előfordulásokról (Report on Hungary's refractory clay deposits). Manuscript.

Földvári – Vogl (1954): Agyagásványok kémiai és fizikai vizsgálata (Chemical and physical investigations of clay minerals). Földtani Közlöny. 84. pp. 121 – 129.

Földvári – Vogl (1958): A DTA szerepe az ásványtanban és a földtani nyersanyag-kutatásban (The role of DTA in mineralogy and geological prospecting). Műszaki Könyvkiadó.

KORRELATIONSMATRIX ALS ANALOGIE-INDEX VON METEOROLOGISCHEN FELDERN

F. RÁKÓCZI

(Meteorologischer Lehrstuhl der Eötvös Loránd Universität Budapest)

(Eingegangen am 25.3.1972)

SUMMARY

In meteorology model experiments may be replaced by investigations of analogue situations. We can expect that the development of analogue weather situations will also remain analogous.

The grade of analogy should be measured by applying an analogy-index. The present paper uses as analogy-index the correlation matrix between zonal and meridional components of two average flow systems and it proves that the systems dealt with are analogous. The method discussed may serve as basis for an objective classification of weather situations.

Einleitung

In der Meteorologie kommt dem Versuch – wegen der Grossräumkeit der Prozesse – nur eine beschränkte Rolle zu. Im Falle zweier identischer Wetterlagen ist es zu empfehlen, die Analogie der mit der Wetterlage verknüpften Felder nachzuweisen. Bei der Untersuchung der Analogien werden sowohl subjektive [4], als auch objektive [1, 2] Methoden benutzt. Bei den subjektiven Methoden besteht die Gefahr, dass identische oder nahezu identische Wetterlagen von zwei verschiedenen Authoren mit verschiedenen Benennungen belegt werden. [3].

Die objektiven Methoden haben auch den Vorteil, dass sie nicht nur das Vorhandensein der Analogie eindeuting nachweisen, sondern auch für den Grad der Analogie eine Information liefern, da sie diesen durch einen numerischen Wert kennzeichnen. Die Untersuchung der Analogien ist also im Stande, die in den technischen Wissenschaften so verbreiteten Modellversuche zu ersetzen. Diese Untersuchung ist auch darum wichtig, weil die weitere Entwicklung der analogen Situationen geht auch in analoger Weise vorsich.

In Zusammenhang mit den analogen Situationen kann man auch die Frage Untersuchen, dass bei der Vorhersage der analogen Situationen welches Prognosenmodell sich als am meisten geeignet erweist und die grösste Treffwahrscheinlichkeit aufweist.

Zur Feststellung der Realität einer Analog-Situation werden wir – auf Vorschlag von Bagrow [1] – die Korrelationsmatrix der zwei Felder benutzen, obwohl auch andere Indikatoren für die quantitative Erfassung der Analogie bekannt sind [2, 3].

1. Mathematische Grundlagen

Im Falle zweier synoptischer Situationen können wir nur von Ähnlichkeit sprechen, die sich nie zur Identität entwickeln kann. Irgend ein Element einer synoptischen Lage, z. B. der Druck oder der Druckgradient kann als ein Vektor X von n Dimensionen aufgefasst werden im n-dimensionalen Zufallsraum:

$$X = (X_1, X_2, \ldots, X_n) . \tag{1}$$

Wir wollen annehmen, dass X eine Kolonnenmatrix darstellt. Ihre Transponierte ist die Zeilenmatrix X^*. Das Quadrat der Länge des Vektors X wird durch das Matrizenprodukt

$$|X|^2 = X^* X = X_1^2 + X_2^2 + \ldots + X_n^2 \tag{2}$$

gegeben.

Die Streuungsmatrix oder Autokorrelations-Matrix des Vektors wird durch die Formel

$$D(X) = E\{(X - \overline{X})(X - \overline{X}^*)\} \tag{3}$$

dargestellt, wobei E für die mathematische Expektanz steht und das Quadrat des Vektors durch die diagonale Glieder representiert wird. Wenn wir annehmen, dass $\overline{X} = 0$, so wird die Allgemeinheit zwar bewahrt, die Ableitungen werden sich aber einfacher gestalten:

$$D_X = \begin{Vmatrix} \overline{X_1 X_1} & \overline{X_1 X_2} & \ldots & \overline{X_1 X_n} \\ \overline{X_2 X_1} & \overline{X_2 X_2} & \ldots & \overline{X_2 X_n} \\ & \ldots & & \\ \overline{X_n X_1} & \overline{X_n X_2} & \ldots & \overline{X_n X_n} \end{Vmatrix} \tag{4}$$

Wird das entsprechende Element der anderen Wetterlage durch den n-dimensionalen Vektor Y dargestellt, dann erhalten wir für D_Y:

$$D_Y = \begin{Vmatrix} \overline{Y_1 Y_1} & \overline{Y_1 Y_2} & \ldots & \overline{Y_1 Y_n} \\ & \ldots & & \\ \overline{Y_n Y_1} & \overline{Y_n Y_2} & \ldots & \overline{Y_n Y_n} \end{Vmatrix} \tag{5}$$

Ausser den zwei Autokorrelationsmatrizen benötigen wir noch zur Ausführung unserer Rechnungen die Matrix
$M_{yx} = E|Y\, X^*|$, d. h. die Matrix des Korrelationszusammenhanges zwischen den Vektoren Y und X. Ausführlich geschrieben haben wir:

$$M_{yx} = \begin{Vmatrix} \overline{Y_1 X_1} & \overline{Y_1 X_2} & \ldots & \overline{Y_1 X_n} \\ & \ldots & & \\ \overline{Y_n X_1} & \overline{Y_n X_2} & \ldots & \overline{Y_n X_n} \end{Vmatrix}, \tag{6}$$

wobei der übergesetzte Horizontalstrich – wie früher – als Symbol für Durchschnittsbildung gilt. Wie wir sehen, sind (4) und (5) symmetrische Matrizen, während (6) asymmetrisch ausfällt.

Wir müssen noch – als Indikator des Zusammenhanges der X – and Y – Vektoren – die normalisierte Korrelationsmatrix, d. h. die Matrix K der Korrelationskoeffizienten:

$$K = D_y^{-1/2} M D_x^{-1/2} \tag{7}$$

einführen.

Aus dieser Definition der Matrix K folgt, dass wenn die Komponenten des Vektors X sowie von Y unabhängig voneinander sind, dieElemente der Matrix K in die Korrelationskoeffizienten zwischen den verschiedenen Komponenten der Vektoren übergehen. In der Folge unserer Rechnungen benötigen wir noch die Transponierte K^* von K, die folgenderweise geschrieben werden kann:

$$K^* = D_x^{-1/2} M^* D_y^{-1/2} . \tag{8}$$

Zur Erreichung des erwünschten Resultats bestimmen wir noch die Produkte $K\,K^*$ und K^*K. Diese können wie folgt hingeschrieben werden:

$$K\,K^* = D_y^{-1/2} A\,B\,D_y^{-1/2} , \tag{9}$$

$$K^*K = D_x^{-1/2} B\,A\,D_x^{-1/2} . \tag{10}$$

Ein jeder dieser Produkte ist zu den Quadraten der Korrelationskoeffizienten analog und representiert die Regression zwischen Y und X, bzw. X und Y.

Die Regressionsmatrizen A und B können durch Einführung der Matrix der Korrelationskoeffizienten wie folgt ausgedrückt werden:

$$A = D_y^{1/2} K D_x^{-1/2} , \tag{11}$$

$$B = D_x^{1/2} K^* D_y^{-1/2} . \tag{12}$$

Als numerischen Indikator der Korrelation benutzen wir den Eigenwert der Matrizen KK^*, bzw. $K^*\,K$. Diese Matrizen besitzen dieselben Eigenwerte $\lambda_1, \ldots, \lambda_n$, wobei diese lediglich die Quadrate der entsprechenden Korrelationskoeffizienten darstellen.

Für uns sind nicht nur die Quadrate der Korrelationskoeffizienten von Wichtigkeit; vielmehr müssen – im Interesse der Möglichkeit der Vorzeichenbestimmung – die Korrelationskoeffizienten selbst errechnet werden. Wenn die Dimensionen der Matrizen nicht übereinstimmen – in unserem Falle haben wir mit Vektoren gleicher Dimension zu tun – dann müssen wir von den Matrizen $K\,K^*$ und $K\,^*K$ mit derjenigen zu operieren welche von grösserer Ordnung ist. Nehmen wir die Dimensionen von X und Y als gleich an, und untersuchen wir die quadratische Matrix K.

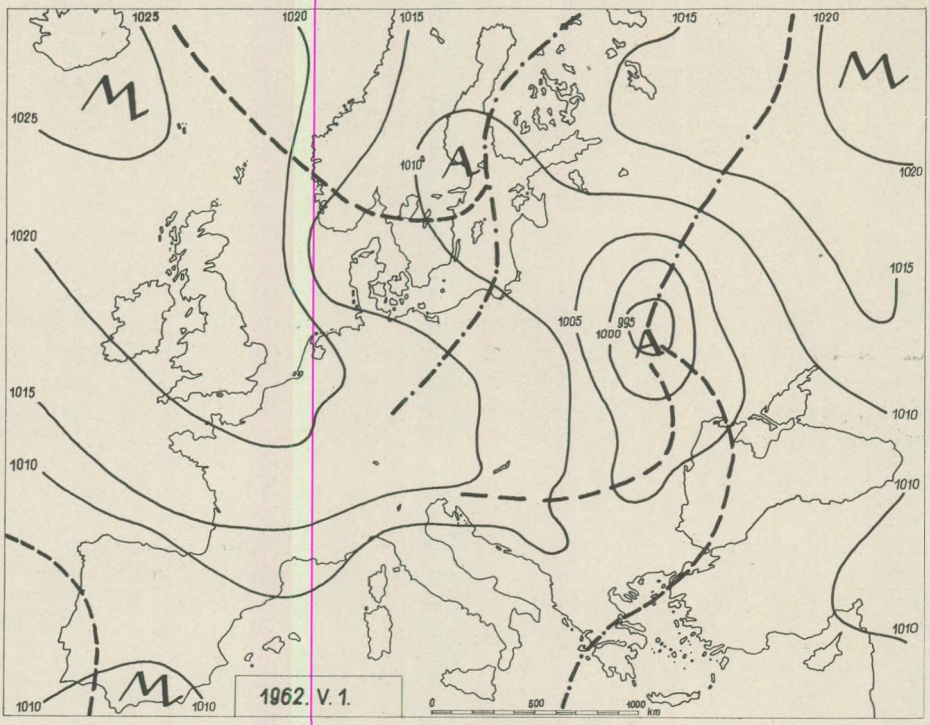

Fig. 1.

Theoretisch kann eine beleibige quadratische Matrix als ein Produkt von drei Matrizen aufgeschrieben werden, wie folgt:

$$K = HRG^*, \tag{13}$$

wobei R ist eine Diagonalmatrix

$$R = \begin{Bmatrix} r_1 & & & \\ & r_2 & & \\ & & \cdot & \\ & & & \cdot \\ & & & r_n \end{Bmatrix}, \tag{14}$$

H und G sind orthogonale Matrizen, für welche die Relationen

$$HH^* = E, \quad GG^* = E \tag{15}$$

bestehen, wobei E eine Einheitsmatrix representiert. Wir bilden nun die Matrizen $K\,K^*$, bzw. $K^*\,K$. Wir erhalten zuerst:

$$KK^* = HRG^*\,GR^*\,H^*, \tag{16}$$

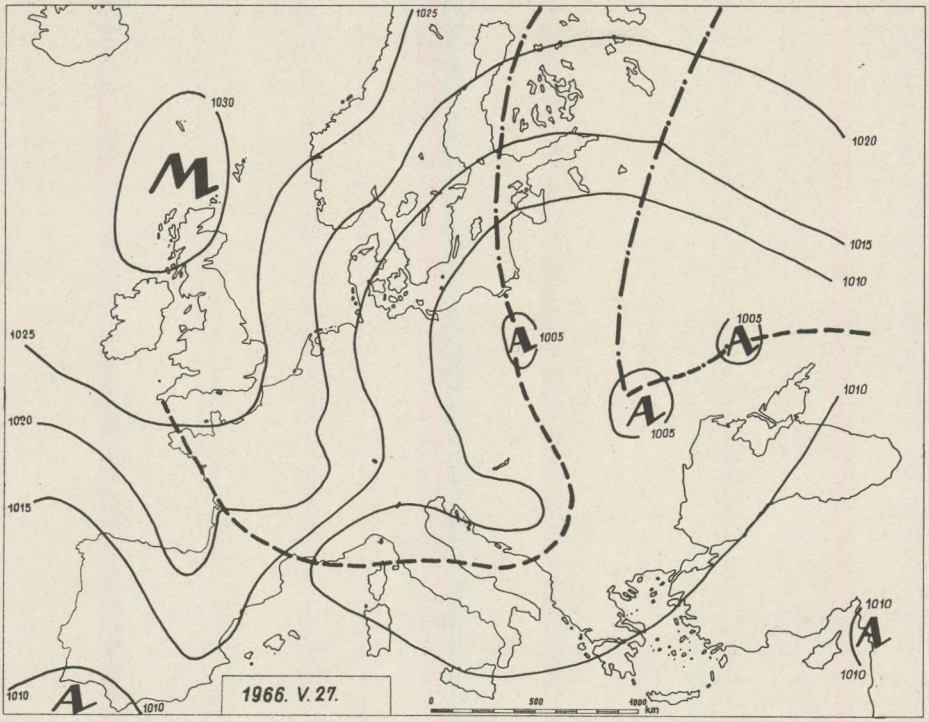

Fig. 2.

d. h.

$$KK^* = HR^2 H^* . \tag{17}$$

Ähnlicherweise erhalten wir:

$$K^* K = GR^2 G^* . \tag{18}$$

Die zwei letzten Gleichungen zeigen, dass $K\,K^*$ und $K^*\,K$ mit Hilfe der diagonalen Matrix R^2 erhalten werden können. Diese Transformationen ändern nicht die Eigenwerte der behandelten Matrizen.

Wir müssen noch auf die Interpretation der Matrizen H und G eingehen. Betrachten wir eine quadratische Matrix $-C\,C$, und formen wir aus den Eigenwerten $\lambda_1, \lambda_2 \ldots, \lambda_n$ dieser Matrix die Diagonalmatrix, wie folgt:

$$\Lambda = \begin{Vmatrix} \lambda_1 & & & \\ & \lambda_2 & & \\ & & \cdot & \\ & & & \cdot \\ & & & \lambda_n \end{Vmatrix} . \tag{19}$$

Die Eigenvektoren $U_1, U_2, \ldots, U_n$ dieser Matrix bilden auch eine Matrix, die wie folgt aufgeschrieben werden kann:

$$U = \begin{Vmatrix} U_{11}\ U_{12} \ldots U_{1n} \\ U_{ij} \\ U_{n1}\ U_{n2} \ldots U_{nn} \end{Vmatrix}, \tag{20}$$

wobei die λ_j Eigenwerte der j-ten Kolonne entsprechen.
Dann können wir die Identität

$$CU = U\,\Lambda \tag{21}$$

hinschreiben. Aus dieser folgt, dass

$$C = U\,\Lambda\,U^{-1} \tag{22}$$

gilt.

Wenn wir die zu C^* gehörigen Eigenvektoren mit V bezeichnen, dann besteht die Gleichung:

$$UV^* = E\,, \tag{23}$$

folglich:

$$C = U\,\Lambda\,V^*\,, \tag{24}$$

Betrachten wir nun den Unterschied zwischen (13) und (24). Alle Matrizen von (13) enthalten nur reelle Elemente, die Matrizen H und G sind orthogonal. Im Gegensatz dazu, die Matrix R ist nicht eine Matrix der Eigenwerte von K. In (24) Λ ist eine Eigenwertsmatrix, aber die U und V Matrizen sind Matrizen der Eigenwerte der Matrizen C und C^*, in Übereinstimmung mit (23).

Ist die Matrix C symmetrisch, dann fallen die Matrizen U und V zusammen und U wird orthogonal nach (23). Wir können daher für symmetrische Matrizen folgendes schreiben:

$$C = U\,\Lambda\,U^*\,. \tag{25}$$

Nun sollen wir (16) und (17) ins Auge fassen. Wir sehen, dass H die Matrix der Eigenwerte des $K\,K^*$ Matrizenvektors ist und G ist dieselbe für die Eigenwerte des Matrizenvektors $K\,^*\,K$. Damit haben wir die Bedeutung der vorkommenden Matrizen beleuchtet und wir können nun aus (13) die Formel für die Berechnung der gewünschten Diagonalmatrix R hinschreiben, wie folgt:

$$R = H^*\,KG\,. \tag{26}$$

In der Haupt diagonale der Matrix stehenden $r_1, r_2, \ldots, r_n$ Zahlen representieren die Korrelationskoeffizienten zwischen den entsprechenden Elementen des zu behandelndten Feldes, die sich demzufolge für eine objektive Bestimmung der Analogie zwischen den Feldern eignen.

Über die Ausführung der bei der als Beispiel angeführten Tage benötigten Berechnungen s. Referenz [5].

2. Beispiel der Analogie von Feldern

Als Beispiel untersuchen wir, inwieweit die Durchschnittskarten des Bodendruckes gewonnen aus der Vereinigung der Karten vom 27 – 29 sten Mai 1966 und 1 – 3 ten Mai 1962 als analog betrachtet werden können. Wir wählten diese zwei Perioden, da beide dadurch charakterisiert sind, dass in diesen Tagen über Ungarn eine Temperaturanomalie von – 4,5 C° und darunter auftrat.

Das untersuchte Gebiet wird durch die Breitengrade $\varphi = 70°$ N – $35°N$ sowie durch die Längenwerte $20°W - 40°E$ begrenzt. Als Netzpunkte wurden dabei die Schnittpunkte der Breiten-und Längenlinien von 5 zu 5 Graden benutzt. So erhielten wir im angeführten Gebiet insgesamt 104 Netzpunkte. Die X und Y zweidimensionalen Vektoren representieren die zonalen und meridionalen Druckunterschiede. So hatten wir auf Grund der 104 Netzpunkte $12 \times 7 = 84$ Ausgangsdaten. Für die erste Wetterlage bezeichneten wir die Differenz der benachbarten Netzpunkt-Druckwerte – von W nach Ost fortschreitend – durch x_1, und in der Richtung N – S durch x_2. Diese stellen Werte dar die mit dem Druckgradient proportional sind, sodass wir hier mit einer Untersuchung der dynamischen Analogie der Felder zu tun haben. Für die zweite Lage werden die entsprechenden Komponenten mit y_1 bzw. y_2 bezeichnet.

Zur Grundlage für unsere Rechnungen dienen die folgenden Ausgangswerte:

	x_1	x_2	y_1	y_2	x_1^2
$\sum$	– 17,1	1,4	– 14,3	– 55,9	480,6
$\frac{1}{N}\sum$	– 0,2035	0,1666	– 0,1702	– 0,6647	5,7214
	$x_1 x_2$	x_2^2	y_1^2	$y_1 y_2$	y_2^2
$\sum$	351,6	560,8	1117,0	390,3	807,7
$\frac{1}{N}\sum$	4,1857	6,6762	13,2976	4,6464	9,6155
	$y_1 x_1$	$y_1 x_2$	$y_2 x_1$	$y_2 x_2$	
$\sum$	134,0	– 67,8	18,7	94,8	
$\frac{1}{N}\sum$	1,5952	– 0,8071	0,2226	0,1129	

Wie wir sehen, $\overline{x_1}$, $\overline{x_2}$, $\overline{y_1}$, $\overline{y_2}$, ..., $\overline{y_2 x_2}$ sind nicht gleich Null. Dies kann so berücksichtigt werden, dass D_x, D_y und M_{yx} wie folgt hingeschrieben werden:

$$D_x = \begin{Vmatrix} \overline{x_1 x_2} & \overline{x_1 x_2} \\ \overline{x_2 x_1} & \overline{x_2 x_2} \end{Vmatrix} - \begin{Vmatrix} \overline{x}_1 \overline{x}_2 & \overline{x}_1 \overline{x}_2 \\ \overline{x}_2 \overline{x}_1 & \overline{x}_2 \overline{x}_2 \end{Vmatrix}, \tag{27}$$

$$D_y = \begin{Vmatrix} \overline{y_1 y_1} & \overline{y_1 y_2} \\ \overline{y_2 y_1} & \overline{y_2 y_2} \end{Vmatrix} - \begin{Vmatrix} \overline{y}_1 \overline{y}_1 & \overline{y}_1 \overline{y}_2 \\ \overline{y}_2 \overline{y}_1 & \overline{y}_2 \overline{y}_2 \end{Vmatrix} \tag{28}$$

Und

$$M_{yx} = \begin{Vmatrix} \overline{y_1 x_1} & \overline{y_1 x_2} \\ \overline{y_2 x_1} & \overline{y_2 x_2} \end{Vmatrix} - \begin{Vmatrix} \overline{y}_1 \overline{x}_1 & \overline{y}_1 \overline{x}_2 \\ \overline{y}_2 \overline{x}_1 & \overline{y}_2 \overline{x}_1 \end{Vmatrix}. \tag{29}$$

Auf Grund dieser Ausdrücke können wir aus den folgenden Matrizen ausgehen:

$$D_x = \begin{Vmatrix} 5{,}679 & 4{,}220 \\ 4{,}220 & 6{,}648 \end{Vmatrix}, \quad D_y = \begin{Vmatrix} 13{,}269 & 4{,}533 \\ 4{,}533 & 9{,}173 \end{Vmatrix}, \quad M_{yx} = \begin{Vmatrix} 1{,}560 & -0{,}779 \\ 0{,}087 & 0{,}224 \end{Vmatrix},$$

Auf Grund der Matrizen D_x und D_y erhalten wir für $D_x^{-1/2}$ und $D_y^{-1/2}$ folgendes:

$$D_x^{-1/2} = \begin{Vmatrix} 0{,}537 & -0{,}204 \\ -0{,}204 & 0{,}492 \end{Vmatrix}.$$

$$D_y^{-1/2} = \begin{Vmatrix} 0{,}317 & -0{,}076 \\ -0{,}076 & 0{,}303 \end{Vmatrix}.$$

Im Besitze dieser Matrizen sowie der Matrix M_{yx}, bei der Anwendung der Formel (7) erhalten wir für K:

$$K = \begin{Vmatrix} 0{,}3158 & -0{,}2293 \\ -0{,}0754 & 0{,}0813 \end{Vmatrix}.$$

Von hier aus haben wir für K^*:

$$K^* = \begin{Vmatrix} 0{,}3158 & -0{,}0754 \\ -0{,}2293 & 0{,}0813 \end{Vmatrix}.$$

Wir haben noch die Produkte dieser Matrizen, d. h. $K\,K^*$ und $K^*\,K$ zu bilden. Nach bekannten Regeln der Matrizen-Multiplikation erhalten wir:

$$KK^* = \begin{Vmatrix} 0{,}1523 & -0{,}0424 \\ -0{,}0424 & 0{,}0123 \end{Vmatrix}, \quad K^*K = \begin{Vmatrix} 0{,}1054 & -0{,}0785 \\ -0{,}0785 & 0{,}0592 \end{Vmatrix}.$$

Diese zwei Matrizen besitzen dieselben Eigenwerte, die nicht anderes sind, wie die Quadrate der entsprechenden Diagonalelemente der Korrelationsmatrix. Die Eigenwerte λ_1 und λ_2 sind wie folgt:

$$\lambda_1 = 0{,}1691\,, \quad \lambda_2 = 0{,}0005\,.$$

Für die Zwecke weiterer Berechnungen müssen die Werte der Matrizen H und G hergestellt werden. Wie bekannt, besteht H aus den Eigenvektoren von $K\,K^*$, G aber aus den Eigenvektoren von K^*K. Sowohl $K\,K^*$, als auch $K^*\,K$ sind symmetrische Matrizen, so dass H und G beide leicht berechnet werden können. [5]. Als Resultat, ergibt sich folgendes:

$$H = \begin{Bmatrix} 0{,}9631 & -0{,}2689 \\ -0{,}2689 & 0{,}9631 \end{Bmatrix},$$

$$G = \begin{Bmatrix} 0{,}8006 & -0{,}5993 \\ -0{,}5993 & -0{,}8006 \end{Bmatrix}.$$

Nun haben wir alle die benötigten Werte und können durch die Formel

$$R = H^*\,KG$$

R wie folgt erhalten:

$$R = \begin{Bmatrix} 0{,}405 & -0{,}000 \\ 0{,}000 & 0{,}021 \end{Bmatrix}.$$

Damit haben wir aber die gewünschten Korrelationskoeffizienten berechnet.

3. Schlußfolgerungen

a) Die aus den zwei untersuchten Wetterperioden abgeleiteten Durchschnittskarten können auch aus dynamischem Gesichtspunkte als analog betrachtet werden. Diese Analogie ist aber nicht zu streng, wie es aus den Korrelationskoeffizienten ersehen werden kann.

b) Die Analogie gestaltet sich besser, wenn das meridionale Strömungsystem in Betracht gezogen wird, als im Falle der zonalen Strömung.

c) Zur Ausführung der Berechnungen, die recht grosse Sorgfalt beanspruchen, ist es vorteilhaft, eine Rechenmaschine zu benutzen.

d) Auf Grund von Untersuchungen, die sich auf ein grösseres Material erstrecken, ist es möglich, eine objektive Klassifizierung der Wetterlagen aufzubauen.

LITERATUR

Bagrow, N. A. (1963): Indeksz analogicsnosztyi vektornüj polej. Trudü C. I. P. Vüp. 123. 4–17.

Bagrow, N. A. (1963): Sztatiszticseszkaja entropija kak pokazatyel szhodsztva ili razlicsija meteorologicseszkih polej. Met. i Gidr., 1963, No. 1.

Cehak, K. (1962): Die Verwendung von orthogonalen Polynomen in der Meteorologie. Archiv f. Met. Geoph. u. Bioklim. S. A. B. 12. 40–61.

Péczely Gy. (1957): Grosswetterlagen in Ungarn. Budapest 1957.

Lovas – Nagy V. (1956): Mátrixszámítás. Tankönyvkiadó.

PETROGRAPHICAL AND GEOCHEMICAL INVESTIGATIONS OF THE MESOZOIC ON THE LEFT BANK OF THE DANUBE

by
J. RÓZSAVÖLGYI

(Department of Petrography and Geochemistry, L. Eötvös University, Budapest)
(Received: 28th March, 1972)

ZUSAMMENFASSUNG

Die mesozoischen Schollen an der Linksseite der Donau bestehen vorwiegend aus karnischem und norischem Raibler Kalkstein, Dolomit und Dachsteinkalk, auf dessen verkarsteter, unebener Oberfläche während der terrestrischen Periode, die von der Kreide bis zum unterenEozän dauerte, sich stellenweise roter und grauer Ton und Krusteneisenstein ablagerten (Vashegy); an anderen Stellen häuften sich Bauxite in den Dolinen an (Nézsa).

In den Karbonatgesteinen der Obertrias weisen die Elemente Co, Ag, As, Cu, Ba, Sr und Mo beträchtliche Anreicherungen im Vergleich mit den von K. K. Turekian und K. H. Wedepohl (1961) angegebenen Durchschnittswerten auf. Angesichts der intensiven, epigenen Verkieselung des Kalksteins sowie des Auftretens von Fluorit und Baryt sind die überdurchschnittlichen Grössen der Mehrheit der Spurenelement-konzentrationen dem Mobilisationseffekt des tertiären Vulkanismus der Umgebung und den weitgehenden Ausstrahlungen dieses Effektes zuzuschreiben. Der Kaolinit, das vorwiegende Mineral des Lösungsrückstandes des Kalksteins, ist wahrscheinlich von allothigenem Ursprung.

Die Durchschnittsmenge der Spurenelemente des Diasporbauxits von Nézsa bleibt bei den meisten Elementen unterhalb des Durchschnittswertes der ungarischen Bauxite, die zumeist von gibbsitischer Zusammensetzung sind. Die Spurenelementkonzentration des säurigen Lösungsrückstandes der obertriadischen Karbonatgesteine, welche das Liegende des Bauxits bilden, ist jener des Bauxits ähnlich. In den Pisolithen ist die Menge des Goethits und Kaolinits grösser, als im originalen Gestein. Die an seltenen Elementen reichsten Bildungen der am Linksufer der Donau gelegenen Schollen und des ganzen Cserhát-Gebirges sind die kretazischen, terrestrischen roten und grauen Tone sowie der limonitführende Krusteneisenstein. Ihre Verbreitung an der Tagesoberfläche ist wegen der starken Denudation nur auf kleinere Flecken beschränkt.

Introduction

Oldest rocks exposed in the Cserhát Mountains, the blocks on the left bank of the Danube emerge like diapiric horsts from the surrounding Tertiary sedimentary mantle. They are constituted for the most part by Upper Triassic limestones and dolomites. On the karsted paleorelief of these, red and grey clays and a limonitic ironstone coat were formed (Vashegy) and, elsewhere, bauxite bodies were accumulated in dolinas (Nézsa) under the terrestrial regime that lasted from the Cretaceous to the Early Eocene.

According to drilling information, the Mesozoic horsts, fractured and down-faulted for several hundred metres with regard to one another, can be traced for considerable distances under the contemporary surface (*Mrs.* Csongrádi – J. Kővári – L. Majzon, 1959). Their stratigraphy and fault structure are ties connecting them with the SW – NE trending Transdanubian Central Mountains, even though their immediate connection with these is interrupted by the Tertiary volcanics of the Szentendre – Visegrád Mountains. Their connection with the E – W trending Triassic formations of the Bükk Mountains to the northeast is not clear either, as deep drilling and geophysical data have shown the basement of the intervening Cserhát and Mátra Mountains to consist partly of crystalline schists (G. Csiky 1968, I. Kubovics 1970, T. Szalai 1962).

Triassic

Including frequent intercalations of marls, the bituminous, cherty limestones belong to the Raibl Horizon of the Carnian the Dachsteinkalk and the unfossiliferous dolomites to the Norian (E. Vadász 1910, Cs. Detre 1970). According to J. Oravecz (1963), the dolomites are older than the Raibl limestone which seems to be evidenced by the sequence of the borehole drilled in recent years at Csővár: 2,00 to 522,00 m – Carnian cherty limestones; 522,00 to 613,00 m – Carnian-Ladinian dolomites with chert nodules; 613,00 to 1200 m – Ladinian Diplopora dolomites.

On the basis of the examination under the microscope of the Carnian of Csővár and the quantity of the insoluble residue the following rock variants have been distinguished: 1. microcrystalline limestone, 2. micritic limestone, 3. banded limestone, 4. biogenic limestone, 5. clayey limestone, and 6. calcareous marl, of which the first three are predominant. Their common feature is that they contain, in addition to allothigenic, detrital quartz, a considerable amount of SiO_2 concentrated partly in the chert nodules visible to the naked eye, partly in nests of chalcedony, fan-like, interlaced with calcite, 150 to 200 μm in diametre. With a view to the abundance of silica, the process of silicification could not have been fed by the dissolution and re-precipitation of the SiO_2 of siliceous fossils alone. Ascendent solutions may later have contributed to silicification, as supported by the fluorite and baryte crystals occurring in the cavities of the Raibl limestone (L. Jugovics, 1912).

As indicated by the frequently corroded surface of the quartz grains and the narrow fissures intersecting the accumulations of epigenic chalcedony, filled with well-crystallized calcite grains, the alkaline water, from which $CaCO_3$ precipitated, must have attacked the quartz grains, and the carbonic acid of calcium carbonate must have replaced a part of the silica. Accordingly, the precipitation-crystallization order was the following: 1. calcite, 2. SiO_2 modifications, 3. calcite, fluorite and baryte.

With the increase of the quantity of the insoluble residue the mean diametre of the calcite grains usually decreases. Predominant clay mineral of the fraction insoluble in diluted hydrochloric acid is kaolinite to which some montmorillonite, limonite and organic matter are associated (Fig. 1). The antagonism between the alkaline pH necessary for the precipitation of carbonates on the one hand and the acidic pH favourable for the formation of kaolinite on the other is eliminated by the assumption of detrital sources for kaolinite. As shown by G. Millot (1964), the kaolinite of limestones is almost always of detrital, inherited, origin.

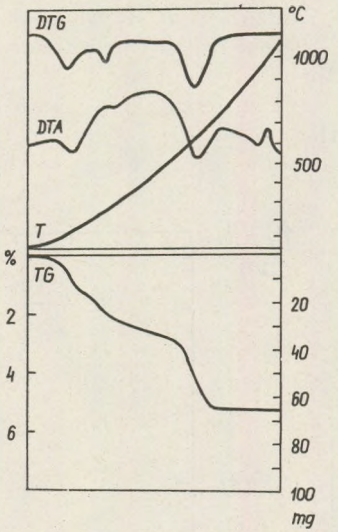

Fig. 1. Derivatogram of the insoluble residue of banded limestone. Quarry at Csővár.

As suggested by both the rock texture and the quantity of insoluble residue, the following two variants of the Norian dolomites of Vashegy can be distinguished: one characterized by an equigranular texture and an insoluble residue of 1–2 per cent and one having an inequigranular texture of brecciated habit due to the netlace of fissures filled up by calcite and detrital guartz grains. This second variety is also characterized by the 1–2% ratio of the insoluble residue which may sometimes attain, however, a striking value of 10 per cent or so. In the case of the Csővár limestone and the Vashegy dolomite there is not even a faint correlation of positive trend between the intensity of dolomitization and the quantity of the insoluble residue (unlike in the case discussed by R. W. Fairbridge, G. V. Chilingar and H. J. Bissel, 1967). This is due to the fact that the insoluble residue of limestone has been largely increased by epigenetic silicification, whilst the dolomite has not undergone any silicification of this kind.

The hanging wall of the bauxite at Nézsa is constituted by Dachsteinkalk consisting of calcite grains some 1 to 3 μm in diametre. Containing extremely little terrigenous material, if any, it is characterized by an insoluble residue on the average lower than 1 per cent.

The trace elements of the rock samples were determined semi-quantitatively by J. Nagy – Balogh (1971) by emmission spectral analyses. The values of Co, Ag, As, Cu, Ba, Sr and Mo in the limestones and those of Co, As, Cu and Ba in the dolomites are by one or two orders of magnitude higher as compared to the averages calculated for the carbonate rocks by K. K. Turekian and K. H. Wedepohl (1961.) The quantities of the other elements, too, are either higher than, or about the same as, the averages of Turekian and Wedepohl. A striking exception to the rule is only the manganese whose average is lower

by one order (Table 1). With a view to intensive epigenic silicification and to the occurrence of fluorite and baryte, the over-average concentrations of most of the trace elements can be ascribed to the far-reaching radiation, the mobilizing effect, of the Tertiary volcanism of the region.

Out of the trace elements of limestone and dolomite, it is alone strontium that shows a striking difference in favour of limestone which is justified by the size ratios of ionic radii (Sr^{2+} = 1.27 Å; Ca^{2+} = 1.06 Å; Mg^{2+} = 0.78 Å).

Comparing the quantities of three elements, Sr, Ba and Mn, with their counterparts in the Triassic carbonate rocks of other mountains, the present autor examined them separately in the original rock on the one

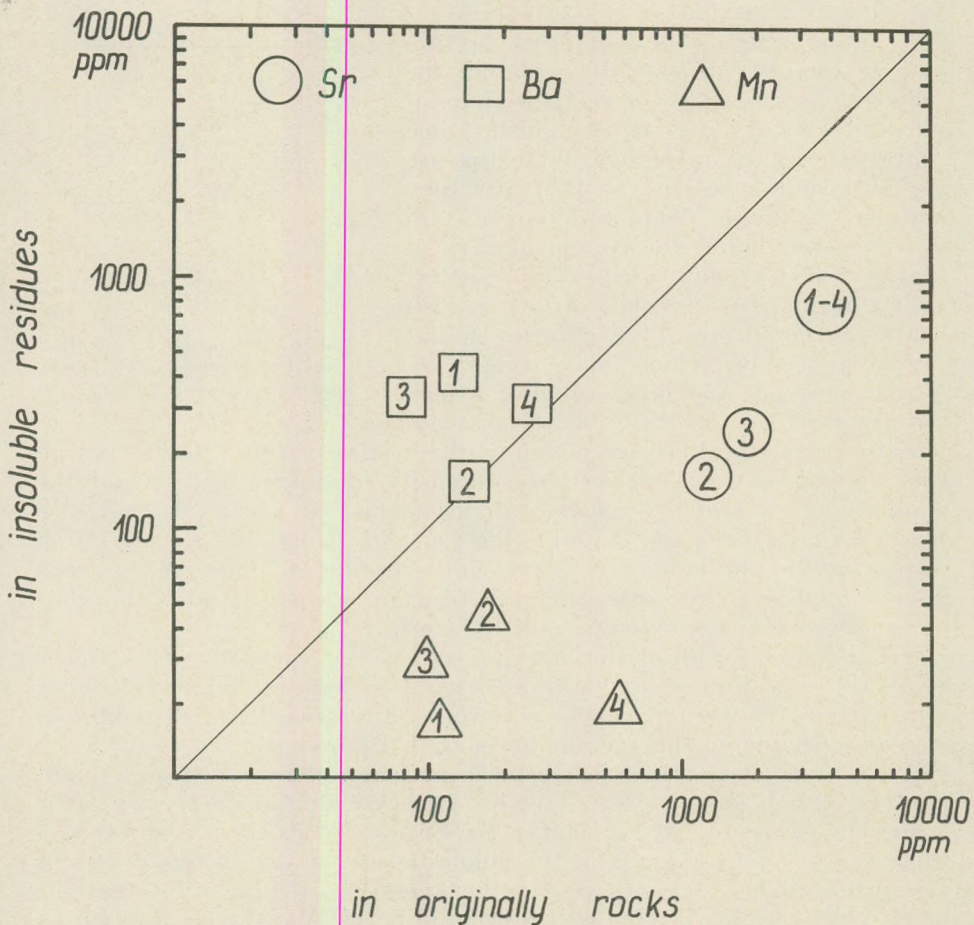

Fig. 2. Average concentrations of strontium, barium and manganese in the original rocks and their insoluble residues.

1. Transdanubian Central Mountains, 2. blocks on the left bank of the Danube, 3. Bükk Moutains, 4. Mecsek Mountains.

hand, and its residue insoluble in acids on the other. The solubility conditions of the Sr^{2+}, Ba^{2+} and Mn^{2+} ions are similar, all three belonging to Goldscmiedt's carbonate group with ionic potentials ranging from 1.5 to 3.0. The distribution of manganese and, the more so, that of strontium really relate to the fact that these two elements are connected preferentially with the carbonate fraction of the rock, while barium shows a relative enrichment in the insoluble residue (Fig. 2).

According to W. M. Bausch (1968), the strontium content of old basin limestones is considerably higher than that of reef limestones. He observed, however, that the strontium content cannot be used for the purpose of facies analysis, a statement confirmed by the author's own investigations. On the basis of the strontium content the Alpin-type geosynclinal sequence of the Transdanubian Central Mountains and the Mecsek's epicontinental Trias of partly German-type would belong to one and the same group, whereas the Alpin-type blocks on the Danube's left bank would form another group with Bükk's Trias of partly Dinaric type. Accordingly, the concentration of trace elements is controlled by the lithology of the source area rather than by stratigraphy.

Table 1

Trace element content in ppm of the Triassic horsts on the left bank of the Danube

		1	2	3
Number of samples		27	6	–
Siderophile elements	Co	10.2	18.9	0.1
	Ni	20	47.4	20
Calcophile elements	Ag	0.5	–	0.0
	As	24.4	24.5	1
	Cu	26.8	18.3	4
	Ga	4.3	1.6	4
	Pb	8.6	7.2	9
	Zn	56.5	163.1	20
Lithophile elements	Ba	139	158.7	10
	Sr	1330	518.3	610
Pegmatophile elements	Cr	22	10.5	11
	Mn	165	104.5	1100
	Mo	11.5	–	0.4
	Ti	393	286.5	400
	V	24	2.4	20
Sedimentophile elements	B	16.4	10	20

1. Average trace element content of the carbonate roks of the quarry at Csővár; 2. Average trace element content of the Vashegy dolomites; 3. Average values given for carbonate rocks by K. K. Turekian and K. H. Wedepohl (1961).

The quantity of manganese in all of the investigated mountain blocks was found to fall short of the international standards (K. K. Turekian – K. H. Wedepohl 1961; A. P. Vinogrodov 1962). Therefore Gy. Bárdossy's and G. Csajághy's conclusion (1966) that one of the special geochemical features of the Hungarian Mesozoic is the over-average quantity of iron, titanium and manganese can be restricted to apply, in respect of manganese, to the Jurassic and Cretaceous only.

The Ba/Sr ratios with 0.03 on the Transdanubian Central Mountains, 0.10 and 0.30, respectively, on the Danube's left bank, 0.04 in the Bükk Mountains and 0.06 in the Mecsek Mountains show a good agreement with the values calculated by A. Puchelt (1967) for carbonate rocks. The faint maximum observable in the horsts of the Danube's left banks is probably due to the occurrence of baryte.

Cretaceous to Lower Eocene

The exact age of the formations of the terrestrial period having followed the Late Triassic emergence is uncertain. M. Vendel (1937), relying on the analogy with the Transdanubian bauxite deposits, assigned these rocks to the Lower Cretaceous, though, because of the lack of knowledge of the overlying rocks, he did not exclude their Lower Eocene age either. The Eocene transgression began to reach the territory of the Cserhát Mountains as late as the Lutetian.

Main mineral of the dark red and hard, pisolitic bauxite, already stripped off is diaspore which beside the Nézsa deposit is present in considerable amount in the Nagyszál and Nagyharsány deposits. Its occurrence may be ascribed to tectonic effects, the presence of a primary deposit (autochtony) being highly improbable (Gy. Bárdossy 1961). Diaspore is accompanied by kaolinite and limonite in varying amounts. According to the DTG analyses, the quantity of goethite and kaolinite in the pisolites is higher than in the bauxite on the whole. This relates to the fact that the migration of the iron compounds, most mobile of all, and their local enrichment are primarily responsible for the origin of pisolites (Fig. 3 and 4). Within the bauxite body all kinds of transitions of bauxite, clayey bauxite, bauxitiferous clay and clay can be shown to occur. The decrease of the amounts of diaspore and goethite and the increase of the kaolinite content are usually accompanied by a bleaching of the rock this turning white. Clayey bauxite variants, variegated with red-and-white mottles, are rather frequent.

On the basis of the micromineralogical analyses of the bauxite of Nézsa, J. Kiss (1952) suggests the bauxite to have originated by a complex process from two different types of mother rock. Similar is the opinion of Gy. Bárdossy (1961) who believes the material of the Transdanubian bauxite deposits to derive from the erosion of metamorphic and

igneous rocks. The Nézsa deposit is rather poor in trace elements as compared to other Hungarian bauxites. Out of the metals other than aluminium that might be recovered for industrial purposes, neither gallium, nor vanadium does attain the average of the Hungarian bauxites. The trace element concentrations of the deposit are similar to those of the residue insoluble in acids of the Upper Triassic carbonate rocks.

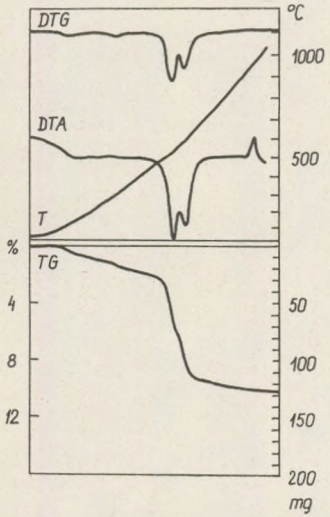

Fig. 3. Derivatogram of red pisolitic bauxite. Nézsa.

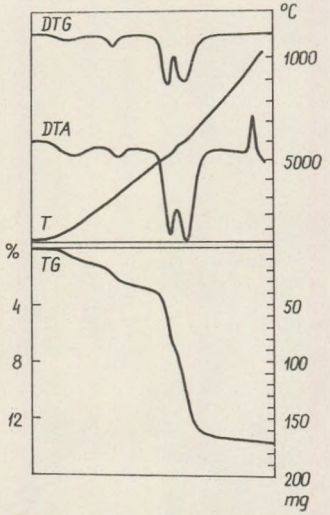

Fig. 4. Derivatograms of pisolites. Nézsa.

The more so, these rocks are characterized by a higher average of all rare metals except arsenic (Table 2). This fact can be interpreted in two different ways. According to one of these, the material of the bauxites may partly derive from the alkaliinsoluble residue of the underlying carbonate rocks which would account for the similar concentrations of trace elements in both formations. (Gy. Komlóssy 1967). The othere more plausible, interpretation is that the source rocks of the Upper Cretaceous sedimentary basin were of the same character as the sources of the bauxites. This hypothesis seems to be confirmed by the kaolinite of detrital origin present in the insoluble residue of the Triassic limestones, a fact suggesting a source area made up of crystalline schists and granites liable to weathering.

As shown by the results of investigations by H. M. Köster (1966), the residual clays produced by the kaolinitization of granites retain strontium less effectively than barium can be retained. Therefore the autochtonous clays are much more abundant in barium than the allochtonous ones. Should this statement be applied to the kaolinitiferous bauxites in which no barium could be detected, this would relate to the rede-

Table 2

Average concentrations of trace elements in the bauxite of Nézsa, the terrestrial weathering products of Vashegy and in the insoluble residue of the limestone sequence of Csővár

Quantity of samples		1 8 specimens	2 6 specimens	3 25 specimens
Siderophile elements	Co	24.6	65.2	9.5
	Ni	98.2	196.6	184.5
Calcophile elements	Ag	–	–	–
	As	116.5	163	23.5
	Cu	17.5	150.8	201.5
	Ga	21.2	23.9	6.9
	Pb	40.4	36.7	10.3
	Zn	129.8	400	456
Lithophile elements	Ba	–	733.3	133
	Sr	443.7	733.3	175
Pegmatophile elements	Cr	87.8	98.3	45.6
	Mn	260.7	391.8	47.5
	Mo	5.6	7.7	39.3
	Ti	7700	4276.6	1459
	V	110.1	215	142
Sedimentophile elements	B	10	39.2	26.1

1. Average trace element content of the Nézsa bauxite formation; 2. Average trace element content of the terrestrial weathering products of Vashegy; 3. Average trace element content of the insoluble residue of the carbonate rocks of Csővár.

position of the bauxite and suggest crystalline schists and granites as sources.

Formations similar to the barren minerals of bauxites have filled up the dolinas of the Vashegy dolomite, where the fractured, breccious dolomite carries an ironstone coat and grey clays of irregularly varying thickness and then gravelly red clays of greater thickness (Fig. 5). The ironstone coat is of nodular porous-cavernous habit, less frequently stalactitic, showing an iris-patterned stain. According to thermal analyses, it consists predominantly of goethite. Essential mineral components of the red clays are candite-type fire-clay and goethite (Fig. 6). Occurring among the gravels of the red clays, the dolomite debris and the poor sorting of the material are indicative of the presence of a residual terrestrial sediment which may have undergone a transportation for a very short distance, if any. The relatively high barium content and the unusually high Ba/Sr = 1 ratio are also arguments for their being residual sediments. They would be the formations richest in trace elements and worthy of further pros-

pecting of the central and western Cserhát, if their probable extension was not limited to minor patches as a result of vast denudation.

The continental period, which lasted for the greater part of the Mesozoic, ended with the Eocene sedimentary cycle starting with a slow subsidence of the territory.

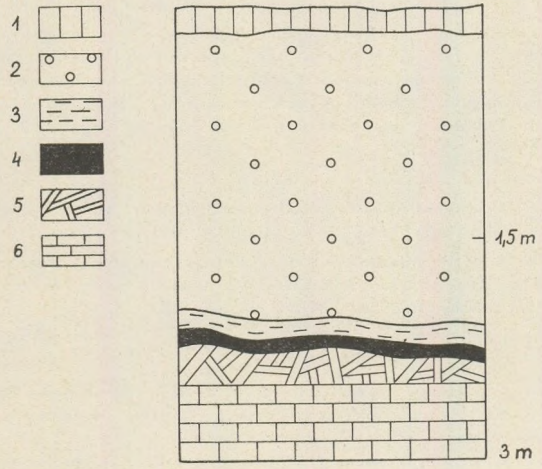

Fig. 5. Profile of dolina-filling sediments. Vashegy.
1. soil, 2. red clay with gravels, 3. grey clay, 4. limonitic coat, 5. brecciated dolomite, 6. dolomite.

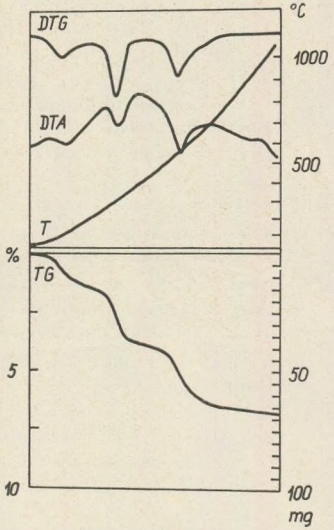

Fig. 6. Derivatogram of red clay. Vashegy.

REFERENCES

Bausch, W. M. (1968): Outlines of distribution of strontium in marine limestones. – in: Recent developments in carbonate sedimentology in Central Europe. Springer V. pp. 106–115.

Bárdossy, Gy. (1961): A magyar bauxitok összetételnek és keletkezésének kérdései (Problems of the composition and origin of the Hungarian bauxites). Földt. Int. Évkönyve 49. pp. 815–823.

Bárdossy, Gy.– Csajághy, G. (1966): Geochemical data on the mesozoic of Hungary. – Acta Geologica 10. pp. 117–131.

Csiky, G. (1968): A szénhidrogénkutatások újabb eredményei és kilátásai az északi paleogénmedencében (Recent results and perspectives of prospecting for oil and natural gas in the Northern Paleogene Basin). Földtani Közlöny 98. pp. 29–40.

Csongrádi, B. – Kővary, J. – Majzon, L. (1959): Adatok a Budapest környéki medencerészek rétegsorához (Contribution to the stratigraphy of the subbasins in the vicinity of Budapest). Földt. Közl. 89. pp. 407–412.

Detre, Cs. (1970): Őslénytani és üledékföldtani vizsgálatok a Csővár, Nézsa és Keszeg környéki triász rögökön (Paleontological and lithological investigations of the Triassic horsts near Csővár, Nézsa and Keszeg). Földt. Közl. 100. pp. 173–184.

Fairbridge, R. W. – Chilingar, G. V. – Bissel, H. J. (1967): Introduction. – in: Carbonate Rocks. Elsevier Publ. Comp. pp. 1–28.

Jugovics, L. (1912): Ásványtani Közlemények (Contributions to mineralogy). Annales Mus. Nat. Hung. 10. pp. 593–598.

Kiss, J. (1952): La constitution minéralogique de la bauxite de Nézsa. – Acta Geologica 1. pp. 113–132.

Komlóssy, Gy. (1967): Contribution à la connaissance de la genèse des bauxites hongroises. – Acta Geologica 11. pp. 477–489.

Köster, H. M. (1966): Zur Röntgen-Fluoreszenz Spektralanalyse von Rubidium, Strontium, Barium und Blei in Kaolinen und Tonen. – Contr. Mineral. and Petrol. 12. pp. 168–172.

Kubovics, I. (1970): Északkelet- és Nyugat-Mátra ásvány-kőzettani vizsgálata (Mineralogical and petrographical investigations of the northeastern and westerm Mátra Mountains). – in: Vulkanológiai vizsgálatok a Mátrában és a Börzsönyben (Volcanological investigations in the Mátra and Börzsöny). Ak. Kiadó. Bp. pp. 7–160.

Millot, G. (1964): Géologie des argiles. – Masson Ed. Paris.

Nagyné – Balogh, J. (1971):. Vorrichtung zur halbquantitativen Auswertung von Emissionsspektren. – Spectrochimica Acta. 26B. pp. 609–611.

Oravecz, J. (1963): A Dunántúli Középhegység felsőtriász képződményeinek rétegtani és fácieskérdései (Problems of stratigraphy and lithology of the Upper Triassic of the Trandsdanubian Central Mountains). Földt. Közl. 93. pp. 63–73.

Puchelt, H. (1967): Zur Geochemie des Bariums im exogenen Zyklus. – Springer V. Heidelberg.

Szalai, T. (1962): A Cserhát-Mátra gravitációs anomáliáinak tektonikai értelmezése és kristályos kőzeteinek helyzete a Ny-i Kárpátok rendszerében (Tectonic interpretation of the gravimetric anomalies of the Cserhát Mountains and the position of their crystalline rocks within the system of the Western Carpathians). Magyar Geofizika 3. pp. 31–40.

Turekian, K. K. – Wedepohl, K. H. (1961): Distribution of the elements in some major units of the Earth's crust. – Bull. Geol. Soc. America 72. pp. 175–192.

Vadász, E. (1910): A Duna-balparti idősebb rögök őslénytani és földtani viszonyai (Paleontology and geology of the older blocks on the left bank of the Danube). Földt. Int. Évkönyve. 18. pp. 101–172.

Vendel, M. (1937): Über die geologischen Verhältnisse der Umgebung von Nézsa. – Bánya és Kohómérn. Oszt. Közl. 9. pp. 327–372.

Vinogradov, A. P. (1962): Srednije soderzanija himiceskih elementov v glavnüh tipah izverzenüh gornüh parod zemnoj korü. – Geohimija 7. pp. 555–571.

DETERMINATION OF SATELLITE AND STATION POSITIONS BY MEANS OF GEOMETRICAL DOPPLER GEODETIC METHODS

by
GY. TARCSAI
(Geophysical Institute of Loránd Eötvös University, Budapest)

and
J. ÁDÁM
(Polytechnical University, Budapest)
(Received: 1st March, 1972)

РЕЗЮМЕ

Излагаются два независимых допплеровских метода, которые можно применять и вместе. Один из них способствует определению положения спутника при помощи синхронного измерения интегрального допплеровского сдвига на пяти станциях известного положения.

Спомощью второго метода можно определять координаты самостоятельной допплеровской станции, при условии, что ею измеряется интегральный допплеровский сдвиг на такой дуге орбиты, которая включает в себя по крайней мере пять известных пунктов.

Оба метода полностью независимы от различных возмущений орбиты спутника и приводят к системе линейных уравнений.

Были начаты вычисления на ЭВМ для определения возможностей и ограничений методов.

Introduction

The geodetical methods based on the Doppler shifted radio signals of artificial satellites are mainly of dynamical character (beside the station coordinates providing the orbital elements and often the coefficients of the Earth's gravitational potential also), consequently require cumbersome computations. In the following a simple and rigorous method will be given for the determination of station position, based on integrated Doppler measurements over such an arc of the orbit, which contains at least five known points. These points can be obtained either from simultaneous Doppler measurements carried out at five stations with known coordinates (C a r r a r a et al., 1961.) or by other means.

The methods for determining satellite positions and station coordinates from integrated Doppler measurements will be described in detail. Both methods are completely independent of any perturbations in the satellite motion.

The integrated Doppler-shift

Suppose that an observer receives continuously the radio transmission of a satellite and at the moment t observes a Doppler-shift $\Delta f(t)$. Neglecting refraction and relativistic effects (which can be satisfactorily eliminated) one may write:

$$\Delta f(t) = -\frac{f_0}{c} \frac{d\varrho(t)}{dt} \tag{1}$$

where f_0 is the frequency of the signal transmitted by the satellite, c is the velocity of light in free space and $\varrho(t)$ is the distance between satellite and observer. Integrating $\Delta f(t)$ over the time interval $\Delta t = t - t_0$, we get the corresponding change of distance:

$$\varrho(t) - \varrho(t_0) = -\frac{c}{f_0} \int_{t_0}^{t} \Delta f(t)\, dt \tag{2}$$

Thus, if the distance $\varrho(t_0)$ is known for a given t_0 then $\varrho(t)$ can be computed for any moment using the integrated Doppler-shift

$$\varrho(t) = \varrho(t_0) - \frac{c}{f_0} \int_{t_0}^{t} \Delta f(t)\, dt \tag{3}$$

The efficiency of geodetic Doppler measurements generally is strongly limited by the absence of such a known $\varrho(r_0) = \varrho_0$ initial distance.

Determination of satellite positions

If we have several Doppler stations with known coordinates then the problem really reduces to the determination of the ϱ_{i0} initial distances (where the subscript i refers to the i-th station). Namely, if we know the initial distances at least for three stations, then using (3) the individual satellite-station distances, and consequently the satellite position also, can be determined. Since up to the present time only the principle of determining the initial distances was published (Carrara et al., 1961), therefore we discuss the problem in more detail.

The distance between the i-th station and the satellite at the moment t_k is related to the (x_i, y_i, z_i) station and (x_{sk}, y_{sk}, z_{sk}) satellite coordinates as

$$(x_{sk} - x_i)^2 + (y_{sk} - y_i)^2 + (z_{sk} - z_i)^2 = \varrho_{ik}^2 \tag{4}$$

(the chosen system of coordinates is fixed to the Earth). At a given instant this second order equation contains four unknowns: x_{sk}, y_{sk}, z_{sk} and ϱ_{i0}. Writing (4) for four stations and subtracting the first equation from the others we arrive at a linear system of equations for the satellite coordinates belonging to the moment t_k:

$$\begin{aligned} Ax_{sk} + Dy_{sk} + Gz_{sk} + L &= \varrho_{2k}^2 - \varrho_{1k}^2 \\ Bx_{sk} + Ey_{sk} + Hz_{sk} + M &= \varrho_{3k}^2 - \varrho_{1k}^2 \\ Cx_{sk} + Fy_{sk} + Kz_{sk} + N &= \varrho_{4k}^2 - \varrho_{1k}^2 \end{aligned} \tag{5}$$

where

$$A = 2(x_1 - x_2) \qquad D = 2(y_1 - y_2) \qquad G = 2(z_1 - z_2)$$

$$B = 2(x_1 - x_3) \qquad E = 2(y_1 - y_3) \qquad H = 2(z_1 - z_3)$$

$$C = 2(x_1 - x_4) \qquad F = 2(y_1 - y_4) \qquad K = 2(z_1 - z_4)$$

$$L = R_2^2 - R_1^2 \qquad M = R_3^2 - R_1^2 \qquad N = R_4^2 - R_1^2$$

$$R_i^2 = x_i^2 + y_i^2 + z_i^2 \qquad (i = 1, 2, 3, 4)$$

Solving (5) for the satellite coordinates:

$$\begin{bmatrix} z_{sk} \\ y_{sk} \\ x_{sk} \end{bmatrix} = \begin{bmatrix} a & b & c & d & e \\ f & g & h & l & m \\ n & o & p & q & r \end{bmatrix} \begin{bmatrix} \varrho_{1k}^2 \\ \varrho_{2k}^2 \\ \varrho_{3k}^2 \\ \varrho_{4k}^2 \\ 1 \end{bmatrix} \tag{6}$$

where

$$a = \frac{AA'}{G'} \qquad b = -\frac{AD'}{G'} \qquad c = \frac{BD' - CA'}{G'}$$

$$d = \frac{CA' + AD' - AA' - BD'}{G'} \qquad e = \frac{C'D' - F'A'}{G'} \qquad f = \frac{A - aE'}{D'}$$

$$g = -\frac{bE'}{D'} \qquad h = -\frac{C + cE'}{D'} \qquad l = \frac{C - \alpha E' - A}{D'}$$

$$m = -\frac{F' + eE'}{D'} \qquad n = -\frac{Df + aG}{A} \qquad o = -\frac{Dg + bG}{A}$$

$$p = -\frac{Gc + Dh - 1}{A} \qquad q = -\frac{Gd + Dl + 1}{A} \qquad r = -\frac{L + Ge + Dm}{A}$$

$$A' = AE - BD \qquad B' = AN - GB \qquad C' = AM - BL$$

$$D' = AF - DC \qquad E' = AK - CG \qquad F' = AN - CL$$

$$G' = A'E' - B'D'$$

In addition to the satellite coordinates, in equation (6) also the ϱ_{ik} distances are unknown (through the ϱ_0 initial distances), therefore first of all these must be determined. For this, substituting the satellite coordinates from (6) into the equation of type (5) for the fifth station, after reductions we get the following second order equation for the ϱ_{ik} unknowns:

$$w\varrho_{5k}^2 + s\,\varrho_{4k}^2 + t\,\varrho_{3k}^2 + u\,\varrho_{2k}^2 + v\,\varrho_{1k}^2 + \text{const} = 0 \tag{7}$$

where the coefficients are functions of the known coordinates of the stations.

Let us introduce the

$$A_{ik} = -\frac{c}{f_0} \int_{t_0}^{t_k} \Delta f_i(t)\, dt \tag{8}$$

notation, where $\Delta f_i(t)$ is the Doppler-shift that can be measured at the i-th station. Using the relation

$$\varrho_{ik} = \varrho_{i0} + A_{ik}$$

equation (7) can be rewritten:

$$w(\varrho_{50} + A_{5k})^2 + s(\varrho_{40} + A_{4k})^2 + t(\varrho_{30} + A_{3k})^2 + u(\varrho_{20} + A_{2k})^2 + v(\varrho_{10} + A_{1k})^2 + \text{const} = 0 \tag{9}$$

In this equation only the ϱ_{i0} initial distances are unknown, as the quantities A_{ik} are measured at the stations. In order to eliminate the second order members it is suitable to write equation (9) for six points of the orbit (for six different values of k), then subtract the first equation from the others. Thus we obtain a linear inhomogeneous system of equations for the five initial distances, in matrix notation:

$$\overline{\overline{A}}\, \bar{\varrho}_0 = \bar{b} \tag{10}$$

where the columns of the matrix $\overline{\overline{A}}$ are as follows:

$$a_{j1} = 2v\,(A_{1,j+1} - A_{11}) \qquad a_{j3} = 2t\,(A_{3,j+1} - A_{31})$$
$$a_{j2} = 2u(A_{2,j+1} - A_{21}) \qquad a_{j4} = 2s(A_{4,j+1} - A_{41})$$
$$a_{j5} = 2w\,(A_{5,j+1} - A_{51}) \qquad (j = 1, 2, 3, 4, 5)$$

furthermore

$$\bar{\varrho}_0 = \begin{bmatrix} \varrho_{10} \\ \varrho_{20} \\ \varrho_{30} \\ \varrho_{40} \\ \varrho_{50} \end{bmatrix} \qquad \bar{b} = \begin{bmatrix} b_1 \\ b_2 \\ b_3 \\ b_4 \\ b_5 \end{bmatrix}$$

where

$$b_j = w(A_{51}^2 - A_{5,j+1}^2) + s(A_{41}^2 - A_{4,j+1}^2) + t(A_{31}^2 - A_{3,j+1}^2) + u(A_{21}^2 - A_{2,j+1}^2) + v(A_{11}^2 - A_{1,j+1}^2)$$
$$(j = 1, 2, 3, 4, 5)$$

From equation (10) the unknown ϱ_{i0} distances can be computed. The computation requires that the determination of A_{ik} defined by (8), be completed simultaneously at five known stations for six different t_k values.

If the initial distances ϱ_{i0} once have been determined, then from equations (6) or from other expressions (based only on three stations) the satellite coordinates can be computed, provided that the stations observe the integrated Doppler-shift simultaneously.

It is to be noted that the initial distances are "initial" only in the sense that all the other distances are computed using them and the integrated Doppler-shifts (and not in chronological sense).

In the preceding a method was described for satellite positioning which is based entirely on Doppler measurements. In Doppler measurements the accomplishment of synchronous observations does not meet so serious difficulties as in the photographic and laser methods. This is due to the continuous character and technique (electronic) of the measurements and the rather weak dependence on meteorological factors. On the other hand a great advantage of the method that based on the highly advanced measuring, recording, data transmission and data processing techniques the determination of satellite positions can be almost entirely automated.

Determination of the coordinates of a Doppler station

Suppose that the position of the satellite is determined (by photographic, laser, Doppler etc. methods) at five different moments. If a station measures the integrated Doppler-shift over such a time interval which includes this five points then equation (4) can be written for each of the five known points of the trajectory (of course, the subscript i can be omitted), with

$$\varrho_k = \varrho_0 + A_k = \varrho_0 - \frac{c}{f_0} \int_{t_0}^{t_k} \Delta f(t)\, dt$$

It is useful to coincide t_0 with one of the t_k values. Then, subtracting the first equation from the others we get the following equation for the unknown quantities x, y, z and ϱ_0:

where
$$\overline{\overline{C}} \cdot \overline{T} = \overline{d} \tag{11}$$

$$\overline{T} = \begin{bmatrix} x \\ y \\ z \\ \varrho_0 \end{bmatrix} \qquad \overline{d} = \begin{bmatrix} d_1 \\ d_2 \\ d_3 \\ d_4 \end{bmatrix}$$

$$d_j = R_{s1}^2 - R_{s,j+1}^2 + A_{j+1}^2 - A_1^2; \quad R_{sj}^2 = x_{sj}^2 + y_{sj}^2 + z_{sj}^2$$

and the columns of the matrix $\overline{\overline{C}}$ are given as:

$$C_{j1} = 2(x_{s1} - x_{s,j+1}) \qquad C_{j3} = 2(z_{s1} - z_{s,j+1})$$
$$C_{j2} = 2(y_{s1} - y_{s,j+1}) \qquad C_{j4} = 2(A_1 - A_{j+1})$$
$$(j = 1, 2, 3, 4)$$

The solution of (11) for $\overline{T}$ thus yields the coordinates of the Doppler station and the satellite-station distance at the moment t_0.

Model computations

For the methods described in the preceding computer programs have been written. The efficiency of the methods might be checked by computing the "measured" data, deviating them from their accurate values by an amount corresponding to the probable measurement errors, then computing the satellite or station coordinates. After this the actual coordinates can be compared to the computed ones and the deviations will be characteristic for the effect of measurement errors.

In connection with the determination of satellite position the model computations might answer to the following questions:

a) Accuracy conditions under ideal circumstances and in the case of different kinds of measurement errors
b) the effect of synchronization errors
c) the effect of inaccuracies in the positions of stations
d) the influence of the relative position of stations
e) the influence of orbital parameters
f) optimal execution of the measurements.

Questions concerning the determination of the position of a Doppler station:

a) applicability of the method under ideal conditions and in the case of different kind of errors in the Doppler measurements
b) the effect of inaccuracies in the satellite positions
c) the influence of the relative position between the sation and the satellite orbit; optimal configuration
d) optimal execution of the measurements.

REFERENCES

Carrara, N., Checcacci, P. F., Ronchi, L. (1961): Determination of the orbit of an artificial satellite by means of four Doppler stations, in: Space Research II, North-Holland, Amsterdam.

Drahos, D., Horváth F., Tarcsai, Gy. (1969): Determination of the geodetical position from the Doppler curves of artificial satellites using the method of differential corrections, in: Observation of artificial satellites of the Earth, No. 8., Budapest.

Ferencz, Cs., Ferencz I., Drahos, D., Horváth, F., Tarcsai, Gy. (1970): Some theoretical contributions concerning Doppler geodetical measurements, in: Space Research X, North-Holland, Amsterdam.

Tarcsai, Gy. (1969): Thesis, Budapest.

Tarcsai, Gy., Horváth, F. (1970): Relativistic effects and optimalization in Doppler geodetical measurements, in: Observation of artificial satellites of the Earth. No. 9., Warszawa.

SPECULATIONS ON FOOD SUPPLY AND BATHYMETRY IN THE MEDITERRANEAN JURASSIC SEA

by
A. VÖRÖS

(Institute of Paleontology, Eötvös University, Budapest)
(Received: 1th March, 1972)

РЕЗЮМЕ

Единственным основным источником питания открытого океана Тетхис мог являться фитопланктон. Его количество в течении периода юры (из за причин эволюции) постепенно увеличивалось несмотря на то, что Тетхис расширялся или, что то же самое, нутрианс источник отодвигался назад. Итак, причиной уменьшения бентоса в средиземноморском районе могла быть не всё усиливающийся характер открытого моря, а как Garrison и Fischer (1969) установили, такое явление могла причинять увеличивающаяся глубина моря. Это предположение потверждает и исследование бентонических соединений леаса, найденных в горах Баконь (Венгрия). Экстраполяция результатов современной морской билогии указывает на то, что максимальная глубина Мединерранского моря периода юры могла превзойти 3000 метров.

Introduction

The bathymetric criteria of the Mediterranean Jurassic was recently discussed by H a l l a m (1971). The depth-dependent physical and chemical factors seem to be – at least separately – ineffective to the sediments. The biological factors appear to be more usable, since the fossil remains and the traces of the organic activity can approximately date the smaller water depth down to the lower boundary of the photic zone. The relatively shallow-water deposition of certain condensed red limestones could be demonstrated in this way (W e n d t 1970, S t u r a n i 1971, J e n k y n s 1971). However, the majority of the Mediterranean Jurassic sediments formed in greater depth as compared to the latter. The embedded benthonic fauna shows no direct indication to the depth. The aim of this work is to discuss the food-supply problems and to drow some indirect conclusions from these to the bathymetry.

Food-supply and feeding in the Mediterranean Jurassic sea

The two most conspicuous and general feature of the Mediterranean Jurassic rocks, i. e. the red colour and the sparsity of the benthonic faunal elements equally suggest bottom circumstances of poor in organic matter (H a l l a m 1967). The red colour is due to the higher oxidizing state iron (Fe^{3+}), showing that in the sediment reductive zone was not formed. The rate of bacterial sulphate reduction is a function of the available amount of organic matter (B e r n e r 1970), in this case, therefore, the

organic material falling onto the bottom was mineralized in the uppermost sediment layer, or still in the water column, precluding in this way the activity of sulphate-reducing bacteria. The sparsity of benthonic faunal elements is especially striking when compared to the coeval strata of other European areas. To explain these differences the formerly suggested factors (temperature, salinity, etc.) are insufficient, the most important reason could be that the benthonic populations became increasingly distant from the food-source (Garrison – Fischer 1969, Hallam 1971). Brachiopod studies led directly to the conclusion suggesting food-deficiency: as shown by Ager (1965) and more exactly Vogel (1966) on the basis of functional morphologic studies, the pygopids and sulcate terebratulids characteristic to the Mediterranean Jurrassic are examples of adaptation to environment with reduced food-supply.

Beside of other paleontological and sedimentological evidences, it is justified to assume from the above mentioned facts, that the Tethys was a wide open sea of order of 1000 km. The principal food-source of the open oceans is the phytoplankton. The importance of the land-derived detrital and dissolved organic matter, as well as the role of the shallow-water benthonic algal vegetation is negligible (Bordovskiy 1965).

Phytoplankton and nutrients

Inorganic nutrients essential for the phytoplankton are derived finally from continents, and their amount diminishes gradually towards the open ocean. However, only the phosphate and nitrate depletion becomes critical (Clarke 1954, p. 280). It is shown that nitrate could be formed in open seas by electric discharges (Pitrat 1970), but the absence of nitrate in itself checks the life-limits of plants. Consequently the amount of the phytoplankton decreases away from the continents.

Assuming oceanic dimensions to the Tethys in the Jurassic similar distribution is expected. In the Mediterranean areas from the lowermost Jurassic onwards calcareous nannofossils can be found in rock-forming quantity (Bernoulli – Jenkyns 1970), suggesting productive or not completely barren surface waters.

During the course of the Jurassic the Tethys graditionally expanded, partly by the drifting away of the African and European lithospheric plates (Géczy 1973), partly by eustatic sea-level rise (Hallam 1969), and/or the submergence of the marginal regions (e. g. Russian Platform) of the two continents. With the shifting back of the nutrient-source a gradual phytoplankton impoverishment is expected. On the contrary the Mediterranean Jurassic is characterized by a considerable phytoplankton enrichment (cf. thick pelagic limestones in the Upper Jurassic). This flourishing is a global evolutionary phenomenon (Tappan – Loeblich 1971), and it is clear therefore, that the evolution, and not the nutrient-distribution was the critical factor in the temporal change of the phytoplankton quantity. Within the Tethys nutrients must have been available in excess during the whole Jurassic.

Food-Chain

The food-chain of the Recent seas is inextricably interwoven, and to reconstruct any Jurassic food-chain is evidently impossible. As an approximation merely the so-called biomass pyramid can be outlined (see for example A g e r 1963, p. 219) to show the biomass relation of the groups of organisms living on a given area. The base of the pyramid represents the primary producers, the second step is of the herbivores, and the third (or ocassionally the additional) one is of the carnivores (or parasites, scavengers, etc.). The biomasses of the succeeding stages differ by more than an order of magnitude. The fossilization eliminates the organisms without hard parts, but trusting that this selection equally concerns all of the trophic levels, we can attempt to outline a biomass pyramid for the Mediterranean Jurassic (The table below contains only the most important fossil groups, in estimated biomass order within the certain columns).

Table I

	PRODUCERS: Phytoplankton	
	CONSUMERS:	
	Living in the water column	Living on the bottom
HERBIVORES	ammonoids, bivalves, foraminifers, radiolarians	crinoids, sponges, brachiopods, bivalves, gastropods, echinoids, foraminifers
CARNIVORES	belemnoids, cephalopods with Rhynchoteuthis, fishes, ammonoids (?)	gastropods (?) echinoderms (?)

In contrast to that of the NW European (L e h m a n n 1971), there are no direct data on the food of the Mediterranean Jurassic ammonites. Some species could have been carnivores, but the majority should be reasonably ranged into the herbivores. If we placed this megafossil group of much the greatest biomass onto the top of the pyramid, the lower trophic levels should be increased by order of magnitude, but this is not justified by the fossil record.

According to G a s i o r o w s k i (1971), the "Cephalopods with Rhynchoteuthis" represents a distinct group of pelagic carnivores.

The worms and arthropods certainly took an important part, but the rare trace fossils do not permit to estimate their quantity.

The two-column separation of the above table is justified by the conspicuous and essential differences between the pelagic and benthonic groups. The *pelagic community* represents a greater biomass, showing well-organized ecosystem; the food-chain is complex with many carnivores. These suggest favourable food-supply. During the course of the Jurassic this community follows in diversity and even more in biomass the rise of the phytoplankton. On the other hand the *benthonic community* appears to be of primitively organized, with few carnivores. On the

Mediterranean areas marked decline can be recognized oppositing the rise of the phytoplanktonic community. This fact was firstly emphasized by Garrison and Fischer (1969), who convincingly demonstrated that the decline of the benthos can be due to the starvation related to the increasing water depth.

In the following – beside some further discussion – this opinion will be supported by a factual example.

The feeding of the benthos

Glancing over the feeding habits of the benthonic communities of the Mediterranean Jurassic it becomes clear that the suspension feeders (crinoids, sponges, brachiopods, bivalves) were in vast majority; the organic matter produced by the phytoplankton was directly available to them. As it was shown by McCammon (1969) the brachiopods chiefly feed dissolved organic matter, but this is ultimately of phytoplanktonic origin. The deposit-feeders could have been represented by some echinids, gastropods and worms only. According to Sokolova (1959) the dominance of suspension-feeders is characteristic to areas of slow deposition and relatively high concentration of suspended organic matter. This circumstance can be well generalized to the Mediterranean Jurassic.

The spatial distribution of the benthos is not as uniform as that of the plankton or nekton, but rather patchy. This result was obtained from the study of the Lower Jurassic sections of the Bakony Mountains (Hungary); as an explanation the submarine relief differences appeared (Galácz – Vörös 1972). It is reasonable to present an example concerning this.

Ibex zone benthonic faunas of three different Bakony mountains sections

The three sections (i. e. Közöskút, Kericser, Lókút) were uncovered by the Hungarian Geological Institute. The lithology and biostratigraphy was disscussed by Konda (1970) and Géczy (1971a) respectively. A more detailed description of the Kericser Section can be found in Géczy (1971b.) The location, lithology and presumed paleobathymetric situation of the localities are shown on Fig. 1.

The Közöskút Section is considerably discontinous: on the uneven surface of the Hettangian massive limestone succeeds disconformably a pink limestone with manganese-coated fossils, representing the Ibex Zone exclusively. The overlying red Toarcian limestone with basal ferromanganese crust is similarly separated by a hiatus from the succeeding Bajocian ammonitico rosso limestone (Humphriesianum Zone, A. Galácz pers. comm.). These lithologic features are generally accepted as characteristics of the submarine swell (seamount) deposition. The hardgrounds has not yielded so far any traces indicating the photic zone, therefore, the seamount was probably situated in relatively great (several hundred metres) depth.

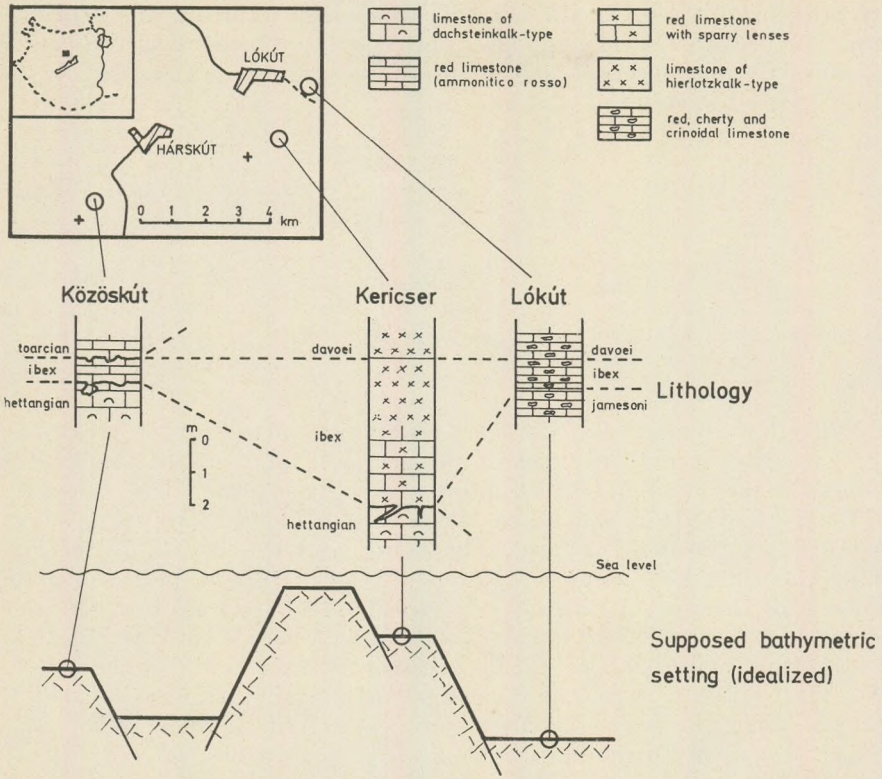

Fig. 1. The location and lithology of the Közöskút, Kericser and Lókút sections, and their supposed bathymetric situation in the Ibex Zone.

In the Kericser Section the Ibex Zone is represented by a relatively thick sequence, overlying the jointed surface of the Hettangian limestone. In its lower levels some lenses of Hierlatz-type limestone, containing ammonites, brachiopods and crinoids are intercalated with the red limestone. The former lithology becomes predominant and continuous in the Davoei Zone as well. The sessile benthonic megafossils can be regarded as allochtonous elements (G é c z y 1971b); these originally lived on a seamount nearby, and subsequently were carried down by slumping. The bathymetric position of the seamount is given by some recently found algal borings: a few tens of metres (V ö r ö s 1973).

In the Lókút Section the Carixian, as well as the underlying Sinemurian, attaining almost 100 m in thickness, is represented by cherty crinoidal limestones. On the basis of studies carried out on other Mediterranean areas (cf. B e r n o u l l i – J e n k y n s 1970) it is interpreted as an interseamount, basinal sequence; the biogenic cherts and limestones are of allodapic origin.

Table II. shows the distribution of the benthonic megafossils in the

coeval strata of the certain sections. (Specimen numbers are referred to 2 m^2 surface) (N. B. The sponges and crinoids, representing the greatest biomass are not enable to specimen-number indication because of their disintegrated skeleton).

Table II

	Közöskút	Kericser	Lókút
Brachiopoda, specimen number	56	890	2
Brachiopoda, diversity index	1.7	5.2	–
Bivalvia, specimen number	13	72	1
Gastropoda specimen number	8	61	1
Hexacorallia specimen number	2	1	–
Echinoidea specimen number	–	2	–

The fossil material of the Kericser Section reflecting the most elevated seamount is not only richest in specimen number, but the diversity index of the brachiopod community is high as well. (The calculation of the diversity index was based on the S i m p s o n – formula as suggested by A g e r 1963, p. 240). The benthos of the Közöskút Section is much poorer, the brachiopod fauna of low diversity index is mainly consists of the species *Propygope? aspasia* (M e n e g h i n i), wich can be regarded as very efficient suspension-feeder (A g e r 1965). In the Lókút Section the shelly benthos is only represented by a few specimen.

The explanation for these conspicuous differences might be that the basinal sequence of the Lókút Section (suggesting evidently soft substrate), contrarily to the hard bottom of the seamounts was not advantageous for the attaching of the sessile benthos. But the Lókút Section did not yield any burrowing bivalves, hence in this case not the bottom circumstances, but the food-supply could have been decisive.

The organic matter of the plankton living in the surface waters of the Recent open seas relatively quickly mineralizes by aerob bacterial activity in the course of the slow postmortal sinking. This decomposition process ends at about 2000 and 1000 m depth in the case of the pteropods (V i n o g r a d o v 1961), and the foraminifers (B e l i a e v a 1962) respectively, but its highest rate falls within the uppermost some hundreds of metres. Consequently, considering some hundreds of metres elevation differences to the bottom-elements in the Bakony Mountains example (and this seems to be quite resonable), it will clearly explanate the differences of the benthonic communities.

* * *

The above example supports the suggestion of G a r r i s o n and F i s c h e r (1969), namely that the graditional impoverishment of the benthos in the Mediterranean Jurassic can be due to the increasing water-depth and connecting food-absence. It is a matter of further consideration that what a water-depth is involved with complete starvation occured on Mediterranean areas in the Middle and/or Upper Jurassic.

The Recent marine food-web contains vertically migrant organisms which transport the living organic matter down to 8000 m depth (V i n o g r a d o v 1968, p. 279), and this is the exclusive food-supply of the abyssal depths. But while the Recent organic world represents the mature stage of the ecosystem succession, in the Jurassic the global ecosystem was in an early stage (T a p p a n 1971), with presumably much simpler and shorter food-chain. This means that such a well developed food-transport mechanism as the Recent, vertically several kilometres' migrant organisms can be left out of account in the Jurassic, thus the food could not reach so deep as today.

On the other hand the mineralization of organic matter of the organisms lived in the upper, productive zone ends only at 2000 – 3000 m depth (V i n o g r a d o v 1961), a fact that can be more probably extrapolated to the Jurassic. Taking this into account, the conclusion seems not to be hazardous that the depth of the Mediterranean Jurassic sea-floor – at least in the periods characterized by the total absence of benthos – could be greater than 3000 metres.

Conclusions

In the open Tethyan ocean the phytoplankton must have been the only fundamental food-supply. During the course of the Jurassic its quantity increased gradually (by evolutionary causes), in spite of the fact that the Tethys opened and the nutrient-source shifted back. Therefore the benthos-impoverishment can be due to not the increasing pelagicity, but rather – as suggested by G a r r i s o n and F i s c h e r (1969) – to the increasing water-depth. The quick mineralization of the organic matter sinking from shallow into deep zones is reflected by the benthonic communities even in the upper hundreds of metres, but the total decomposition can be expected at 2 – 3000 m depth only. The maximum depth of the Mediterranean Jurassic sea-floor, judging from the total absence of the benthos, would exceed this figure.

This is consistent with the modern paleogeographic and tectonic concepts, which reveals that the Mediterranean Jurassic sediments deposited on submerged parts of a carbonate platform (B e r n o u l l i 1971). This platform belonged to the southern continental margin of the Tethys (L a u b s c h e r 1971), subsequently perhaps existed as a "microcontinent" (W e z e l 1970), thus was surrounded by newly formed oceanic crust. The vast (locally several thousand metres') submergence of the areas characterized by continental (granitic) crust can be understood by the mechanism outlined by B o t t (1971).

REFERENCES

A g e r, D. V. (1963): Principles of palaeoecology. New York.

A g e r, D. V. (1965): The adaptation of Mesozoic brachiopods to different environments. Palaeogeogr., Palaeocolimatol., Palaeoecol. I. 2.

B e l i a e v a, N. V. (1962): The distribution of the plankton foraminifera in the water masses of the Indian Ocean. Biull. Mosk. Isp. Prir. Otd. Geol. 37., 3. (in Russian).

Berner, R. A. (1970): Sedimentary pyrite formation. Amer. J. Sci. 268., 1.
Bernoulli, D. – Jenkyns, H. C. (1970): A Jurassic basin: Glasenbach Gorge, Salzburg, Austria. Verh. Geol. Bundesanst. (1970), 4.
Bordovskiy, O. K. (1965): Accumulation and transformation of organic substances in marine sediments, Marine Geol. 3., 1/2.
Bott, M. H. P. (1971): Evolution of young continental margins and formation of shelf basins. Tectonophysics, 11, 5.
Clarke, G. L. (1954): Elements of ecology. New York (1965) Rev. print.
Galácz A. – Vörös A. (1972): An outlined evolution of the Jurassic of the Bakony Mountains (Hungary) based on sedimentological phenomena. Földt. Közl., 102., 2. (in Hungarian, with English abst.)
Garrison, E. R. – Fischer, A. G. (1969): Deep-water limestones and radiolarites of the Alpine Jurassic. SEPM Spec. Publ. No. 14.
Gasiorowski, S. M. (1971): Distribution in facies and mode of life of cephalopods with Rhynchoteuthis in the Jurassic and Neocomian. Bull. Acad. Polon. Sci., Ser. Sci. Terr. XIX., 3.
Géczy B. (1971a): The Pliensbachian of the Bakony Mountains. Acta Geol. Acad. Sci. Hung. 15.
Géczy B. (1971b): The Pliensbachian of Kericser Hill, Bakony Mountains, Hungary. Ann. Univ. Sci. Budapest., Sec. Geol. XIV.
Géczy B. (1973): The origin of the Jurassic faunal provinces and the Mediterranean plate tectonics. Ann. Univ. Sci. Budapest., Sec. Geol. XV. (in press).
Hallam, A. (1967): Sedimentology and palaeogeographical significance of certain red limestones and associated beds in the Lias of the Alpine region. Scott. J. Geol. 3., 2.
Hallam, A. (1969): Tectonism and eustasy in the Jurassic. Earth-Sci. Rev. 5., 1.
Hallam, A. (1971): Evaluation of bathymetric criteria for the Mediterranean Jurassic. Ann. Inst. Geol. Publ. Hung. LIV., 2.
Jenkyns, H. C. (1971): The genesis of condensed sequences in the Tethyan Jurassic. Lethaia 4., 3.
Konda, J. (1970): Lithologische und Fazies-Untersuchung der Jura-Ablagerungen des Bakony-Gebirges. Ann. Inst. Geol. Publ. Hung. L.
Laubscher, H. P. (1971): Das Alpen-Dinariden-Problem und die Palinspastik der südlichen Tethys. Geol. Rundschau. 60., 3.
Lehman, U. (1971):. Jaws, radula and crop of Arnioceras (Ammonoidea). Palaeontology. 14., 4.
Mc Cammon, H. M. (1969): The food of articulate brachiopods. J. Paleont. 43., 4.
Pitrat, C. W. (1970): Phytoplankton and the Late Paleozoic wave of extinction. Palaeogeogr., Palaeoclimatol., Palaeocecol. 8., 11.
Sokolova, M. N. (1959): On the distribution of deep-water bottom animals in relation to their feeding habits and the character of sedimentation. Deep-Sea Res. 6., 1.
Sturani, C. (1971): Ammonites and stratigraphy of the "Posidonia alpina" beds of the Venetian Alps. Mem. Ist. Geol. Min. Univ. Padova. XXVIII.
Tappan, H. (1971): Microplankton, ecological succession and evolution. Proc. North Amer. Paleont. Conv. (H).
Tappan, H. – Loeblich, A. J. Jr. (1971): Geobiologic implications of fossil phytoplankton evolution and time – space distribution. Geol. Soc. Amer., Spec. Paper 127.
Vinogradov, M. E. (1961): Food sources of deep-water faunas. Dokl. Akad. Nauk. S. S. S. R. 138., 6. (in Russian).
Vinogradov, M. E. (1968): Vertical distribution of the oceanic zooplankton. Moscow. (in Russian).
Vogel, K. (1966): Eine functionsmorphologische Studie an der Brachiopodengattung Pygope (Malm bis Unterkreide). N. Jb. Geol. Pal., Abh. 125., 1 – 3.
Vörös A. (1973): Traces of boring algae from the Lias of Kericser (Bakony Mountains, Hungary). Földt. Közl. 103. (in press) (in Hungarian with English abstr.)
Wendt, J. (1970): Stratigraphische Kondensation in triadische und jurassische Cephalopodenkalken der Tethys. N. Jb. Geol. Pal., Mh. (1970), 7.
Wezel, F. C. (1970): Interpretazione dinamica della "eugeosinclinale meso-mediterranea". Riv. Miner. Sicil. XXI., no. 124 – 126.

INDEX

A kiadásért felelős: az Eötvös Loránd Tudományegyetem rektora — A kézirat nyomdába érkezett: 1973. január — Megjelent: 1974. február — Terjedelem: 19 (A/5) ív + 3 db mell. — Példányszám: 750 — Készült monó szedéssel, íves magasnyomással, az MSZ 5601—59 és az MSZ 5602—55 szabvány szerint.
73.61. Állami Nyomda, Budapest